

HYDRAULICS

AUTHORS:

Prof.^o Dr.^o Sérgio António Neves Lousada
Eng.^o Rafael Freitas Camacho
Eng.^o Adhony's Alexander Rincon Rodrigues

Technical Specifications

Title	Hydraulics: Theory
Authors	Sérgio António Neves Lousada Rafael Freitas Camacho Adhony's Alexander Rincon Rodrigues
Editors	University of Madeira
Edition	1 st
Edition Years	2018
Volume	I
ISBN	978-989-8805-48-5
Support	Electronic
Format	PDF

Index

CHAPTER 1 - Introduction.....	27
1.1 Small approach about hydraulic history	27
1.2 Hydraulics branches.....	28
1.3 Definition of fluid	29
1.4 Unit system. International unit system.....	29
1.4.1 Systems used in hydraulics	29
1.4.2 International System (IS)	29
1.5 Physical properties of fluids	30
1.5.1 Weight and mass. Volumetric weight and volumetric mass	30
1.5.2 Density	30
1.5.3 Isotropy.....	31
1.5.4 Continuity	31
1.5.5 Compressibility	31
1.5.6 Viscosity	32
1.5.7 Cohesion	33
1.5.8 Superficial tension and capillarity	34
1.5.9 Liquid steam tension.....	35
1.5.10 Gas solubility in water.....	35
1.5.11 Elastic waves propagation speed	35
1.6 Equations of fluid mechanics	35
1.6.1 Lagrange variables	38
1.6.2 Euler Variables	38
1.6.3 Kraichnan variables	39
1.6.4 Types of equations of Fluid Mechanic and Hydraulic	40
Chapter 2 - Fundamental Equations of Fluid Movement	43
2.1 Parameters of hydrokinetic character.....	43
2.1.1 Trajectory. Stream lines. Filaments lines. Fluid lines.....	43
2.1.2 Lagrange's and Euler's Variables.....	44
2.1.3 Flow rate. Flows medium velocity	46
2.1.4 Acceleration.....	47
2.1.5 Vorticity.....	50
2.2 Types of movements.....	51
2.2.1 Permanents and non-permanents movements.....	51
2.2.2 Rotational and irrotational Movements/Flows	53
2.2.3 Laminar, transition and turbulent Movements/Flows	53
2.2.4 External, internal and in porous media flows	54
2.3 Continuity equation	55
2.3.1 Deduction of the general equation.....	55
2.3.2 Application to a stream tube (stream pipe)	57
2.4 Equation of dynamic equilibrium	58
2.4.1 Consequences in Fluids	59
2.4.2 Notion of dynamic equilibrium	60
2.4.3 Characterization of the state of tension	60
2.4.4 Equations of dynamic equilibrium	61
2.4.5 Euler's Equations.....	61

2.4.6 Navier-Stokes Equations. Borders conditions	62
Chapter 3 - Hydrostatic.....	69
3.1 General equations of fluids equilibrium	69
3.1.1 General case	69
3.1.2 Equilibrium of a fluid at constant temperature	70
3.1.3 Heavy fluids equilibrium.....	70
3.1.4 Equilibrium of heavy liquids	71
3.1.5 Absolutes and effectives pressures	72
3.1.6 Equilibrium of liquids with different densities	73
3.1.7 Equilibrium of liquid under non-exclusive gravitational forces fields	73
3.2 Liquid manometer	76
3.3 Hydrostatics impulsions in surfaces	80
3.3.1 Concept	80
3.3.2 Hydrostatics impulsions on plain surfaces	80
3.3.3 Hydrostatics impulsions in curved surfaces	85
3.3.4 Hydrostatics impulsions on closed surfaces	87
3.3.5 Uniform pressures applied to the liquid mass	87
3.4 Pascal Principle	89
3.5 Equilibrium in floating bodies	90
3.5.1 Impulsion. Arquimedes Principles.....	90
3.5.2 Definitions. Fundamental theorems	92
3.5.3 Equilibrium condition in buoyancy or floating bodies	98
Chapter 4 - Bernoulli Theorem and applications.....	101
4.1 Bernoulli theorem in local aspect.	101
4.1.1 Deduction of the local equation of Bernoulli	101
4.1.2 Interpretation of the local expression of Bernoulli theorem	103
4.1.3 Bernoulli theorem applied to a permanent regime	106
4.2 Bernoulli's theorem in global aspect	108
4.2.1 Application of the Bernoulli's theorem to a stream tube.....	108
4.2.2 Global coefficients of Bernoulli's equation	110
4.2.3 Global expression of Bernoulli's theorem	115
4.2.4 Interpretation of the global expression of Bernoulli's theorem	116
4.2.5 Application of global equations to permanent regime	118
4.3 Application of Bernoulli's theorem	120
4.3.1 Measure of velocity by using a Pitot Pipe (Tube)	120
4.3.2 Diffusor of a hydraulic turbine	121
4.3.3 Charge and piezometric lines in hydraulic machine installation.....	123
4.3.4 Occurrence of cavitation.....	125
Chapter 5 - Theorem of amount of movement and its applications	129
5.1 Expression of the amount of movements theorem	129
5.1.1 Principle of amount of movement applied to fluids mechanics	129
5.1.2 Theorem of amount of movement applied to a stream tube or pipe	131
5.2 Application of the theorem of amount of movement.....	134
5.2.1 Pipe with a gradual reduction of transversal section.....	135
5.2.2 Reduction of section and direction change.....	135
5.2.3 Action of a jet over a fixed curved surface	136
5.2.4 Action of a jet in a plain surface.....	137

5.2.5 Forces in movables solid surfaces.....	138
5.2.6 Kutta-Joukowski's Theorem	139
Chapter 6 - Flows through orifices and spillways.....	141
6.1 Flows through orifices	141
6.1.1 General scheme of an orifice.....	141
6.1.2 Classification	142
6.1.3 Orifices of thin walls.....	143
6.1.4 Orifices of thick walls. Additional pipes.....	150
6.1.5 Draining time in reservoir.....	156
6.1.6 Configuration of liquid jets	157
6.2 Flows through spillways	158
6.2.1 Spillways classification	159
6.2.2 Influence of the liquid veins shape.....	160
6.2.3 Spillway of thin crest or threshold	162
6.2.4 Unloader or spillways of thick crest	169
6.2.5 Normal crest spillway or unloaders.....	170
6.2.6 Cares when using spillways for flow rate measurements	171
Chapter 7 - Dimensional or design Analysis	173
7.1 Introduction	173
7.2 Units and dimensions.....	174
7.3 Theorems of Dimensional Analysis	175
7.3.1 Applications of the Theorem of $\pi\pi\pi$ to a problem of Fluids Mechanics....	177
7.3.2 Physical meaning of the dimensionless parameters.....	179
Chapter 8 - Similarity	181
8.1 Mechanical and Hydraulics Similarity.....	181
8.1.1 Euler, Froude and Reynolds's Similarity.....	182
8.1.2 Usual dimensionless parameters.....	184
8.1.3 Similarities to consider in a study of a model.....	184
8.1.4 Similarity in hydraulics turbomachines.....	185
8.1.5 Generalities about models.....	186
Chapter 9 - Flows under pressure.....	189
9.1 Generalities.....	189
9.1.1 Flow establishment.....	192
9.1.2 Rugosity of the tube's walls	192
9.1.3 Regimes of flows. Experiences of Nikuradse	193
9.2 Uniform charge losses in flows under pressure	194
9.2.1 Charge losses in laminar regime	195
9.2.2 Charge losses in turbulent regime hydraulically smooth.....	195
9.2.3 Charge losses in turbulent rough regime	195
9.2.4 Charge losses in commercial pipes or conduits	195
9.3 Localized charge losses in flows under pressure.....	197
9.3.1 Charge losses in an abrupt enlargement.....	197
9.3.2 Charge losses in a gradual enlargement	198
9.3.3 Charge losses in a passage from a conduit or pipe to a reservoir	198
9.3.4 Charge losses in an abrupt narrowing or abrupt reduction	199
9.3.5 Charge losses in a passage from a reservoir to a conduit.....	200
9.3.6 Charge losses in directions changes	200

9.3.7 Charge losses in bifurcation	202
9.3.8 Charge losses in valves.....	202
9.3.9 Charge losses in grills	205
9.3.10 Equivalent distance or length to a localized charge loss	205
9.4 Problems of uniform movement in tubes or pipes	206
9.4.1 Generalities	206
9.4.2 Types of problems	207
9.4.3 Determination of the piezometric elevations when flow rate and diameters are known.....	207
9.4.4 Determination of the flow rate when diameters and charge losses are known	207
9.4.5 Determination of the diameters when flow rate and charge losses are known	208
9.4.6 Position of the conduits depending on the piezometric line	208
9.4.7 Conduits supplied by both extremes.....	212
9.4.8 Dimensioning of gravitational conduits	214
9.5 Dimensioning of elevatory pipes or conduits.....	216
9.5.1 Generalities	216
9.5.2 Economical and resources considerations	216
9.5.3 Expenses structure.....	217
9.5.4 Calculus of the economical diameter.....	218
9.5.5 Influence of consume during the year.....	221
9.5.6 Formulas for an approximated dimensioning.....	221
9.5.7 Dimensioning of the conduit's walls.....	222
9.6 Problems in uniform movement by a group of pipes or conduits.....	222
9.6.1 Conduits in serial connection.....	222
9.6.2 Conduits in parallel	223
9.6.3 Node of conduits.....	223
9.6.4 Web of pipes or conduits. Equation system.....	224
9.6.5 Networks of pipes. Meshes	229
9.6.6 Networks of pipes or conduits. Dispositive of control of pressures and flow rate in networks	232
9.7 Varied movement in conduits.....	235
9.7.1 Charge losses in a varied movement	235
9.7.2 Problems of varied movement in conduits.....	236
Chapter 10 - Permanent Flow in conduits conditioned by hydraulic machines	239
10.1 Hydraulics Turbines	239
10.1.1 Characteristic of operation.....	239
10.1.2 Operation of integrated turbines at installations	243
10.1.3 Selection of adequate turbines for an installation	261
10.2 Hydraulic pumps	263
10.2.1 Operation Description.....	263
10.2.2 Operation of pumps integrated to an installation	275
10.2.3 Selection of adequate pumps at some installation.....	283
Chapter 11 - Flows with a free surface	287
11.1 Generalities.....	287
11.1.1 Flows Classifications	288

11.1.2 Types of channels	289
11.1.3 Geometry of a channel	290
11.2 Applications of the Bernoulli's theorem to Flow with free surface	296
11.2.1 Expression of the Bernoulli's theorem	296
11.2.2 Distribution of pressure in the transversal section	297
11.2.3 Distribution of velocity in the transversal section	298
11.2.4 Energy losses. Resistance formulas.....	300
11.2.5 Specific Energy.....	304
11.2.6 Surfaces of energy	305
11.2.7 Critical values	307
11.3 Application of theorem of amount of movement to flows of free surface	309
11.3.1 Principles and definitions.....	309
11.3.2 Total amount of movement. Specific force	310
11.3.3 Surfaces of total quantity of movement	312
11.3.4 Relation between the total amount of movement and the specific energy	314
11.4 Uniform regime in channels	316
11.4.1 Conditions of establishment of uniform regime in channels.....	316
11.4.2 Normal height	316
11.4.3 Section of maximum flow rate	319
11.4.4 Problems of uniform movement in channels.....	321
11.4.5 Critical uniform regime.....	321
11.5 Permanent regime gradually varied in channels or channels.....	322
11.5.1 Theoretical equations of movement gradually varied in channels	322
11.5.2 Backwater in prismatic channels with constant flow rate	323
11.5.3 Backwater in channels of variable flow rate.....	330
11.6 Permanent regime rapidly varied in channels	331
11.6.1 General considerations.....	331
11.6.2 Hydraulic rebound	332
11.6.3 Other types of rapidly varied flows.....	344
REFERENCES	345

Figure Index

Figure 1 – Viscosity.	32
Figure 2 – Relation between deformation and tension or stress.	32
Figure 3 – Superficial tension (White, 1948).	34
Figure 4 – Adherence.	34
Figure 5 – Tensor of tension (https://commons.wikimedia.org).	36
Figure 6 – Diagram of action of a force over a layer of fluid (http://www.mspc.eng.br).	36
Figure 7 – Vector Speed (Junior & Colvara, 2010).	36
Figure 8 – Mixture of oil, water and sand (http://mundoeducacao.bol.uol.com.br/)...	37
Figure 9 – Immersion thermometer (https://www.3bscientific.es).	37
Figure 10 – Lagrange variables (Pinho et al., 2011).	38
Figure 11 – Euler variables (Pinho et al., 2011).	38
Figure 12 – Study of flow's turbulence (www.turbulencia.coppe.ufrj.br/).	39
Figure 13 – Volume of control and Control surface (Pinho et al., 2011).	40
Figure 14 – Trajectory (Pinho et al., 2011).	43
Figure 15 – Stream Lines (Pinho et al., 2011).	43
Figure 16 – Stream pipe (Pinho et al., 2011).	44
Figure 17 – Fluid Lines (Pinho et al., 2011).	44
Figure 18 – Representation of velocity in terms of Lagrange's variables (Vasconcelos, 2005).	45
Figure 19 – Representation of Velocity in terms of Euler's Variables (Vasconcelos, 2005).	46
Figure 20 – Illustration where flow rate, is the volume crossing the surface S with velocity V (adapted from Pinho et al., 2011).	47
Figure 21 – Representation of acceleration using Euler's Representation (Vasconcelos, 2005).	48
Figure 22 – Shear deformation in (x, y) plane of a portion of fluid in flow (Gobbi et al., 2011).	50
Figure 23 – Non-permanent movement (Pinho et al., 2011).	52
Figure 24 – Varied permanent movement (Pinho et al., 2011).	52
Figure 25 – Uniform permanent movement (Pinho et al., 2011).	52
Figure 26 – Graphical representation of laminal flow or movement (Pinho et al., 2011).	53
Figure 27 – Graphical representation of a turbulent flow or movement (Pinho et al., 2011).	54
Figure 28 – Control surface (Pinho et al., 2011).	56
Figure 29 – Stream pipe or stream tube (Pinho et al., 2011).	57
Figure 30 – Example of incompressible fluids in permanent movement (Pinho et al., 2011).	58
Figure 31 – Volume forces or mass forces (Pinho et al., 2011).	59
Figure 32 – Surface forces or contact forces (Pinho et al., 2011).	59
Figure 33 – Dynamic equilibrium (Pinho et al., 2011).	60
Figure 34 – Axis transformation (Baliño, 2017).	63
Figure 35 – Borders conditions in a free surface (kinematics) (Baliño, 2017).	66
Figure 36 – Borders conditions in free surfaces (normal) (Baliño, 2017).	67

Figure 37 – Borders conditions in surfaces between fluids (Baliño, 2017).	67
Figure 38 – Equilibrium of heavy liquids (adapted from Pinho et al., 2011).	71
Figure 39 – Fundamental principle of Hydrostatics (Pinho et al., 2011).	72
Figure 40 – Liquid mass constituted by liquids of different densities (Pinho et al., 2011).	73
Figure 41 – Liquid under constant acceleration (Pinho et al., 2011).	73
Figure 42 – Equilibrium of a liquid in an animated vessel of constant angular velocity (Pinho et al., 2011).	74
Figure 43 – Angular velocity ω_0 where the vertex of the parabola hits the bottom of the reservoir (Pinho et al., 2011).	76
Figure 44 – Connection (Pinho et al., 2011).	76
Figure 45 – Vertical piezometers (Pinho et al., 2011).	77
Figure 46 – Inclined piezometer (Pinho et al., 2011).	77
Figure 47 – High effective pressures (Pinho et al., 2011).	78
Figure 48 – Low effective pressures (Pinho et al., 2011).	78
Figure 49 – Differential manometers, $\gamma_m > \gamma$ (Pinho et al., 2011).	78
Figure 50 – Differential manometers, $\gamma_m < \gamma$ (Pinho et al., 2011).	79
Figure 51 – Manometers in reservoirs (Pinho et al., 2011).	80
Figure 52 – Hydrostatic impulsion on an element of plain surface (Pinho et al., 2011).	81
Figure 53 – Plain surface submerge in liquid (Pinho et al., 2011).	81
Figure 54 – Example of hydrostatic impulsion on a plain surface (Pinho et al., 2011).	82
Figure 55 – Example of a curved surface (Pinho et al., 2011).	85
Figure 56 – Horizontal component of the pressure force (Pinho et al., 2011).	85
Figure 57 – Vertical component of pressure force (Pinho et al., 2011).	86
Figure 58 – Hydrostatics impulsions in closed surfaces (Pinho et al., 2011).	87
Figure 59 – Uniform pressures applied to a liquid mass (Pinho et al., 2011).	88
Figure 60 – Cylindrical body subjected to uniform pressure (boiler or pipe under pressure) (Pinho et al., 2011).	88
Figure 61 – Resultant of pressure forces in transversal direction (Pinho et al., 2011).	89
Figure 62 – Resultant of the pressure forces in longitudinal direction (Pinho et al., 2011).	89
Figure 63 – Pascal Principle (Pinho et al., 2011).	89
Figure 64 – Hydraulic press (Pinho et al., 2011).	90
Figure 65 – Impulsion (http://blogcfqmariana.blogspot.pt/2015/).	91
Figure 66 – Classical unidimensional representation of a system with a meta-state (1), unstable state (2) and a stable state (3) (https://commons.wikimedia.org/).	92
Figure 67 – Immersed block (Martins, 2010).	93
Figure 68 – Edited picture showing and whole Iceberg floating with most of its body immersed (https://commons.wikimedia.org/).	94
Figure 69 – Center of floatability or buoyancy and impulsion (adapted from PNA, 1988).	96
Figure 70 – Transversal section (uniform) of a ship (Martins, 2010).	97
Figure 71 – Longitudinal equilibrium condition (Fonte: Lewis, 1988).	98
Figure 72 – Conditions of equilibrium (adapted from, 2010).	98

Figure 73 – Condition of equilibrium of immersed bodies (adapted from Lewis, 1988).	99
Figure 74 – Condition of equilibrium for floating bodies (adapted from Lewis, 1988).	100
Figure 75 – Fluid particle that displace along its trajectory (Pinho et al., 2011).	101
Figure 76 – Piezometric and energy line or charge (Pinho et al., 2011).	105
Figure 77 – Difference between two types of loss of charge (Pinho et al., 2011).	108
Figure 78 – Stream tube (Pinho et al., 2011).	109
Figure 79 – Free surface flow.	110
Figure 80 – Distribution of pressures (Pinho et al., 2011).	111
Figure 81 – Distribution of pressures in free surface flows (Pinho et al., 2011).	112
Figure 82 – Fillets parallels to a vertical plane (Pinho et al., 2011).	113
Figure 83 – Piezometric line and energy line (Pinho et al., 2011).	117
Figure 84 – Association of a piezometric and a Pitot Tube in order to determine the velocity diagram at a transversal section in a flows tube. (Vasconcelos, 2005).	120
Figure 85 – Typical arrangement of and hydraulic turbine (Tavares, 2014).	121
Figure 86 – Graphical approach of an impeller or rotator: a) with a diffusor; b) without a diffusor (Coelho, 2006).	121
Figure 87 – Hydraulic circuit (Vasconcelos, 2005).	123
Figure 88 – Energy and piezometric line of a hydraulic-elevator pipe circuit (Vasconcelos, 2005).	124
Figure 89 – Energy line and piezometric line in a hydraulic-gravitational pipe circuit with a turbine (Vasconcelos, 2005).	125
Figure 90 – Model of the propeller that creates cavitation in an experimental water tunnel (https://commons.wikimedia.org).	125
Figure 91 – Damages created by cavitation in a Francis turbine (https://commons.wikimedia.org).	126
Figure 92 – Spectrum of vibration collected in a pump bearing (Oliveira, 2007).	127
Figure 93 – Rotor destroyed by cavitation, used to belong to a water pump (Oliveira, 2007).	128
Figure 94 – Scheme of an centrifugal pump (http://www.ebah.com.br) and bearing (https://commons.wikimedia.org).	128
Figure 95 – Current Tube (Brunetti, 2008).	132
Figure 96 – Pressures, tensions and gravity field (Brunetti, 2008).	133
Figure 97 – Components of a resultant force (Brunetti, 2008).	134
Figure 98 – Pipe with gradual reduction of section (Brunetti, 2008).	135
Figure 99 – Reduction of section and direction change (Brunetti, 2008).	135
Figure 100 – Jet acting over a curved laminate (Brunetti, 2008).	136
Figure 101 – Filling jet on a flat plate (Brunetti, 2008).	137
Figure 102 – Filling jet on a moving curve plate (Brunetti, 2008).	138
Figure 103 – (a): Evolution of a fluid mass when steps with a body; (b): Volume of control used in the determination of a sustentation force acting in the body (Pontes & Mangiavacchi, 2013).	140
Figure 104 – General scheme of an orifice (adapted from Silva, 2014).	142
Figure 105 – Orifices of thin walls (Junior L. B., 2005).	143
Figure 106 – Flow rate drained through orifices of small dimensions (Pinho et al., 2011).	143

Figure 107 – Flow rate drained through orifices of great dimensions. Rectangular shape (Pinho et al., 2011).....	146
Figure 108 – Totally submerged orifice (DRHGSA, 2007).....	148
Figure 109 – Orifices partially submerged (DRHGSA, 2007).	150
Figure 110 – Orifices of thick walls (Junior L. B., 2005).....	150
Figure 111 – Orifices of rounded edges (https://pt.slideshare.net/IsaqueEliasCorreia/instrumentacaobasica2-pdf).	151
Figure 112 – (a) Full contraction (in all orifices faces); (b) Partial contraction (only at the top) (Junior L. B., 2005).	151
Figure 113 – Short pipe addition (Pinho et al., 2011).	153
Figure 114 – Additional pipe with adherent liquid vein (Pinho et al., 2011).	154
Figure 115 – Additional cylindrical pipe (Pinho et al., 2011).	155
Figure 116 – Additional conical divergent pipe (Pinho et al., 2011).	155
Figure 117 – Draining of a reservoir of variable section (Pinho et al., 2011).	156
Figure 118 – Draining of a reservoir of constant section (Pinho et al., 2011).	157
Figure 119 – Inversion of the liquid vein (Pinho et al., 2011).	158
Figure 120 – Configuration of a liquid vein (Pinho et al., 2011).	158
Figure 121 – Scheme of a rectangular unloader or spillway with a free strand blade (Queiroz, 2017).....	159
Figure 122 – Spillway (a) without lateral contractions, (b) with one lateral contraction, (c) with two lateral contractions (adapted from Queiroz, 2017).....	160
Figure 123 – Free laminate (Queiroz, 2017).....	161
Figure 124 – Depressed laminate (Queiroz, 2017).....	161
Figure 125 – Adherent laminate (Queiroz, 2017).....	162
Figure 126 – Drowned laminate (Queiroz, 2017).....	162
Figure 127 – Square spillway of thin crest or threshold, without lateral contractions and free discharge, or Bazin's spillway (Queiroz, 2017).....	162
Figure 128 – Triangular discharger (Queiroz, 2017).....	165
Figure 129 – Trapezoidal spillway (Queiroz, 2017).	166
Figure 130 – Trapezoidal spillway (Cipolletti) (Queiroz, 2017).	167
Figure 131 – Circular spillway (Queiroz, 2017).....	167
Figure 132 – Vertical pipe spillway of free discharge (Queiroz, 2017).....	168
Figure 133 – Rectangular spillway of thick crest (Queiroz, 2017).....	169
Figure 134 – Creager profile (Queiroz, 2017).....	170
Figure 135 – Profile WES (EUA) (Queiroz, 2017).....	171
Figure 136 – Study of physical phenomenon's (adapted from Vasconcelos, 2005).	173
Figure 137 – Schematically representation of physical similarity (adapted from Vasconcelos, 2005).	181
Figure 138 – Similarities (adapted from Vasconcelos, 2005).....	182
Figure 139 – Circular conduit or pipe (Pinho et al., 2011).	190
Figure 140 – Absolute rugosity (Pinho et al., 2011).....	192
Figure 141 – Artificial rugosity of Nikuradse (Pinho et al., 2011).	193
Figure 142 – Experimental results of Nikuradse (Pinho et al., 2011).....	193
Figure 143 – Flows regimes in conduits (http://slideplayer.com.br/slide/7750390/#).	194

Figure 144 – Moody diagram (source: https://en.wikipedia.org/wiki/Moody_chart#/media/File:Moody_EN.svg).	194
Figure 145 – Charge loss in an abrupt enlargement (Pinho et al., 2011).	197
Figure 146 – Gradual enlargement (KSB, 2003).	198
Figure 147 – Passage with sharp edge from a conduit to a reservoir (Pinho et al., 2011).	198
Figure 148 – Passage with gradual enlargement from a conduit to a reservoir (Pinho et al., 2011).	199
Figure 149 – Abrupt reduction (Pinho et al., 2011).	199
Figure 150 – Passage with sharp edge from a reservoir to a conduit (Pinho et al., 2011).	200
Figure 151 – Passage with gradual reduction from a reservoir to a conduit (Pinho et al., 2011).	200
Figure 152 – Gradual change of direction in a tube of circular section (curves) (KSB, 2003).	201
Figure 153 – Abrupt change of direction in a tube of circular section (knee or elbow) (KSB, 2003).	201
Figure 154 – Gate valve (adapted from http://www.globalspec.com).	203
Figure 155 – Butterfly valves (adapted from http://www.sohanengg.com).	203
Figure 156 – Spherical valve (adapted from http://www.histarmar.com.ar and Pinho et al., 2011).	204
Figure 157 – Backstop retention valve (adapted from http://www.solucoesindustriais.com.br and https://www.unival.com.br).	204
Figure 158 – Grill (adapted from Pinho et al., 2011).	205
Figure 159 – Schematic representation of a flow inside a tube (Pinho et al., 2011).	206
Figure 160 – Conduit under the effective piezometric line in its complete extension (Pinho et al., 2011).	208
Figure 161 – Conduit above the effective piezometric line (at CD), but below the absolute piezometric line (Pinho et al., 2011).	209
Figure 162 – Conduit coinciding with the effective piezometric line in its complete extension (Pinho et al., 2011).	209
Figure 163 – The conduit crosses the effective charge line (in CD), staying under the absolute piezometric line (Pinho et al., 2011).	210
Figure 164 – The conduit crosses the absolute piezometric line (at CD) but does not achieve the effective charge line (Pinho et al., 2011).	210
Figure 165 – The conduit crosses the absolute piezometric line and overpass the effective charge line (Pinho et al., 2011).	211
Figure 166 – Condition of maximum transportation (Pinho et al., 2011).	211
Figure 167 – Reservoir at constant level.	212
Figure 168 – Partially open valve.	212
Figure 169 – Operation from R1 to R2 reservoir (Pinho et al., 2011).	212
Figure 170 – Operation with a T bifurcation, flow rate q and piezometric $T > R2$ (Pinho et al., 2011).	213
Figure 171 – Operation with a T bifurcation, flow rate q and piezometric line in $T = R2$ (Pinho et al., 2011).	213

Figure 172 – Operation with a T bifurcation, flow rate q and piezometric at $T < R_2$ (Pinho et al., 2011).	214
Figure 173 – Operation with a T bifurcation, flow rate q and piezometric at $T = T$ (Pinho et al., 2011).	214
Figure 174 – Examples of application (Pinho et al., 2011).	215
Figure 175 – Example of an elevatory pipe or conduit (Pinho et al., 2011).	216
Figure 176 – Investment costs (initial costs) (Pinho et al., 2011).	216
Figure 177 – Operating costs (annual costs, most significant: energy cost) (Pinho et al., 2011).	217
Figure 178 – Initial costs or expenses (C_1) (Pinho et al., 2011).	217
Figure 179 – Monetary-time flows diagrams (Pinho et al., 2011).	219
Figure 180 – Flow rate/energy in function of time (Pinho et al., 2011).	221
Figure 181 – Example of an application (Pinho et al., 2011).	222
Figure 182 – Conduits in serial connection (Pinho et al., 2011).	222
Figure 183 – Conduits in parallel (Pinho et al., 2011).	223
Figure 184 – Nodes of conduits (Pinho et al., 2011).	223
Figure 185 – Equations in Nodes (Pinho et al., 2011).	225
Figure 186 – Application examples of equations in Q (Pinho et al., 2011).	226
Figure 187 – Example of application of equations in H (Pinho et al., 2011).	227
Figure 188 – Example of application in equations in ΔQ (Pinho et al., 2011).	228
Figure 189 – Method to solve problems involving meshes (adapted from Pinho et al., 2011).	229
Figure 190 – Example of application of the method Hardy-Cross (Pinho et al., 2011).	230
Figure 191 – Arbitration of flow rate (Pinho et al., 2011).	230
Figure 192 – Determination of the pressures in nodes of the network (Pinho et al., 2011).	231
Figure 193 – Reservoir of control of pressures and flow rate (Pinho et al., 2011). ..	232
Figure 194 – Retention valve (Pinho et al., 2011).	232
Figure 195 – Characteristic curve of the pump (Pinho et al., 2011).	233
Figure 196 – Pressure reduction valve (http://www.vaportec.com.br).	234
Figure 197 – Example of a network of pipes with regulating devices (Pinho et al., 2011).	234
Figure 198 – Pipe with route distribution (Pinho et al., 2011).	235
Figure 199 – Example of a problem involving varied movement in conduits (Pinho et al., 2011).	236
Figure 200 – Pelton Turbine (https://www.zeco.it).	240
Figure 201 – Francis Turbine (https://hydrotu.en.ec21.com).	241
Figure 202 – Kaplan Turbine (https://www.zeco.it).	242
Figure 203 – Kaplan Turbine (bulb) (https://www.zeco.it).	242
Figure 204 – Dériaz Turbine (http://www.directindustry.com/).	243
Figure 205 – The loss of charge ΔE_T at a singularity that can be converted in a useful fall at a turbine (Cruz, 2006).	243
Figure 206 – Examples of the definition of useful falls H in Kaplan (a), Francis (b), of horizontal axis (c) and Pelton (d) turbines (Cruz, 2006).	245
Figure 207 – Euler Theorem applied to a control volume contained in an impeller/wheel of a turbine (Cruz, 2006).	245

Figure 208 – Triangle of velocities (adapted from Cruz, 2006).....	247
Figure 209 – Efficiency versus power (https://pt.slideshare.net/buti_81/hidraulica-turbinas).....	251
Figure 210 – Variation of efficiency with rotation velocity (http://www.antonioguilherme.web.br.com).....	252
Figure 211 – Efficiency/flow rate for turbines: (1) Pelton, (2) Francis, (3) Kaplan, (4) Bulb (Cruz, 2006).	252
Figure 212 – Schema of a diffusor of a turbine of reaction and definition of aspiration height (adapted from http://slideplayer.com.br/slide/1473748/).	258
Figure 213 – Graphic with a typical field of application of the three types of turbines (www.hacker.ind.br).....	261
Figure 214 – Field of application of turbines (Filho, 2015).....	262
Figure 215 – Axial pump (Universidade Federal do ABC, 2013).	264
Figure 216 – Example of a closed impeller (a), partially open (b) and open (propeller) (c) (http://hidromachinesudeg.blogspot.pt/2016/02/componentes-de-bombas-y-turbinas.html).....	264
Figure 217 – Radial flow pump (sectional cut) (http://www.tecpa.es).	264
Figure 218 – Mix flow pump (http://xylemappliedwater.pt).....	265
Figure 219 – Volute pump of duplex aspiration (www.sulzer.com).	265
Figure 220 – Pumps of simple staging of horizontal diffusor style (www.sulzer.com).	266
Figure 221 – Single cell pump (http://www.bombaszeda.com).....	266
Figure 222 – Multicellular pumps (http://www.efaflu.pt).	266
Figure 223 – Application example (determination of H) (Pinho et al., 2011).....	268
Figure 224 – Ascending pumping between reservoirs (Pinho et al., 2011).....	270
Figure 225 – Plain of reference for NPSH (adapted from http://www.nuevaingenieria.com/tag/cavitacion/).	271
Figure 226 – Elevated pump (Pinho et al., 2011).	272
Figure 227 – Pump in charge (Pinho et al., 2011).	273
Figure 228 – Relation between specific velocity in some impellers, efficiency and flow rate (Escola da Vida, 2018).	275
Figure 229 – Influence of the specific velocity in form of the characteristic curves of a pump (adapted from Pinho et al., 2011).	276
Figure 230 – Characteristic curves of a pump (adapted from Area Mecânica, 2011).	277
Figure 231 – Example of a characteristic curve of an installation (Pinho et al., 2011).	277
Figure 232 – Example of application of the concept of an installation characteristic curve (Pinho et al., 2011).....	278
Figure 233 – Variation of a flow rate due to a deviation produced by the change of operation conditions (Pinho et al., 2011).	279
Figure 234 – Regulation of the flow rate admission (Pinho et al., 2011).....	280
Figure 235 – Use of a “Bypass” (Pinho et al., 2011).....	280
Figure 236 – Variation of the rotation velocity of the impeller (Pinho et al., 2011)..	280
Figure 237 – Change of the impeller diameter (reduction) (Pinho et al., 2011).	281
Figure 238 – Pipes or conduits of branched compression (Pinho et al., 2011).....	282
Figure 239 – Operation of parallel pumps with common pipe (Pinho et al., 2011)..	282

Figure 240 – Operation of pumps in serial connection at same pipes (Pinho et al., 2011).	283
Figure 241 – Field of pump application (Henn, 2006).	284
Figure 242 – Example of a hill diagram (http://www.escoladavida.eng.br/mecfluquimica/aulasfei/ccb.htm).	284
Figure 243 – Example of mosaics of pumps uses, to pre-selection of a pump (adapted from Catálogo das Bombas KSB).	285
Figure 244 – Levada das 25 Fontes, Calheta. Channel (solid walls); Water (with a free surface) (Origin: Autor).	287
Figure 245 – Classification of flows.	288
Figure 246 – Types of channels (Origin: author).	289
Figure 247 – Representation of the type of channel section (adapted from Costa & Lança, 2011).	290
Figure 248 – Representation of the geometrical characteristics in a longitudinal profile.	290
Figure 249 – Representation of the geometric characteristics in a plain section (Costa & Lança, 2011).	291
Figure 250 – Water heights and slope of the section (adapted from Costa & Lança, 2011).	291
Figure 251 – Rectangular section of the channel.	292
Figure 252 – Channel of trapezoidal section.	292
Figure 253 – Circular section of the channel.	293
Figure 254 – Channel's circular section (geometrical relations) (adapted from Netto, 1998).	294
Figure 255 – Irregular section of the channels (graphical relationship).	294
Figure 256 – Irregular section of the channel (relationship through a monomial form).	295
Figure 257 – Representation for deduction of Bernoulli's Theorem simplification (Costa & Lança, 2011).	296
Figure 258 – Distribution of pressures in the transversal section, rectilinear flow (Soares, 2011).	297
Figure 259 – Distribution of pressures in the cross-section, concave (a) and convex flow (b) (Soares, 2011).	297
Figure 260 – Example of a non-rectilinear flow, spillway (Soares, 2011).	298
Figure 261 – Isostatics curves for different sections (adapted from Soares, 2011).	298
Figure 262 – Distribution of velocities (Costa & Lança, 2011).	299
Figure 263 – Distribution of flow rate (http://www.escoladavida.eng.br/mecflubasica/aula2_unidade3.htm).	299
Figure 264 – Composed section.	303
Figure 265 – Energy surface.	306
Figure 266 – Curve of energy variation with the water height.	306
Figure 267 – Curve of flow rate variation with the water height.	307
Figure 268 – Curve of flow rate and energy variation with the water height.	307
Figure 269 – Graphical method for the irregular section.	308
Figure 270 – Theorem of amount of movement in the direction of flow.	310
Figure 271 – Variation of the Total Quantity of Movement with the water height ($Q = Q_0 \text{ cst.}$).	313

Figure 272 – Variation of the flow rate with the water height ($M = M_0$ cst.).....	313
Figure 273 – Relationship between the Total Amount of Movement and the specific energy.	314
Figure 274 – Determination of the normal height by the graphical method.	317
Figure 275 – Rectangular section.....	317
Figure 276 – Trapezoidal section.	318
Figure 277 – Circular section.....	318
Figure 278 – Rectangular section.....	319
Figure 279 – Trapezoidal section.	319
Figure 280 – Semi-circular section.	320
Figure 281 – Slope.	323
Figure 282 – Backwater curve in channels of weak slope (adapted from Barbosa, 1982).	324
Figure 283 – Backwater curves in channels of critical slope or inclination (adapted from Barbosa, 1982).....	325
Figure 284 – Backwater curves in channels of strong slope (adapted from Barbosa, 1982).	326
Figure 285 – Backwater curves in channels of null inclination (adapted from Barbosa, 1982).	327
Figure 286 – Backwater curves in channels of negative slope (adapted from Barbosa, 1982).	328
Figure 287 – Numerical integration of backwater curves.....	328
Figure 288 – Distance between S_{i+1} and S_i	329
Figure 289 – Examples of permanents flows rapidly varied (Vasconcelos, 2005)..	332
Figure 290 – Hydraulic rebound (adapted from Barbosa, 1982).....	332
Figure 291 – Undulated hydraulic rebound (adapted from Barbosa, 1982).	333
Figure 292 – Ordinary hydraulics rebound (adapted from Barbosa, 1982).....	333
Figure 293 – Drowned rebound (adapted from Nalluri & Featherstone, 2001).	334
Figure 294 – Forms of hydraulic rebounds (Lencastre, 1983).	335
Figure 295 – Energy losses in function of the conjugated heights of the rebound (adapted from Barbosa, 1982).....	337
Figure 296 – Rebound length (adapted from Barbosa, 1982).....	337
Figure 297 – Thresholds of Venturi (Henriques et al., 2006).	339
Figure 298 – Threshold of Parshall (Henriques et al., 2006).	340
Figure 299 – Rebound at downstream waters produced by a thick threshold or super elevation (Barbosa, 1982).....	341
Figure 300 – Rebound at upstream waters produced by a thick threshold or super elevation (Barbosa, 1982).....	342
Figure 301 – Rebound produced by an abrupt change of slope (Barbosa, 1982). .	342
Figure 302 – Rebound caused by a gate with strong slope (Barbosa, 1982).	343
Figure 303 – Rebound caused by a gate in a channel of weak slope (Barbosa, 1982).	343
Figure 304 – Drowned rebound (Barbosa, 1982).	344

Table Index

Table 1 – International system (IS).....	29
Table 2 – Weight and volumetric mass of water and air.	30
Table 3 – Density of some liquids.....	30
Table 4 – Values of viscosity (kinematic and dynamic) in function of temperature... 33	
Table 5 – Water steam saturation tension at different temperatures.	35
Table 6 – Centers of gravity and momentums of inertia for commons plain surfaces (Gaspar, 2005).	84
Table 7 – Values for C_v at different charges values and orifices diameters (adapted from Netto, 1998).....	144
Table 8 – Values of C_c for different values of charge and orifices diameters (adapted from Netto, 1998).....	144
Table 9 – Values of C_d for different values of charge and Orifice diameters (adapted from Netto, 1998).....	145
Table 10 – Values of correction, x (adapted from DRHGSA, 2007).....	147
Table 11 – Values of $C_{d,s}$ for drowned orifices (Smith, 1886).	149
Table 12 – Relation between perimeters, k for different positions of a rectangular orifice (Junior L. B., 2005).	152
Table 13 – Value of C_d according Eytelwein and for very short pipes of cast iron (Silva, 2014).	153
Table 14 – C_d for conical converged nozzle (Silva, 2014).	155
Table 15 – Values of k in function of D_e (adapted from Queiroz, 2017).	168
Table 16 – Magnitudes of base and unit of base of the international system (IS) (adapted from Ignácio & Nóbrega, 2004).	174
Table 17 – Examples of derivatives magnitudes or quantities and its units (adapted from Ignácio & Nóbrega, 2004).....	174
Table 18 – Units system MLT (adapted from Vasconcelos, 2005).	178
Table 19 – Representation of forces in the system (adapted from Vasconcelos, 2005).	179
Table 20 – Usual dimensionless parameters (adapted from NETeF, 2012).	184
Table 21 – Value of K in function of the angle β (KSB, 2003).....	198
Table 22 – Values of K and C_c in function of the sections of input and output, according to Weisbach (Pinho et al., 2011).....	199
Table 23 – Equivalent lengths of charge losses in bifurcations, expressed in meters (adapted from http://hidrossanitariasutfprcm.blogspot.pt/).....	202
Table 24 – Values of K in function of the relationship h/D and depending of the sections form (adapted from Pinho et al., 2011).	203
Table 25 – Values of K in function of θ and depending of the section's forms (adapted from Pinho et al., 2011).	203
Table 26 – Values of K in function of θ and depending of the sections form (adapted from Pinho et al., 2011).	204
Table 27 – Values of K for absolute opening (adapted from Pinho et al., 2011).....	204
Table 28 – Values of K in function of the opening angle, for $D_0 = 0,73 D$ (adapted from Pinho et al., 2011).	204
Table 29 – Values of β in function of the section profile of the bars (adapted from Pinho et al., 2011).....	205

Table 30 – Velocities and maximum flow rate recommended for asbestos cement (Pinho et al., 2011).	215
Table 31 – Resume of the calculations (adapted from Pinho et al., 2011).	231
Table 32 – Pressures in network nodes (Pinho et al., 2011).	231
Table 33 – Calculus of flow rate (adapted from Pinho et al., 2011).	237
Table 34 – Barometric height in function of the local elevation (adapted from Cruz, 2006).	259
Table 35 – Height of water evaporation in function of temperature (adapted from Cruz, 2006).	259
Table 36 – Coefficient Thoma in function of n_s (adapted from http://slideplayer.es/slide/4161770/).	261
Table 37 – Primary selection of the type of turbine, function of the fall and turbined flow rate (adapted from Cruz, 2006).	262
Table 38 – Denominations /Basic units (adapted from Pinho et al., 2011).	267
Table 39 – Values of C_B in function of the type of channel walls.	301
Table 40 – Values of C_K in function of the nature or type of walls.	301
Table 41 – Formulas of Thijsse for C , in function of the flow's regime.	302
Table 42 – Formulas of Powell for C , in function of the flow's regime.	302
Table 43 – Values of K in function of the material.	302
Table 44 – Values of K in function of the nature of the walls.	303
Table 45 – Values of $(\sin\theta - J)$	323
Table 46 – Values of $1 - Fr\cos\theta$	324
Table 47 – Discretization of backwater curves in channels of weak slope.	324
Table 48 – Discretization of the backwater curves in channels of strong slope.	326
Table 49 – Review of the proposals for the rebound length calculus.	338

List of symbols and abbreviations

Symbols

δ_{ij}	Symbol of Kronecker
∇	Gradient of deformation
a	Acceleration; Dimension; index
A	Area
b	Dimension; Index
c	Dimension; Index; Velocity of elastic waves propagation
C	Coefficient; Costs
C'	Factor of contraction
C_1	Initial costs
C_2	Annual energy costs
C_c	Contraction coefficient
C_d	Discharge or download coefficient
C_p	Specific heat
C_v	Specific heat; Coefficient of velocity
d	Dimension; Index
D	Diameter
E	Energy
Eu	Number of Euler
F	Force
f	Function
g	Gravitational acceleration
H	Charge; Energy
h	Height; Elevation; level
i	Inclination; Index; Slope
I	Moment of inertia
J	Unitary charge losses
k	Coefficient
K	Coefficient of rugosity
Kn	Number of Kundsens
L	Support; Length
l	Dimension; Index
M	Number of Mach; Total quantity of movement or total impulsion
n	Coefficient; Index; Rotation velocity
N	Number of rotations
p	Pressure
P	Perimeter; Position; Power; Pressure
Q	Flow rate; Matrix of transformation
q	Instantaneous Flow rate
r	Radius
R	Hydraulic radius or radius
S	Cross Section Area; Capacity of aspiration; Plain surface

s	Length of a Line
St	Number of Strouhal
T	Tensor of tensions; Temperature; Torque
t	Time
U	Average velocity or speed
v	Velocity
V	Velocity; Volume
We	Number of Weber
x	Coordinate
y	Height; Coordinate
Z	Topographic height
Δ	Variation
ΔH	Charge losses
Φ	Function
Ψ	Function
rot	Rotational
α	Angle; Coefficient
α'	Coefficient of Boussinesq
γ	Angle; Volumetric weight
δ	Coefficient of superficial tension
ε	Coefficient; Grade of reaction of turbines; Parameter of rugosity of Nikuradse
η	Coefficient; efficiency/yield; Specific rotation
θ	Angle
λ	Coefficient; Function; Charge loss;
μ	Coefficient of dynamic viscosity or absolute viscosity
ρ	Volumetric mass or density
σ	Superficial Tension
τ	Tension
ν	Coefficient of kinematic or relative viscosity
χ	Wet or slinked perimeter
ω	Angular velocity; Vorticity
ϵ	Tensor rate of deformation

ABBREVIATIONS

Approx..	Approximately
Cf.	According
CG	Gravity center
CGS	System Centimetre–Gram–Second
Cst.	Constant
Eq.	Equation
NA	Level of Water
NPSH	Net Positive Suction Head
RAM	<i>Região Autónoma da Madeira</i>
S.L. or F.S.	Free surface
SI	International system
T.Q.M.	Theorem of the amount of movement
Theo.	Theorem
US	United States
USBR	United States Bureau of Reclamation
VRP	Pressure reduction valve
WES	Waterways Experiment Station

CHAPTER 1 - INTRODUCTION

1.1 Small approach about hydraulic history

ANCIENTS TIMES

- **EGIPT-MESOPOTÂMIA**
 - Construction of channels for militar defense and irrigation
- **GREECE (CTESIBIOS, HERO, ARQUIMEDES [287-212 A.C.])**
 - Hydrostatic Law & Impulsion
 - Hydraulic equipment Projects (Piston pump, Water watch, Arquimedes's screw)
- **ROME [de 400 A.C. until Cristianism Begin]**
 - Massive Hydraulic Projects

RENAISSANCE

- **LEONARDO DA VINCI [1452-1519]**
 - Flows Description
- **GALILEO GALILEI [1564-1642]**
 - Experimental Mechanics Begins

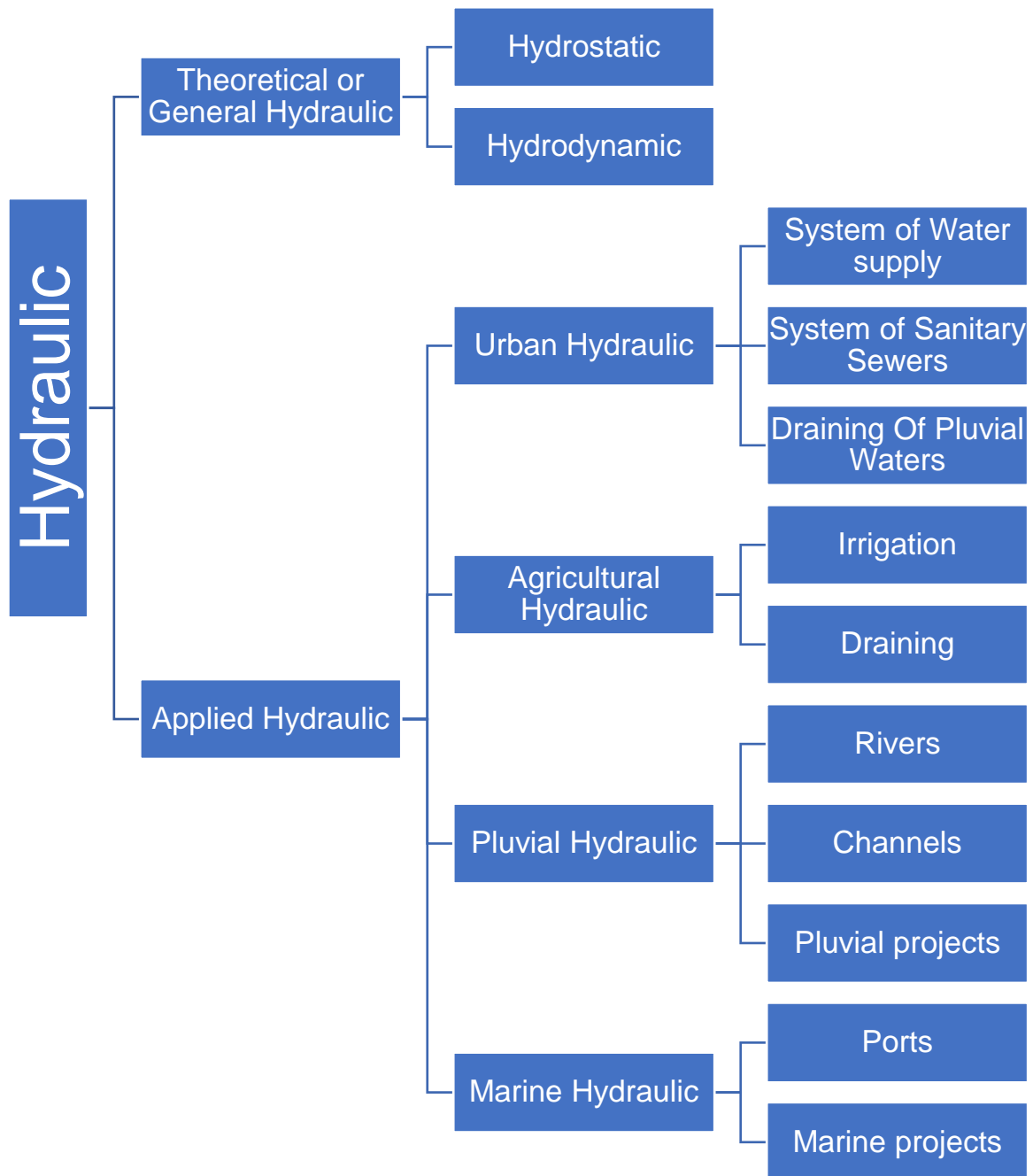
XVII & XVIII CENTURY

- **NEWTON, BERNOULLI, EULER & D'ALEMBERT**
 - Hydrodynamic (Theorical and Mathematical approach of a perfect fluid)
 - Hydraulic (Applied or Experimental approach of a real fluid)

XX CENTURY

- **PRANDTL [1875-1953]**
 - Concept of "border layer"

1.2 Hydraulics branches



1.3 Definition of fluid

A **fluid** is a substance that deforms continuously when submitted to tangential forces (it does not matter how small applied forces can be) (Pinho et al., 2011).

This definition applies for liquid and gases, which differences each other by its grade of compressibility, because liquids almost does not compress by a certain pressure while gases do it. In addition, liquids have a free defined limit surface while expand until it occupies all the circumscribed volume of its container (Pinho et al., 2011).

1.4 Unit system. International unit system

1.4.1 Systems used in hydraulics

Between the most used system, stands out:

- **CGS** - Fundamental units: cm, g, s;
- **Metric Gravitational System (M, K_p, S)** - Fundamental units: m, kgf, s;
- **International System (IS)** - Fundamental units: m, kg, s;
- **English Industrial System** - Fundamental units: foot, pound, s.

At any homogeneous dimensional equation (L, M, T) all units must be expressed in the same system (Pinho et al., 2011).

1.4.2 International System (IS)

Table 1 – International system (IS).

Quantities	Units	IS Symbols
Basic Units		
Distance	Meter	m
Mass	Kilogram	kg
Time	Second	s
Electrical Current or Stream	Ampere	A
Thermodynamic Temperature	Kelvin	K
Substance Quantity	Mol	mol
Luminous intensity	Candle	cd
Additional units		
Plain Angle	Radian	rad
Solid Angle	Steradian	sr

1.5 Physical properties of fluids

1.5.1 Weight and mass. Volumetric weight and volumetric mass

By defining:

- **Mass** - Quantity of mater of the body [kg];
- **Volumetric Mass** - Mass per unit of volume: ρ [kg/m³];
- **Weight** - Attractive forces applied by Earth mass over the body [m/s²];
- **Volumetric Weight** - Weight per unit of volume: $\gamma = \rho \times g$ [N/m³].

Table 2 shows weights and volumetric mass of water and air in function of temperature.

Table 2 – Weight and volumetric mass of water and air.

Temperature	Volumetric Weights				Volumetric Mass			
	Water		Air		Water		Air	
°C	$\frac{N}{m^3}$	$\frac{kgf}{m^3}$	$\frac{N}{m^3}$	$\frac{kgf}{m^3}$	$\frac{kg}{m^3}$	* $\frac{UMM}{m^3}$	$\frac{kg}{m^3}$	* $\frac{UMM}{m^3}$
0	9809	999.9	12.68	1.293	999.9	101.93	1.293	0.132
4	9810	1000.0	12.50	1.274	1000.0	101.94	1.274	0.130
20	9792	998.2	11.81	1.204	998.2	101.75	1.204	0.123
40	9733	992.2	11.08	1.129	992.2	101.14	1.129	0.115
60	9645	983.2	10.42	1.062	983.2	100.22	1.062	0.108
80	9533	971.8	9.90	1.009	971.8	99.06	1.009	0.103
100	9402	958.4	9.28	0.946	958.4	97.70	0.946	0.096

*the metric unit of mass (UMM) is the mass in which a force of 1 **kgf** (kilogram-force) creates an acceleration of 1 **m/s²**. Such unit is used to measure mass when forces are measured in kilograms-force.

1.5.2 Density

Density is the quotient between mass of a certain volume of a substance and the mass of same volume of water at a temperature of 4 °C. Table 3 shows density of some liquids (Pinho et al., 2011).

Table 3 – Density of some liquids.

Liquid	Density
Ethyl Alcohol (100%)	0.79
Terebinthinate	0.86
Oil	0.912-0.918
Lubricating oils	0.880-0.935
Fuel oil	0.820-0.950
Glycerine (100%)	1.26
Carbon Tetrachloride	1.594
Mercury (Hg)	13.6

1.5.3 Isotropy

Isotropy is a property of continuous bodies, in which all points and all directions have the same molecular structure. (Homogeneous material and same behaviour independent of the coordinate system of references applied) (Pinho et al., 2011).

1.5.4 Continuity

In fluid mechanics is consider its averages values at any point inside its domain, by considering it as a continuous medium. (Pinho et al., 2011).

1.5.5 Compressibility

Compressibility is a decrease of fluid volume corresponding to an increase in pressure or external stress. (Pinho et al., 2011).

The difference between **liquid** and **gas** is the different behaviour of each one, when submitted at an increase of pressure:

- Liquid: small compressibility
- Gases: great compressibility

Coefficient of compressibility, α

$$\alpha = \frac{dV}{V dp} \text{ ou } \alpha = -\frac{1}{V} \frac{dV}{dp}$$

Where:

dV/V is the relative variation of volume, V ;

dp is the differential increase of pressure, p ;

$\alpha(\text{H}_2\text{O}) = 5.1 \times 10^{-10} [\text{m}^2/\text{N}]$.

Coefficient or modulus of volume elasticity, ε

$$\varepsilon = \frac{1}{\alpha} [\text{N}/\text{m}^2]$$

Coefficient of Kinematic Elasticity, η

$$\eta = \frac{\varepsilon}{\rho} \Rightarrow \varepsilon = K\rho$$

It's provable that the coefficient of elasticity is proportional to pressure, where K it's the coefficient of proportionality for an isothermal (constant temperature) and adiabatic process (No thermic border exchange).

1.5.6 Viscosity

Viscosity is related to deformation resistance of a fluid in movement. It does not occur in rest. (Pinho et al., 2011).

Viscosity interactions represent a type of internal friction, occurring between contiguous particles, which move at different speeds (Figure 1).

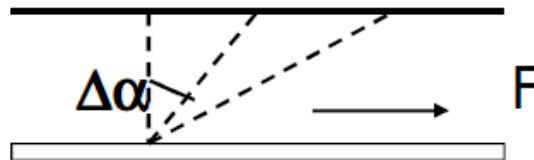
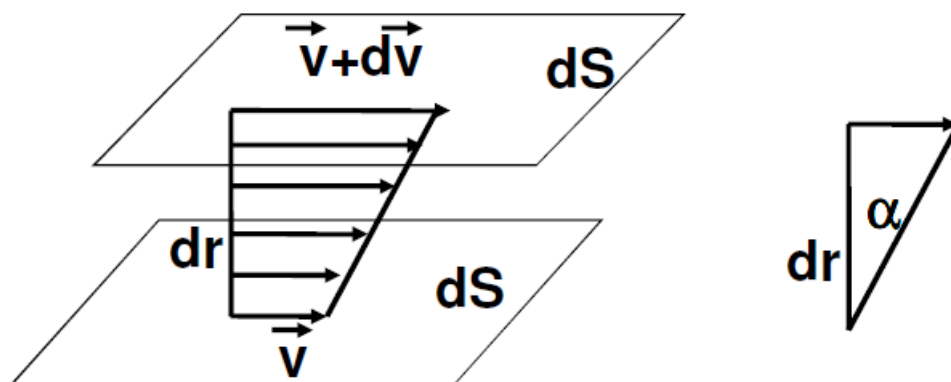


Figure 1 – Viscosity.

Newtonian fluid and newtonian viscosity

Fluid in which exist a linear relation between applied tangential tension and angular deformation speed (variation of $\Delta\alpha$ in time), as show in Figure 2.



$$dF = \mu dS \frac{dv}{dr} \Rightarrow \tau = \mu \frac{dv}{dr}; \alpha = \tan \alpha = \frac{dv}{dr}$$

Figure 2 – Relation between deformation and tension or stress.

Coefficient of absolute or dynamic viscosity $[ML^{-1}T^{-1}]$ $[N.s/m^2]$:

$$\mu = \tau \times \frac{dr}{dv}$$

The physic unit of viscosity on the International Unit System is pascal-second [Pa.s], which is equivalent to 1 N.s/m² or 1 kg/(m.s).

In the Unit System CGS, **dynamic viscosity** is poise [P], in honour of Jean Louis Marie Poiseuille. But it is more used its multiple: o centipoise [cP]. The centipoise is more used, because water have a viscosity of 1,0020 cP at 20°C and 0,891 cP at 25°C:

- 1 poise = 100 centipoise = 1 g/(cm.s) = 0,1 Pa.s;
- 1 centipoise = 1 mPa.s.

Coefficient of relative or kinematic viscosity [L²T⁻¹] [m²/s]:

Quotient between dynamic viscosity and density. Its unit on IS [m²/s]. The physical unit of **kinematic viscosity** in CGS System stokes (S or St), in honour of George Gabriel Stokes. Sometimes it is used as centistokes (cS ou cSt).

$$\nu = \frac{\mu}{\rho}$$

Table 4 shows the values of kinematic and dynamic viscosity, depending on temperature.

Table 4 – Values of viscosity (kinematic and dynamic) in function of temperature.

Temperature °C	Kinematic viscosity		Dynamic viscosity		
	m ² /s	centistokes	N.s/m ²	kgf.s/m ²	centipoises
0	1.78x10 ⁻⁶	1.78	1.78x10 ⁻³	181x10 ⁻⁶	1.78
4	1.56x10 ⁻⁶	1.56	1.56x10 ⁻³	159x10 ⁻⁶	1.56
10	1.31x10 ⁻⁶	1.31	1.31x10 ⁻³	134x10 ⁻⁶	1.31
20	1.01x10 ⁻⁶	1.01	1.01x10 ⁻³	103x10 ⁻⁶	1.01
30	0.81x10 ⁻⁶	0.81	0.81x10 ⁻³	82x10 ⁻⁶	0.81
40	0.66x10 ⁻⁶	0.66	0.66x10 ⁻³	67x10 ⁻⁶	0.66
50	0.56x10 ⁻⁶	0.56	0.55x10 ⁻³	56x10 ⁻⁶	0.55
60	0.47x10 ⁻⁶	0.47	0.47x10 ⁻³	48x10 ⁻⁶	0.47
80	0.36x10 ⁻⁶	0.36	0.35x10 ⁻³	36x10 ⁻⁶	0.35
100	0.28x10 ⁻⁶	0.28	0.27x10 ⁻³	28x10 ⁻⁶	0.27

Non-newtonian fluid

Fluid in which addressed relation are not linear.

1.5.7 Cohesion

Medium property due to attractive actions between liquids (giving resistance to tractional forces, even for small forces) (Pinho et al., 2011).

1.5.8 Superficial tension and capillarity

Coefficient of superficial tension, δ

Represent the superficial energy per unit area [MT^{-2}] [N/m].

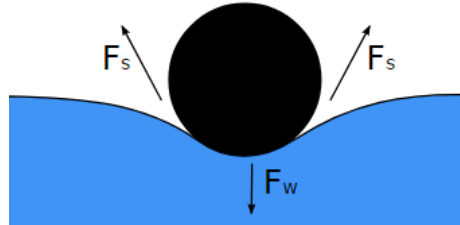


Figure 3 – Superficial tension (White, 1948).

Figure 3 shows the transversal section of a needle, that is over the superficial tension of water. Its weight (F_w) creates a force against water surface, and it is equilibrated by superficial tension forces at both sides (F_s) (Pinho et al., 2011).

Adherence

Manifest of superficial tension in presence of solid walls. The combination of adherence forces and cohesion forces explains the phenomenon of capillarity (Pinho et al., 2011).

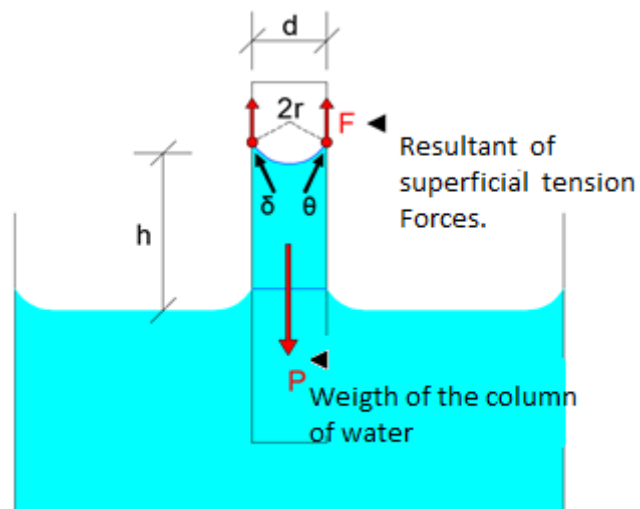


Figure 4 – Adherence

Explaining Figure 4:

- Liquids that wet the pipe walls: **ascension**;
- Liquids that not we the pipe walls: **depression**;
- Tangential tension force over internal surface of the: $2\pi r\delta$;
- Component from internal wall of the pipe: $F=2\pi r\delta \cos \theta$;

- Weight of the column of liquid on height h : $P = \pi r^2 \delta h \gamma$;
- Height h : $h = (2\sigma / \gamma \cdot r) \cdot \cos \theta$.

1.5.9 Liquid steam tension

Liquid steam tension (p_v) is the pressure applied over a certain volume (Pinho et al., 2011).

Steam saturation tension is the steam saturation tension over a certain volume (Ex.: Table 5) (Pinho et al., 2011).

Table 5 – Water steam saturation tension at different temperatures.

T [°C]	4	10	20	30	50	80	100
p_v [kPa]	0.814	1.226	2.333	4.247	12.36	47.38	101.3

1.5.10 Gas solubility in water

Coefficient of gas solubility is the quotient between volume of dissolved gas and the volume of dissolvent liquid, in condition of saturation. For a certain temperature, it is determined the amount of gas that can be dissolved until saturation on a certain liquid (Pinho et al., 2011).

1.5.11 Elastic waves propagation speed

Elastic waves propagation speed is the speed of propagation of pressure variation in a liquid. Most of the times is assumed as speed of propagation of sound in a fluid, because is coincident (Pinho et al., 2011).

$$c = \sqrt{\frac{\epsilon}{\rho}} \text{ [m/s]}; \quad c_{\text{ar}} = 340 \text{ m/s}; \quad c_{\text{água a } 10^\circ\text{C}} = 1425 \text{ m/s}$$

1.6 Equations of fluid mechanics

Considering a fluid as a continuous medium, the resolution of any **problem of fluid dynamics** is approached by knowing any point of the domain at any time of **23** parameters (Pinho et al., 2011):

- **9** elements of tensor of tension (Figure 5);

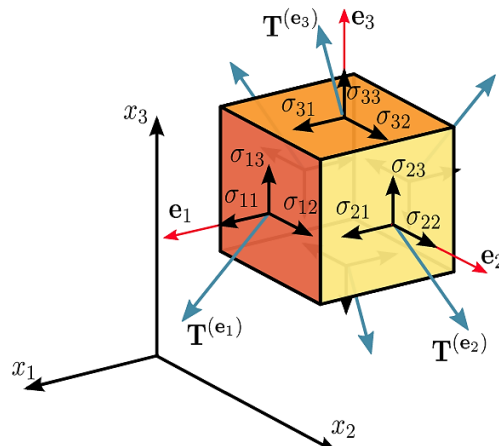


Figure 5 – Tensor of tension (<https://commons.wikimedia.org>).

- **9** elements of the deformation speed tensor (Figure 6);

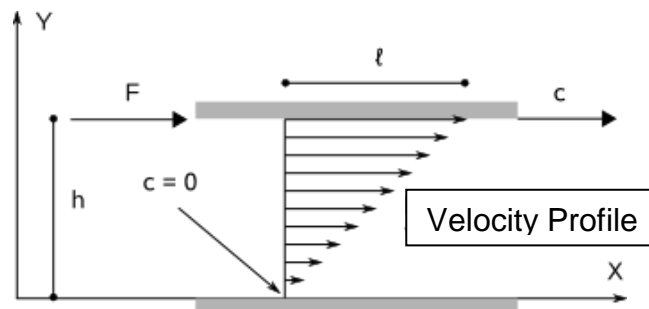


Figure 6 – Diagram of action of a force over a layer of fluid (<http://www.mspc.eng.br>).

- **3** components of speed (Figure 7);

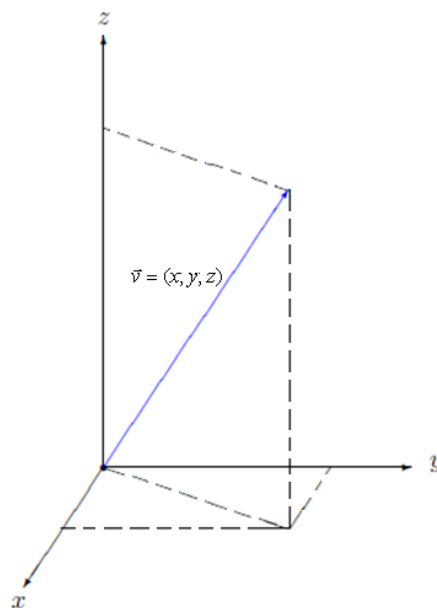


Figure 7 – Vector Speed (Junior & Colvara, 2010).

- **Volumetric mass** (Figure 8);



Figure 8 – Mixture of oil, water and sand (<http://mundoeducacao.bol.uol.com.br/>).

- **Temperature** (Figure 9).



Figure 9 – Immersion thermometer (<https://www.3bscientific.es>).

However, to determine 23 parameters, it's enough to know 6, which are (Pinho et al., 2011):

- Pressure at any point and at any time: $p = p(P, t)$;
- Volumetric mass at any point and at any time: $\rho = \rho(P, t)$;
- Temperature at any point and at any time: $T = T(P, t)$;
- The three components of the speed vector: in **Lagrange** or **Euler** variables, or Kraichnan variables.

1.6.1 Lagrange variables

Particles – Elements of Fluid Volume

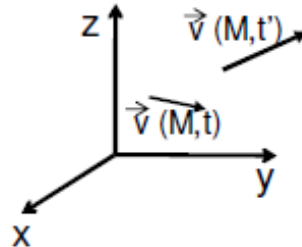


Figure 10 – Lagrange variables (Pinho et al., 2011).

The application point of velocity $\vec{v}(M, t)$ vary from t to t' . velocity is the derivate of the position vector of the particle:

$$\vec{v} = \frac{d\vec{r}(M, t)}{dt}$$

So, it is possible, to adopt the components of the position vector instead of the velocity vector.

If x, y, z were function of x_0, y_0, z_0 and t , the movement of the fluid is determined:

$$\begin{cases} x = x(x_0, y_0, z_0, t) \\ y = y(x_0, y_0, z_0, t) \\ z = z(x_0, y_0, z_0, t) \end{cases}$$

In practice is quite difficult to define the particle trajectory because its individuality is not preserving due to molecular diffusion. (Pinho et al., 2011).

1.6.2 Euler Variables

At each point of fluid domain, the velocity is referred to each instant t .

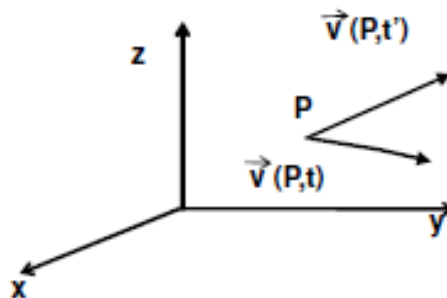


Figure 11 – Euler variables (Pinho et al., 2011).

At point $P(x, y, z)$:

- At instant t pass a particle with velocity $\vec{v}(x, y, z, t)$;
- At instant t' pass another particle with velocity $\vec{v}(x, y, z, t')$.

Velocity is not the derivate of the position vector (P) in order of time. In this form, it is pursued to determine the velocity of the particles that pass through certain points of the fluid domain. Euler variables consist in the projections u, v, w over the velocity coordinate axis (v) of the particle that pass at point $P(x, y, z)$ at instant t :

$$\begin{cases} u = u(x_0, y_0, z_0, t) \\ v = v(x_0, y_0, z_0, t) \\ w = w(x_0, y_0, z_0, t) \end{cases}$$

Its defined **viatorial field** (velocities field) and three **scalar fields** (pressure, volumetric mass, temperature).

Euler representation is simpler and more suitable for the practical objectives of fluid mechanics (Pinho et al., 2011).

1.6.3 Kraichnan variables

$\vec{v}(P, t_1/t_2)$: velocity at instant t_2 of a particle which match with the P at instants t_1 (applies to the mathematical study of turbulence, cf. Figure 12) (Pinho et al., 2011).

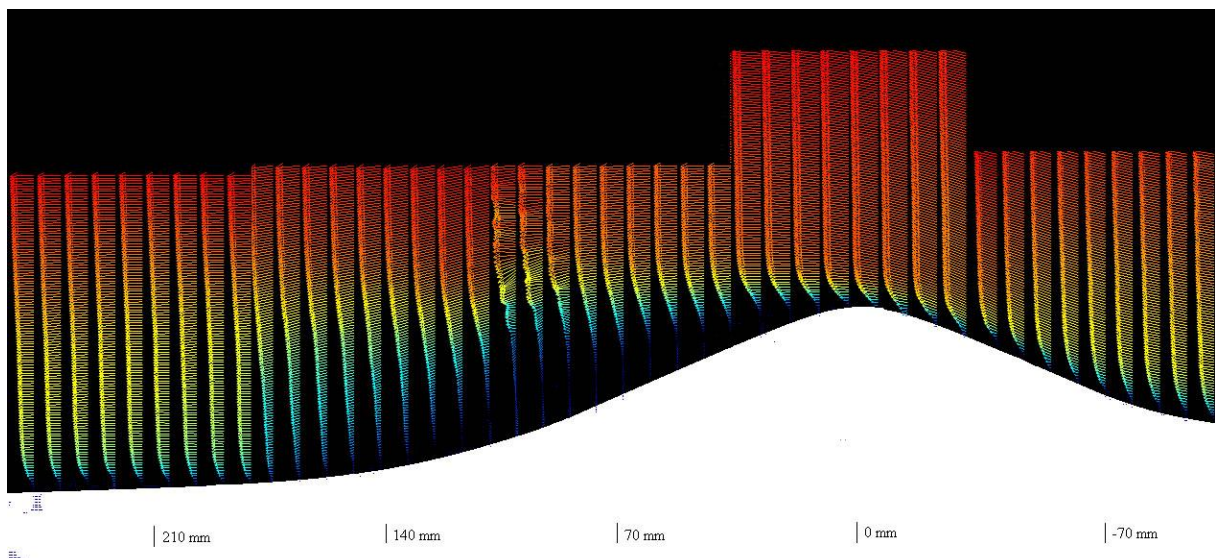


Figure 12 – Study of flow's turbulence (www.turbulencia.coppe.ufrj.br/).

1.6.4 Types of equations of Fluid Mechanic and Hydraulic

Notion of control volume

Well-defined region, where is made the analysis of physical quantities variation, limited by a closed surface, **control surface (S)**, which is the border of the region (Figure 13) (Pinho et al., 2011).

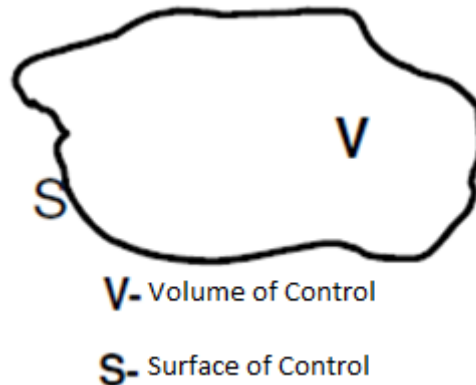


Figure 13 – Volume of control and Control surface (Pinho et al., 2011).

A – Local equations and global equations

Local equations – Apply to every point of fluid domain or each particle, defining local conditions of flow (Pinho et al., 2011).

Global equations – Apply to individualized regions of fluid domain or until totality of flow at certain sections (Pinho et al., 2011).

B – Equation of conservation and balance

Equation of conservation – quantities keep its global value invariable inside the regions. Ex.: Mass, Energy and Quantity of Movement, are quantities that have conservation properties in relation of specific closed systems (Pinho et al., 2011).

Equations of balance - regions work as open systems, with incomes and outcomes through its borders. It can be written mathematical equations like (Pinho et al., 2011):

$$\Phi_S - \Phi_E = \Delta G_I$$

Where:

Φ_S outcoming quantity;

Φ_E incoming quantity;

ΔG_I decrease in the global value of the quantity inside the control surface.

In order to solve any **problems of fluid dynamics**, it is necessary to know the local values of 6 variables (volumetric mass, pressure, temperature, components of velocity vector). Then is necessary 6 equations (Pinho et al., 2011):

- **Equation of continuity**: represent the principle of mass (**property of continuity**);
- **Equation of dynamic equilibrium**: vector eq. corresponding to 3 equations of projections depending on the coordinate's axis. Stating Relations between the state of tension and velocity of deformation, and by assuming the behaviour of a Newtonian Viscous Fluid, these are the **Navier-Stokes equations**;
- **State of fluid equation**: relate pressure, mass, volumetric mass and temperature;
- **Principle of energy conservation**: **thermodynamic complementary equation**, that in normal cases is assumed as a balance equation.

CHAPTER 2 - FUNDAMENTAL EQUATIONS OF FLUID MOVEMENT

2.1 Parameters of hydrokinetic character

2.1.1 Trajectory. Stream lines. Filaments lines. Fluid lines

Trajectory

Trajectory is the geometrical place of the different positions of a fluid particle in time (related with fluid particles and an interval of time, cf. Figure 14) (Pinho et al., 2011).

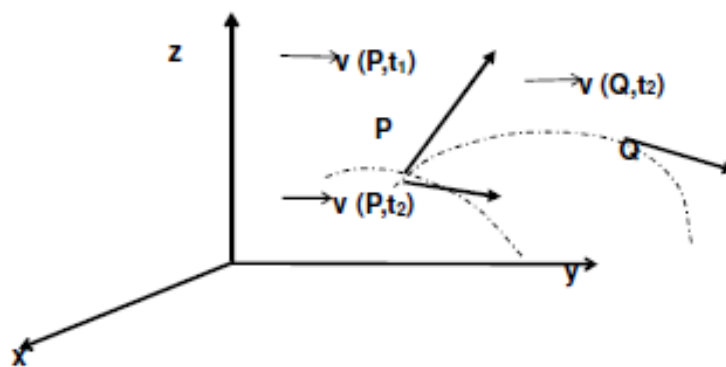


Figure 14 – Trajectory (Pinho et al., 2011).

Stream lines

Stream lines are tangential curves to the velocity vector in every point. Streams lines are defined at every instant. (Figure 15) (Pinho et al., 2011).

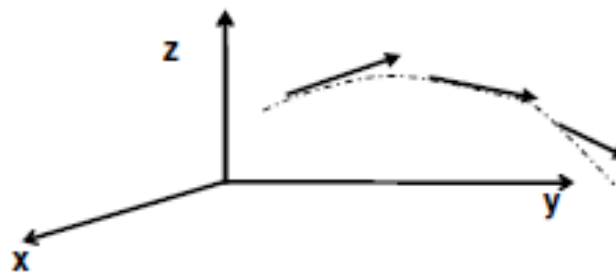


Figure 15 – Stream Lines (Pinho et al., 2011).

Filaments lines

Filaments lines are the geometrical descriptions of the particles that pass through a point at a certain instant. **In every instant** the stream lines are tangential to the trajectory of the particles in points, where the particles are at that instant. **In permanent movement** trajectories, streams lines and filaments lines are coincident (gives same geometrical description) (Pinho et al., 2011).

Stream pipe

Stream pipe is the geometrical description conformed by the stream lines that coincided with a closed contour (C) (the contour is not formed by the stream lines, but stream lines adopt the contour form) (Figure 16) (Pinho et al., 2011).

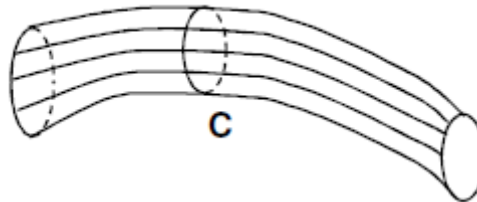


Figure 16 – Stream pipe (Pinho et al., 2011).

Fillet

Fillet is a stream pipe with infinitesimal transversal section area (Pinho et al., 2011).

Fluid Lines

Fluid lines are lines that in time, **are always** constituted by the same fluid particles (Figure 17) (Pinho et al., 2011).

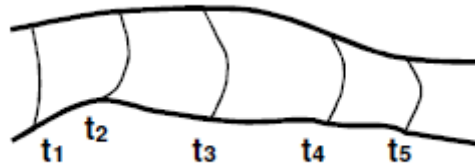


Figure 17 – Fluid Lines (Pinho et al., 2011).

Fluid surface

Fluid surface is a surface that in time, **is always constituted** by the same particles of the fluid (Pinho et al., 2011).

2.1.2 Lagrange's and Euler's Variables.

Consider any quantity (G) scalar or vectoral, that can be studied in function of time (Pacífico, 2016).

Lagrange's Method (Joseph L. Lagrange, 1736 until 1813): consist in follow and study the particle along his trajectory, form an initial position A, so that at every second, is

possible to determine the value of that quantity $G = G_L(x_A, y_A, z_A, t)$. Be aware, that the point (x_A, y_A, z_A) is defined as the initial point – “its name” – of each particle. This method applied to Fluid mechanics involves to follows and study many particles, which turn to be a quite hard an endless work. However, exist some situation where Lagrange method is still useful, for exp: description of Buoy's movement, Birds migration, Satellite tracking of vehicles(Pacífico, 2016).

Euler's Method (Leonhard Euler, 1707 to 1783): consist in study a fixed geometrical point $P(x_P, y_P, z_P)$ to determine the physical quantity associated to the particles, that pass through P. Then, $G = G_F(x_P, y_P, z_P, t)$. At this case, the pursued quantities are function of space and time. The physical studied region of flows, studied with this method, are called **flow field** (Pacífico, 2016).

Generally, Euler method is the most used (Pacífico, 2016):

- Majority of cases, particles does not conserve its physical individuality (due to diffusion or turbulence), so the descriptions is affected (then, is used Lagrange Method);
- Physical laws obtained by Euler's method are easier to apply in real situations;
- The dimensions of the particles of a flow, turn to impossible to use instruments, that can be apply along its trajectory.

Lagrange's Variables

The representation of the velocity vector in term of LaGrange's variables, means the study of the behaviour of each particle along time. It is recording the data of each particle (Vasconcelos, 2005).

Notation used is $\vec{v} = \vec{v}(M, t)$, that means, **velocity at instant t**. It is important to know the velocity of each particle at different instant Figure 18 (Vasconcelos, 2005).

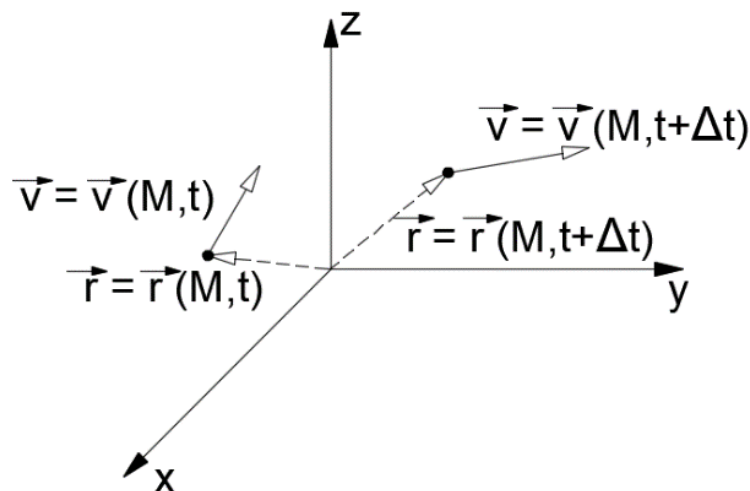


Figure 18 – Representation of velocity in terms of Lagrange's variables (Vasconcelos, 2005).

Velocity is a variation of **position Vector \vec{r}** , of **particle M**, in time (Vasconcelos, 2005):

$$\vec{v}(M, t) = \frac{d\vec{r}(M, t)}{dt}$$

In Fluids Mechanics this representation turns to be difficult, because is not possible to follow every single particle at every single instant into sine of the fluids volume. (Vasconcelos, 2005).

Euler's Variables

At this case are studied the characteristic of the particles that pass in a certain position in the fluid's domain at a certain time. At every instant, is determined the velocity of particles that at such instant are in some positions of the fluid's domain. (Vasconcelos, 2005).

In each position of fluids domain, correspond to a velocity vector and a value of pressure (relate to the particle in that position), constituting a vector field and a scalar field. (Vasconcelos, 2005).

The notation $\vec{v} = \vec{v}(P, t)$ means that the **velocity of the particle in position P at instant t**, Figure 19 (Vasconcelos, 2005).

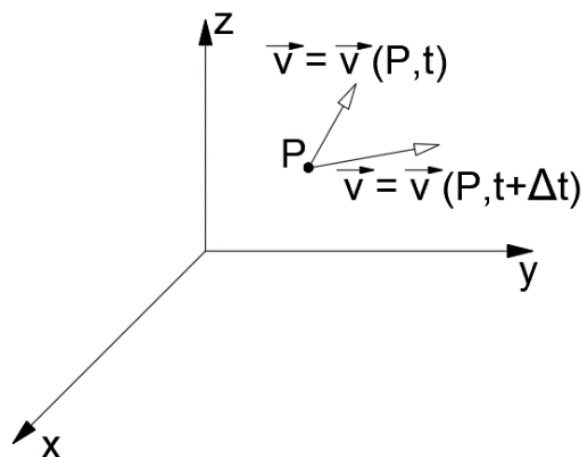


Figure 19 – Representation of Velocity in terms of Euler's Variables (Vasconcelos, 2005).

In Hydraulics Engineering will be applied this representation. (Vasconcelos, 2005).

2.1.3 Flow rate. Flows medium velocity

Flow rate (Q) is the fluids volume that goes through a certain surface per unit of time. (Figure 20) (Pinho et al., 2011).

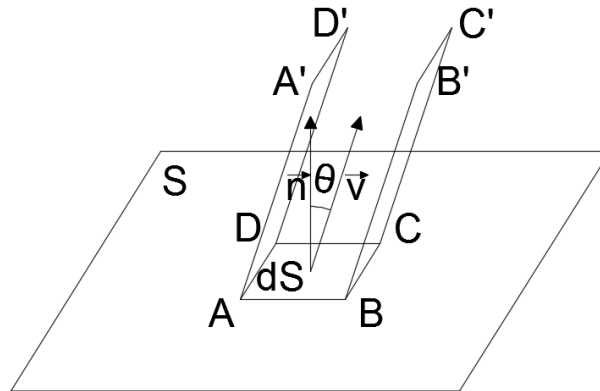


Figure 20 – Illustration where flow rate, is the volume crossing the surface S with velocity V (adapted from Pinho et al., 2011).

$$\begin{aligned} v &= \text{cst. in } dt \\ \overline{AA'} &= \overline{BB'} = \overline{CC'} = \overline{DD'} = v \, dt \\ dV &= v \, dt \cos \theta \, dS \\ dQ &= v \cos \theta \, dS \\ dQ &= \vec{v} \cdot \vec{n} \, dS \\ Q &= \int_S \vec{v} \cdot \vec{n} \, dS \end{aligned}$$

In the same way, **flow rate** can be defined as the flows of velocity vector through the area (S) (Pinho et al., 2011).

Flows medium velocity (medium speed) (U) is the value of the normal component of velocity if were constant at every point of the surface. It is normally defined for the normal transversal section of a stream pipe, in which walls coincide with flows borders. (Pinho et al., 2011).

$$v_n = \vec{v} \cdot \vec{n} \Rightarrow U = \frac{Q}{S} = \frac{\int_S v_n \, dS}{S}$$

2.1.4 Acceleration

Acceleration measure the velocity variation in time and space. In Euler's representation, is related to each position contained in volume of control, that means, related to the fluid's particles, that are located inside the volume of control. (Vasconcelos, 2005).

By Euler's method, acceleration is represented by the gradient of velocity of particles located at different positions in the volume of control, at a certain instant, and by the gradient of velocity over time, Figure 21 (Vasconcelos, 2005).

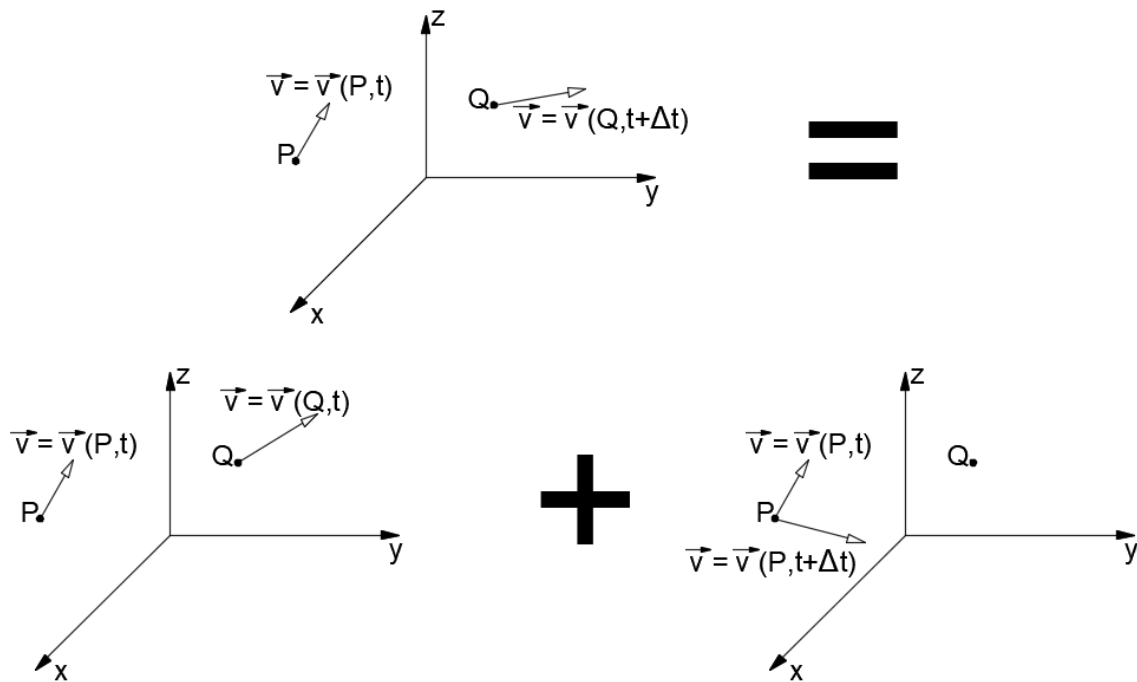


Figure 21 – Representation of acceleration using Euler's Representation (Vasconcelos, 2005).

In a general case, velocity vector depends on the independent's variables, time and position in the fluid's media. (Vasconcelos, 2005).

$$\begin{cases} \vec{v} = \vec{v}(t, x, y, z) \\ v_x = v_x(t, x, y, z) \\ v_y = v_y(t, x, y, z) \\ v_z = v_z(t, x, y, z) \end{cases}$$

Based on the variable's definition, acceleration is determined by:

$$\vec{a} = \frac{d\vec{v}}{dt} = \lim_{\Delta t \rightarrow 0} \frac{\vec{v}(Q, t + \Delta t) - \vec{v}(P, t)}{\Delta t}$$

If we add and rest in the numerator of the mentioned equation, the value of velocity in position **P** and instant **t + Δt**, then:

$$\begin{aligned} \vec{a} &= \lim_{\Delta t \rightarrow 0} \frac{[\vec{v}(Q, t + \Delta t) - \vec{v}(P, t + \Delta t)] + [\vec{v}(P, t + \Delta t) - \vec{v}(P, t)]}{\Delta t} \Rightarrow \\ \Rightarrow \vec{a} &= \lim_{\Delta t \rightarrow 0} \frac{[\vec{v}(Q, t + \Delta t) - \vec{v}(P, t + \Delta t)]}{\Delta t} + \lim_{\Delta t \rightarrow 0} \frac{[\vec{v}(P, t + \Delta t) - \vec{v}(P, t)]}{\Delta t} \end{aligned}$$

The first part of the right member of the equations, represents the variation of velocity in space, while the second part, represents the variation of velocity in time, for a certain position. (Vasconcelos, 2005).

The variation in space can be decomposed in each direction of the orthogonal coordinate system (Vasconcelos, 2005).

$$\vec{a} = \lim_{\substack{\Delta t \rightarrow 0 \\ \Delta x \rightarrow 0}} \frac{[\vec{v}(Q, t + \Delta t) - \vec{v}(P, t + \Delta t)] \Delta x}{\Delta x \Delta t} + \lim_{\substack{\Delta t \rightarrow 0 \\ \Delta y \rightarrow 0}} \frac{[\vec{v}(Q, t + \Delta t) - \vec{v}(P, t + \Delta t)] \Delta y}{\Delta y \Delta t} + \\ + \lim_{\substack{\Delta t \rightarrow 0 \\ \Delta z \rightarrow 0}} \frac{[\vec{v}(Q, t + \Delta t) - \vec{v}(P, t + \Delta t)] \Delta z}{\Delta z \Delta t} + \lim_{\Delta t \rightarrow 0} \frac{[\vec{v}(P, t + \Delta t) - \vec{v}(P, t)]}{\Delta t}$$

The limits of the equation correspond to partial derivatives of the velocity vector respect to the independent's variables, time and position in fluids medium (Vasconcelos, 2005).

$$\vec{a} = \frac{\partial \vec{v}}{\partial x} \frac{dx}{dt} + \frac{\partial \vec{v}}{\partial y} \frac{dy}{dt} + \frac{\partial \vec{v}}{\partial z} \frac{dz}{dt} + \frac{\partial \vec{v}}{\partial t}$$

The variation of the components in a system of cartesian axis, the independent variable known as position in the fluid, with the independent variable known as time, equals the respective component of velocity and the acceleration vector equation is (Vasconcelos, 2005):

$$\vec{a} = \frac{\partial \vec{v}}{\partial x} v_x + \frac{\partial \vec{v}}{\partial y} v_y + \frac{\partial \vec{v}}{\partial z} v_z + \frac{\partial \vec{v}}{\partial t}$$

The components of the upper equation, respect of each cartesian axis are:

$$\begin{cases} a_x = \frac{\partial v_x}{\partial x} v_x + \frac{\partial v_x}{\partial y} v_y + \frac{\partial v_x}{\partial z} v_z + \frac{\partial v_x}{\partial t} \\ a_y = \frac{\partial v_y}{\partial x} v_x + \frac{\partial v_y}{\partial y} v_y + \frac{\partial v_y}{\partial z} v_z + \frac{\partial v_y}{\partial t} \\ a_z = \frac{\partial v_z}{\partial x} v_x + \frac{\partial v_z}{\partial y} v_y + \frac{\partial v_z}{\partial z} v_z + \frac{\partial v_z}{\partial t} \end{cases}$$

By introducing the definition of **grad** into the equation that represents acceleration, it becomes:

$$\vec{a} = \frac{\partial \vec{v}}{\partial t} + (\vec{v} \cdot \overrightarrow{\text{grad}}) \vec{v}$$

The first part of the second member of the upper equation correspond to a variation of velocity in time, that is called local acceleration; while the second term correspond to a variation of velocity in space, that is called convective acceleration. (Vasconcelos, 2005).

2.1.5 Vorticity

Rotational (Vortex vector)

The **rotational** of a vector is a vector defined in the cartesian coordinates by (Gobbi *et al.*, 2011):

$$\text{rot } \mathbf{v} = \nabla \times \mathbf{v} = \begin{vmatrix} \mathbf{e}_x & \mathbf{e}_y & \mathbf{e}_z \\ \frac{\partial}{\partial x} & \frac{\partial}{\partial y} & \frac{\partial}{\partial z} \\ v_x & v_y & v_z \end{vmatrix}$$

Where is used the notation of a vector product. Vertical bars represent the determinant in which, first line is filled with Normal Unit Vectors of the cartesian system, second line hold the components of ∇ , and the third line contains a vector field \mathbf{v} . In case the vector field is a velocity field in a continuous media, the rotational of it at each point is equal to two times the local vector of angular velocity, which is the reason to be called rotational. In fluids mechanics, the **rotational of a velocity field** is called **vorticity or vortex**: $\boldsymbol{\omega} = \nabla \times \mathbf{v}$ (Gobbi *et al.*, 2011).

Rotation of a fluid: vorticity

Consider Figure 22, in which we assume that the angles α and β have the same rotational direction (in Figure 22 angles are in opposite directions) (Gobbi *et al.*, 2011).

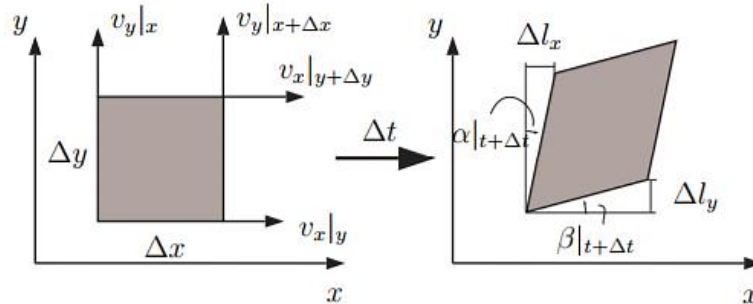


Figure 22 – Shear deformation in (x, y) plane of a portion of fluid in flow (Gobbi *et al.*, 2011).

It is clear, that at this case, is more like a rotation than a deformation. So, is defined the rate of rotation analogous to a rate of shear deformation. Then, one of the angles have an opposite signal. (Gobbi *et al.*, 2011):

$$\frac{1}{2} \left(\frac{d\beta}{dt} - \frac{d\alpha}{dt} \right) = \frac{1}{2} \lim_{\Delta t \rightarrow 0} \left(\frac{\beta|_{t+\Delta t} - \beta|_t}{\Delta t} - \frac{\alpha|_{t+\Delta t} - \alpha|_t}{\Delta t} \right)$$

Similar to a deformation case, is concluded:

$$\frac{1}{2} \frac{d(\beta - \alpha)}{dt} = \frac{1}{2} \left(\frac{\partial v_y}{\partial x} - \frac{\partial v_x}{\partial y} \right)$$

Which essentially leads to the local angular velocity of a fluid's particle around Z axis., It is possible to define velocity as the component z of an angular velocity vector. By applying the same analogy to rotation in planes (x,z) and (y,z), an angular velocity vector is obtained. (Gobbi *et al.*, 2011):

$$\frac{1}{2} \left(\frac{\partial v_z}{\partial y} - \frac{\partial v_y}{\partial z}, \frac{\partial v_x}{\partial z} - \frac{\partial v_z}{\partial x}, \frac{\partial v_y}{\partial x} - \frac{\partial v_x}{\partial y} \right)$$

The expression between parentheses in last equation, is called **vorticity**, a vector that is two times the angular velocity of a fluid in a certain point, therefore, measure the rate of rotation in the point. Clearly, is obvious that vorticity (ω) is equal to a rotational of a velocity field (Gobbi *et al.*, 2011):

$$\omega = (\omega_x, \omega_y, \omega_z) = \left(\frac{\partial v_z}{\partial y} - \frac{\partial v_y}{\partial z}, \frac{\partial v_x}{\partial z} - \frac{\partial v_z}{\partial x}, \frac{\partial v_y}{\partial x} - \frac{\partial v_x}{\partial y} \right) = \nabla \times \mathbf{v}$$

Lines and vortex tube

Let's (\mathbf{v}) be a vectoral velocity field, in order to calculate its vorticity field (ω) by applying a rotational operator to \mathbf{v} . By doing this, the stream lines are defined as lines to which velocity vectors are tangent to, so analogously, it is defined lines, to which vorticity vectors are tangent to. The last definition is also called, **vorticity Lines**. Those lines are represented by the following equations:

$$\frac{dx}{\omega_x} = \frac{dy}{\omega_y} = \frac{dz}{\omega_z}$$

Analogously to a stream pipe or stream tube, a Vorticity tube is a surface generated by adjacent vorticity lines. A practical example similar to a vorticity tube (or vortex tube) is the funnel or vortex formed by a tornado or a hurricane (Gobbi *et al.*, 2011).

If a region that belong to a flows domain has no vorticity, (vorticity operator gives a null vector), $\omega = \nabla \times \mathbf{v} = \mathbf{0}$, such Flow is called **irrotational or potential flow**, in that region (Gobbi *et al.*, 2011).

2.2 Types of movements

2.2.1 Permanents and non-permanents movements

Non-permanent movement occur while at least one variable is dependent of time (Figure 23) (Pinho *et al.*, 2011).

$$\frac{\partial}{\partial t} \neq 0$$

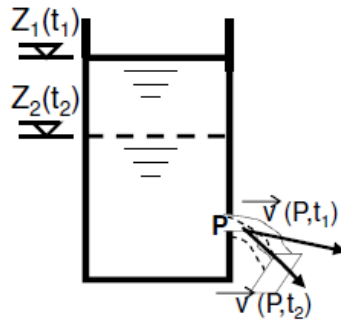


Figure 23 – Non-permanent movement (Pinho et al., 2011).

Permanent movement occurs when all variables involved are independent of time (Pinho et al., 2011).

$$\frac{\partial}{\partial t} = 0$$

Varied permanent movement occurs when velocity varies across all trajectory (Figure 24) (Pinho et al., 2011).

$$\frac{\partial}{\partial t} = 0, \frac{d\vec{v}}{ds} \neq 0$$

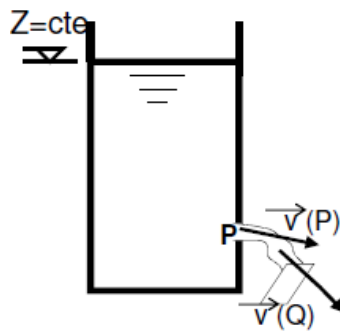


Figure 24 – Varied permanent movement (Pinho et al., 2011).

Uniform Permanent Movement occurs when velocity is constant across all trajectory (Figure 25) (Pinho et al., 2011).

$$\frac{\partial}{\partial t} = 0, \frac{d\vec{v}}{ds} = 0$$

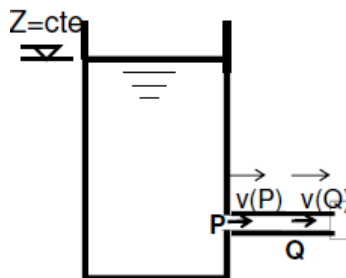


Figure 25 – Uniform permanent movement (Pinho et al., 2011).

2.2.2 Rotational and irrotational Movements/Flows

This classification is stated depending on the existence of **rotation** or not of particles in movement, where ω is vorticity or vortex vector (Pinho et al., 2011).

Rotational Movement/Flow

Flow or movement where particles are under an angular velocity, in relation to its mass or gravity center. A typical example is the phenomenon of relative equilibrium in an open cylinder of a fluid that rotates around its vertical axis. Due to viscosity, any real fluids flow behaves as a rotational flow (at least at one point of the fluid domain) (Pordeus, 2015).

$$\omega = \nabla \times v \neq 0$$

Irrotational Movement/Flow

Flow or movement that is just an approximation, in which is considered no rotational particles in the fluid. (without vortex or tornados), so the studied flow is considered as irrotational, by applying the classical principles of fluids dynamics. On these types of theoretical flows, particles are non-deformable, viscosity effects are ignored, and it created a mathematical modelling of the flow (that apply for every point in fluids domain) (Pordeus, 2015).

$$\omega = \nabla \times v = 0$$

2.2.3 Laminar, transition and turbulent Movements/Flows

Laminar Movements/Flows

Stream lines are totally independent from each other, do not share any common point, and its tangents are always parallel to each other's. So, it constitutes a regular and stable field in such way, that any external perturbation is rapidly suppress (Figure 26) (Pinho et al., 2011).

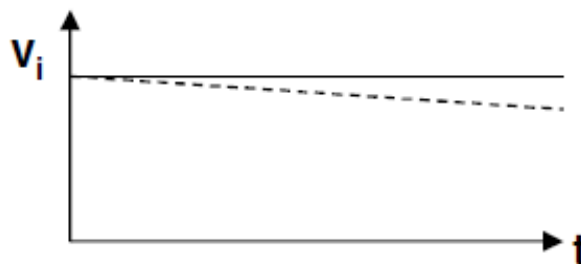


Figure 26 – Graphical representation of laminar flow or movement (Pinho et al., 2011).

Transitional Movements/Flows

It is a regime between laminar and turbulence regimes (Pinho et al., 2011).

Turbulence Movements/Flows

The laminar structure totally dissipates and disperse, leading to great fluctuations of physical quantities in space and time (Figure 27) (Pinho et al., 2011).

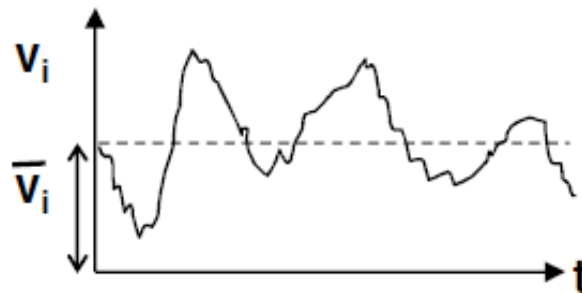


Figure 27 – Graphical representation of a turbulent flow or movement (Pinho et al., 2011).

$$v_i = \bar{v}_i + v_i'$$

2.2.4 External, internal and in porous media flows

This classification is based on the **relative position** of fluids domain and the solid walls that are in contact (Pinho et al., 2011).

External flows

The fluid in movement **surround absolutely** all solid walls that constitute the flows borders, an example is the transversal section of an airplane wing surrounded by air flow, great size buildings or the water flows around a bridge column (Pinho et al., 2011).

Internal flows

The fluids flow is **totally or partially surrounded** by solid walls. This type of flow has two sub-division (Pinho et al., 2011):

- **Flow under pressure**: can be find inside pipes, when the fluid fills the whole section of it, creating pressures in all point of the surrounding walls, those pressures are usually different to atmospheric pressure;
- **Flow with a free surface** are in permanent contact with an external gas media, generally, the atmosphere.

Flows in porous media

Enclose characteristics of both types of flows (external and internal). It is verified when exist a permanent contact between fluid flow and the porous media (Pinho et al., 2011).

2.3 Continuity equation

In order to solve problems of **Fluid Dynamics** is necessary to have **6 equations** (Pinho et al., 2011):

- Continuity Equation;
- 3 Equations of Dynamic Equilibrium;
- Equation of Fluids State;
- Equation of Energy Balance.

In order to solve problems of **Fluid Mechanics** is necessary to have **4 equations** (Pinho et al., 2011):

- Continuity Equation;
- 3 Equations of Dynamic Equilibrium.

Equations based on Euler's variables are consider as valid for laminar flows and turbulent flows at instantaneous values. Equations are deduced or built in local terms by giving to each geometrical point of space of Fluid's domain a set of values that correspond to certain tensorial quantities, that are typical of a fluid or flow (Pinho et al., 2011):

- Tensor field of zero order or scalar: **ρ, γ, T** ;
- Tensor field of first order: **velocity, vorticity, forces**;
- Tensor fields of second order: **tension, angular deformation velocity**.

2.3.1 Deduction of the general equation

Continuity Equation or **Mass Conservation** state the property of mass conservation and is written-down as a balance equation applied to a surface of control (**S**) related to an axis references system, limiting a certain volume of control (**V**) (Pinho et al., 2011).

$$(1): \Phi_S - \Phi_e = \Delta G_I$$

Where:

$\Phi_S - \Phi_E$ is the difference between quantities that cross in and out the systems border; ΔG_I represent a decrease in the global value of the measured quantity inside the surface of control (Figure 28).

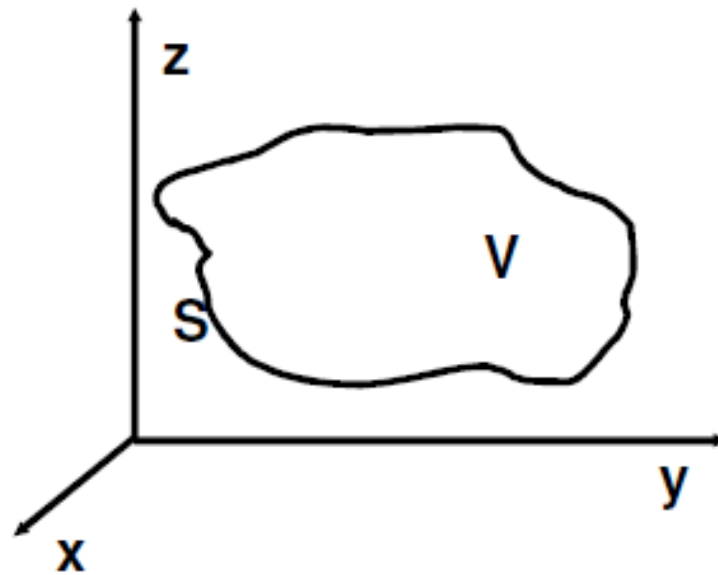


Figure 28 – Control surface (Pinho et al., 2011).

General Expression

It is necessary to define the difference ($\Phi_S - \Phi_E$) between fluids mass that cross a closed surface from inside to outside (leave the system) and the fluids mass that flows in opposite direction, at some interval of time (Pinho et al., 2011).

Mass that cross an element of area (dS) per unit time:

$$dm = \rho \vec{v} \cdot \vec{n} dS \text{ (Positive when flows outwards (from inside to outside))}$$

by integrating the whole surface of control (S), is obtained:

$$(2): \Phi_S - \Phi_E = \int_S \rho \vec{v} \cdot \vec{n} dS$$

It is necessary to define the decrease (ΔG_I) of mass, that exist inside the volume of control, per unit time (Pinho et al., 2011).

Total mass contained in control surface (S):

$$m = \int_V \rho dV$$

Variation of mass per unit time:

$$(3): \Delta G_I = -\frac{\partial}{\partial t} \int_V \rho dV$$

Being the limits of the integer independent of time:

$$\text{Transf. (1) em: } (\Phi_S - \Phi_e) - \Delta G_I = 0$$

$$\text{and including (2) and (3), we get (4): } \int_S \rho \vec{v} \cdot \vec{n} \, dS + \frac{\partial}{\partial t} \int_V \rho \, dV = 0$$

$$\text{And by applying the Ostrogradsky Theorem: } \int_S \vec{v} \cdot \vec{n} \, dS = \int_V \text{div} \vec{v} \, dV$$

$$\text{Then (4) becomes (5): } \int_V \left[\text{div}(\rho \vec{v}) + \frac{\partial \rho}{\partial t} \right] dV = 0$$

Being volume (**V**) totally arbitrary:

$$\text{div}(\rho \vec{v}) + \frac{\partial \rho}{\partial t} = 0 \quad \text{or} \quad \frac{\partial(\rho v_i)}{\partial x_i} + \frac{\partial \rho}{\partial t} = 0$$

For **permanent flows**:

$$\frac{\partial}{\partial t} = 0 \wedge \text{div}(\rho \vec{v}) = 0$$

For **incompressible fluids**:

$$\rho = \text{cst.} \wedge \text{div} \vec{v} = 0$$

2.3.2 Application to a stream tube (stream pipe)

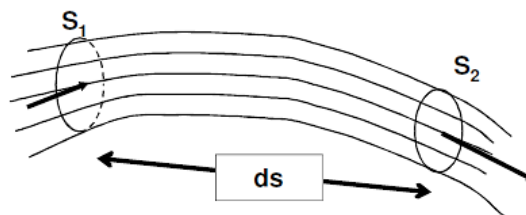


Figure 29 – Stream pipe or stream tube (Pinho et al., 2011).

Mass that cross surface **S₁** in an interval of time **dt**:

$$\rho Q dt$$

Mass that cross surface **S₂** in an interval of time **dt**:

$$\left[\rho Q + \frac{\partial(\rho Q)}{\partial s} ds \right] dt$$

Decrease of mass in volume (**V**):

$$- \frac{\partial(\rho Q)}{\partial s} ds dt$$

Considering **S** as the area of an average transversal section a long distance **ds**:

$$dV = S ds$$

Variation of mass inside the volume of control per interval of **dt**:

$$- \frac{\partial(\rho S)}{\partial t} dt ds$$

Equation of continuity applied to a **stream tube**:

$$\frac{\partial(\rho Q)}{\partial s} + \frac{\partial(\rho S)}{\partial t} = 0$$

For **incompressible fluids**:

$$\frac{\partial Q}{\partial s} + \frac{\partial S}{\partial t} = 0$$

For **incompressible fluids and permanent movement/flow**:

$$Q = U \cdot S = \text{cst.}$$

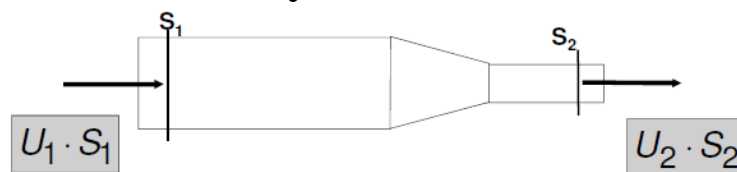


Figure 30 – Example of incompressible fluids in permanent movement (Pinho et al., 2011).

$$U_1 \cdot S_1 = U_2 \cdot S_2$$

2.4 Equation of dynamic equilibrium

The **Equation of Dynamic Equilibrium** result from applying the general equations of particle systems dynamics to a fluid movement/flow (Pinho et al., 2011).

$$\vec{F} = m\vec{a} \text{ (Newton's Equation)}$$

2.4.1 Consequences in Fluids

A **fluid surface** (S) limiting a volume (V) in movement is submitted to two types of forces distributions (Pinho et al., 2011):

1. **Mass forces or volume forces (gravity forces)** – results from attraction or repulsion created by the fluid media, and such forces are proportional to the volume or mass of the fluid corresponding to each differential element of volume.
2. **Surface forces or contact forces** – results from actions made over surface S by the surrounding fluid, that is inside the mentioned surface.

Volume forces or mass forces

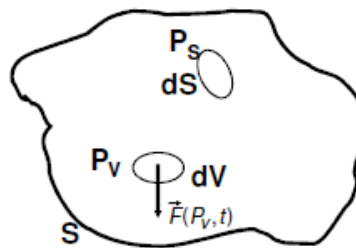


Figure 31 – Volume forces or mass forces (Pinho et al., 2011).

Resultant from volume forces inside S :

$$\int_V \vec{F}(P_v, t) dV$$

Force per unit mass:

$$\vec{G}(P_v, t) = \frac{\vec{F}(P_v, t)}{\rho}$$

Surface forces or contact forces

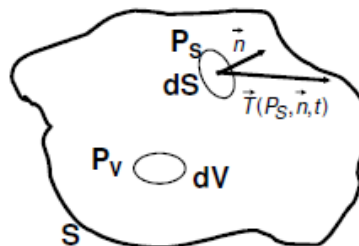


Figure 32 – Surface forces or contact forces (Pinho et al., 2011).

Resultant from forces distribution in P_s :

$$d\vec{\Phi}$$

Resultant of tension in dS :

$$\vec{T}(P_S, \vec{n}, t) = \frac{d\vec{\Phi}}{dS}$$

In S :

$$\int_S \vec{T}(P_S, \vec{n}, t) dS$$

2.4.2 Notion of dynamic equilibrium

Dynamic Equilibrium means that the main vector of the forces' system, the resultant moment and inertial forces of the same system, are all equal to null vector or totally zero. (Figure 33) (Pinho et al., 2011).

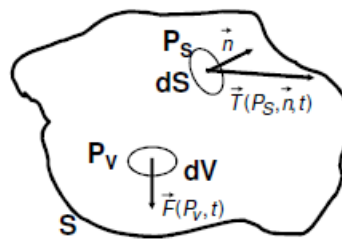


Figure 33 – Dynamic equilibrium (Pinho et al., 2011).

$$\int_V \vec{F}(P_v, t) dV + \int_S \vec{T}(P_S, \vec{n}, t) dS - \int_V \rho \vec{a}(P_v, t) dV = 0$$

Where $\vec{a}(P_v, t)$ is an acceleration vector in point P_v at instant t (Pinho et al., 2011).

By using forces per unit time:

$$\int_V \rho \vec{G} dV + \int_S \vec{T} dS = \int_V \rho \vec{a} dV$$

Or in cartesian tensorial notation:

$$\int_V \rho G_i dV + \int_S T_i dS = \int_V \rho a_i dV$$

2.4.3 Characterization of the state of tension

By assuming that the tension corresponding to any orientation of a face, is given from knowing two elements of the tensor of tension (Pinho et al., 2011):

$$\vec{T}(P_S, \vec{n}) = \tau_{ji}(P_S) n_j$$

Following **Euler** expression of acceleration:

$$a_i = \frac{D_{v_i}}{D_t} = \frac{\partial v_i}{\partial t} + v_j \frac{\partial v_i}{\partial x_j} \Rightarrow$$

$$\Rightarrow a_i = \underbrace{\frac{\partial v_i}{\partial t}}_{\text{Local Acceleration}} + \underbrace{v_1 \frac{\partial v_i}{\partial x_1} + v_2 \frac{\partial v_i}{\partial x_2} + v_3 \frac{\partial v_i}{\partial x_3}}_{\text{Convective Acceleration}}$$

2.4.4 Equations of dynamic equilibrium

Thereby, the **dynamic equilibrium Equations** can assume the following form (Pinho et al., 2011):

$$\int_V \rho a_i dV = \int_V \rho G_i dV + \int_S \tau_{ji} n_j dS$$

ou

$$\int_V \rho a_i dV = \int_V \rho G_i dV + \int_S \frac{\partial \tau_{ji}}{\partial x_j} dS$$

Having an arbitrary volume:

$$a_i = G_i + \frac{1}{\rho} \frac{\partial \tau_{ji}}{\partial x_j} \quad \text{ou} \quad \frac{\partial v_i}{\partial t} + v_j \frac{\partial v_i}{\partial x_j} = G_i + \frac{1}{\rho} \frac{\partial \tau_{ji}}{\partial x_j}$$

For example, for **i = 1**, the expression takes the following form:

$$\frac{\partial v_1}{\partial t} + v_1 \frac{\partial v_1}{\partial x_1} + v_2 \frac{\partial v_1}{\partial x_2} + v_3 \frac{\partial v_1}{\partial x_3} = G_1 + \frac{1}{\rho} \frac{\partial \tau_{11}}{\partial x_1} + \frac{1}{\rho} \frac{\partial \tau_{21}}{\partial x_2} + \frac{1}{\rho} \frac{\partial \tau_{31}}{\partial x_3}$$

2.4.5 Euler's Equations

Considering meaningless all distortional (perfect fluid) and considering the tensor of the tensions as spherical, it is reduced to a hydrostatic tensor (Pinho et al., 2011):

$$\tau_{ij} = -p \delta_{ij}$$

Where **Kronecker delta**:

$$\delta_{ij} = \begin{cases} 0, i \neq j \\ 1, i = j \end{cases}$$

$$\frac{\partial \tau_{ji}}{\partial x_j} = -\frac{\partial p}{\partial x_j} \delta_{ji} = -\frac{\partial p}{\partial x_i}$$

$$\frac{\partial v_i}{\partial t} + v_j \frac{\partial v_i}{\partial x_j} = G_i - \frac{1}{\rho} \frac{\partial p}{\partial x_i} \quad \begin{array}{l} \text{Component of pressure} \\ \text{gradient in } O_{x_i} \text{ direction} \end{array}$$

A vectorial equation that is decomposed into three scalar equations of projection depending on the coordinate axis (Pinho et al., 2011).

In **Hydrostatic**, viscosity has no effect:

$$G_i = \frac{1}{\rho} \frac{\partial p}{\partial x_i} \quad \text{ou} \quad \vec{G} = \frac{1}{\rho} \text{grad } p$$

2.4.6 Navier-Stokes Equations. Borders conditions

Constitutive relation for a newtonian fluid

It is the simplest relation between the tensor of state of tension and the tensor of rate of deformation (Claude-Louis Navier, 1822; George Gabriel Stokes, 1845). Based in three arguments/postulates (Baliño, 2017):

1. The fluid is continuous and the **tensor of tension (T)** is at maximum a linear function of the **tensor of rate of deformation (ε)**. **Corollary**: there is no effect of translation, rotation, or older situations (*stress*);
2. The fluid is isotropic (properties are independent of the reference system (direction)), so the relation law is independent of the coordinate axis selected to express it. **Corollary**: Main axis of the related tensors coincide;
3. In absence of rate of deformation, the state of tension is reduced to a hydrostatic state **T = -pI**.

By selecting main axis (x_1, y_1, z_1) to state the constitutive relation. At these axes, the associated matrix to tensors are diagonal, resulting from the following hypothesis: (Baliño, 2017):

$$T_{11} = -p + C_1 \epsilon_{11} + C_2 \epsilon_{22} + C_3 \epsilon_{33}$$

By isotropic conditions, the perpendicular direction to x_1 are equivalents, that means, $C_2 = C_3$, which lead to two independents coefficients (Baliño, 2017):

$$T_{11} = -p + (C_1 - C_2) \epsilon_{11} + C_2 (\epsilon_{11} + \epsilon_{22} + \epsilon_{33}) = -p + k \epsilon_{11} + C_2 (\nabla \cdot V)$$

Where, $k = C_1 - C_2$. And analogously for other components:

$$T_{22} = -p + k \epsilon_{22} + C_2 (\nabla \cdot V)$$

$$T_{33} = -p + k \epsilon_{33} + C_2 (\nabla \cdot V)$$

It is made a transformation to axis (x, y, z) , where its associated matrix has also non-diagonal elements. If T_1 and ϵ_1 are the associated matrixes to main axis, while T and ϵ are matrix associated to the transformed axis, its result in (Baliño, 2017):

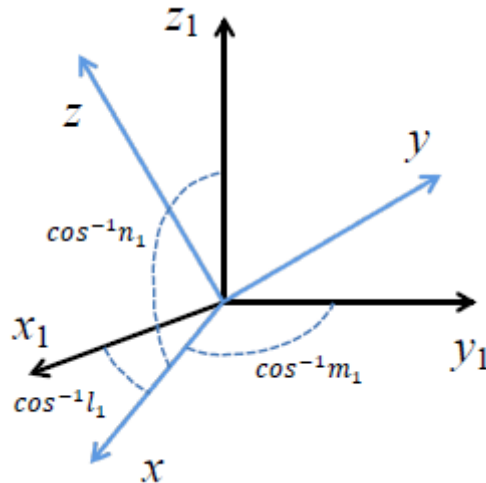


Figure 34 – Axis transformation (Baliño, 2017).

$$T = Q^T \cdot T_1 \cdot Q$$

$$\epsilon = Q^T \cdot \epsilon_1 \cdot Q$$

Where Q is the **transformation matrix** (director cosines of transformed axis ordered in columns) (Baliño, 2017):

$$\{Q\} = \begin{pmatrix} l_1 & l_2 & l_3 \\ m_1 & m_2 & m_3 \\ n_1 & n_2 & n_3 \end{pmatrix}; \begin{cases} \check{i}_1 = l_1 \check{i} + l_2 \check{j} + l_3 \check{k} \\ \check{i}_2 = m_1 \check{i} + m_2 \check{j} + m_3 \check{k} \\ \check{i}_3 = n_1 \check{i} + n_2 \check{j} + n_3 \check{k} \end{cases}$$

The transformation for a diagonal element (for example T_{xx} and ϵ_{xx}) and a non-diagonal element (for example T_{xy} and ϵ_{xy}) result (Baliño, 2017):

$$T_{xx} = l_1^2 T_{11} + m_1^2 T_{22} + n_1^2 T_{33} \quad \wedge \quad \epsilon_{xx} = l_1^2 \epsilon_{11} + m_1^2 \epsilon_{22} + n_1^2 \epsilon_{33}$$

$$T_{xy} = l_1 l_2 T_{11} + m_1 m_2 T_{22} + n_1 n_2 T_{33} \quad \wedge \quad \epsilon_{xy} = l_1 l_2 \epsilon_{11} + m_1 m_2 \epsilon_{22} + n_1 n_2 \epsilon_{33}$$

By replacing tensions in main directions and knowing that:

$$\begin{cases} \check{i} \cdot \check{i} = l_1^2 + m_1^2 + n_1^2 \\ \check{i} \cdot \check{j} = l_1 l_2 + m_1 m_2 + n_1 n_2 = 0 \end{cases}$$

$$\begin{aligned} T_{xx} &= l_1^2 [-p + k\epsilon_{11} + C_2(\nabla \cdot V)] + m_1^2 [-p + k\epsilon_{22} + C_2(\nabla \cdot V)] + n_1^2 [-p + k\epsilon_{33} + C_2(\nabla \cdot V)] = \\ &= -p(l_1^2 + m_1^2 + n_1^2) + k(l_1^2 \epsilon_{11} + m_1^2 \epsilon_{22} + n_1^2 \epsilon_{33}) + C_2(\nabla \cdot V)(l_1^2 + m_1^2 + n_1^2) = \\ &= -p + k\epsilon_{xx} + C_2(\nabla \cdot V) \end{aligned}$$

$$T_{xy} = l_1 l_2 [-p + k\epsilon_{11} + C_2(\nabla \cdot V)] + m_1 m_2 [-p + k\epsilon_{22} + C_2(\nabla \cdot V)] + n_1 n_2 [-p + k\epsilon_{33} + C_2(\nabla \cdot V)] =$$

$$= -p(l_1 l_2 + m_1 m_2 + n_1 n_2) + k(l_1 l_2 \epsilon_{11} + m_1 m_2 \epsilon_{22} + n_1 n_2 \epsilon_{33}) + C_2(\nabla \cdot V)(l_1 l_2 + m_1 m_2 + n_1 n_2) = k\epsilon_{xy}$$

By defining $k = 2\mu$ and $C_2 = \lambda$, where μ is **dynamic viscosity** and λ is the **second coefficient of viscosity**, finally (Baliño, 2017):

$$T_{xx} = -p + 2\mu\epsilon_{xx} + \lambda(\nabla \cdot V)$$

$$T_{yy} = -p + 2\mu\epsilon_{yy} + \lambda(\nabla \cdot V)$$

$$T_{zz} = -p + 2\mu\epsilon_{zz} + \lambda(\nabla \cdot V)$$

$$T_{xy} = 2\mu\epsilon_{xy}$$

$$T_{yz} = 2\mu\epsilon_{yz}$$

$$T_{zx} = 2\mu\epsilon_{zx}$$

In compact form:

$$T_{ij} = [-p + \lambda(\nabla \cdot V)]\delta_{ij} + 2\mu \cdot \epsilon_{ij} = [-p + \lambda(\nabla \cdot V)]\delta_{ij} + \mu \left(\frac{\partial u_i}{\partial x_j} + \frac{\partial u_j}{\partial x_i} \right)$$

$$T = [-p + \lambda(\nabla \cdot V)]I + 2\mu\epsilon = [-p + \lambda(\nabla \cdot V)]I + \mu(\nabla V + \nabla V^T)$$

Mechanical pressure and thermodynamic pressure

By adding normal tensions, the first invariant of the tensor became:

$$I_1 = -3p + 2\mu(\epsilon_{xx} + \epsilon_{yy} + \epsilon_{zz}) + 3\lambda(\nabla \cdot V) = -3p + (2\mu + 3\lambda)(\nabla \cdot V)$$

And by defining mechanical pressure as:

$$\bar{p} = -\frac{I_1}{3}$$

Results in:

$$\bar{p} = p - \left(\lambda + \frac{2}{3}\mu \right) (\nabla \cdot V)$$

Mechanical pressure is different from thermodynamic pressure. The problematic term is related to compressible flows, (where $\nabla \cdot V = 0$ is irrelevant), which is controversial. Stokes solved by stating next condition: $\bar{p} = p$, that means, $\lambda = -(2/3)\mu$, which is known as **Stokes hypothesis** (Baliño, 2017).

Force term of the state of tension

It must be added, in conservation equations of linear momentum, the force terms of the state of tension ($\nabla \cdot T$):

$$\begin{aligned}\nabla \cdot T &= \nabla \cdot \{[-p + \lambda(\nabla \cdot V)]I + \mu(\nabla V + \nabla V^T)\} = \\ &= -\nabla p + (\nabla \cdot V)\nabla\lambda + \lambda\nabla(\nabla \cdot V) + (\nabla V + \nabla V^T) \cdot \nabla\mu + \mu\nabla \cdot (\nabla V + \nabla V^T)\end{aligned}$$

By calculating last term, using **Einstein's summation convention** (when an index is duplicated, means it must be a summation of all its values) (Baliño, 2017):

$$\begin{aligned}[\nabla \cdot (\nabla V + \nabla V^T)]_i &= \frac{\partial}{\partial x_j} \left(\frac{\partial u_i}{\partial x_j} + \frac{\partial u_j}{\partial x_i} \right) = \frac{\partial^2 u_i}{\partial x_j^2} + \frac{\partial}{\partial x_i} \left(\frac{\partial u_j}{\partial x_j} \right) = (\nabla^2 V)_i + [\nabla(\nabla \cdot V)]_i \\ \nabla \cdot (\nabla V + \nabla V^T) &= \nabla^2 V + \nabla(\nabla \cdot V)\end{aligned}$$

So, when replacing, it's obtained:

$$\nabla \cdot T = -\nabla p + (\nabla \cdot V)\nabla\lambda + (\lambda + \mu)\nabla(\nabla \cdot V) + (\nabla V + \nabla V^T) \cdot \nabla\mu + \mu\nabla^2 V$$

In terms of genuine operators, the Laplacian vector results:

$$\nabla^2 V = \nabla(\nabla \cdot V) - \nabla \times (\nabla \times V)$$

The conservation equation of linear moment finally results in:

$$\frac{dV}{dt} = \frac{\partial V}{\partial t} + \nabla V \cdot V = -\frac{1}{\rho}\nabla p + G + v\nabla^2 V + \frac{1}{\rho}[(\lambda + \mu)\nabla(\nabla \cdot V) + (\nabla \cdot V)\nabla\lambda + (\nabla V + \nabla V^T) \cdot \nabla\mu]$$

The upper relations show the coupling to energy equations, through the specific mass and the viscosity gradient (Baliño, 2017).

Navier-Stokes equations

Considering the Stokes hypothesis and constant viscosity, its results:

$$\frac{dV}{dt} = \frac{\partial V}{\partial t} + \nabla V \cdot V = -\frac{1}{\rho}\nabla p + G + v\nabla^2 V + \frac{1}{3}v\nabla(\nabla \cdot V)$$

Finally, considering a non-compressible flow, results in **Navier-Stokes equations** (Baliño, 2017):

$$\frac{dV}{dt} = \frac{\partial V}{\partial t} + \nabla V \cdot V = -\frac{1}{\rho}\nabla p + G + v\nabla^2 V$$

Navier-Stokes equations is of second order in velocity and is not coupled to energy equation. In cartesian coordinates, the x components result in (Baliño, 2017):

$$\frac{du}{dt} = \frac{\partial u}{\partial t} + u \frac{\partial u}{\partial x} + v \frac{\partial u}{\partial y} + w \frac{\partial u}{\partial z} = -\frac{1}{\rho} \frac{\partial p}{\partial x} + G_x + \nu \left(\frac{\partial^2 u}{\partial x^2} + \frac{\partial^2 u}{\partial y^2} + \frac{\partial^2 u}{\partial z^2} \right)$$

Borders conditions in fluid-solid interface

In a fluid-solid interface, by ignoring microscale effects characterized by the large numbers of Knudsen ($Kn = l/L < 0.1$, where l is the free average distance of molecules and L is the characteristic distance of the problem), and is normal to assume a non-slipping condition (Baliño, 2017);

$$V(r_s, t) = V_s(t)$$

If the solid where permeable (for example, in case of suction or injection of fluid) or if it exists a phase-change (evaporation, condensation, sublimation, deposition), the normal component of velocity slows-down, which means, $V_n(r_s, t) \neq 0$ (Baliño, 2017).

Borders conditions on a free surface (kinematic)

In case of an ideal free surface, that creates a knowing pressure in the interface, characterized by its position $z = \eta(x, y, t)$ (Baliño, 2017):

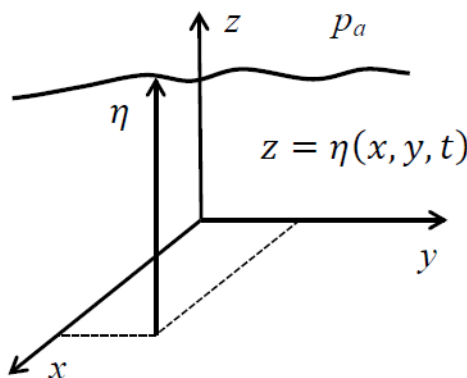


Figure 35 – Borders conditions in a free surface (kinematics) (Baliño, 2017).

Apply to kinematics conditions in which particles on surface, stay on surface; that means, the particles velocity in a vertical direction is equal to its vertical displacement following particles (Baliño, 2017):

$$w(x, y, \eta, t) = \frac{d\eta}{dt} = \frac{\partial \eta}{\partial t} + u \frac{\partial \eta}{\partial x} + v \frac{\partial \eta}{\partial y}$$

When ignoring the surface angle, results:

$$w(x, y, \eta, t) \cong \frac{\partial \eta}{\partial t}$$

Border conditions in free surfaces (normal)

The **curvature** in the interface is related to a force in the normal direction (Baliño, 2017):

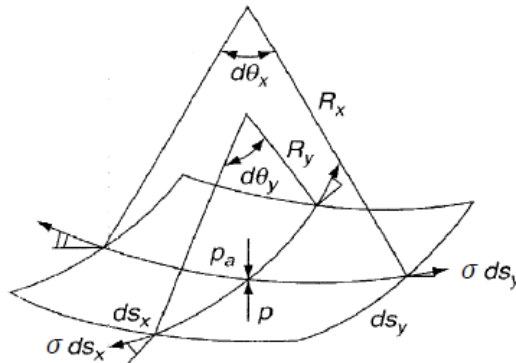


Figure 36 – Borders conditions in free surfaces (normal) (Baliño, 2017).

A balance in the normal direction to the interface results in **Young-Laplace equation**:

$$p(x, y, \eta, t) = p_a - \sigma \left(\frac{1}{R_x} + \frac{1}{R_y} \right)$$

$$\frac{1}{R_x} + \frac{1}{R_y} = \frac{\frac{\partial^2 \eta}{\partial x^2} + \frac{\partial^2 \eta}{\partial y^2}}{\left[1 + \left(\frac{\partial \eta}{\partial x} \right)^2 + \left(\frac{\partial \eta}{\partial y} \right)^2 \right]^{3/2}}$$

Where, σ is a superficial tension. By ignoring superficial tension effects or great curvature radius, results in $p \cong p_a$ (Baliño, 2017).

Border conditions in surface between fluids

Considering that, the interface has ignorable inertia and considering the possibility of tensions variations all over the surface (Marangoni Flow) (Baliño, 2017):

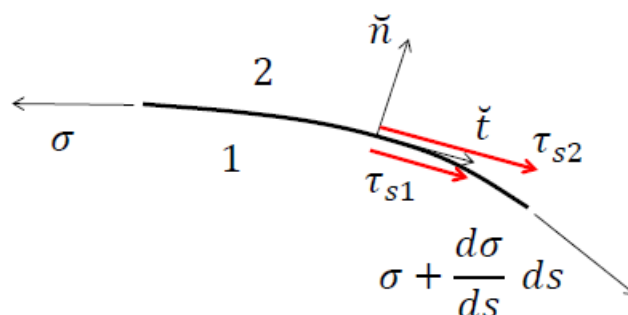


Figure 37 – Borders conditions in surfaces between fluids (Baliño, 2017).

Borders conditions results in (Baliño, 2017):

Continuity of velocity

$$V_1 = V_2$$

Balance in tangential direction

$$\tau_{s1} + \tau_{s2} = -\frac{d\sigma}{ds}$$

Where:

$$\tau_{s2} = (\tau_2 \cdot \vec{n}) \cdot \vec{t}$$

$$\tau_{s1} = -(\tau_1 \cdot \vec{n}) \cdot \vec{t}$$

CHAPTER 3 - HYDROSTATIC

3.1 General equations of fluids equilibrium

Introduction to pressure

Pressure is an acting load normal to a surface with unit area, applied in a certain point, acting on a determinate plain (direction) inside a fluids mass in rest. Pressure in some point inside a fluid in rest, is independent of direction (Pinho et al., 2011).

$$p = \gamma \times g$$

3.1.1 General case

Resolution of a fluid's statics problem consist in determine **3** variables: **pressure**, **volumetric mass**, **temperature**, in every point of fluids domain, from the knowing the external forces field. So, it is necessary **3 equations** (Pinho et al., 2011).

1^a Equation - from dynamic equilibrium equations applied to a fluid in rest:

$$\frac{1}{\rho} \text{grad } p = \vec{G} \quad \text{Resultant of external forces per unit mass}$$

Projecting over 3 orthogonal cartesian axis:

$$G_i = \frac{1}{\rho} \frac{\partial p}{\partial x_i} \Rightarrow \begin{cases} G_1 = \frac{1}{\rho} \frac{\partial p}{\partial x} \\ G_2 = \frac{1}{\rho} \frac{\partial p}{\partial y} \\ G_3 = \frac{1}{\rho} \frac{\partial p}{\partial z} \end{cases} \quad \text{or} \quad \begin{cases} G_1 dx = \frac{1}{\rho} \frac{\partial p}{\partial x} dx \\ G_2 dy = \frac{1}{\rho} \frac{\partial p}{\partial y} dy \\ G_3 dz = \frac{1}{\rho} \frac{\partial p}{\partial z} dz \end{cases}$$

And by adding:

$$\frac{1}{\rho} \left(\frac{\partial p}{\partial x} dx + \frac{\partial p}{\partial y} dy + \frac{\partial p}{\partial z} dz \right) = G_1 dx + G_2 dy + G_3 dz$$

Where:

$$\frac{1}{\rho} dp = G_1 dx + G_2 dy + G_3 dz$$

Fundamental equation of fluids statics

2^a Equation - equation of state:

$$f(p, \rho, T) = 0$$

3^a Equation - complementary equation of thermodynamics type, related with the principle of conservation or balance of energy.

3.1.2 Equilibrium of a fluid at constant temperature

When, **T = constant** the number of incognitos or unknowns variables is reduced to two, then is only necessary two equations (Pinho et al., 2011).

1^a Equation:

$$\rho = \rho(p)$$

2^a Equation:

$$\left\{ \begin{array}{l} \rho G_1 = \frac{\partial p}{\partial x} \\ \rho G_2 = \frac{\partial p}{\partial y} \\ \rho G_3 = \frac{\partial p}{\partial z} \end{array} \right. \text{ which can proof that: } \left\{ \begin{array}{l} \frac{\partial G_1}{\partial x} = \frac{\partial G_2}{\partial y} \\ \frac{\partial G_2}{\partial y} = \frac{\partial G_3}{\partial z} \\ \frac{\partial G_3}{\partial z} = \frac{\partial G_1}{\partial x} \end{array} \right.$$

Where:

$$G_1 dx + G_2 dy + G_3 dz = dU, \text{ with } U(x_1, x_2, x_3) \quad \text{or} \quad dU = \frac{dp}{\rho}$$

A fluid with **a constant temperature** can only be in rest if **the forces field applied is conservative**:

$$G_1 dx + G_2 dy + G_3 dz = 0$$

3.1.3 Heavy fluids equilibrium

Heavy fluids are a type of fluid under external forces (static forces), that are only induced or created by the **action of gravity** (Pinho et al., 2011).

Them:

$$G_1 = 0, G_2 = 0, G_3 = -g$$

In which g is acceleration due to gravity effects.

From statics fundamental equation:

$$\frac{1}{\rho} dp = -g dz \quad \text{or} \quad dp + \gamma dz = 0$$

For heavy fluids at **constant temperature**:

$$\gamma dz = 0 \Rightarrow dz = 0 \Rightarrow z = \text{cst.}$$

In case of heavy fluids, the **equipotential surfaces** are horizontal, also called **level surfaces** (Pinho et al., 2011).

3.1.4 Equilibrium of heavy liquids

For **heavy liquids** ($\gamma = \text{cte.}$) and by integrating:

$$dp + \gamma dz = 0$$

Between two point of quotas z_0 and z_1 and pressures of p_0 and p , where:

$$p_1 - p_0 = \gamma(z_0 - z_1)$$

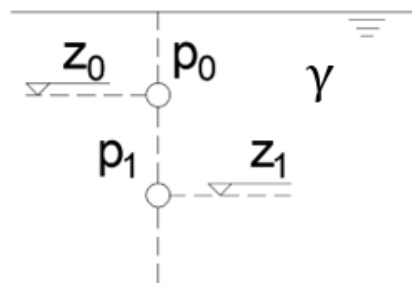


Figure 38 – Equilibrium of heavy liquids (adapted from Pinho et al., 2011).

Fundamental Principle of Hydrostatics

The difference of pressure between two points of a heavy liquid mass in rest is equal to the weight of a liquid column with base of unit area, and which height is the level difference between the considered points (Pinho et al., 2011).

The integral of $dp + \gamma dz = 0$ can be write as $p + \gamma z = \text{cst.}$ or yet:

$$z + \frac{p}{\gamma} = h = \text{cst.}$$

Where:

z is the topographical quota of the considered point [L];

p/γ is the piezometric height [L];

h is the piezometric height [L].

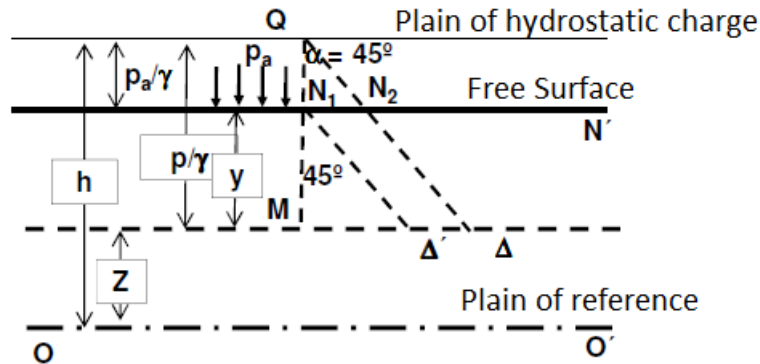


Figure 39 – Fundamental principle of Hydrostatics (Pinho et al., 2011).

$$\frac{p}{\gamma} = y + \frac{p_a}{\gamma} \Rightarrow p = p_a + \gamma y$$

M is the point with deep y a pressure p :

$$p = \gamma(h - Z) = \gamma \overline{MQ}$$

3.1.5 Absolutes and effectives pressures

Absolute pressure is a total pressure at a certain point or place, that means, it is the summation of all pressures that contributes to it final value (increase or decrease). Its determination depends on different factors that can lead to an increase or decrease of the pressure on the system (Pinho et al., 2011).

Effective pressure is the pressure created by the fluid on a point, apart from the pressure created by the atmospheric pressure (Pinho et al., 2011).

$$p = p_a + \gamma \cdot h$$

Where:

p is absolute pressure;

p_a is atmospheric pressure;

$\gamma \cdot h$ is effective pressure.

In Hydrostatics (as Hydrodynamics) the pressures are normally considerate as effectives (Pinho et al., 2011).

3.1.6 Equilibrium of liquids with different densities

If a mass of liquid is constituted by different liquids, non-miscible, with different volumetric weights, so that it overlaps one over another by a decreasing density order (Figure 40) (Pinho et al., 2011).

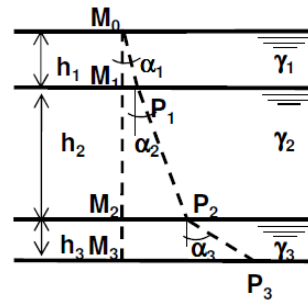


Figure 40 – Liquid mass constituted by liquids of different densities (Pinho et al., 2011).

$$p_1 = \gamma_1 h_1; \alpha_1 = K_1(\gamma_1)$$

$$p_2 - p_1 = \gamma_2 h_2; \alpha_2 = K_2(\gamma_2)$$

$$p_3 - p_2 = \gamma_3 h_3; \alpha_3 = K_3(\gamma_3)$$

$$\text{With } \alpha_3 > \alpha_2 > \alpha_1$$

$$p_3 = \gamma_1 h_1 + \gamma_2 h_2 + \gamma_3 h_3$$

For n liquids with volumetric weights $\gamma_i (i = 1, 2, \dots, N)$, in rest, forming layers of thickness h_i , can be stated that:

$$p_n = \sum_{i=1}^n \gamma_i h_i$$

3.1.7 Equilibrium of liquid under non-exclusive gravitational forces fields

Equilibrium of a liquid under constant acceleration

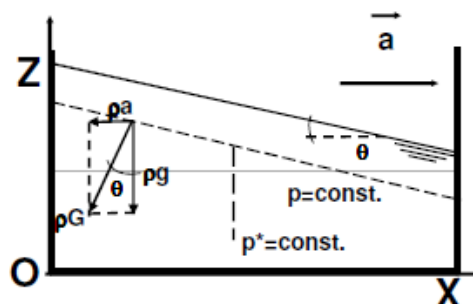


Figure 41 – Liquid under constant acceleration (Pinho et al., 2011).

Where:

\vec{a} is the constant horizontal acceleration;

$\rho \vec{G}$ are the resultant forces per unit volume $\begin{cases} \rho \vec{g} \text{ (weight)} \\ \rho \vec{a} \text{ (inertia)} \end{cases}$;

p^* is dynamical pressure.

And:

$$\vec{a} = \vec{G} - \frac{1}{\rho} \text{grad } p$$

Projecting in **OX** and **OZ**:

$$\begin{cases} -\rho a - \frac{\partial p}{\partial x} = 0 \\ -\rho g - \frac{\partial p}{\partial z} = 0 \end{cases} \quad \text{adding} \quad \begin{cases} -\rho a dx - \rho g dz = \frac{\partial p}{\partial x} dx + \frac{\partial p}{\partial z} dz \\ -\rho a dx - \rho g dz = dp \end{cases}$$

For **equipotential surfaces** coincident with **isobarics** (Pinho et al., 2011):

$$dp = 0 \text{ (} p = \text{cst.} \text{)} \Rightarrow -\rho a dx - \rho g dz = 0$$

Integrating:

$$z = -\frac{a}{g}x + \text{cst.}$$

The surfaces $p = \text{cst.}$ is normal to the vector \vec{G} and are inclined planes with angle θ respect to the horizon: $\tan \theta = -a/g$. Surfaces $p^* = \text{cst.}$ are normal to vector \vec{a} .

Equilibrium of a liquid in an animated vessel of constant angular velocity

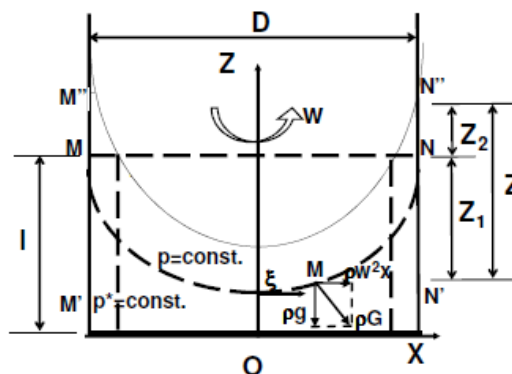


Figure 42 – Equilibrium of a liquid in an animated vessel of constant angular velocity (Pinho et al., 2011).

Where w is a constant velocity in circular uniform movement around Z .

Forces Equilibrium - particle **M** located at the free surface is in rest and under a force $\rho \vec{G}$ per unit of volume, equilibrated by its weight (vertical force, $-\rho g$) and by the horizontal component of the inertial force (centrifugal force, $\rho w^2 r$) (Pinho et al., 2011).

Projecting the equation of equilibrium over **OX** and **OZ**:

$$\begin{cases} \rho w^2 r - \frac{\partial p}{\partial x} = 0 \\ -\rho g - \frac{\partial p}{\partial z} = 0 \end{cases} \Rightarrow dp = \rho w^2 r dx - \rho g dz$$

Integrating:

$$p = \frac{\rho w^2}{2} x^2 - \rho g z + \text{cst.}$$

The **isobarics** $p = \text{cst.}$ have the equation:

$$w^2 \frac{x^2}{2} - g z = \text{cst.}$$

The **isobarics** are paraboloids of revolution of axis **OZ**, in every point, normal to vector \vec{G} , resulting from the gravitational and inertial forces (Pinho et al., 2011).

By referring the equation to the “parabola” in axis **OZ** and **Oξ//OX**, with origin in its vertex:

$$w^2 \frac{x^2}{2} - g z = 0 \Rightarrow z = \frac{w^2 \xi^2}{2g} = \frac{v^2}{2g}$$

Where velocity in a consider point is $v = w\xi$.

The **ordinate at any point** related to a plain that contains the vertex of the paraboloid, is equal to its Kinetics heights ($v^2/2g$), that correspond to velocity v (Pinho et al., 2011):

$$h_c = \frac{v^2}{2g}$$

In **rest**:

$$\text{volume } \mathbf{M'N'M''N''} \sim \text{water: } \pi D^2/4Z_1; \text{ air: } \pi D^2/4Z_2$$

In **movement**:

$$\text{volume } \mathbf{ar} \sim 1/2 \pi D^2/4Z = \pi D^2(Z_1 + Z_2)/2$$

Because volumes of air are equals:

$$\pi D^2/4Z_2 = \pi D^2(Z_1 + Z_2)/2 \Rightarrow Z_2 = (Z_1 + Z_2)/2 \quad \text{or} \quad Z_1 = Z_2$$

Angular Velocity w_0 , where the vertex of the parabola hits the bottom of the reservoir:

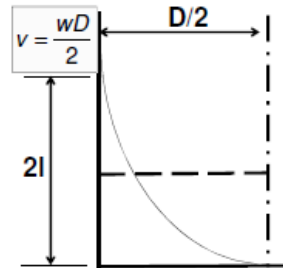


Figure 43 – Angular velocity w_0 where the vertex of the parabola hits the bottom of the reservoir (Pinho et al., 2011).

$$2I = \frac{v^2}{2g} = \frac{w_0^2 D^2}{8g} \Rightarrow w_0 = \frac{4\sqrt{gI}}{D}$$

Where, I is the height of water in rest.

For $w > w_0$ it is created an empty circular area with increasing radius proportional to w (Pinho et al., 2011).

Surfaces $p^* = \text{cte.}$ are cylinders of revolutions with axis coincident with two paraboloids of equation (Pinho et al., 2011):

$$\rho \frac{w^2 x^2}{2} = \text{cst.}$$

3.2 Liquid manometer

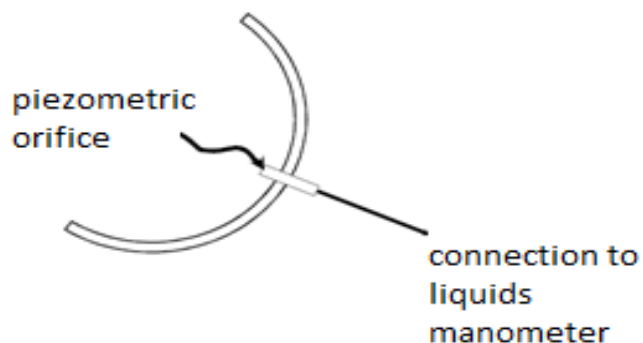


Figure 44 – Connection (Pinho et al., 2011).

Vertical piezometers

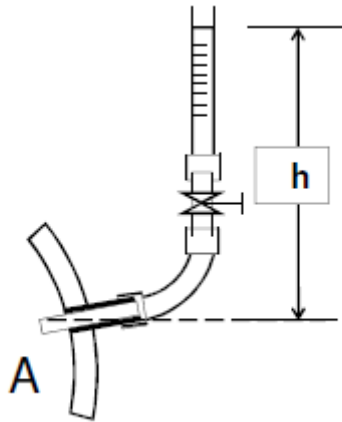


Figure 45 – Vertical piezometers (Pinho et al., 2011).

Effective pressure in A:

$$p = \gamma h$$

Where:

γ is the liquids specific weight (cst.);

h are the differences of level between the free surface of the liquid and the point A.

Inclined piezometers

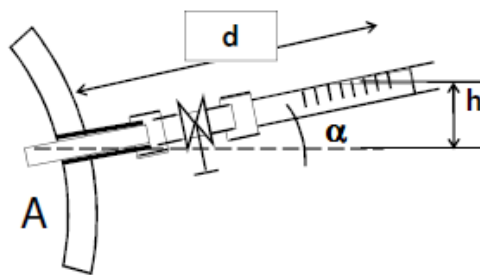


Figure 46 – Inclined piezometer (Pinho et al., 2011).

$$\text{For } h \ll d: d = \frac{h}{\sin \alpha}$$

$$p = \gamma h = \gamma d \sin \alpha$$

Manometers of U-Tube

Manometers of U-Tube are normally use for effectives pressures that are too high or too low (Pinho et al., 2011).

For high effective pressures:

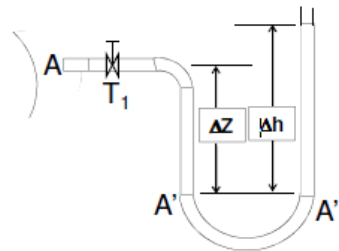


Figure 47 – High effective pressures (Pinho et al., 2011).

$$\gamma_m > \gamma \wedge p_{A'} = p_{A''} \Rightarrow p_A + \gamma \Delta Z = \gamma_m \Delta h \Rightarrow p_A = \gamma_m \Delta h - \gamma \Delta Z$$

For low effective pressures:

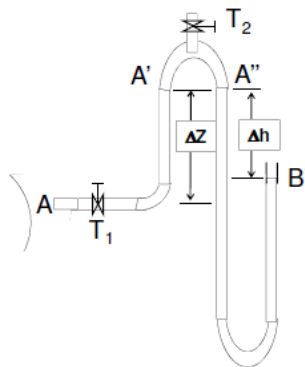


Figure 48 – Low effective pressures (Pinho et al., 2011).

$$\gamma_m < \gamma \wedge p_{A'} = p_{A''} \Rightarrow p_A - \gamma \Delta Z = -\gamma_m \Delta h \Rightarrow p_A = \gamma \Delta Z - \gamma_m \Delta h$$

For manometers **with different liquids non-miscible** is used the **adopted methodology** (Pinho et al., 2011).

Differential manometers

$\gamma_m > \gamma$

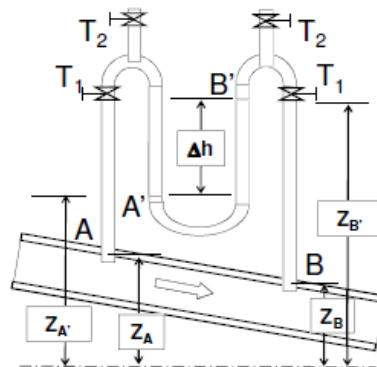


Figure 49 – Differential manometers, $\gamma_m > \gamma$ (Pinho et al., 2011).

In the last figure, T_1 and T_2 represent, respectively, sectioning valves or isolation valves and purge valves (Pinho et al., 2011).

$$A \rightarrow A': \quad Z_A + \frac{p_A}{\gamma} = Z_{A'} + \frac{p_{A'}}{\gamma} \quad (1)$$

$$B \rightarrow B': \quad Z_B + \frac{p_B}{\gamma} = Z_{B'} + \frac{p_{B'}}{\gamma} \quad (2)$$

$$A' \rightarrow B': \quad Z_{A'} + \frac{p_{A'}}{\gamma_m} = Z_{B'} + \frac{p_{B'}}{\gamma_m} \Rightarrow p_{A'} - p_{B'} = \gamma_m(Z_{B'} - Z_{A'}) \quad (3)$$

$$(1) - (2): \left(Z_A + \frac{p_A}{\gamma} \right) - \left(Z_B + \frac{p_B}{\gamma} \right) = \frac{p_{A'} - p_{B'}}{\gamma} + Z_{A'} - Z_{B'} \Rightarrow$$

$$\Rightarrow \text{replacing. (3):} \left(Z_A + \frac{p_A}{\gamma} \right) - \left(Z_B + \frac{p_B}{\gamma} \right) = \frac{\gamma_m - \gamma}{\gamma} (Z_{B'} - Z_{A'}) \Rightarrow$$

$$\Rightarrow p_A - p_B = (\gamma_m - \gamma)\Delta h - \gamma(Z_A - Z_B) \Rightarrow$$

$$\Rightarrow p_A - p_B = (\gamma_m - \gamma)\Delta h$$

$$\gamma_m < \gamma$$

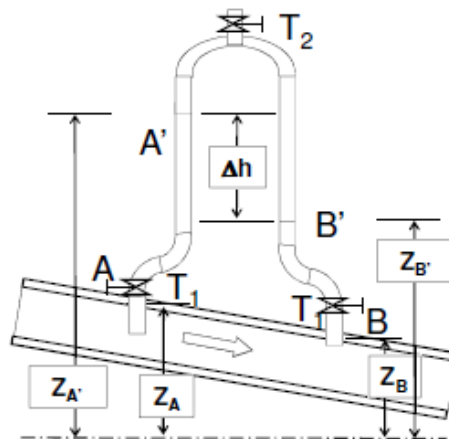


Figure 50 – Differential manometers, $\gamma_m < \gamma$ (Pinho et al., 2011).

In upper figure, T_1 and T_2 represent, respectively, isolation or sectioning valves and purge valves (Pinho et al., 2011).

Reservoirs

$$p_A - p_B = (\gamma - \gamma_m)\Delta h - \gamma(Z_A - Z_B) \Rightarrow$$

$$\Rightarrow p_A - p_B = (\gamma - \gamma_m)\Delta h$$

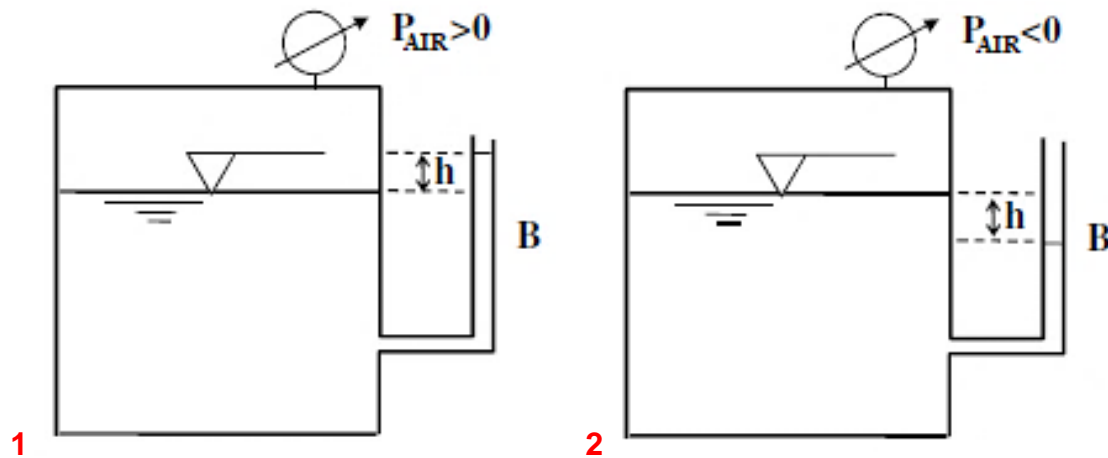


Figure 51 – Manometers in reservoirs (Pinho et al., 2011).

$$h = \frac{p_{AIR}}{\gamma} \text{ for } p_{AIR} > 0 \text{ (Fig. 51.1)}$$

or

$$p_{AIR} < 0 \text{ (Fig. 51.2)}$$

3.3 Hydrostatics impulsions in surfaces

3.3.1 Concept

It is called **hydrostatic impulsion** to the resultant forces of pressure, that a fluid creates over a contact-surface (if exists the resultants forces or force) (Vasconcelos, 2005).

It is called elemental pressure force over an elemental area (**dA**), where pressure is considered constant (Vasconcelos, 2005).

Pressure forces has only a o unique resultant force, if elemental forces are concurrent or parallels, which happens on plain, cylindrical or spherical curved surfaces (Vasconcelos, 2005).

Due to its uniqueness, it must be defined: the modulus, direction, sense and application point. The application point of impulsion is called center of impulsion (Vasconcelos, 2005).

3.3.2 Hydrostatics impulsions on plain surfaces

Hydrostatics impulsions on an element of plain surface (Pinho et al., 2011):

$$dF_1 = (p_a + \rho gZ) dS \wedge dF_2 = p_a dS$$

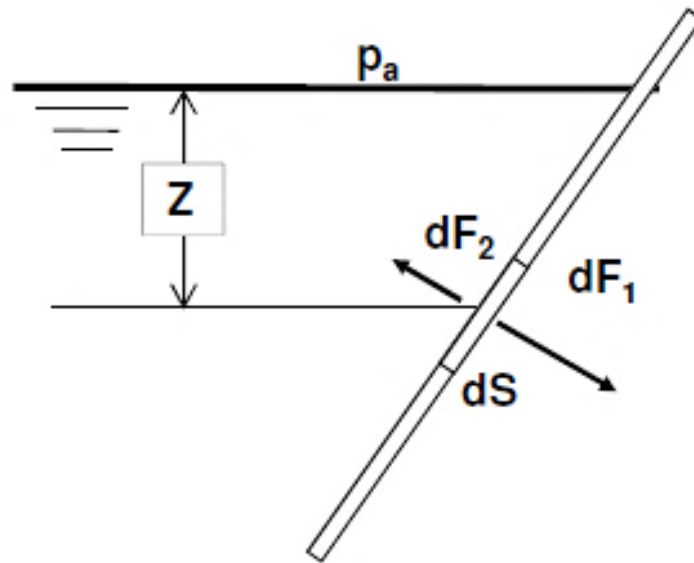


Figure 52 – Hydrostatic impulsion on an element of plain surface (Pinho et al., 2011).

Resultant:

$$dF = dF_1 - dF_2 = \gamma Z dS$$

Considering a plain surface (S) submersed in liquid, with angle θ respect to the horizontal (free surface) (Pinho et al., 2011):

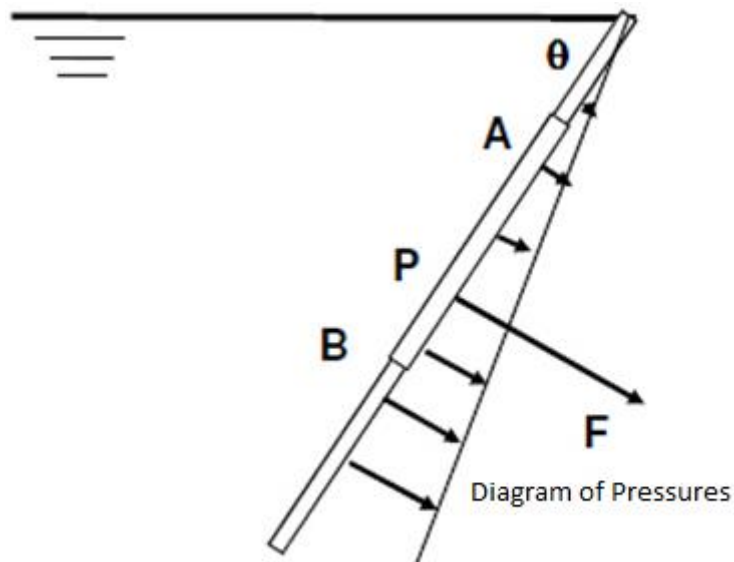


Figure 53 – Plain surface submerge in liquid (Pinho et al., 2011).

Where:

F is the resultant of pressures;

P is the center of pressure (application point of F).

Methodology

It's pretended to determine **the value of F** and the **position of the application point of F (Z_P)** (Pinho et al., 2011):

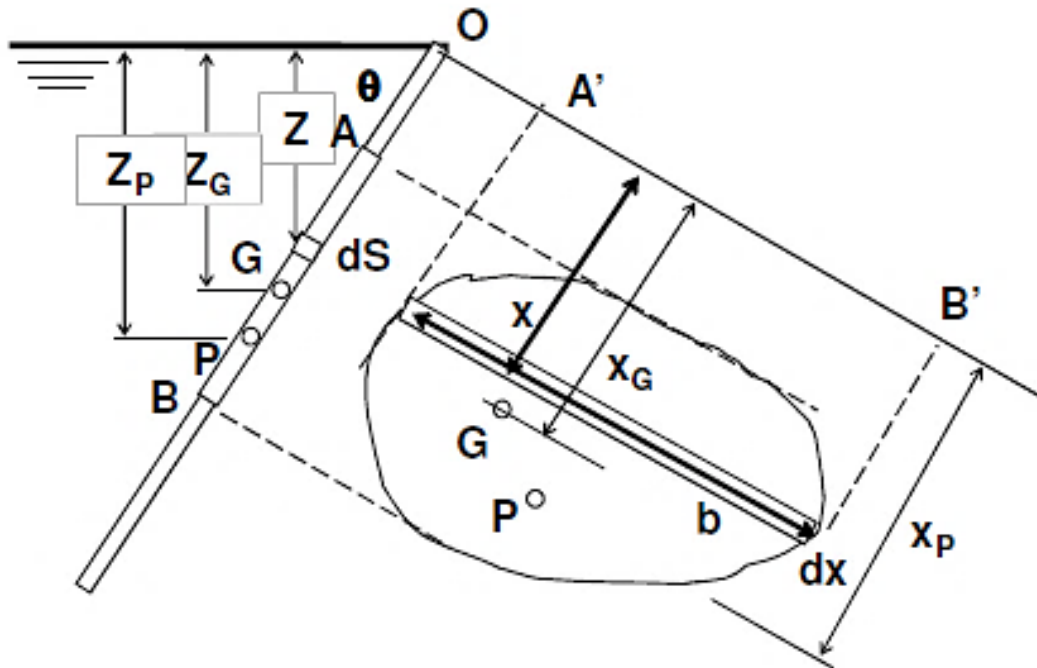


Figure 54 – Example of hydrostatic impulsion on a plain surface (Pinho et al., 2011).

1. Value of F:

In dS , it is possible to assume the constant hydrostatical pressure as γZ .

Leading to a resultant:

$$dF = \gamma Z dS = \gamma Z b dx \quad \text{ou} \quad dF = \gamma b x dx \sin \theta$$

Where, when integrating the resulting of the whole surface S is:

$$F = \gamma \sin \theta \int b x dx$$

And by knowing that, the static moment in S related to OB' :

$$\int b x dx = S x_G = S \frac{Z_G}{\sin \theta}$$

Then:

$$F = \gamma \sin \theta S \frac{Z_G}{\sin \theta} \Rightarrow F = \gamma S Z_G$$

2. Value of Z_P :

The resultant momentum is equal to the summation of the component's momentums (in relation to **OB'**) (Pinho et al., 2011):

$$F_{x_P} = \gamma \sin \theta \int b x^2 dx$$

$$\begin{cases} F = \gamma S Z_G \\ x_P = \frac{Z_P}{\sin \theta} \end{cases} \Rightarrow \gamma S Z_G x_P = \gamma \sin \theta \int b x^2 dx \Rightarrow S Z_G Z_P = \sin^2 \theta \int b x^2 dx \Rightarrow$$

$$\Rightarrow Z_P = \frac{\sin^2 \theta \int b x^2 dx}{S Z_G}$$

Knowing that the momentum of inertia **I'** of **S** related **OB'**:

$$\int b x^2 dx = I'$$

Then:

$$Z_P = \frac{I' \sin^2 \theta}{S Z_G}$$

For surface **S**, that is perpendicular to the free surface ($\theta = \pi/2$, $\sin^2 \theta = 1$):

$$Z_P = \frac{I}{S Z_G}$$

It is important to realize that, the center of pressure is always under the center of gravity:

$$Z_P = \frac{I' \sin^2 \theta}{S Z_G} \Rightarrow x_P \sin \theta = \frac{I' \sin^2 \theta}{S x_G \sin \theta} \Rightarrow x_P = \frac{I'}{S x_G}$$

By **Huyghens Theorem**:

$$I' = I_G + S x_G^2$$

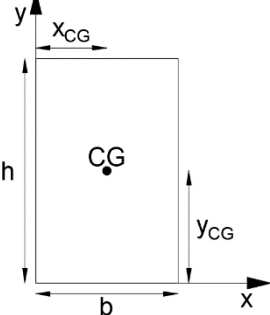
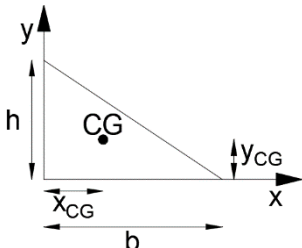
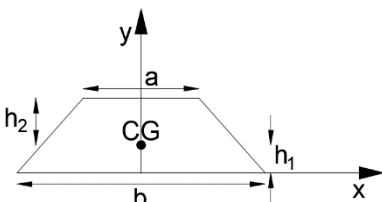
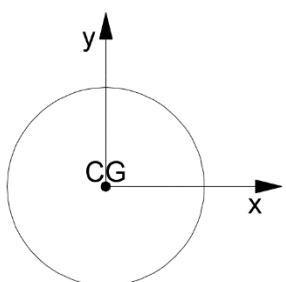
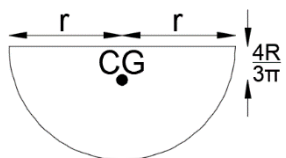
Then:

$$x_P = x_G + \frac{I_G}{S x_G} > 0$$

$$x_P > x_G$$

Gravity centers and momentum of inertia

Table 6 – Centers of gravity and momentums of inertia for commons plain surfaces (Gaspar, 2005).

Plain Surface	Center	Inertia
Rectangle 	$x_{CG} = \frac{b}{2}$ $y_{CG} = \frac{h}{2}$	$I_{x_{CG}} = \frac{bh^3}{12}$
Triangle 	$x_{CG} = \frac{b}{3}$ $y_{CG} = \frac{h}{3}$	$I_{x_{CG}} = \frac{bh^3}{36}$
Trapezium 	$h_2 = \frac{h}{3} \cdot \frac{a + 2b}{a + b}$ $h_1 = \frac{h}{3} \cdot \frac{2a + b}{a + b}$	$I_{x_{CG}} = \frac{h^3(a^2 + 4ab + b^2)}{36(a + b)}$
Circle 	$x_{CG} = 0$ $y_{CG} = 0$	$I_{x_{CG}} = \frac{\pi r^4}{4}$
Semicircle 	$y_{CG} = \frac{4r}{3\pi}$	$I_{x_{CG}} = 0,1098 r^4$

3.3.3 Hydrostatics impulsions in curved surfaces

When a surface is **not plain**, elemental forces are not paralleling and the force system is **not equivalent** to a unique force. So, it is possible to re-define the components of the resultant vector in the coordinate's axis (Pinho et al., 2011):

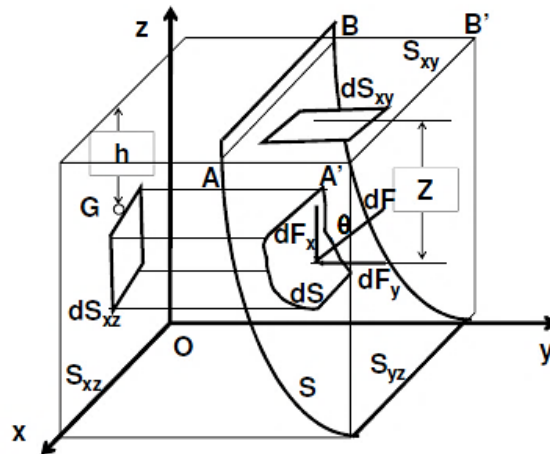


Figure 55 – Example of a curved surface (Pinho et al., 2011).

Where θ is the angle of dF respect OZ .

The pressure force applied in the elemental area dS :

$$dF = p \, dS$$

Being Z , the deepness of the elemental area dS :

$$dF = \rho g z \, dS \rightarrow \begin{cases} \text{Horizontal Component: } dF_y = \rho g z \, dS \sin \theta \\ \text{Vertical Component: } dF_z = \rho g z \, dS \cos \theta \end{cases}$$

Horizontal component

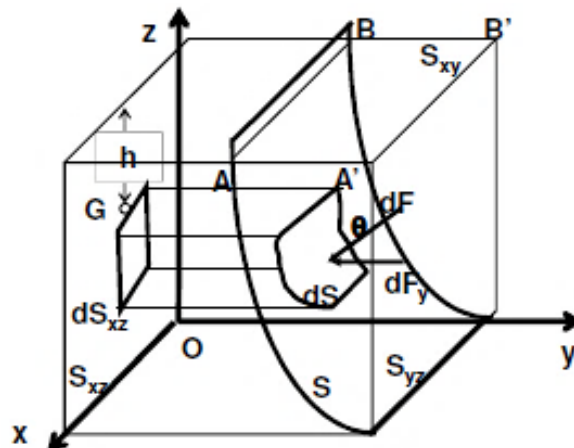


Figure 56 – Horizontal component of the pressure force (Pinho et al., 2011).

As $dS \sin \theta$ is the projection of dS_{xz} in a surface dS on the plain OXZ (Pinho et al., 2011),

$$dF_y = \rho g z dS_{xz}$$

and when expanding over all surface S :

$$F_y = \rho g \int_S z dS_{xz}$$

Being h the deepness of the gravity center of S_{xz} :

$$F_y = \rho g h S_{xz}$$

Where F_y is the hydrostatic resultant that is applied to the projection S_{xz} of the surface over a normal plain to OY .

Vertical component

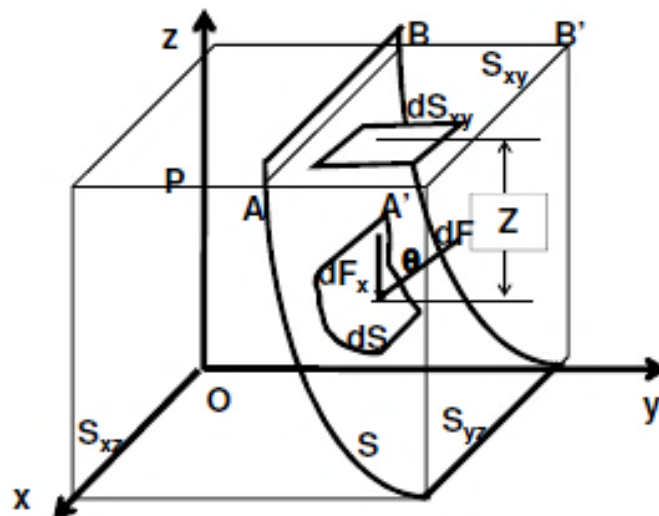


Figure 57 – Vertical component of pressure force (Pinho et al., 2011).

As $dS \cos \theta$ is the projection dS_{xy} of surface dS applied over plain OXY (Pinho et al., 2011),

$$dF_z = \rho g z dS_{xy}$$

Expanding over all surface S :

$$F_z = \rho g \int_S z dS_{xy}$$

Being h the deepness of gravity center of S_{xy} :

$$F_Z = \rho g h S_{XY}$$

Leading to, that F_Z is equal to the weight of the liquid that rest over the curved surface.

3.3.4 Hydrostatics impulsions on closed surfaces

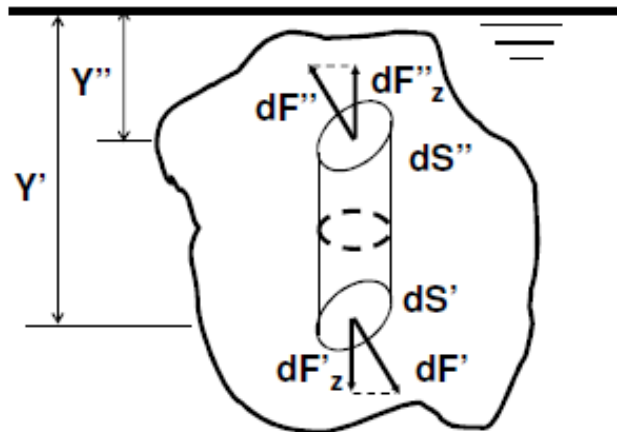


Figure 58 – Hydrostatics impulsions in closed surfaces (Pinho et al., 2011).

$$\begin{cases} dF' = \gamma y' dS' \\ dF'' = \gamma y'' dS'' \end{cases} \xrightarrow{\text{In vertical projection}} \begin{cases} dF'_Z = \gamma y' dS \\ dF''_Z = \gamma y'' dS \end{cases}$$

By extracting in order:

$$dF'_Z - dF''_Z = \gamma(y' - y'') dS$$

Where $\gamma(y' - y'') dS$ is the liquid's weight inside an elemental cylinder.

The vertical component of the resultant F_Z of pressure forces (Pinho et al., 2011):

$$F_Z = \int_S (dF'_Z - dF''_Z) = \text{Total Liquid's Weight}$$

The resultant force of pressure forces inside a closed surface is vertical and equal to the weight of the liquid contained inside. **With other words:** a solid immerse in a liquid is submitted to an upward impulsion, equal to the weight of the displaced volume, such reaction is known as the **Arquimedes Principle** (Pinho et al., 2011).

3.3.5 Uniform pressures applied to the liquid mass

Let's S be a curved surface that enclose a volume of a non-heavy liquid at some pressure p (Pinho et al., 2011):

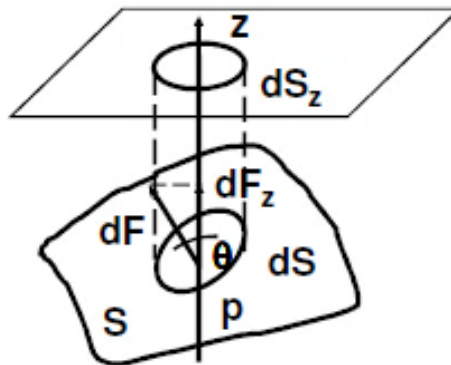


Figure 59 – Uniform pressures applied to a liquid mass (Pinho et al., 2011).

Over dS acts some force:

$$dF = p \, dS$$

And its component according to the projection in OZ :

$$dF_z = p \, dS \cos \theta = p \, dS_z$$

By integrating:

$$F_z = p \int_S dS_z$$

F_z , resultant of the forces created by uniform pressure projected according OZ , that act over a curved surface, is equal to the force of uniform pressure that acts in the projection of that surface over a plane perpendicular to OZ axis. **Note:** this conclusion is valid for any direction (Pinho et al., 2011).

Practical approach: dimension of a cylindrical body under a uniform pressure (boiler or pipe under pressure), cf. Figure 60 (Pinho et al., 2011).

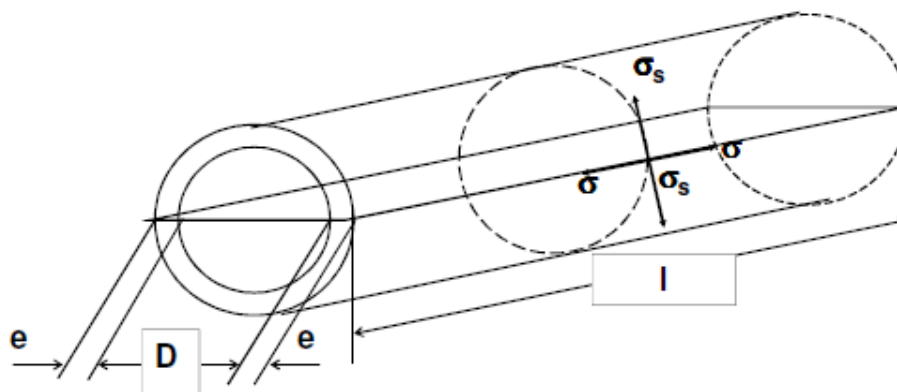


Figure 60 – Cylindrical body subjected to uniform pressure (boiler or pipe under pressure) (Pinho et al., 2011).

By studying the upper part (a longitudinal cut cylinder of two equals parts) (Pinho et al., 2011):

1. Resultant of pressure forces in transversal direction

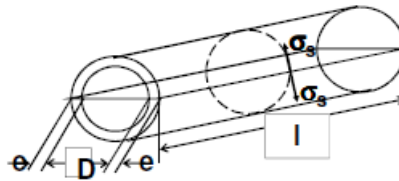


Figure 61 – Resultant of pressure forces in transversal direction (Pinho et al., 2011).

$$F_p = D \cdot l \cdot p$$

Where, $D \cdot l$ is the projected area of the lateral surface on a diametral plain.

To this force resist a plate with two sections of area $e \cdot l$, and if the material is under some tension σ_s (Pinho et al., 2011), then:

$$Dlp = 2el\sigma_s \Rightarrow e = \frac{pD}{2\sigma_s} \Rightarrow \sigma_s = \frac{pD}{2e}$$

2. Resultant of pressure forces in longitudinal direction

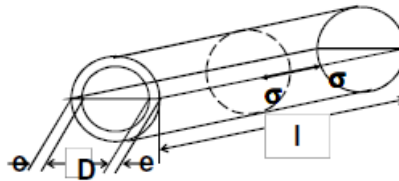


Figure 62 – Resultant of the pressure forces in longitudinal direction (Pinho et al., 2011).

$$F_p = p \frac{\pi D^2}{4}$$

$$p \frac{\pi D^2}{4} = \pi De\sigma \Rightarrow e = \frac{pD}{4\sigma} \Rightarrow \sigma = \frac{pD}{4e} = \frac{\sigma_s}{2}$$

3.4 Pascal Principle

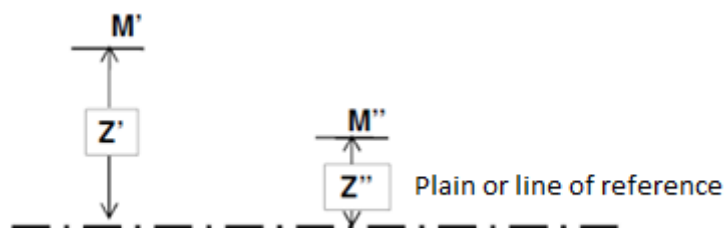


Figure 63 – Pascal Principle (Pinho et al., 2011).

By admitting a liquid in equilibrium (Pinho et al., 2011):

$$p'' - p' = -\gamma(z'' - z')$$

If pressure vary, without affecting equilibrium in M' of $\Delta p'$, then in M'' pressure will increase $\Delta p''$. As an **incompressible liquid** (Pinho et al., 2011):

$$(p'' + \Delta p'') - (p' + \Delta p') = -\gamma(z'' - z') \Rightarrow \Delta p' = \Delta p''$$

Pascal Principle: At a liquid mass in equilibrium, pressures variations are integrally and equally transmitted to every point of the liquid mass (Pinho et al., 2011).

Practical approach: Hydraulic press (Figure 64) (Pinho et al., 2011).

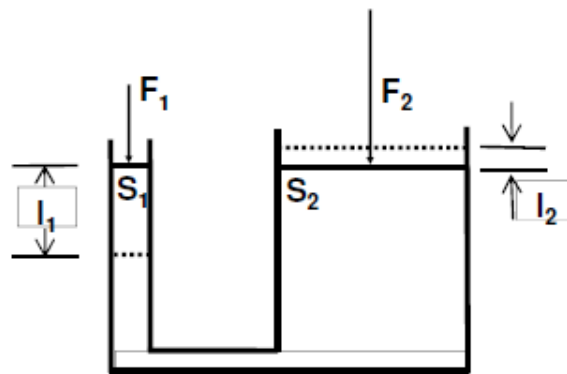


Figure 64 – Hydraulic press (Pinho et al., 2011).

$$\begin{cases} F_1 = pS_1 \\ F_2 = pS_2 \end{cases} \wedge S_1 l_1 = S_2 l_2 \Rightarrow \frac{F_1}{F_2} = \frac{S_1}{S_2} = \frac{l_2}{l_1} \therefore \underbrace{F_1 l_1 = F_2 l_2}_{\text{Equations that shows work conservation}}$$

3.5 Equilibrium in floating bodies

3.5.1 Impulsion. Arquimedes Principles

A floating body must have a lower weight than the weight of the displaced liquid volume. So, in order to have a floating body, its volumetric mass or density must be lower than liquid's one (Mata-Lima, 2010).

In this case, total body weight is equal to the product of the immerse volume and its specific or volumetric weight. The immersed portion of the body is called by Brazilian literature, as *carena* or *querena*, that in English is well-known as keel (Mata-Lima, 2010).

It also is usual to call the center of gravity of the immersed part as a **floating center** (or *carena*), which correspond to the impulsion's application point (Mata-Lima, 2010).

Arquimedes principle was announced for first time by Arquimedes, and can be stated as: “Any body immerse in a fluid in rest, is under the action of an upward vertical force created by the displaced fluid and which intensity (I) is equal to the weight of that displaced fluid (P).”, cf. Figure 65 (UALG, 2018)

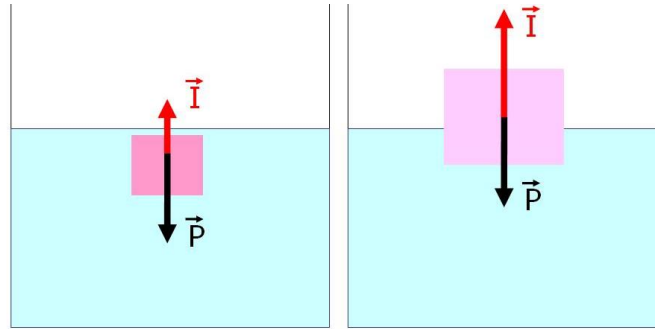


Figure 65 – Impulsion (<http://blogcfqmariana.blogspot.pt/2015/>).

Notation:

m , immersed fluid mass;
 V , immersed fluid volume;
 ρ , density or specific mass of the fluid;
 g , gravitational acceleration;
 I , impulsion force.

The Arquimedes Principle is expressed by the equation (UALG, 2018):

$$I = gV\rho$$

As the weight of the body is given by the product between the mass and the gravitational acceleration ($m \cdot g$), it can be said that (UALG, 2018):

- $V\rho < m$, the body sink;
- $V\rho = m$, the body stay in **metastable equilibrium**;
- $V\rho > m$, the body floats.

When a body is denser than fluid, immerse totally (sinks), and it can be appreciated that the value of its weight is apparently lower than in the air. The difference between those two values (real weight and apparent weight) correspond to the impulsion created by the displaced fluid (UALG, 2018):

$$\text{Apparent Weight} = \text{Real Weight} - \text{Impulsion}$$

If the mass of the immersed body is expressed as the product of its average density (ρ_c) and volume (V), then, Arquimedes criteria assumed the next mathematical form or interpretation (UALG, 2018):

- $\rho < \rho_c$, the body sink;
- $\rho = \rho_c$, the body stay in **metastable equilibrium**;
- $\rho > \rho_c$, the body floats.

3.5.2 Definitions. Fundamental theorems

Metastable state

A **metastable** correspond to any state different than the state of stable equilibrium, (different than thermodynamic equilibrium) which have associated a restriction that avoid any transition to a more stable state without any significant external perturbation. So, the system can stay in such state for a long period of time, without changing to a more stable state. At any case, under the influence of an external or internal action, the system will tend to transit to a more stable state (Eisberg & Resnick, 1979):

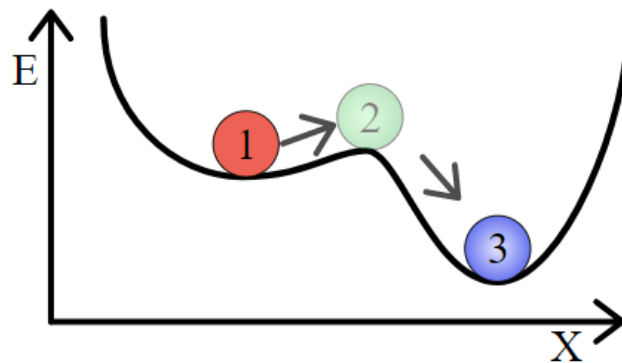


Figure 66 – Classical unidimensional representation of a system with a meta-state (1), unstable state (2) and a stable state (3) (<https://commons.wikimedia.org/>).

The ball is assumed to be static in each of the indicated points. In the vertical axis is represented the height, that is directly related to the systems potential energy, which in this case correspond to total system energy, and the horizontal axis correspond to the spatial position of the ball along the ramp (Eisberg & Resnick, 1979).

Hydrostatic Pressure and Impulsion

Pressure is defined as force per unit area. Pressure in a point located at some deepness **h** in a fluid is obtained by **Stevin Law** (Martins, 2010):

$$p = p_o + \rho gh = p_o + \gamma h$$

Where:

- p pressure at that point;
- p_o pressure at surface;
- ρ fluids density;
- g gravitational acceleration;
- h immersion deepness;
- γ fluids specific weight.

Active pressure at some point, correspond to the fluids weight per unit area, located above such point, and including **the acting atmospheric pressure at fluids surface**

(p_0). When we deal with **water**, pressure increase around **1 atm (10^5 N/m^2) each 10 immersed meters** (Martins, 2010).

The hydrostatic pressure that acts along the surface of a sunken body, create a force. When this force is integrated along bodies contour, results in **impulsion (I)**, which is responsible of its fluctuation (Martins, 2010).

So, to determine an impulsion, the acting pressure field must be integrated along surface, expressed as (Martins, 2010):

$$\vec{I} = \oint_S p \, d\vec{S}$$

Where **S** is bodies surface and **p** the acting pressure in the element of area **dS**.

When a block is totally immersed, the acting pressure field in its faces can be represented as in Figure 67. The figure shows a body in such position, that face is parallel to fluids surface (Martins, 2010).

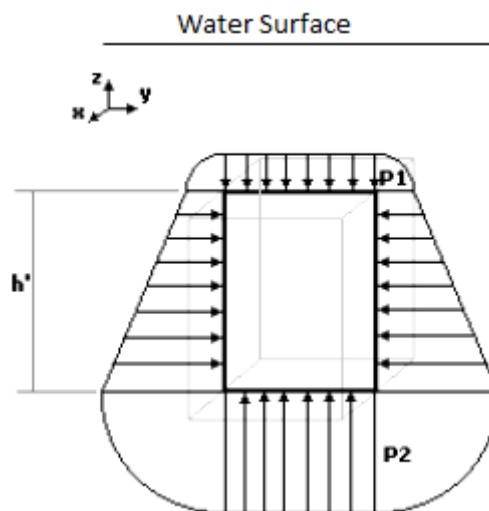


Figure 67 – Immersed block (Martins, 2010).

The acting pressures fields in the vertical faces of the block are identical, because the acting pressure at some deepness is constant. So, therefore, the resultant of the forces that act in the horizontal direction are null (Martins, 2010).

The resultant force in the superior face has a modulus of $F_s = A_s \cdot p_s$, where p_s is the acting pressure acting in that face and A_s is the area of the face. Analogously, the resultant force in the inferior face has a modulus of $F_i = A_i \cdot p_i$, where p_i is the acting pressure in the inferior face and A_i is area of that face (Martins, 2010).

As $p_i = \rho \cdot g \cdot h' + p_s$ and impulsion is the resultant of the acting forces due to the hydrostatic pressure field, can be expressed (Martins, 2010):

$$I = F_i - F_s = (\rho g h' + p_s) A_s - p_s A_s$$

Leading to:

$$I = \rho g \nabla$$

Where ∇ represents the immersed volume of the body or the volume of the displaced fluid.

By this way, the Impulsion modulus is equal to the displaced liquid weight. So, it can be verified that if the space occupied by a body in equilibrium and totally immerse in a stationary fluid, is filled with the same fluid, the acting pressure over this portion of fluid will be the same as the one acting on the body. In the same way, this portion of fluid, will also stay in equilibrium, can be affirmed that its weight is counteracted by impulsion (Martins, 2010).

This fact leads again to the Arquimedes Principle: “*Any body immerse in a fluid in rest, is under the action of an upward vertical force created by the displaced fluid and which intensity (I) is equal to the weight of that displaced fluid (P).*” (Martins, 2010)

Then, based in such principle, it is not necessary to integrate the pressures field over a body, in order to determine impulsion. So, it will be only necessary to know the weight of the displaced body. (Martins, 2010).

First example: when a body is composed by a material that is less dense than fluid in which it is immerse, can have an equilibrium position, floating in surface. Such a typical case are icebergs (Figure 68), which stay stable floating in water when the immerse portion creates enough impulsion to sustain its weight (Martins, 2010).

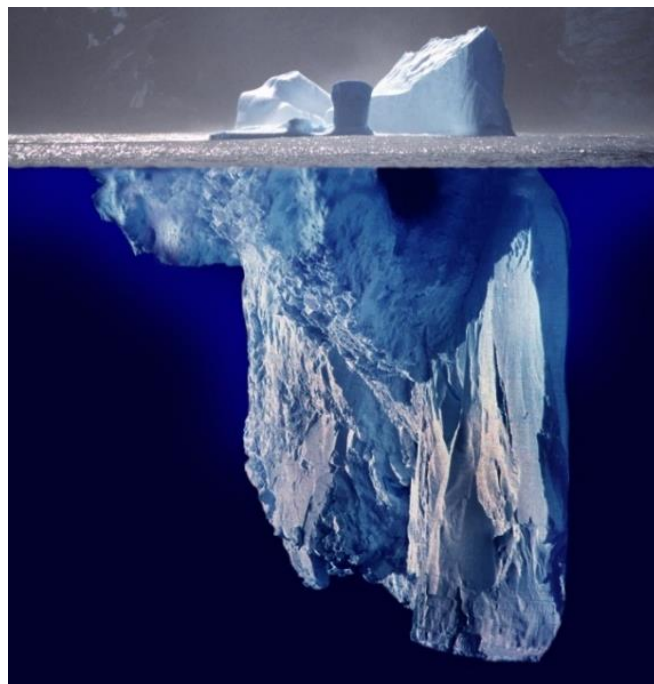


Figure 68 – Edited picture showing and whole Iceberg floating with most of its body immersed (<https://commons.wikimedia.org/>).

Then, let set V_i as the sunken volume of the iceberg, V_T is total volume and ρ_g ice density, the equilibrium condition turns to:

$$I = \rho V_i = \rho_g V_T$$

Resolving in order to V_i :

$$V_i = \frac{\rho_g}{\rho} V_T = \frac{0.92 \text{ g/cm}^3}{1 \text{ g/cm}^3} V_T = 0.92 V_T$$

Then, is obtained that the immersed volume of an iceberg is equal to 92% of its total volume, letting only 8% over water surface; such condition leads to the phrase: *"It is just the top of the iceberg!"*.

Second example: an iron solid block of density 8.0 g/cm^3 with 80 kg is founded at the bottom of a water pool, (density 1.0 g/cm^3 and deepness 3.0 m). Then, it is tight with a cable up, and pushed out of water with constant velocity. Consider $g = 10 \text{ m/s}^2$. Which is the intensity of the force applied to the cable? Consider cable weight as zero (Martins, 2010).

The force on the cable will be the difference between the block weight and the acting impulsion, that is:

$$F = P - I$$

Where $P = m \cdot g = (80 \text{ kg}) \cdot (10 \text{ m/s}^2) = 800 \text{ N}$ and impulsion is:

$$I = V \cdot \rho_{\text{water}} \cdot g = \frac{m_{\text{block}}}{\rho_{\text{block}}} \cdot \rho_{\text{water}} \cdot g = \frac{(80 \text{ kg})}{(8.0 \text{ g/cm}^3)} \cdot (1.0 \text{ g/cm}^3) \cdot (10 \text{ m/s}^2) = 100 \text{ N}$$

Finally, $F = 800 \text{ N} - 100 \text{ N} = 700 \text{ N}$.

Displacement and Center of buoyance

Displaced volume (∇) of a body, is the volume of the fluid displaced by the immersed portion of the body, associated with the condition of **draft** (distance between the keel and the float-line, which represent the immersed portion of the ship or body). Can be applied a numerical method of integration (First Simpson Rule or Trapezius Rule) to calculate the displacement of a ship by its Immersed body geometry (Martins, 2010).

Knowing fluid density implicated, it is possible to determine **the weight of the displaced fluid (P)**, then:

$$P = \rho g \nabla$$

Remembering Arquimedes Principle, the acting buoyancy in the immersed portion will be also equal to **P**, and as it will be approached in the next section, the full body weight must be also equal to **P** in order to ensure floatability of it at this case (Martins, 2010).

It is usual to refer to loading condition of a ship by the term: **“displacement (Δ)”** instead of **“displacement volume (∇)”**. At this case, it will refer the ship’s weight instead of is displacement volume (Martins, 2010). Leading to:

$$\Delta = \gamma \nabla$$

where **γ** is the volumetric specific weight of the fluid [t/m^3].

Thus, is quite common to [ton] as a unit, where 1 metric tons of mass is equal to the mass of one tone of “sweet-water” (Martins, 2010).

Floatability center (B) is a theorical point in the center of the displaced volume, where all floatability can be considered. (The force) floatability or buoyancy always act upward. Can be calculated by a numerical method (Trapezium Rule or First Simpsons Rule), or by simple’s forms, by using some tables like Table 6 (Martins, 2010).

Note: in case of a composed figure, the center of gravity of that figure is calculated by the expression (Martins, 2010):

$$x_{CG} = \frac{\sum_{i=1}^n x_i A_i}{\sum_{i=1}^n A_i}; y_{CG} = \frac{\sum_{i=1}^n y_i A_i}{\sum_{i=1}^n A_i}$$

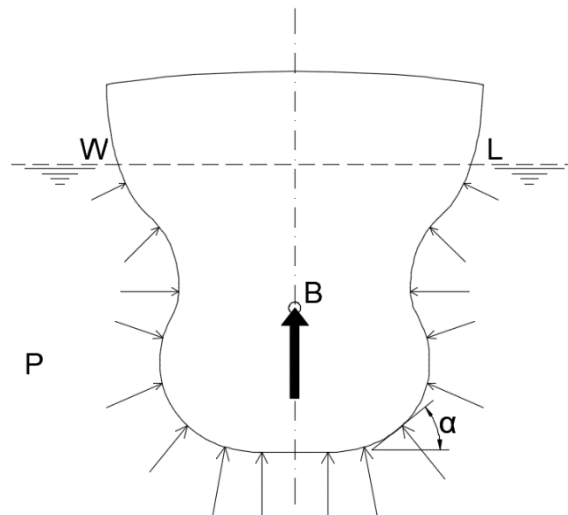


Figure 69 – Center of floatability or buoyancy and impulsion (adapted from PNA, 1988).

First example: Which is the draft and the buoyancy center of a ship that is 100 m long (c), with displacement $\Delta = 7000 \text{ t}$ and with uniform transversal section, like in Figure 70 (Martins, 2010).

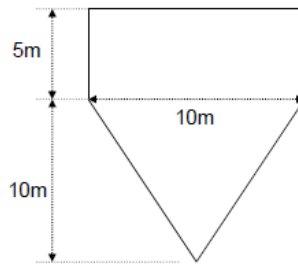


Figure 70 – Transversal section (uniform) of a ship (Martins, 2010).

In order to obtain the **value of draft**:

- Mass of the displaced water (Δ) is equal to the mass of the immersed part of the ship, with volume of displacement:

$$\nabla = \frac{\Delta}{\gamma} = \frac{7000 \text{ t}}{1 \text{ t/m}^3} = 7000 \text{ m}^3$$

- Knowing that the total volume of the ship is:

$$V_t = A \times c = (A_{\text{tri}} + A_{\text{ret}}) \times c = \left(\frac{10^2/2}{50} + \frac{10 \times 5}{50} \right) \times 100 = 10000 \text{ m}^3$$

- And knowing that the volume of the triangular section is $50 \times 100 = 5000 \text{ m}^3$, then, the draft or calado is above of it, and have a value greater than 10 m. where rest 2000 m^3 of water, that through the equation

$$\frac{2000 \text{ m}^3}{V_{\text{rect}} = 50 \times 100 = 5000 \text{ m}^3} = 0.4$$

- It is concluded that the sunken volume of the rectangular section corresponds to a height of immersion of $0.4 \times h_{\text{ret}} = 0.4 \times 5 \text{ m} = 2 \text{ m}$.

In this way, the **draft of the ship = 10 + 2 = 12 m**.

In order to obtain its **buoyancy center or floatability center (B_x, B_y)**:

- Using symmetry of the transversal section, it is admitted that the axis YY is located exactly in the center or gravity, leading to $B_x = 0 \text{ m}$;
- The axis XX is in the keel B_y will be determined based on the composed figure, rectangle of section $2 \times 10 \text{ m}^2$ (including draft) and a triangle of base 10 m and height of 10 m:

$$B_y = \frac{y_{\text{ret}} A_{\text{ret}} + y_{\text{tri}} A_{\text{tri}}}{A_{\text{ret}} + A_{\text{tri}}} = \frac{(1 + 10) \times (2 \times 10) + (10 - 10/3) \times (10^2/2)}{(2 \times 10) + (10^2/2)} \cong 7.9 \text{ m}$$

The **center of buoyance or floatability** has next **coordinates (0, 7.9) m**, in relation to the keel.

3.5.3 Equilibrium condition in buoyancy or floating bodies

The condition for anybody to stay in equilibrium, is a null resultant force and moments (summation), then (Martins, 2010):

$$\begin{cases} \sum F_{\text{externals}} = \vec{0} \\ \sum M_{\text{externals}} = \vec{0} \end{cases}$$

For a floating body, the first conditions are to have same weight as impulsion value, the second, that weight forces and impulsion act on the same influence lines. The second condition, means that the center of gravity and the center of buoyancy are on the same vertical axis, as shows Figure 71 (Martins, 2010).

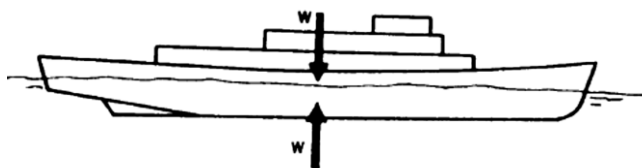


Figure 71 – Longitudinal equilibrium condition (Fonte: Lewis, 1988).

This **equilibrium position** is called **stable or positive**, if a small perturbation induces to forces or momentums that act in order to return the body back to its initial position. And if a small displacement or perturbation induce forces or momentums that does not return the body to its initial position, instead the opposite, the equilibrium position is called **unstable or negative**. But there is also an estate of **neutral or indifferent equilibrium**, where any displacement or perturbation always lead to a new position of equilibrium. Figure 72 shows such conditions (Martins, 2010).

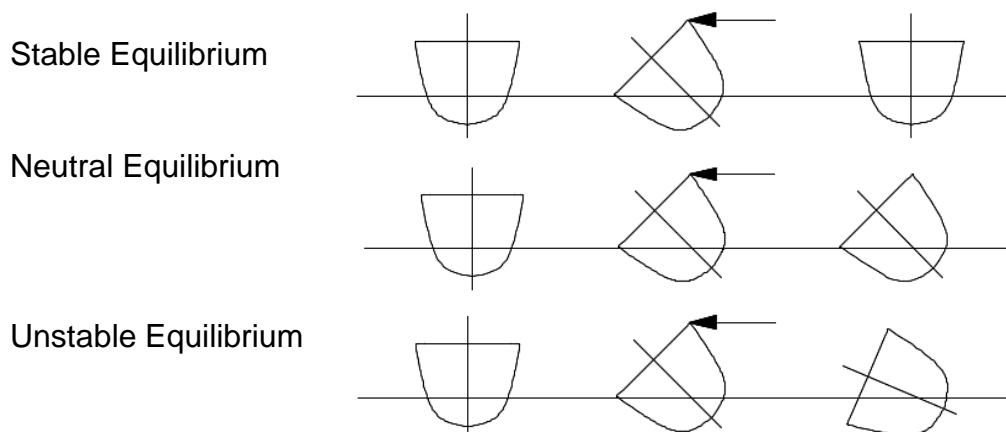


Figure 72 – Conditions of equilibrium (adapted from, 2010).

The position **related to the center of gravity or floatability center** define also the **equilibrium condition**. In totally immersed bodies, the position of the buoyancy center or floatability is fixed due to no variation of immerse geometry (is sunken) when a perturbation to the equilibrium condition is applied; such condition is known defined by the position of the center of gravity. In case **the center of gravity is over the center of floatability**, the equilibrium position will be **unstable**; **if it is under** will be **stable** and if **both coincide** equilibrium will be **indifferent** (Martins, 2010).

Figure 73 shows **conditions of stable and unstable equilibrium of sunken bodies**. In this figure, condition (a) represents a body in **unstable** equilibrium, with a center of gravity over the center of buoyancy. In such situation, a small perturbation will change the equilibrium position due to a binary that tend to increase the effect of the perturbation, as show situation (b). Case (c) represents a body in **stable** equilibrium, with gravitational center under buoyancy center. In such situation, a small perturbation will be consumed, and the position of equilibrium will remain due to a binary that acts attempting to return the body to its initial position, as shows situation (d) (Martins, 2010).

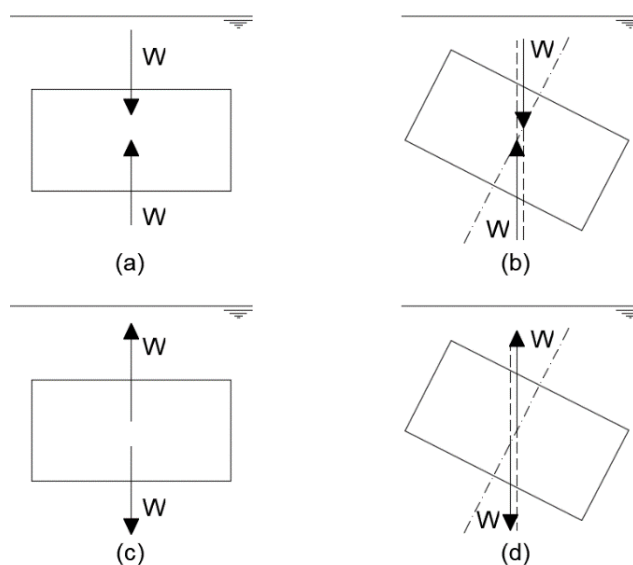


Figure 73 – Condition of equilibrium of immersed bodies (adapted from Lewis, 1988).

For **floating bodies, partially immerse**, the fact, that the center of gravity is above the center of floatability, does not implied necessarily a stable equilibrium condition. It is verified due to the change of the position of the center of buoyancy after a perturbation that modifies the geometry of the immersed body. Case (a) of Figure 74 shows such situation, where it is appreciable a condition of **stable** equilibrium. As the center of gravity get closer to its center of buoyance, a restoring moment (binary) increase, as confirmed in cases (c) and (d) of same figure. As the center of gravity elevates, the equilibrium point tents to instability (Martins, 2010).

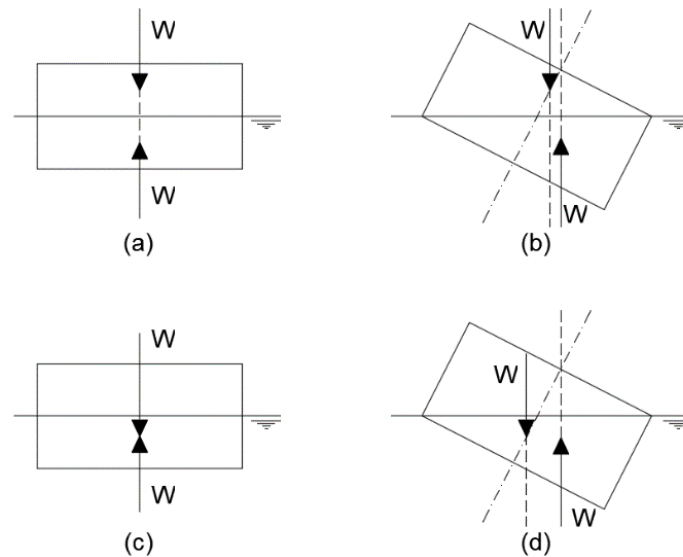


Figure 74 – Condition of equilibrium for floating bodies (adapted from Lewis, 1988).

Solved example: consider a recipient with **volume** equal to **v** and weight equal to **p** floating in sweet water. Until volume **(V)** of **liquid density ρ** , higher than water, is introduced in the recipient before losing its floatability (Martins, 2010).

At these types of exercises is essential to decompose the problem:

1. Floating recipient (Impulsion, I) in sweet water (density, ρ_a), of weight p and volume v;
2. Introducing a liquid of density ρ , that occupy a certain volume V and therefore with weight p_ρ ;
3. So, it has 3 forces: p (given data), $p_\rho = \rho \cdot V \cdot g$ e $I = \rho_a \cdot v \cdot g$. By following the statement, the total weight of the considered system is $p_T = p + p_\rho$, which must be inferior to I (following theory), so, in order to keep its buoyancy (start point) is state:

$$\begin{aligned}
 p_T &= p + p_\rho < I \Rightarrow \\
 \Rightarrow p + \rho V g &< \rho_a v g \Rightarrow \\
 \Rightarrow \rho V g &< \rho_a v g - p \Rightarrow \\
 \Rightarrow V &< \frac{\rho_a v g}{\rho g} - \frac{p}{\rho g} \Rightarrow V < \frac{\rho_a}{\rho} \cdot v - \frac{p}{\rho g}
 \end{aligned}$$

CHAPTER 4 - BERNOULLI THEOREM AND APPLICATIONS

4.1 Bernoulli theorem in local aspect.

4.1.1 Deduction of the local equation of Bernoulli

Flow's characteristic parameters are considered and expressed in term of **Lagrange variables**. For a system of material particles, **Lagrange equations** can be written as (Pinho et al., 2011):

$$\frac{d}{dt} \left(\frac{\partial L}{\partial \dot{q}_K} \right) - \frac{\partial L}{\partial q_K} = 0 \quad (K = 1, 2, \dots, n)$$

Where:

L Lagrange function of the particles system;

q_K is the general generic coordinate ($K = 1, 2, \dots, n$, system with n grades of freedom);

\dot{q}_K is the total derivative in order of time of the generalized coordinate q_K .

Apply it to a fluid particle that displace along its **trajectory** (only one grade of freedom) (Pinho et al., 2011):

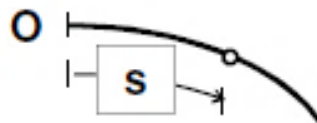


Figure 75 – Fluid particle that displace along its trajectory (Pinho et al., 2011).

$$\frac{d}{dt} \left(\frac{\partial L}{\partial \dot{s}} \right) - \frac{\partial L}{\partial s} = 0$$

as:

$$\dot{s} = \frac{ds}{dt} = v \Rightarrow \frac{d}{dt} \left(\frac{\partial L}{\partial v} \right) - \frac{\partial L}{\partial s} = 0$$

Where, Lagrangian (**L**) is defined by:

$$L = \underbrace{T}_{\text{kinetic Energy}} - \underbrace{U}_{\text{Potential Energy}}$$

Kinetic energy of a particle, of volume **dV** (mass **ρdV**), with speed **v** (Pinho et al., 2011):

$$T = \frac{1}{2} \rho v^2 dV \quad (\text{only in order of } v \text{ and not } s)$$

Potential energy of the same particle, explicit function of s . Can be decomposed in three parts (actions) (Pinho et al., 2011):

1. Forces per unit mass, \vec{G} : in hydraulics of heavy fluid is reduced to only gravitational actions;

2. Pressure forces, H_{ij} : acting perpendicular to the considered surface;

$$H_{ij} = \frac{1}{3} \tau_{kk} \delta_{ij} \quad (\text{Hidrostatic tensor})$$

3. Forces that express resistance of the medium, τ'_{ij} : represent an action that works in a opposite direction to movement.

$$\delta'_{ij} \quad (\text{Distorsional tensor})$$

Potential corresponding energies:

1. Potential energy due to particle weight (potential energy of position);

$$U_1 = \gamma z \, dV$$

Where, z is the vertical coordinate with upward direction.

2. Potential energy of pressure (piezometric potential energy);

$$U_2 = p \, dV$$

3. Potential energy due to mediums resistance.

$$U_3 = -\gamma H_r \, dV$$

Where, H_r is potential energy of resistance forces per unit weight, which means, the particles oppose to movement (H_r represent external actions over particle) (Pinho et al., 2011).

Then, **potential energy** (Pinho et al., 2011):

$$U = U_1 + U_2 + U_3 = \gamma z \, dV + p \, dV - \gamma H_r \, dV$$

Leading to:

$$L = \frac{1}{2} \rho v^2 \, dV - \gamma z \, dV - p \, dV + \gamma H_r \, dV$$

And by knowing that:

$$\frac{d}{dt} \left(\underbrace{\frac{\partial L}{\partial v}}_{\Rightarrow \rho v \, dV} \right) - \underbrace{\frac{\partial L}{\partial s}}_{-\gamma \frac{\partial z}{\partial s} dV - \frac{\partial p}{\partial s} dV + \gamma \frac{\partial H_r}{\partial s} dV} = 0$$

$$\Rightarrow \rho \frac{dv}{dt} dV$$

Also, considering mass (ρdV), weight (γdV) as constants:

$$\rho \frac{dv}{dt} dV + \gamma \frac{\partial z}{\partial s} dV + \frac{\partial p}{\partial s} dV - \gamma \frac{\partial H_r}{\partial s} dV = 0$$

Per unit of particle weight ($/\gamma dV$):

$$\frac{1}{g} \frac{dv}{dt} + \frac{\partial z}{\partial s} + \frac{1}{\gamma} \frac{\partial p}{\partial s} - \frac{\partial H_r}{\partial s} = 0$$

And as:

$$\frac{dv}{dt} = \frac{\partial v}{\partial t} + \frac{\partial v}{\partial s} \frac{ds}{dt} = \frac{\partial v}{\partial t} + \frac{\partial v}{\partial s} v = \frac{\partial v}{\partial t} + \frac{\partial}{\partial s} \left(\frac{v^2}{2} \right) \quad \wedge \quad \frac{\partial H_r}{\partial s} = j$$

Then, in term of Lagrange variables:

$$\frac{\partial}{\partial s} \left(z + \frac{v^2}{2g} \right) + \frac{1}{\gamma} \frac{\partial p}{\partial s} = - \frac{1}{g} \frac{\partial v}{\partial t} - j$$

Generalized local expression of Bernoulli theorem (in Lagrange coordinates), of movement of a particles of a heavy fluid flow along its trajectory and considering that does not exists any local singular resistance through the evaluated section (continuity of H_r and j is admitted). In case of an **incompressible fluid** (most usual in hydraulics) (Pinho et al., 2011):

$$\frac{\partial}{\partial s} \left(z + \frac{p}{\gamma} + \frac{v^2}{2g} \right) = - \frac{1}{g} \frac{\partial v}{\partial t} - j$$

Expression of Bernoulli theorem (valid only for Lagrange variables) for movement of a particle of an incompressible and heavy fluid along its trajectory (Pinho et al., 2011).

4.1.2 Interpretation of the local expression of Bernoulli theorem

Physical meaning (Pinho et al., 2011)

$$\frac{\partial}{\partial s} \left(z + \frac{p}{\gamma} + \frac{v^2}{2g} \right) = - \frac{1}{g} \frac{\partial v}{\partial t} - j$$

z is the elevation related to a horizontal plane of reference corresponding to the potential energy of position per unit weight (topographical height).

p/γ is the piezometric height of a particle. Corresponding to the potential energy of pressure of a fluid's particle per unit weight.

h = z + p/γ is piezometric elevation of the particle.

v²/2g is the kinetic height of a particle. Corresponding to Kinetic energy per unit weight of an animated particle of velocity v.

1/g · ∂v/∂t are inertial local forces per unit weight. Corresponding to the work done by local forces of inertia per unit weight and per unit of trajectory:

- Inertial forces: $F = -ma$;
- Particle of volume dV : $-\rho \cdot \partial v / \partial t \cdot dV$
- Per unit weight: $1/g \cdot \partial v / \partial t$

j is the work done per unit of weight and per unit of trajectory by forces that resist the particle's movement.

Total mechanical energy per unit weight of a particle

$$H = z + \frac{p}{\gamma} + \frac{v^2}{2g}$$

Variation of **H** per unit of trajectory:

$$\frac{\partial H}{\partial s} = \frac{\partial}{\partial s} \left(z + \frac{p}{\gamma} + \frac{v^2}{2g} \right)$$

Energy or **Charge**:

$$H \begin{cases} z, \text{ potential energy of position} \\ \frac{p}{\gamma}, \text{ potential energy of pressure} \\ \frac{v^2}{2g}, \text{ kinetic energy} \end{cases}$$

Per unit weight $\sim [L]$

Work done by forces of local inertia and by forces of medium resistance per unit weight and per unit of trajectory (Pinho et al., 2011):

$$-\frac{1}{g} \frac{\partial v}{\partial t} - j$$

Bernoulli theorem: variation of total mechanical energy is equal to a work done by local forces of inertia and resistance. All energy lost is due to work. **Bernoulli theorem** represents an equation of **energy balance** (Pinho et al., 2011).

Piezometric line and energy line (or charge line)

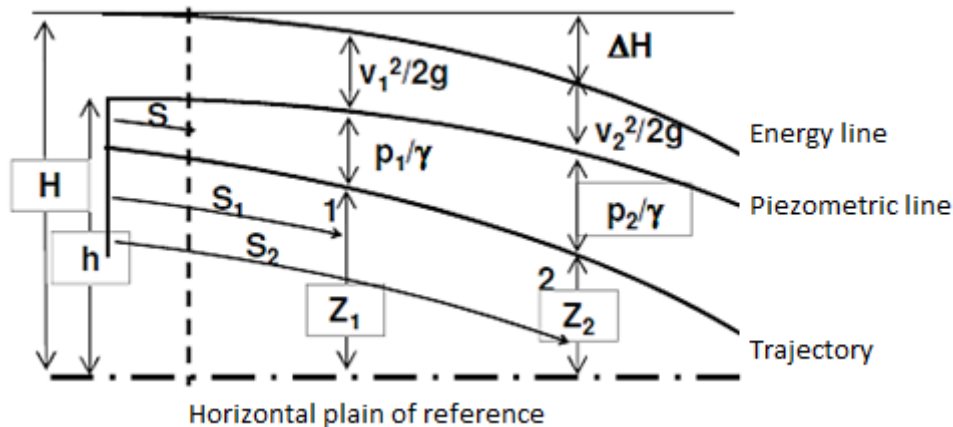


Figure 76 – Piezometric and energy line or charge (Pinho et al., 2011).

Z is the elevation of the points of a trajectory of a particle related to a horizontal plane of reference (topographic elevation) (Pinho et al., 2011).

Piezometric line is the geometric place of points, related to the horizontal plane of reference and the pressure installed in the pipe or system (Pinho et al., 2011):

$$h = z + \frac{p}{\gamma}$$

The piezometric height shows how high will get the fluid at some vertical pipe, open in his extremities and with its bottom connected or located in the considered point, usually, normal to trajectory (piezometer) (Pinho et al., 2011).

Energy line or charge is the geometrical place of points, in which its cartesian ordered is obtained by the summation of the piezometric elevation and the Kinetic elevation ($v^2/2g$) (Pinho et al., 2011):

$$H = z + \frac{p}{\gamma} + \frac{v^2}{2g}$$

Terms as **Charge** or **Energy** are used specially when a flow under pressure or a free surface flow is studied (Pinho et al., 2011).

From:

$$\frac{\partial H}{\partial s} = \frac{\partial}{\partial s} \left(z + \frac{p}{\gamma} + \frac{v^2}{2g} \right)$$

Applying between sections **1** and **2** (Figure 76), integrating:

$$\Delta H = H_1 - H_2 = \int_{S_1}^{S_2} \left(-\frac{1}{g} \frac{\partial v}{\partial t} - j \right) ds$$

where:

H_1 and H_2 represent the energy (charges) corresponding to the positions referenced by S_1 and S_2 , respectively;

ΔH represents energy losses (free surface flows) or loss of charges (flows under pressure).

Applying Bernoulli's equation to positions of particles **1** and **2** (Figure 76), is obtained:

$$z_1 + \frac{p_1}{\gamma} + \frac{v_1^2}{2g} = z_2 + \frac{p_2}{\gamma} + \frac{v_2^2}{2g} + \Delta H$$

The **energy line** is always downward in direction of the flow, since there is not external energy supply (Pinho et al., 2011).

By having **energy exchanges with the exterior** between S_1 and S_2 (supply or transfer), the Bernoulli's equations can be written as:

$$z_1 + \frac{p_1}{\gamma} + \frac{v_1^2}{2g} = z_2 + \frac{p_2}{\gamma} + \frac{v_2^2}{2g} + \Delta H \pm \Delta B$$

When in the expression is used **$+\Delta B$** , means transfer or loss of energy (ex.: turbine) and when is used **$-\Delta B$** , this variation represents energy supply (ex.: pump) (Pinho et al., 2011).

4.1.3 Bernoulli theorem applied to a permanent regime

Simplification from local equation (Pinho et al., 2011)

For a permanent flow:

$$-\frac{1}{g} \frac{\partial v}{\partial t} = 0$$

Form of the equation in terms of **Lagrange** coordinates, coincide with those in terms of **Euler's** variables:

$$\frac{\partial}{\partial s} \left(z + \frac{p}{\gamma} + \frac{v^2}{2g} \right) = -j$$

Where v can be interpreted as a **Euler's** variables.

$$H_r = H$$

In permanent movement, energy or charge represent the potential energy of resistance forces per unit of weight of particles that oppose to movement.

In **uniform regime** (stream tubes coincide with the trajectory of particles):

$$z_1 + \frac{p_1}{\gamma} + \frac{v_1^2}{2g} = z_2 + \frac{p_2}{\gamma} + \frac{v_2^2}{2g} + \Delta H$$

Can be applied, not only to positions **1** and **2** of a particle, but also to the characteristics of the flow in two points of a trajectory, and ΔH express the dissipated energy per unit weight and trajectory, by medium resistance forces.

Valid for two points of a same current line, when flow is incompressible and composed by a heavy fluid.

Losses of charge in uniform regime (Pinho et al., 2011)

Uniform regime:

$$\frac{\partial}{\partial s} \left(\frac{v^2}{2g} \right) = 0 \Rightarrow \frac{\partial}{\partial s} \left(z + \frac{p}{\gamma} \right) = -j \text{ ou } z_1 + \frac{p_1}{\gamma} - \left(z_2 + \frac{p_2}{\gamma} \right) = \Delta H$$

A loss of energy can be expressed by the difference of the piezometric elevations.

Uniform movement: the work of resistance forces per unit of weight and trajectory is constant at any point of its trajectory:

$$\Delta H = H_1 - H_2 = -j \int_{s_1}^{s_2} ds = j(s_2 - s_1)$$

Where L is a distance between **1** and **2**, measured along trajectory.

$$\Delta H = jL$$

$$z_1 + \frac{p_1}{\gamma} - \left(z_2 + \frac{p_2}{\gamma} \right) = \Delta H$$

And $j = \Delta H/L$ represents losses of energy per unit length.

Conclusion: in uniform movement, the line of energy is constant when trajectory is. And the piezometric line is also constant and parallel to the energy line ($v^2/2g = \text{cte.}$).

In sections where movement vary in short extensions, can be considered as abrupt drops of the energy line, which are called **local charges losses** (ΔH_L).

$$\Delta H = jL + \sum_{i=1}^n \Delta H_{L_i}$$

Where:

jL represents loss of uniform charge (main loss, steady);

$\sum \Delta H_{L_i}$ is the summation of all local charge losses (concentrated, accidental).

Considering an exchange of energy with the exterior, Bernoulli's equation for uniform movement can be write as:

$$z_1 + \frac{p_1}{\gamma} - \left(z_2 + \frac{p_2}{\gamma} \right) = jL + \sum_{i=1}^n \Delta H_{L_i} \pm \Delta B$$

Next figure shows graphically, the difference between a **uniform loss of charge** and **localized loss of charge**.

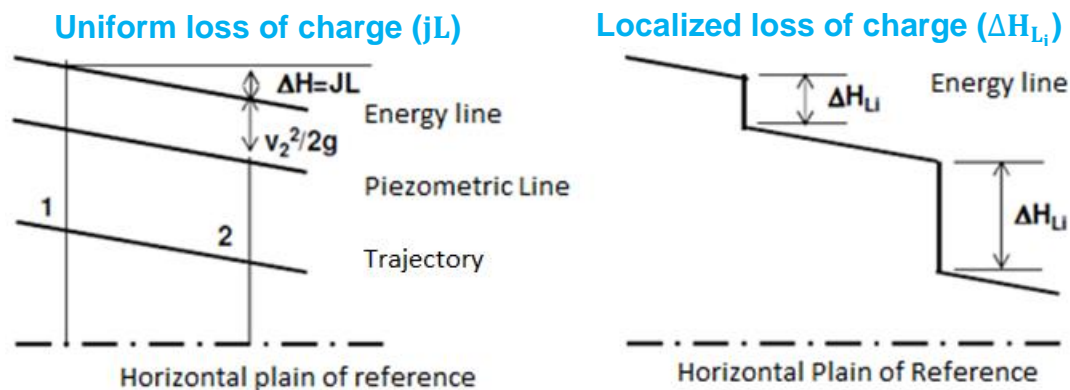


Figure 77 – Difference between two types of loss of charge (Pinho et al., 2011).

4.2 Bernoulli's theorem in global aspect

4.2.1 Application of the Bernoulli's theorem to a stream tube

The local expression of Bernoulli's theorem can be adapted to the totality of the fluid that flows in a **stream tube** (Figure 78) obtaining a **global expression** (Pinho et al., 2011).

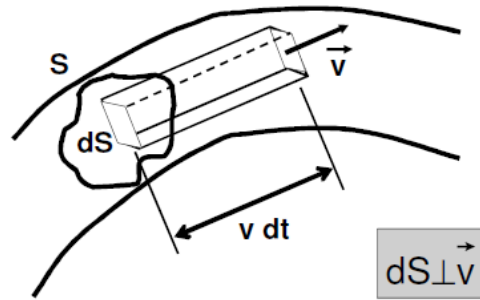


Figure 78 – Stream tube (Pinho et al., 2011).

So, again for a heavy and incompressible fluid, the local expression of Bernoulli's theorem is:

$$\frac{\partial}{\partial s} \left(z + \frac{p}{\gamma} + \frac{v^2}{2g} \right) = -\frac{1}{g} \frac{\partial v}{\partial t} - j \text{ (per unit weight)}$$

Flow rate that pass through **dS**:

$$dQ = v dS$$

Weight of a fluid that pass through **dS** per unit time:

$$\gamma v dS \frac{dt}{ds} = \gamma dQ$$

and now, applying the theorem to that fluids weight:

$$\begin{aligned} \frac{\partial}{\partial s} \left(z + \frac{p}{\gamma} + \frac{v^2}{2g} \right) &= -\frac{1}{g} \frac{\partial v}{\partial t} - j \Rightarrow \\ \Rightarrow \frac{\partial}{\partial s} \left(\left(z + \frac{p}{\gamma} \right) \gamma v dS \right) + \frac{\partial}{\partial s} \left(\frac{v^2}{2g} \gamma v dS \right) &= -\frac{1}{g} \frac{\partial v}{\partial t} (\gamma v dS) - j \gamma v dS \end{aligned}$$

So then, integrating the upper equation along all surface **S**, dividing by **γ** (cst.), which affects **z** and **p** of index **x** (values in a usual point, x, in a section):

$$\text{Knowing that } Q = \int_S v dS \Rightarrow \int_Q \frac{\partial}{\partial s} \left(z_x + \frac{p_x}{\gamma} \right) dQ + \frac{1}{2g} \int_Q \frac{\partial v^2}{\partial s} dQ = -\frac{1}{g} \int_Q \frac{\partial v}{\partial t} dQ - \int_Q j dQ$$

It is demonstrated that can be change at this equation, the order of operations of derivatives and integrals:

$$\frac{\partial}{\partial s} \int_S \left(z_x + \frac{p_x}{\gamma} \right) v dS + \frac{1}{2g} \frac{\partial}{\partial s} \int_S v^3 dS = -\frac{1}{g} \frac{\partial}{\partial t} \int_S v^2 dS - \int_S j v dS$$

4.2.2 Global coefficients of Bernoulli's equation

$$\underbrace{\frac{\partial}{\partial s} \int_S \left(z_x + \frac{p_x}{\gamma} \right) v \, dS}_1 + \underbrace{\frac{1}{2g} \frac{\partial}{\partial s} \int_S v^3 \, dS}_2 = - \underbrace{\frac{1}{g} \frac{\partial}{\partial t} \int_S v^2 \, dS}_3 - \underbrace{\int_S jv \, dS}_4$$

Global aspect of Bernoulli's theorems is obtained by introducing 3 coefficients that are defined as follows (Pinho et al., 2011).

A. Coefficient of pressure distribution (Pinho et al., 2011)

A.1. Linear flows (Pinho et al., 2011)

If trajectories have straight and parallel lines, the distribution of pressures is hydrostatic in that section of flow (straight section).

The piezometric elevation of any point (**x**) is equal to the piezometric height at a point (**P**) of the same section:

$$h_x = z_x + \frac{p_x}{\gamma} = h_p = z + \frac{p}{\gamma}$$

Part **1** takes the form:

$$\frac{\partial}{\partial s} \int_S \left(z_x + \frac{p_x}{\gamma} \right) v \, dS = \frac{\partial}{\partial s} \left[\left(z + \frac{p}{\gamma} \right) \int_S v \, dS \right] = \frac{\partial}{\partial s} \left[\left(z + \frac{p}{\gamma} \right) Q \right]$$

In this way, it will only exist one piezometric height for all section. So, by convention, **Z** refers to:

- Intersection of an axis of the stream tube with the axis's section (flow under pressure);
- So, in the section is the lowest topographic elevation (free surface flows).

Free surface flows:

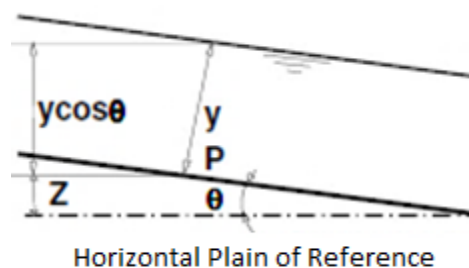


Figure 79 – Free surface flow.

Pressure at point **P**:

$$p = p_a + \gamma y \cos \theta$$

$$z + \frac{p}{\gamma} = z + y \cos \theta + \frac{p_a}{\gamma}$$

where p_a represents pressure in a free surface.

Part **1** takes the form:

$$\frac{\partial}{\partial s} \int_S \left(z_x + \frac{p_x}{\gamma} \right) v \, dS = \frac{\partial}{\partial s} \left[\left(z + y \cos \theta + \frac{p_a}{\gamma} \right) Q \right]$$

Defining $\xi = \cos \theta$ (coefficient of Boudin) and considering effective pressures:

$$\frac{\partial}{\partial s} \int_S \left(z_x + \frac{p_x}{\gamma} \right) v \, dS = \frac{\partial}{\partial s} [(z + \xi y) Q]$$

A.2. General expression of the coefficient of pressures distribution (Pinho et al., 2011)

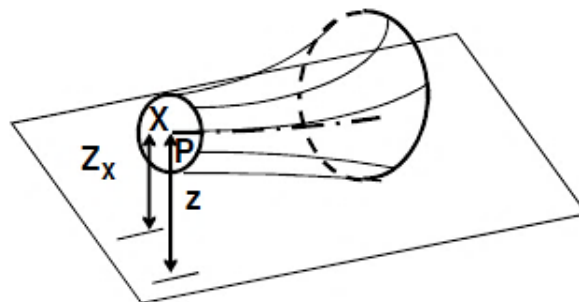


Figure 80 – Distribution of pressures (Pinho et al., 2011).

Due to a curvature and non-hydrostaticity of the distribution of pressures, exist a piezometric gap (p'/γ):

$$h_p - h_x = \frac{p'}{\gamma}$$

$$z_x + \frac{p_x}{\gamma} = z + \frac{p}{\gamma} - \frac{p'}{\gamma}$$

Integral of part **1** takes the form:

$$\int_S \left(z_x + \frac{p_x}{\gamma} \right) v \, dS = \int_S \left(z + \frac{p}{\gamma} \right) v \, dS - \int_S \frac{p'}{\gamma} v \, dS$$

Where, $z + \frac{p}{\gamma}$ is a particular value of the piezometric elevation:

$$\int_S \left(z_x + \frac{p_x}{\gamma} \right) v \, dS = \left(z + \frac{p}{\gamma} \right) Q - \int_S \frac{p'}{\gamma} v \, dS = Q \left[z + \frac{p}{\gamma} \left(1 - \frac{\int_S p' v \, dS}{pQ} \right) \right]$$

Knowing that the coefficient b is called **coefficient of pressure distribution** takes the form:

$$b = 1 - \frac{\int_S p' v \, dS}{pQ}$$

Then:

$$\int_S \left(z_x + \frac{p_x}{\gamma} \right) v \, dS = Q \left(z + b \frac{p}{\gamma} \right)$$

Finally, **piezometric elevation** is defined as:

$$h = z + b \frac{p}{\gamma}$$

in a general form a flow of non-hydrostatics distribution is adapted to a case of hydrostatics distribution of pressures when $b = 1$. And when $b \neq 1$,

- $b > 1$ (p' negative) \sim upward concavity \cup ;
- $b < 1$ (p' positivo) \sim downward concavity \cap .

In free surface flows:

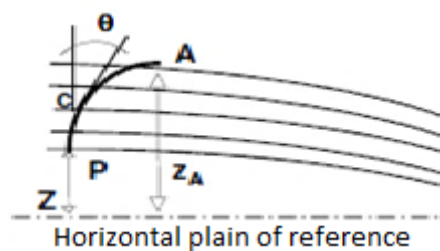


Figure 81 – Distribution of pressures in free surface flows (Pinho et al., 2011).

$$z_A = z + \int_P^A \cos \theta \, dc$$

Where:

z is a point elevation, which in the section is the lowest;

z_A is elevation of the free surface;

$\cos \theta \, dc$ is a projection of the elemental arch dc of a curve of intersection of the section of flow with a plain in which it is analysed.

If effective pressures are considered and a free surface is in contact with atmosphere:

For a hydrostatic distribution of pressure;

$$z_x + \frac{p_x}{\gamma} = z_A$$

- For non-hydrostatics distribution of pressures.

$$z_x + \frac{p_x}{\gamma} = z_A - \frac{\Delta p'}{\gamma} \quad \text{ou} \quad z_x + \frac{p_x}{\gamma} = z + \int_P^A \cos \theta \, dc - \frac{\Delta p'}{\gamma}$$

The integral of part 1 takes the form:

$$\int_S \left(z_x + \frac{p_x}{\gamma} \right) v \, dS = \int_S \left(z + \int_P^A \cos \theta \, dc - \frac{\Delta p'}{\gamma} \right) v \, dS = ZQ + \int_S \int_P^A \cos \theta \, v \, dc \, dS - \int_S \frac{\Delta p'}{\gamma} v \, dS$$

Defining a **coefficient of pressure distribution b'** :

$$b' = \frac{1}{cQ} \left(\int_S \int_P^A \cos \theta \, v \, dc \, dS - \int_S \frac{\Delta p'}{\gamma} v \, dS \right)$$

Where:

$\int_S \int_P^A \cos \theta \, v \, dc \, dS$ represents the **curvature of that section**;

$\int_S \Delta p' / \gamma \, v \, dS$ represents **curvatures of “fillets” (centrifugal forces)**.

As $c = \int_P^A dc$ represents the length of the arch of curve \overline{PA} , then:

$$\int_S \left(z_x + \frac{p_x}{\gamma} \right) v \, dS = (z + b'c)Q$$

Considering the case of “fillets” parallels to a vertical plain and $\xi = \cos \theta$ (coefficient of Boudin):

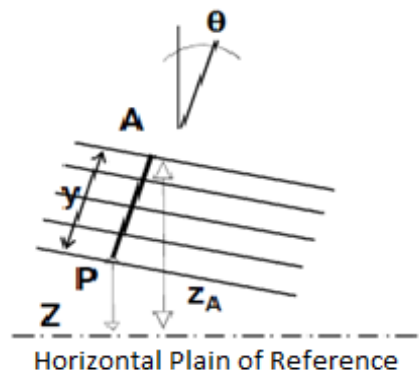


Figure 82 – Fillets parallels to a vertical plane (Pinho et al., 2011).

$$\lambda = \frac{1}{Qy} \left(\int_S y \cos \theta v \, dS - \int_S \frac{\Delta p'}{\gamma} v \, dS \right) \Rightarrow \lambda = \frac{y \cos \theta Q}{Qy} - \frac{\int_S \Delta p' v \, dS}{\gamma Qy} \Rightarrow$$

$$\Rightarrow \lambda = \xi - \frac{\int_S \Delta p' v \, dS}{\gamma Qy} = \xi \left(1 - \frac{\int_S \Delta p' v \, dS}{\gamma Qy \cos \theta} \right) = \xi \left(1 - \frac{\int_S \Delta p' v \, dS}{\gamma Q(z_A - z)} \right)$$

Considering β (**coefficient of Jaeger-Manzanares**) and replacing it in the last equation:

$$\beta = 1 - \frac{\int_S \Delta p' v \, dS}{\gamma Q(z_A - z)} \sim \lambda = \xi \beta$$

where:

$$\int_S \left(z_x + \frac{p_x}{\gamma} \right) v \, dS = (z + \lambda y) Q = (z + \xi \beta y) Q = (z + \beta y \cos \theta) Q$$

B. Coefficient of kinetic energy (Pinho et al., 2011)

$v^2/2g$ represents kinetics energy per unit of weight.

$(v^2/2g) \cdot \gamma v \, dS$ represents potential energy of current (kinetics energy that goes through dS in a unit of time).

Integrating along all section:

$$P = \frac{\gamma}{2g} \cdot \int_S v^3 \, dS$$

Part 2 is related with this potential, if velocity is constant at any point of that section and equal to the average velocity of flow (U),

$$U = \frac{\int_S v \, dS}{S} \sim P_m = \frac{\gamma}{2g} U^3 S$$

Defining α (**coefficient of kinetic energy** or **coefficient of Coriolis**):

$$\alpha = \frac{P}{P_m} = \frac{\text{Kinetik effective potential of flow}}{\text{Kinetik potential of a fictisius flow with } v = U \text{ in all points}} \Rightarrow$$

$$\Rightarrow \alpha = \frac{\frac{\gamma}{2g} \cdot \int_S v^3 \, dS}{\frac{\gamma}{2g} U^3 S} = \frac{\int_S v^3 \, dS}{U^3 S} \sim \frac{1}{2g} \frac{\partial}{\partial s} \int_S v^3 \, dS = \frac{1}{2g} \frac{\partial}{\partial s} (\alpha U^3 S)$$

C. Coefficient of amount of movement (Pinho et al., 2011)

$d\vec{M} = \rho \vec{v} dS \vec{v}$ represents the amount of movement ($m\vec{v}$) referred to fluids mass that pass through dS in a unit of time.

Integrating whole section S , with \vec{n} versor of the resultant direction in which the liquids flows:

$$\vec{M} = \vec{n} \rho \int_S v^2 dS$$

Part 3 is related with this expression. If velocity is constant at any point of that section and equal to the average velocity of flow (U),

$$U = \frac{\int_S v dS}{S} \sim \vec{M} = \vec{n} \rho U^2 S$$

Defining α' (coefficient of amount of movement or coefficient of Boussinesq):

$$\begin{aligned} \alpha' &= \frac{M}{M_m} = \frac{\text{effective amount of movement}}{\text{fictitious amount of movement}} \Rightarrow \\ \Rightarrow \alpha &= \frac{\int_S v^2 dS}{U^2 S} \sim \frac{1}{g} \frac{\partial}{\partial t} \int_S v^2 dS = \frac{1}{g} \frac{\partial}{\partial t} (\alpha' U^2 S) \end{aligned}$$

4.2.3 Global expression of Bernoulli's theorem

When using formulation of the global coefficients of Bernoulli's equation and by adapting, is obtained (Pinho et al., 2011):

$$\frac{\partial}{\partial s} \left[Q \left(z + \frac{bp}{\gamma} \right) \right] + \frac{1}{2g} \frac{\partial}{\partial s} (\alpha U^3 S) = -\frac{1}{g} \frac{\partial}{\partial t} (\alpha' U^2 S) - \int_S jv dS$$

Consider that J represents work done by resistance forces per unit of weight and trajectory, so in global term, this means, a unit of weight respect to the totality of the fluid that pass-through section S in the unit of time:

$$J = \frac{\int_S jv dS}{Q} \sim \frac{\partial}{\partial s} \left[Q \left(z + \frac{bp}{\gamma} \right) \right] + \frac{1}{2g} \frac{\partial}{\partial s} (\alpha U^3 S) = -\frac{1}{g} \frac{\partial}{\partial t} (\alpha' U^2 S) - JQ$$

Considering $\partial Q / \partial s$ too small, so that, $Q = U \cdot S = \text{cte.}$,

$$\frac{\partial}{\partial s} \left(z + \frac{bp}{\gamma} + \frac{\alpha U^2}{2g} \right) = -\frac{1}{g} \frac{\partial}{\partial t} (\alpha' U) - J$$

The generalized global expression of Bernoulli's theorem, (in Lagrange variables) is applicable to a unit of weight of fluid, heavy and incompressible that flows in a stream tube, at any part that has no singular resistances (Pinho et al., 2011).

In local equation:

- Appear coefficients α , α' and b ;
- Appear a global parameter J instead a local parameter j ;
- Appear an average velocity U instead a velocity in a point v .

4.2.4 Interpretation of the global expression of Bernoulli's theorem

Physical meaning (Pinho et al., 2011)

By doing the right adjustments, the meaning will be analogous to the local equation:

$$\frac{\partial}{\partial s} \left(z + \frac{bp}{\gamma} + \frac{\alpha U^2}{2g} \right) = -\frac{1}{g} \frac{\partial}{\partial t} (\alpha' U) - J$$

Z is again the topographic elevation of any point of that section related to a reference plane. Represents the potential energy of position of a unit of weight of liquid that flows in a stream tube:

- **Flows under pressure**, Z correspond to the intersection of the tube's axis with the section axis;
- **Flow with free Surface**, Z correspond to a point located lower in that section.

bp/γ is piezometric height.

$h = z + bp/\gamma$ is piezometric elevation. Represents a summation of the potential energy of position with the potential energy of pressure per unit of weight of flowed liquid (through the section).

$\alpha U^2/2g$ is kinetic height. Represents kinetics energy per unit of flowed liquid through the section.

$-1/g \cdot \partial/\partial t(\alpha' U)$ represents work done by local forces of inertia per unit of weight and trajectory.

J represents work done by resistances forces per unit of trajectory and weight of flowed fluid inside the stream tube.

Bernoulli's theorem (global aspect) represents an equation of **balance of energy** because the **work done by local forces of inertia and resistance are equal to a variation of the total mechanical energy**. Per unit of weight:

$$-\frac{1}{g} \frac{\partial}{\partial t} (\alpha' U) - J = H \left(= z + \frac{bp}{\gamma} + \frac{\alpha U^2}{2g} \right)$$

Piezometric line and energy line (Pinho et al., 2011)

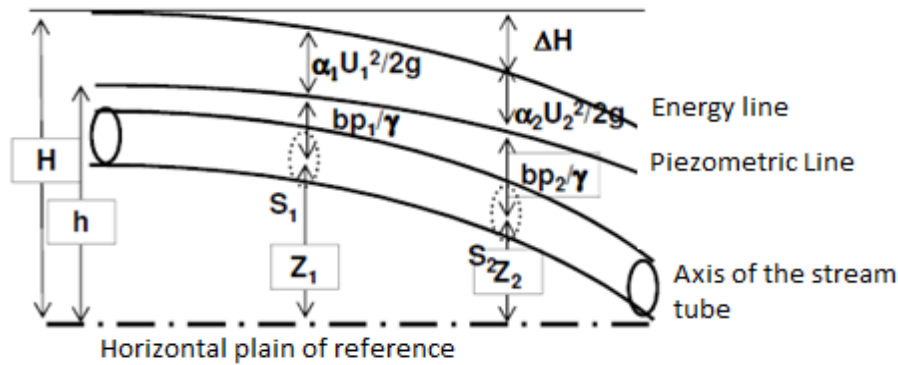


Figure 83 – Piezometric line and energy line (Pinho et al., 2011).

Loss of energy (Pinho et al., 2011)

From:

$$\Delta H = H_1 - H_2 = \int_{S_1}^{S_2} \left(-\frac{1}{g} \frac{\partial}{\partial t} (\alpha' U) - J \right) ds$$

Applying Bernoulli's equation to sections 1 and 2, integrating:

$$Z_1 + \frac{b_1 p_1}{\gamma} + \frac{\alpha_1 U_1^2}{2g} - \left(Z_2 + \frac{b_2 p_2}{\gamma} + \frac{\alpha_2 U_2^2}{2g} \right) = \Delta H$$

Energy exchange with exterior (Pinho et al., 2011)

$$Z_1 + \frac{b_1 p_1}{\gamma} + \frac{\alpha_1 U_1^2}{2g} - \left(Z_2 + \frac{b_2 p_2}{\gamma} + \frac{\alpha_2 U_2^2}{2g} \right) = \Delta H \pm \Delta B$$

where:

+ΔB correspond to loss of energy (ex.: turbine);

−ΔB correspond to a supply of energy (ex.: pump).

Values of global coefficient of Bernoulli's equation (Pinho et al., 2011)

A. Coefficient of distribution of pressures b (Pinho et al., 2011)

b = 1:

- Hydrostatic fields of pressure;
- Pressured pipes (tubes with small and medium diameter and high pressures);
- Flows with free surfaces (curvature of “fillets” poorly accented).

b > 1:

- curvature of “fillets” with upward concavity.

b < 1:

- curvature of “fillets” with downward concavity.

B. Coefficients of kinetics energy and amount of movement, α and α' (are function of the form of the section, rugosity of walls, velocity of flow) (Pinho et al., 2011)

Laminar regime:

- $\alpha = 2 \wedge \alpha' = 4/3$ (Newtonian Viscous fluids \).

Turbulence regime:

- $\alpha = 1.15 \wedge \alpha' = 1.05$ (section of simple shape and small rugosity);
- $\alpha = 1.01 \text{ a } 1.02 \wedge \alpha' = 1.6$ (free surface flow, high rugosity and very low velocity).

Applied hydraulics:

- $\alpha = \alpha' = 1$.

4.2.5 Application of global equations to permanent regime

Simplification of global equation (Pinho et al., 2011)

For a permanent flow:

$$-\frac{1}{g} \frac{\partial v}{\partial t} = 0$$

It is the form of the equations write in **Lagrange's** variables coincide with the form in **Euler's** variables,

$$\frac{\partial}{\partial s} \left(z + \frac{bp}{\gamma} + \frac{\alpha U^2}{2g} \right) = -J$$

Or in **flows with free surface:**

$$\frac{\partial}{\partial s} \left(z + \beta y \cos \theta + \frac{\alpha U^2}{2g} \right) = -J$$

equally,

$$Z_1 + \frac{b_1 p_1}{\gamma} + \frac{\alpha_1 U_1^2}{2g} - \left(Z_2 + \frac{b_2 p_2}{\gamma} + \frac{\alpha_2 U_2^2}{2g} \right) = \Delta H \pm \Delta B$$

Or in **flows with free surface**:

$$Z_1 + \beta_1 y_1 \cos \theta_1 + \frac{\alpha_1 U_1^2}{2g} - \left(Z_2 + \beta_2 y_2 \cos \theta_2 + \frac{\alpha_2 U_2^2}{2g} \right) = \Delta H \pm \Delta B$$

These expressions are valid in terms of Euler variables and is applicable to liquid's mass that pass cross sections **S₁** and **S₂**, and to the characteristic of the flow at those two sections.

In **uniform regime**,

$$\frac{\partial}{\partial s} \left(\frac{U^2}{2g} \right) = 0$$

Current lines coincide with the trajectory of fluid's particles:

$$\frac{\partial}{\partial s} \left(z + \frac{p}{\gamma} \right) = -J$$

$$Z_1 + \frac{p_1}{\gamma} - \left(Z_2 + \frac{p_2}{\gamma} \right) = \Delta H$$

For **free surface flows**,

$$\frac{\partial z}{\partial s} = -J \leadsto Z_1 - Z_2 = \Delta H$$

Uniform movement: the work done by the resistance's forces per unit of weight and trajectory is constant at any section of the flow:

$$\Delta H = H_1 - H_2 = -J \int_{S_1}^{S_2} ds = J(s_2 - s_1)$$

Where **L** is the distance between sections **1** and **2**.

$$\Delta H = JL$$

With **J** representing energy losses per unit of length.

And considering local energy losses and external exchanges of energy to the flow, then:

$$Z_1 + \frac{p_1}{\gamma} - \left(Z_2 + \frac{p_2}{\gamma} \right) = J_L + \sum_{i=1}^n \Delta H_{L_i} \pm \Delta B, \text{ com } \Delta H_L = K \frac{U^2}{2g}$$

Where, K is the **coefficient of localized energy losses (charge loss)**.

4.3 Application of Bernoulli's theorem

4.3.1 Measure of velocity by using a Pitot Tube (Tube)

From a point of view bases in energy balance, Pitot Tube is a traditional application of Bernoulli's theorem along a current line. The association or similarity between the pitot tube and a piezometric tube allow to experimentally determine the kinematic height and indirectly, also the velocity flow of a particle positioned at a current line where the tube is installed (Vasconcelos, 2005).

It is possible by installing a piezometric tube in a section of a flow tube with straight axis, where current lines are straight and parallel and also installing a Pitot Tube at different positions of the transversal section in order to determine the velocity diagram at such section, Figure 84 (Vasconcelos, 2005).

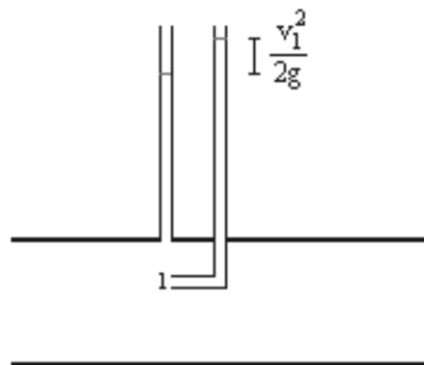


Figure 84 – Association of a piezometric and a Pitot Tube in order to determine the velocity diagram at a transversal section in a flows tube. (Vasconcelos, 2005).

As the Pitot Tube gets closer to the center of gravity of the transversal section of the flows tube, increase the difference of topographic elevation of a free surface between the tubes, because velocity also increase (Vasconcelos, 2005).

Flow's velocity is obtained by the next equation:

$$h = \frac{\Delta p}{\rho g} = \frac{\frac{1}{2} \rho v_1^2}{\rho g} = \frac{v_1^2}{2g} \Rightarrow v_1 = \sqrt{2gh}$$

4.3.2 Diffusor of a hydraulic turbine

The **diffusor** is a fixed part that leads water from the exits of the impeller until the downstream level in order to recover the height between impeller exit and the level of the scape channel, restoring part of the kinetic energy that correspond to the residual velocity of water at the rotator exit (Soares Júnior, 2013).

Those expanded pipes reduce the flow's velocity and increase static pressure. As soon as goes through the diffusor, the flow's velocity is decrease, where a conversion of an amount of energy from kinetic to potential of pressure occurs (Coelho *et al.*, 2006).

It is clear the importance of using a diffusor, when considering the energy of the water that comes from the impeller will be lost without it (Figure 85). In some projects, that energy can raise until 50 % of the total available energy. However, the use of a diffusor absolutely isolated from any gas or air, creates a partial vacuum due to the high speed of water. With these reductions of pressure, the pressure at the impeller's spades tend to gap greater than usually, increasing the **global efficiency of a turbine** (Costa, 2003).

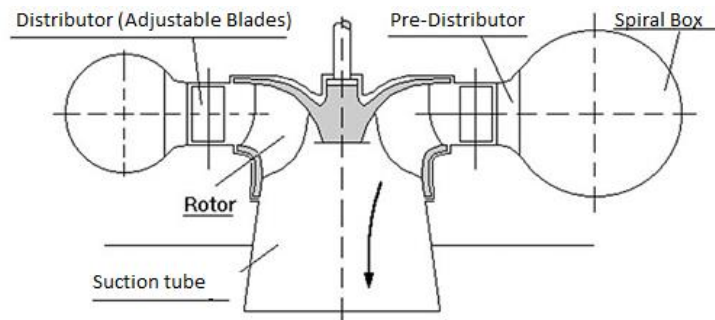


Figure 85 – Typical arrangement of and hydraulic turbine (Tavares, 2014).

For a better understanding of the efficiency or yield theory, two situations are show, one with diffusor and the second without it, as in Figure 86, like it was done by Coelho (2006).

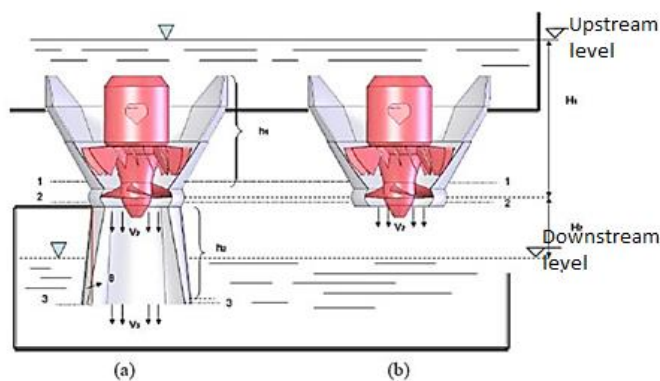


Figure 86 – Graphical approach of an impeller or rotator: a) with a diffusor; b) without a diffusor (Coelho, 2006).

With a reference of the downstream level and specific energy before impeller and by using the energy's conservation's theorem, is given by:

$$E_1 = \frac{p_{\text{atm}}}{\rho} + gH_1 + gH_2 - gh_1$$

Where:

p_{atm} atmospheric pressure;

ρ is specific mass of water;

g is gravitational acceleration;

H_1 is the height of fall referent to upstream;

H_2 is the height of fall referent to downstream;

h_1 represents losses of charge when the flows go through the water outlet before the diffusor.

Analogously, at the exit of the rotor, is obtained:

$$E_2 = \frac{p_2}{\rho} + gH_2 + \frac{v_2^2}{2}$$

Where, $\frac{v_2^2}{2}$ is the specific kinetic energy at impeller exit.

So, the energy consumed by the impeller, obtained from the variation of energies E_1 and E_2 , is given by:

$$\Delta E = E_1 - E_2 = \frac{p_{\text{atm}}}{\rho} - \frac{p_2}{\rho} + gH_1 - \frac{v_2^2}{2} - gh_1$$

Now, analysing without a diffusor, Figure 86 (b), can be appreciated that pressure at impeller exit (p_2) is the same as atmospheric pressure at the entrance of it.

In this way, the difference between those pressures is zero. So, the last equation can be written as:

$$\Delta E_I = gH_1 - \frac{v_2^2}{2} - gh_1$$

Analysing the turbine with a diffusor, Figure 86 (a), the pressure at the impeller exit is different to the atmospheric pressure. Now, using the conservation of energy theorem between points 2 and 3 in figure, is obtained:

$$\frac{p_2}{\rho} = \frac{p_{\text{atm}}}{\rho} - gH_2 - \frac{v_2^2}{2} + \left(gh_2 + \frac{v_3^2}{2} \right)$$

Where, h_2 is the loss of charge in the diffusor.

Then, ΔE_{II} became:

$$\Delta E_{II} = (gH_1 + gH_2) - g \left(\frac{v_3^2}{2g} + h_1 + h_2 \right)$$

4.3.3 Charge and piezometric lines in hydraulic machine installation.

It is quite interesting to study a hydraulic circuit through the analysis of potential energy transfers in substitution of the analysis of energy equilibrium (Vasconcelos, 2005).

Consider a hydraulic circuit formed by two reservoirs of great dimensions with a pipe connecting both allowing an exchange of flow rate (Q) from the upstream reservoir (R_1) to the downstream reservoir (R_2), Figure 87 (Vasconcelos, 2005).

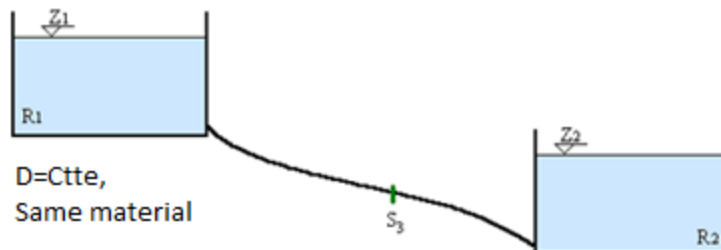


Figure 87 – Hydraulic circuit (Vasconcelos, 2005).

The hydraulic potential of the liquid in the upstream reservoir (of great dimensions), is:

$$P_{esc1} = \gamma Q H_1$$

Where the charge in the upstream reservoir is equal to the topographic elevation of the free surface in it. Such affirmation is due to nonexistence of liquids velocity in the reservoir, verifying the **Law of Hydrostatic Pressures**. If the piezometric elevation is constant, it is also equal to the piezometric elevation of the free surface, where pressure is null, matching the topographic elevation. (Vasconcelos, 2005).

In the same way, the downstream reservoir of great dimensions has a liquid hydraulic potential of:

$$P_{esc2} = \gamma Q H_2$$

The liquid potential in a pipe section (S_3) is:

$$P_{esc3} = \gamma Q H_3$$

Where:

$$H_3 = Z_3 + \beta \frac{p_3}{\gamma} + \alpha \frac{U_3^2}{2g}$$

The flow potential, necessary to transport a flow rate Q between both reservoirs, is:

$$P_{esc\Delta H} = \gamma Q \Delta H$$

Where ΔH is a charge loss along the path, between both reservoirs.

There are two possible cases (Vasconcelos, 2005):

- **1st Case** (Figure 88) – If $\Delta H > H_1 - H_2 \rightarrow$ it is necessary to install a pump that transmit a potential corresponding to a charge, designated by the total height of elevation of the pump, equal to:

$$H_t = \Delta H - (H_1 - H_2) = H_s - H_e$$

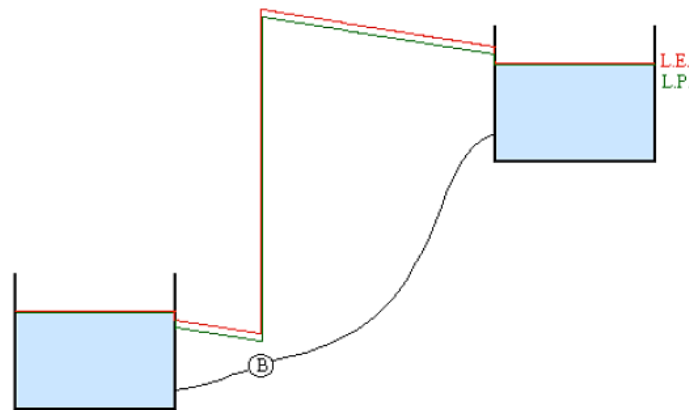


Figure 88 – Energy and piezometric line of a hydraulic-elevator pipe circuit (Vasconcelos, 2005).

The potential transmitted by the pump to the flow is:

$$P_{B-esc} = \gamma Q H_t$$

And the potential of the pump is superior, when including losses in it:

$$P_B = \frac{\gamma Q H_t}{\eta_B}$$

So, finally the necessary potential of the pumps motor is:

$$P_m = \frac{\gamma Q H_t}{\eta_m \eta_B}$$

- **2nd Case** – If $\Delta H < H_1 - H_2 \rightarrow$ can be installed a turbine (Figure 89) that receive a potential from the flow, corresponding to a charge, designated as usable gap, equal to:

$$H_u = (H_1 - H_2) - \Delta H = H_e - H_s$$

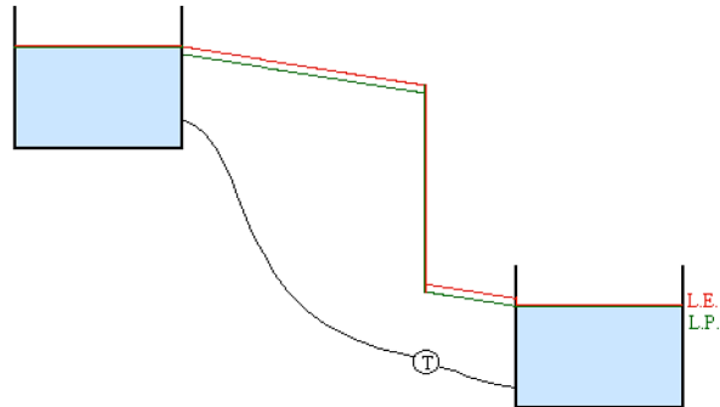


Figure 89 – Energy line and piezometric line in a hydraulic-gravitational pipe circuit with a turbine (Vasconcelos, 2005).

The potential given to the turbine from the flow, is:

$$P_{esc-T} = \gamma Q H_u$$

The potential of the turbine is lower, when including losses in transformation (in turbine):

$$P_T = \eta_T \gamma Q H_u$$

4.3.4 Occurrence of cavitation.

Cavitation is the name given to a phenomenon of vaporization of a liquid by the reduction of pressure, while its movement (Figure 90) (Oliveira, 2007).



Figure 90 – Model of the propeller that creates cavitation in an experimental water tunnel (<https://commons.wikimedia.org>).

For all fluids in liquids state can be establish a curve that relates pressure with the temperature at which vaporizations occurs. As an example: at atmospherically pressure, is necessary a temperature around 100°C to have vaporization. In this way, as lower the pressure is, lower the necessary temperature for such phenomenon (Oliveira, 2007).

Applying Bernoulli's theorem

It is a well know and predictable fact, with help of Bernoulli's theorem, where a fluid flowing, as soon as accelerates, have immediately a reduction of pressure in order to keep a constant mechanical energy. Consider a fluid in a liquid state flowing at some temperature, T_0 and a pressure P_0 (Oliveira, 2007).

In some certain points, due to acceleration of the fluid (like in a spillway, hydraulic turbine or pump, valve or opening) the pressure may fall until a value under the minimal pressure where occurs vaporization of a fluid (P_v) with temperature T_0 . Then, will occurs a local vaporization of the fluid, forming bubbles of vapor. This phenomenon is called **cavitation** (formation of cavities inside the liquid mass) (Oliveira, 2007).

Cavitation is common in pumps of water and oil, valves, turbines, naval propeller, autos pistons and even in channel of concrete at highs speeds, like in a spillway of a dam (Oliveira, 2007).

So, it must be always avoided due to financial expenses (related to destruction generated by associated erosion, in turbine (Figure 91) or pump blades, piston or channels) (Oliveira, 2007).



Figure 91 – Damages created by cavitation in a Francis turbine (<https://commons.wikimedia.org>).

Such bubbles of vapor that form in a flow due to low pressures, are carried and can achieve a region where pressures rise again to a value superior to P_v . Then occurs an implosion of those bubbles. And if the region of implosion is close enough to a solid

surface, the shock waves generated by successive events can lead to micro fractures in the material, that in time, will expand and destroy or displace part of the surface material, creating some cavities due to such local erosion process. This is a physical molecular phenomenon, that expand and spread with time, ruining the rotators, impellers or propellers (Oliveira, 2007).

In practice

In **hydraulic engineering** and mechanical engineering, cavitation is a great concern, as well as the abrasion of the sand and other sediments particles transferred by water inside pumps and turbines, especially due to possible damages in elevator stations and in turbines and spillways of hydroelectrical centrals (Netto, 1998).

Must not be confused the corrosion (chemical phenomenon) with the cavitation or abrasion (physical phenomenon), although, the effects in the blades of turbines and pumps are similar, as also happens in concrete surfaces of spillways channels (Netto, 1998).

Identification

In the vibration spectrum (Figure 92), it is identified cavitation by the emerging of aleatory signals (signals without an exact definition), in the region of low frequency (80 a 200 Hz) of the velocity spectrum and in a high frequency in acceleration spectrum (Oliveira, 2007).

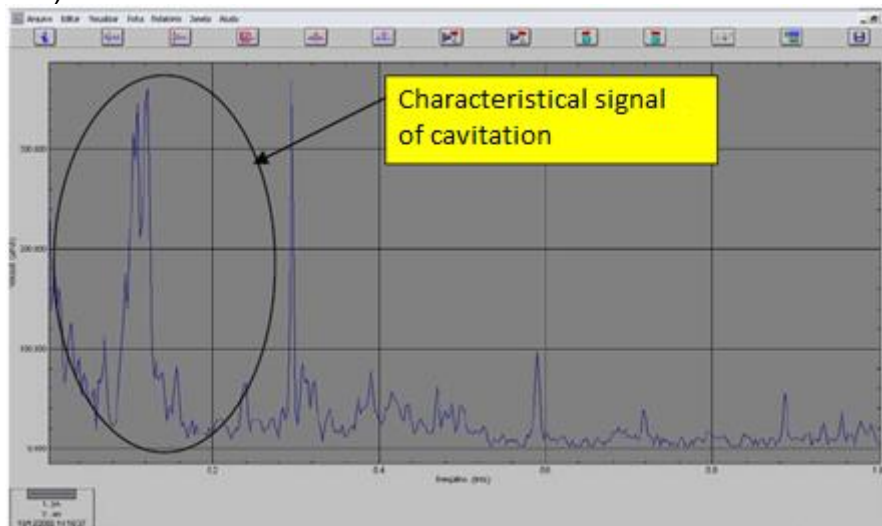


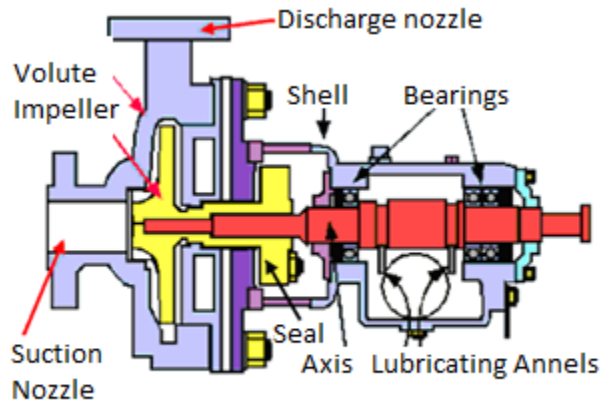
Figure 92 – Spectrum of vibration collected in a pump bearing (Oliveira, 2007).

In a sensitive way, cavitation is finding through the strong sounds at the pump volute, causing an impression that is pumping solid bodies as rocks. For example, (Figure 93) (Oliveira, 2007).



Figure 93 – Rotor destroyed by cavitation, used to belong to a water pump (Oliveira, 2007).

In order to clarify, a **bearing** (Figure 94) is a fixed mechanical dispositive, in steel or melted iron (also of wood), where a rotating, oscillating or slider axis is supported.



Centrifugal Pump

Figure 94 – Scheme of an centrifugal pump (<http://www.ebah.com.br>) and bearing (<https://commons.wikimedia.org>).

CHAPTER 5 - THEOREM OF AMOUNT OF MOVEMENT AND ITS APPLICATIONS

5.1 Expression of the amount of movements theorem

In hydraulics problems, in which its pretended **to determine the forces prosecuted by a fluid over a solid border, it is not sufficient an application of the equation of continuity (Mass Conservation Principle) and the theorem of Bernoulli (Energy Conservation Principle)** being necessary the deduction of an **equation that considers the equilibrium of forces that acts over a certain volume of fluid (Theorem of Amount of Movement or Euler's Theorem)** (Vasconcelos, 2005).

The **Theorem of Amount of Movement** allow to determine forces acting over a solid border in contact with a fluid, so in a particular case of permanents flows, allow the characterization of the flow based only in the border conditions (Vasconcelos, 2005).

This theorem in conjunctions of the Bernoulli's Theorem and the Continuity Equation allow to solve any problem of hydraulics, based in the characterization of a certain volume in the fluid's domain (Vasconcelos, 2005).

5.1.1 Principle of amount of movement applied to fluids mechanics

Following Vasconcelos (2005), Euler's Equation, which express dynamic equilibrium applied to perfect liquids:

$$\vec{g} - \frac{1}{\rho} \overrightarrow{\text{grad } p} - (\vec{v} | \overrightarrow{\text{grad}}) \vec{v} = \vec{0}$$

And the Continuity Equation:

$$\text{div } \rho \vec{v} + \frac{\partial \rho}{\partial t} = 0$$

Constitute a system of two equations that, in tensorial form, are represented by:

$$\begin{cases} \rho g_i - \frac{\partial p}{\partial x_j} - \rho \frac{\partial v_i}{\partial t} - \rho v_j \frac{\partial v_i}{\partial x_j} = 0 \\ \frac{\partial \rho v_j}{\partial x_j} + \frac{\partial \rho}{\partial t} = 0 \end{cases}$$

Now, based in the definition of a derivative of a product, the third and fourth part of Euler's Equations can be replaced by the following equations:

$$\begin{cases} 3^{rd} \text{ part: } \rho \frac{\partial v_i}{\partial t} = \frac{\partial \rho v_i}{\partial t} - v_i \frac{\partial \rho}{\partial t} \\ 4^{th} \text{ part: } \rho v_j \frac{\partial v_i}{\partial x_j} = \frac{\partial \rho v_i v_j}{\partial x_j} - v_i \frac{\partial \rho v_j}{\partial x_j} \end{cases}$$

Obtaining the next form of Euler's Equation:

$$\begin{aligned} \rho g_i - \frac{\partial p}{\partial x_j} &= \left(\frac{\partial \rho v_i}{\partial t} - v_i \frac{\partial \rho}{\partial t} \right) + \left(\frac{\partial \rho v_i v_j}{\partial x_j} - v_i \frac{\partial \rho v_j}{\partial x_j} \right) \Rightarrow \\ \Rightarrow \rho g_i - \frac{\partial p}{\partial x_j} &= \frac{\partial \rho v_i}{\partial t} + \frac{\partial \rho v_i v_j}{\partial x_j} - v_i \left(\frac{\partial \rho}{\partial t} + \frac{\partial \rho v_j}{\partial x_j} \right) \end{aligned}$$

The term between parenthesis of the upper equations cancels if the equations of continuity is verified, obtaining a simplified equation:

$$\rho g_i - \frac{\partial p}{\partial x_j} = \frac{\partial \rho v_i}{\partial t} + \frac{\partial \rho v_i v_j}{\partial x_j}$$

The integration of the upper equation at a certain volume of fluid, volume of control and the application of the Theorem of Divergence of Gauss to the seconds terms of both members, which lead to two integrals in the border surface of the volume of control, allow to obtain the equation:

$$\int_V \rho g_i \, dV + \int_S -p n_j \, dS = \int_V \frac{\partial \rho v_i}{\partial t} \, dV + \int_S \rho v_i v_j n_j \, dS$$

The upper equation represents an **Equation of the Theorem of Amount of Movement, in form of integral applied to perfect liquids**. In **vectoral notation**, it is represented by:

$$\int_V \rho \vec{g} \, dV + \int_S -p \vec{n} \, dS = \int_V \frac{\partial \rho \vec{v}}{\partial t} \, dV + \int_S \rho \vec{v} (\vec{v} | \vec{n}) \, dS = 0$$

Interpretation of the Theorem of Amount of Movement (Vasconcelos, 2005)

- $\int_V \rho \vec{g} \, dV$, forces of mass that acts over the fluid contained inside the control surface, \vec{G} ;
- $\int_S -p \vec{n} \, dS$, impulsión prosecuted along the control surface, by the surrounding fluid or by solid walls (positive with outward direction). In this term, in order to generalize the application of an equation deduced to real liquids, it must be

included the parts corresponding to the tangential tensions at the control surface, $\vec{\Pi}$;

- $\int_V \partial \rho \vec{v} / \partial t \, dV$, local forces of inertia (it is cancelled in permanent flows), \vec{I} ;
- $\int_S \rho \vec{v} (\vec{v} \cdot \vec{n}) \, dS$, quantity of movement across the whole surface of control, which means, the amount of movement that enters in it per unit of time. The integral affected by the negative signal, correspond to an amount of movement that enters, without the amount of movement that leaves the surface of control, $\vec{M}_e - \vec{M}_s$.

In a **simpler way**, the **Theorem of Amount of Movement**, can be write as:

$$\vec{G} + \vec{\Pi} + \vec{I} + \vec{M}_e - \vec{M}_s = \vec{0}$$

5.1.2 Theorem of amount of movement applied to a stream tube or pipe

The equation of amount of movement is only the second Newton's Law of dynamic modified functionally for the study of Fluids Mechanics. According to this law, acceleration of a certain mass implies the existence of a resultant force over it, that at each instant, in the direction of the acceleration. Accelerating a mass means to modify its velocity in modules and/or direction, and by observing this, in order to change a fluid velocity in modulus or direction, it will be necessary to apply a force produced by an external entity, in general, a solid surface in contact with the flow (Brunetti, 2008).

By the principle of action and reaction, if a surface applies a force in the fluid, this one will apply over the surface another force of same modulus but with opposite direction. By observing this fact, it is possible to build an equation of amount of movement, in the desired moulds (Brunetti, 2008). So, being the second Newton's Law of dynamics:

$$\vec{F} = m\vec{a} = m \frac{d\vec{v}}{dt}$$

Notice that the equation must be maintained in its vectorial form, because velocity can vary in any direction in which its modulus is altered. And, because this equation is designed for system with constant mass, then can be write: (Brunetti, 2008):

$$\vec{F} = \frac{d}{dt}(m\vec{v})$$

As $m\vec{v}$ is by definition, an amount of movement of that system, then can be said that the resultant force, that acts in such system, is equal to the variation respect of time, of the amount of movement of the system (Brunetti, 2008).

This is the theorem established in Mechanics and must be used to determine the studied dynamics forces. In this sub chapter, the equation of amount of movement will be establish for a stream tube and for the hypothesis of a permanent regime (Braga, 2014).

As already demonstrated in the sub chapter 2.1.4, acceleration ($\vec{a} = d\vec{v}/dt$) must be composed with a local variation in time ($\partial\vec{v}/\partial t$, variation of velocity in time), plus and variation of transfer from a one point to another of the fluid (variation of velocity in space). When it is a permanent regime, properties do not vary at each point respect time, but may vary in space. A variation of the amount of movement in case of Figure 95 must be understood as a variation between sections (1) and (2) (Brunetti, 2008).

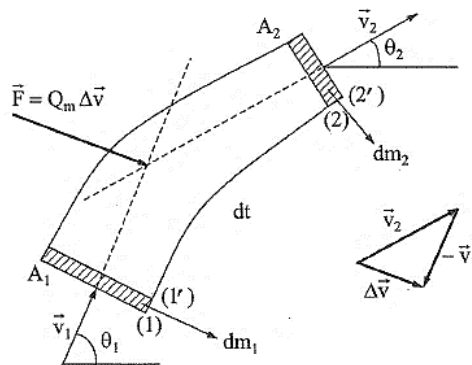


Figure 95 – Current Tube (Brunetti, 2008).

Admitting uniform properties in the section, as some interval of time dt , a mass of fluid that cross the section (1) with velocity \vec{v}_1 will be dm_1 , producing an increase of the amount of movement of the fluid between sections (1) and (2) of $dm_1\vec{v}_1$ (Brunetti, 2008).

At the same interval of time, through the section (2), exist an expulsion of an amount of movement $dm_2\vec{v}_2$. Then, variation of amount of movement between (1) and (2) will be $dm_2\vec{v}_2 - dm_1\vec{v}_1$. So, following the theorem of amount of movement, a resultant force that acts in the fluid between sections (1) and (2) will be (Brunetti, 2008):

$$\vec{F} = \frac{dm_2\vec{v}_2}{dt} - \frac{dm_1\vec{v}_1}{dt} = Q_{m2}\vec{v}_2 - Q_{m1}\vec{v}_1$$

By other side, as a permanent regime, then:

$$Q_{m1} = Q_{m2} = Q_m$$

And, therefore:

$$\vec{F} = Q_m(\vec{v}_2 - \vec{v}_1) = Q_m\Delta\vec{v}$$

The upper equation shows also that \vec{F} has a direction of $\Delta\vec{v} = \vec{v}_2 - \vec{v}_1$, and its point of application can be found in the intersection of the directions \vec{v}_2 and \vec{v}_1 (Figure 95). Also allow to determine the resultant force that acts in a fluid, between (1) and (2), which is not a usual main objective (Brunetti, 2008).

Let's analyse the component of the resultant force \vec{F} (Figure 96).

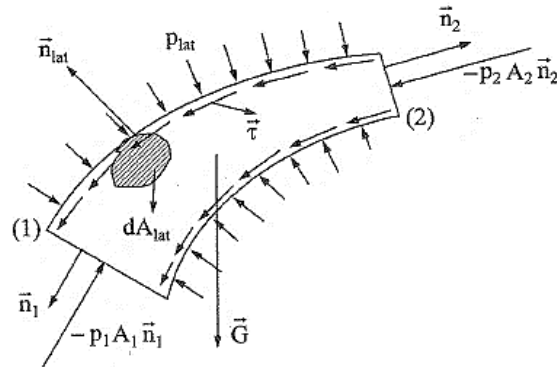


Figure 96 – Pressures, tensions and gravity field (Brunetti, 2008).

The fluid between (1) and (2) is subjected to normal contact force (of pressure) and tangential forces (bearing forces), and the field force caused by the gravity field, that is the weight (\vec{G}) (does not include the existence of other fields) (Brunetti, 2008).

In section (1) and (2), an upstream fluid and downstream fluid of the stream tube ((1) – (2)) apply pressure to the fluid contained in those sections (Brunetti, 2008).

Forces generated by pressures between (1) and (2) are respectively p_1A_1 and p_2A_2 in modulus. For the determination of the vectors of the forces at those two sections, the normal vector to it are adopted, in an outward direction from the stream tube (due to convention). In such way, the forces that acts in the fluid in sections (1) and (2) will be respectively $-p_1A_1\vec{n}_1$ and $-p_2A_2\vec{n}_2$, where negative signals are adopted, due to the convection adopted for the normal, as observed in Figure 96 (Brunetti, 2008).

On a lateral surface, the fluid is subjected to pressures and bearing tensions due to its movement in contact with the media (Brunetti, 2008).

Such pressures and bearing tensions can vary from one point to another in the lateral surface. The resultant of pressures can be obtained by adopting at each point a normal with outward direction, in order to follow the convention (Brunetti, 2008). The resultant at each element (dA_{lat}) in the contour of a point of the lateral surface, will be:

$$d\vec{F}'_s = -p_{lat}\vec{n}_{lat}dA_{lat} + \vec{\tau}dA_{lat}$$

Then, the resultant forces of pressure and bearing tensions in the lateral surface will be:

$$\vec{F}'_s = \int -p_{lat}\vec{n}_{lat}dA_{lat} + \int \vec{\tau}dA_{lat}$$

When such resultant is already defined, Figure 96 can be reduced to Figure 97 (Brunetti, 2008).

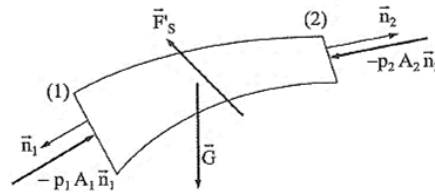


Figure 97 – Components of a resultant force (Brunetti, 2008).

By the exposed before, the resultant force (\vec{F}) that acts in the fluid between (1) and (2) will be the summation of the components represented in Figure 97 (Brunetti, 2008). Then:

$$\vec{F} = \vec{F}'_s + (-p_1 A_1 \vec{n}_1) + (-p_2 A_2 \vec{n}_2) + \vec{G}$$

But $\vec{F} = Q_m(\vec{v}_2 - \vec{v}_1)$, so then:

$$-p_1 A_1 \vec{n}_1 - p_2 A_2 \vec{n}_2 + \vec{G} = Q_m(\vec{v}_2 - \vec{v}_1)$$

In general, the interest for this equation correspond to the cases in which the fluid is in contact with a solid surface, the lateral surface between (1) and (2). In such condition, force \vec{F}'_s represents the resultant forces of contact of the solid surface against the fluid (Brunetti, 2008). By isolating this term in the last equation, is obtained:

$$\vec{F}'_s = p_1 A_1 \vec{n}_1 + p_2 A_2 \vec{n}_2 + Q_m(\vec{v}_2 - \vec{v}_1) - \vec{G}$$

Normally, in practice only interest to determine the force applied by the fluid on the solid surface in contact between sections (1) and (2). As \vec{F}'_s represents a resultant force of the solid surface acting in the fluid, then by the principle of action and reaction, the force \vec{F}_s which the fluid applies in the solid surface will be (Brunetti, 2008):

$$\vec{F}_s = -\vec{F}'_s = -[p_1 A_1 \vec{n}_1 + p_2 A_2 \vec{n}_2 + Q_m(\vec{v}_2 - \vec{v}_1)] + \vec{G}$$

For an easier calculus, the weight of the fluid (\vec{G}) will not be consider; however, must noticed that not always such term can be ignored, and in the practical applications may be necessary to calculate. By the exposed, the upper equation will be used in advance as (Brunetti, 2008):

$$\vec{F}_s = -[p_1 A_1 \vec{n}_1 + p_2 A_2 \vec{n}_2 + Q_m(\vec{v}_2 - \vec{v}_1)]$$

5.2 Application of the theorem of amount of movement

The equations that defines \vec{F}_s is not applied in a vectoral form. Normally, some convenient axis is adopted for solving a problem, so vectors of the equations are projected in those directions (Brunetti, 2008).

All equations vectors will be projected in such directions, determining the components of a force \vec{F}_s at those directions (Brunetti, 2008).

If the results lead to the determination of \vec{F}_s , these two components will be composed vectorially to obtain them (Brunetti, 2008).

5.2.1 Pipe with a gradual reduction of transversal section.

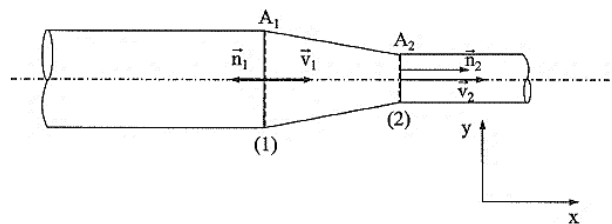


Figure 98 – Pipe with gradual reduction of section (Brunetti, 2008).

Considering a pipe represented above and an incompressible fluid with uniform properties in the sections, flowing in permanent regime. Let's determine the horizontal force of the fluid over the pipe (knowing such force will help to design a system for the pipe fixation). For the piece between sections (1)–(2) can be stated:

$$\vec{F}_s = -[p_1 A_1 \vec{n}_1 + p_2 A_2 \vec{n}_2 + Q_m(\vec{v}_2 - \vec{v}_1)]$$

Projecting in direction of axis x:

$$F_{sx} = -[p_1 A_1(-1) + p_2 A_2(+1) + Q_m(v_2 - v_1)] \Rightarrow$$

$$\Rightarrow F_{sx} = p_1 A_1 - p_2 A_2 + \rho Q(v_1 - v_2)$$

Must notice the advantages of this method is related to the fact that the study is made in the incoming and outgoing sections of a pipe, without any concern of the intermediary distribution of forces. As no vectors of the figure has components in the direction of axis y, $F_{sy} = 0$ (due to ignoring \vec{G}) (Brunetti, 2008).

5.2.2 Reduction of section and direction change.

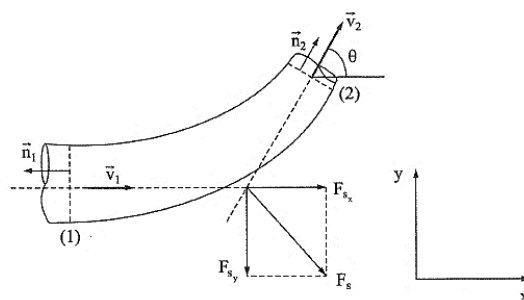


Figure 99 – Reduction of section and direction change (Brunetti, 2008).

Under same last hypothesis:

$$\vec{F}_s = -[p_1 A_1 \vec{n}_1 + p_2 A_2 \vec{n}_2 + Q_m(\vec{v}_2 - \vec{v}_1)]$$

Projecting respect of x:

$$\begin{aligned} F_{sx} &= -[p_1 A_1(-1) + p_2 A_2 \cos \theta + Q_m(v_2 \cos \theta - v_1)] \Rightarrow \\ \Rightarrow F_{sx} &= p_1 A_1 - p_2 A_2 \cos \theta + \rho Q(v_1 - v_2 \cos \theta) \end{aligned}$$

Projecting respect of y:

$$\begin{aligned} F_{sy} &= -[0 + p_2 A_2 \sin \theta + Q_m(v_2 \sin \theta - 0)] \Rightarrow \\ \Rightarrow F_{sy} &= -p_2 A_2 \sin \theta - \rho Q v_2 \sin \theta \end{aligned}$$

Notice that the components \vec{F}_{sx} and \vec{F}_{sy} can be obtained by a resultant force of fluid acting over the pipe, which is (Brunetti, 2008):

$$F_s = \sqrt{F_{sx}^2 + F_{sy}^2}$$

5.2.3 Action of a jet over a fixed curved surface

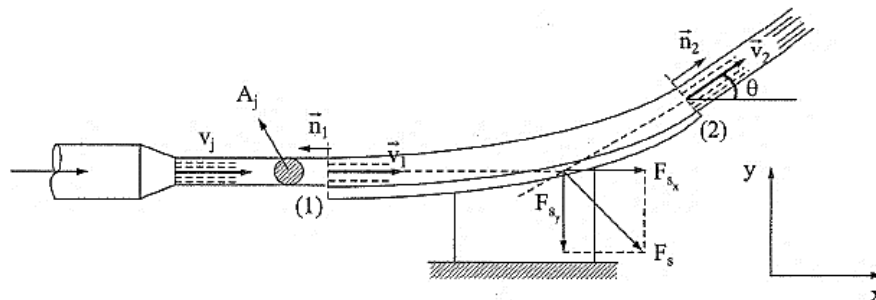


Figure 100 – Jet acting over a curved laminate (Brunetti, 2008).

This case has applications as the blades or spades of an impeller turbine. The fluid projected against the deviator suffers a deflection due to it (Brunetti, 2008).

Notice that by deducing equation of \vec{F}_s , which is produced in a contact between fluid and air, because the fluid is not totally surrounded by the solid surface in sections (1) and (2) (Brunetti, 2008).

Pressure in an effective scale is zero, however, still exists and air friction effect. Then, \vec{F}_s must be a resultant of a force that a fluid applies in a bulkhead in which air friction effect is ignored (Brunetti, 2008). So:

$$\vec{F}_s = -[p_1 A_1 \vec{n}_1 + p_2 A_2 \vec{n}_2 + Q_m (\vec{v}_2 - \vec{v}_1)]$$

As in (1) and (2), a jet is released at atmospheric pressure, $p_1 = p_2 = 0$, then:

$$\vec{F}_s = Q_m (\vec{v}_1 - \vec{v}_2)$$

Projecting in respect of x:

$$F_{sx} = Q_m (v_1 - v_2 \cos \theta)$$

Projecting in respect of y:

$$F_{sy} = Q_m (0 - v_2 \sin \theta) = -Q_m v_2 \sin \theta$$

It is normal at this type of application, to ignore the fluids friction with a solid surface, so the difference between the elevations between (1) and (2), result in $v_1 = v_2 = v_j$ (jet velocity). Thus:

$$F_{sx} = \rho A_j v_j^2 (1 - \cos \theta) \wedge F_{sy} = -\rho A_j v_j^2 \sin \theta$$

A force \vec{F}_s is obtained by a composition of \vec{F}_{sx} and \vec{F}_{sy} , which its point of application will be at a crossing point of those vectors (Brunetti, 2008).

5.2.4 Action of a jet in a plain surface

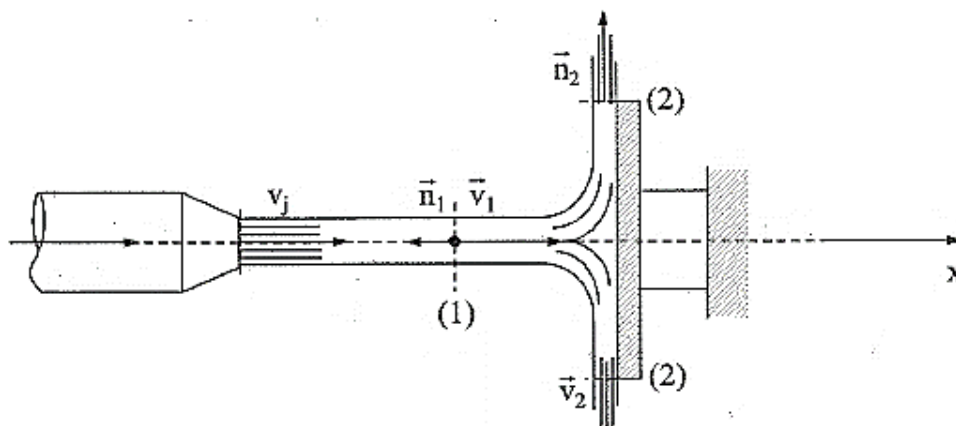


Figure 101 – Filling jet on a flat plate (Brunetti, 2008).

Consider a jet, that hit a plate, where it is totally uniformly spread in all directions (Brunetti, 2008). The velocity v_2 will not have a component in x direction. And as the pressure is atmospheric, it is obtained:

$$F_{sx} = \rho Q v_1$$

5.2.5 Forces in movables solid surfaces

In many problems, the main objective is to determine the action of fluids in solid surfaces in movement. At this sub chapter, it will be considered especially rectilinear and uniform movements, in order to avoid inertia forces due to acceleration (Brunetti, 2008).

With this hypothesis, the problem will be solved in a simpler way, because it will be enough to study in relation of a fixed system of reference in the movable solid surface (Brunetti, 2008).

By this way, a solid surface is again observed in rest, and the fluid will have an altered velocity in relation to that one appreciated from an inertial system of reference (Brunetti, 2008).

At this case, the velocity variation must be studied from a fixed system of reference (fixed to the solid surface). Let's see how some of the already stated expressions are altered when the solid surface is in movement (Brunetti, 2008).

For the study, it will be adopted a particular case for a mayor comprehension. So, in Figure 102 the diverter of a jet in movement with constant velocity (\vec{v}_s) (Brunetti, 2008).

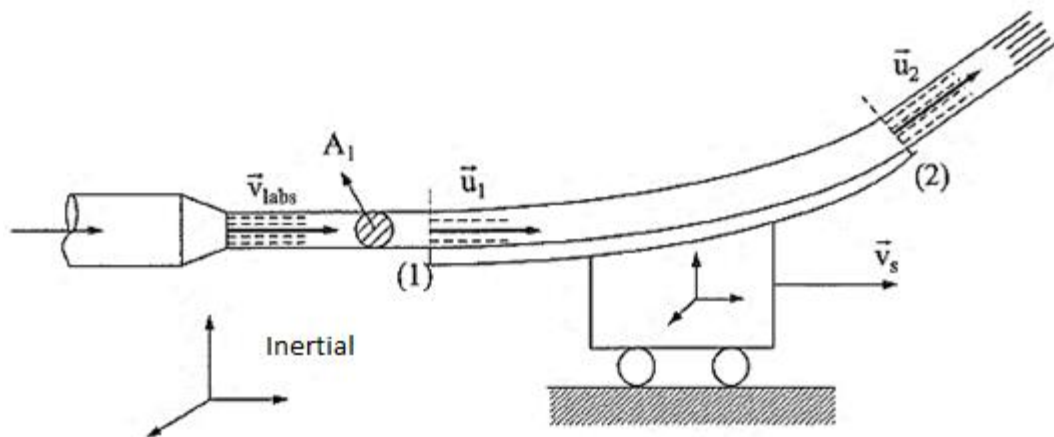


Figure 102 – Filling jet on a moving curve plate (Brunetti, 2008).

It is well-know from mechanics, that $\vec{v}_{abs} = \vec{u} + \vec{v}_s$, where:

\vec{v}_{abs} is absolute velocity in relation to an inertial system;

\vec{v}_s is the diverter velocity, which is the velocity of the fixed system of reference;

\vec{u} is the relative velocity in relation to a movable system of reference, at this case, the jet velocity in relation to the diverter.

A force from the diverter acts against the fluids jet, launched by through the opening, in function of a relative velocity (\vec{u}). It easy to proof such affirmation, because, if a diverter has a higher velocity than the fluid, the force will be nulled, but if a diverter has non velocity, a force will be mayor in it than if the diverter would have had some

velocity. So, as faster the diverter goes, lower is the applied force. In case the solid surface stand with move, go to chapter 5.2.3 (Brunetti, 2008).

At this particular application, flow rate of a jet launched through an opening is $Q_m = \rho A_1 v_1$, however, due to the movement of the solid surface, that flow rate does not really totally approach it (Brunetti, 2008). But what really affects such surface is a flow rate given by:

$$Q_{m_{ap}} = \rho A_1 (v_{abs_1} - v_s) = \rho A_1 u_1$$

Then, the equation that defines \vec{F}_s , will became for relative movement:

$$\vec{F}_s = Q_{m_{ap}} (\vec{u}_1 - \vec{u}_2)$$

So, it is possible to have a hypothesis of rectilinear and uniform movement of a solid surface, so all expression are valid since the relation of velocity $\vec{u} = \vec{v}_{abs} - \vec{v}_s$ and flow rate $Q_{m_{ap}}$ is used instead of Q_m (Brunetti, 2008). So, in a general form,

$$\vec{F}_s = - \left[p_1 A_1 \vec{n}_1 + p_2 A_2 \vec{n}_2 + Q_{m_{ap}} (\vec{u}_1 - \vec{u}_2) \right]$$

5.2.6 Kutta-Joukowski's Theorem

Based in the literature of Pontes and Mangiavacchi (2013), the **Kutta-Joukowski's Theorem** is a fundamental theorem of aerodynamic. Which name comes from the scientists called Martin Wilhelm Kutta (German) and Nikolai Joukowski (Russian) (or Zhukovsky), pioneers in their ideas development at the beginning of the 1920's.

Such theorem said that sustentation generated by a cylinder is proportional to the velocity of the cylinder through the fluid, fluids density and circulation. Circulation is defined as the line integral around a closed cycle surrounding the cylinder or aerofoil, integrating the tangential component of the fluid's velocity to a loop. Magnitude and direction of velocity of a fluid vary along path.

The flow of air in response to the aerofoil presence can be treated as a superposition of a translational flow and a rotational flow (Figure 103). But it is a mistake to think that exist a closed vortex surrounding the cylinder or airplane wing of a flying airplane. And the path of the integral that surround the cylinder does not have an air vortex. (in descriptions of the Kutta-Joukowski's theorem, the aerofoil is generally considered as a circular cylinder or some type of aerofoil of Joukowski).

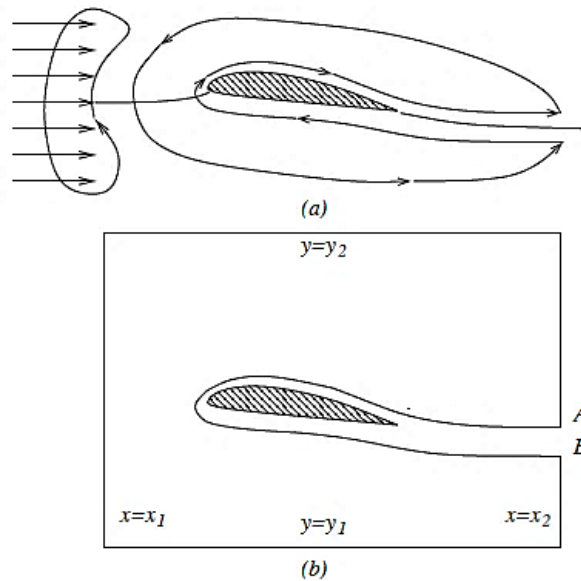


Figure 103 – (a): Evolution of a fluid mass when steps with a body; (b): Volume of control used in the determination of a sustentation force acting in the body (Pontes & Mangiavacchi, 2013).

The theorem refers to a flow of two dimensions around a cylinder (or cylinder on infinite wingspan) and determines the generated sustentation per unit length. When **circulation Γ_∞** is known, **sustentation L** , per unit of cylinders length (N/m, in SI) can be calculated according to the next equation (Kutta-Joukowski's theorems form):

$$L = \rho_\infty V_\infty \Gamma_\infty$$

Where, **ρ_∞ e V_∞ are respectively, fluids density and upstream cylinders velocity**, and Γ_∞ is circulation defined as the line integral:

$$\Gamma_\infty = \oint_{C_\infty} V \cos \theta \, ds$$

Around a path **C_∞ (in complex plane) long-enough and surrounding the cylinder or aerofoil**. Such path must be a region of potential flow and not a border layer of the cylinder. The term **$V \cos \theta$ is a local component of velocity, tangential and oriented in direction of a curve C_∞** that encircles the cylinder, and **ds is the infinitesimal length of such curve**.

CHAPTER 6 - FLOWS THROUGH ORIFICES AND SPILLWAYS

6.1 Flows through orifices

Flows through openings is a subject of great interest in hydraulics for applications, for example (Silva, 2014):

- Flow rate control in general (flow rate measures dispositive, from industrial effluents and water channels);
- Water outlets in supply systems;
- Projects of irrigations and drainage;
- Retention basins for urban floods control;
- Hydroelectrical projects;
- Treatment of water and sewers;
- Shock absorbers in cars, planes and cannon recoil mechanics system;
- Motor oil feeding systems for vehicles;
- Industrial burners;
- Sprinkler irrigation.

Some useful concepts in order to understand the subject (Silva, 2014):

- **Orifice** - any orifice or opening, of closed perimeter, defined geometric form practiced on a wall, reservoir bottom or pipe under pressure, that contains a liquid or a gas, such opening allows the flow to occur;
- **Floodgate** - is a piece adopted to the orifices with variable opening and \one side exposed to a free flow;
- **Penstock** - are orifices of incomplete contraction, adopted in reservoirs, dams or channels, which dimensions of opening can be controlled with a movable surface;
- **Opening or nozzle** – piece adapted to a wall or recipient's bottom or a pipe, in order to set a direction for a liquid jet. The flow through such dispositive has same theoretical foundations as flows through orifices. Measure between 1.5 and 5 times the diameter orifice.

In this way, the part of Hydraulics that explains the study and modulation of flows through holes, orifices, opening or spillways is called **Hydrometrics** (study of different methods to measure velocity and flow rate in channels and pipes) (Mendonça, 2015).

6.1.1 General scheme of an orifice

Flows principle: **Potential energy** \leftrightarrow **kinetical energy** (Silva, 2014).

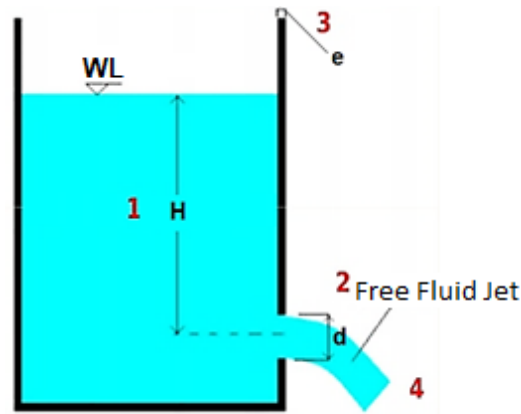


Figure 104 – General scheme of an orifice (adapted from Silva, 2014).

Considering the previous figure:

1. H = charge above an orifice;
2. d = vertical dimension, diameter or height of opening formed by the orifice or hole;
3. e = thickness of orifices walls;
4. The fluid jet emanating from the orifice is called **liquid vein**, forming a parabola.

6.1.2 Classification

Based in Silva (2014):

- **Geometric form**
 - Simple: circular, triangular, rectangular, square, elliptical, etc.;
 - Composed: more than one geometric form;
- **Orientation**
 - Horizontal;
 - Vertical;
 - Inclined;
- **Dimensions**
 - Small dimensions: $d \leq H/3$;
 - Big dimensions: $d > H/3$;
- **Nature of the wall**
 - Thin wall: $e < 0.5d$. The contact of a jet only at a contour line (perimeter) of the orifice;
 - Thick wall: $0.5d \leq e \leq 1.5d$. The contact with the jet with an internal surface of the orifice (adherence of the jet);
 - Openings: $1.5d < e \leq 5d$. Piece adapted to the wall to orientate the jet;
- **Variability of the charge in time**
 - Permanent: all particles that cross the orifice are under the same charge H and have same velocity v ;

- Transition: H is consider variable and particles that cross the opening have different velocities;
- **Type of contraction of an effluent jet**
 - Total;
 - Partial;
- **Pressure of an effluent jet**
 - Free (atmospheric pressure);
 - Partially submerged;
 - Totally submerged.

6.1.3 Orifices of thin walls

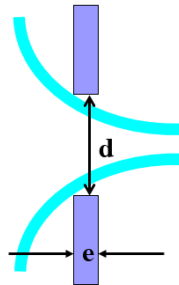


Figure 105 – Orifices of thin walls (Junior L. B., 2005).

Flow rate drained through orifices of small dimensions (vertical dimensions $< 1/3h$)

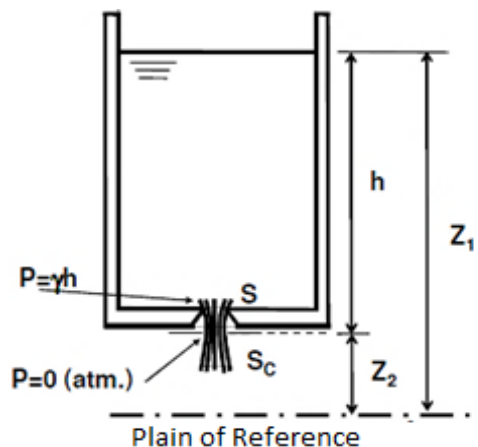


Figure 106 – Flow rate drained through orifices of small dimensions (Pinho et al., 2011).

At this situation, we have:

- S_c , constricted section;
- In permanent movement;

$$\left(Z + \frac{p}{\gamma} + \frac{\alpha U^2}{2g} \right)_{S_L} - \left(Z + \frac{p}{\gamma} + \frac{\alpha U^2}{2g} \right)_{S_C} = \Delta H \rightarrow Z_1 - Z_2 - \frac{\alpha U_c^2}{2g} = K \frac{\alpha U_c^2}{2g}$$

$$U_c = \frac{1}{\sqrt{\alpha + K}} \sqrt{2gh}$$

- **Velocity coefficient** (Table 7);

$$C_v = \frac{1}{\sqrt{\alpha + K}} \quad (0.960 \text{ a } 0.990)$$

Table 7 – Values for C_v at different charges values and orifices diameters (adapted from Netto, 1998).

Charge, H [m]	Orifices diameters, d [cm]				
	2.0	3.0	4.0	5.0	6.0
0.20	0.954	0.964	0.973	0.978	0.984
0.40	0.956	0.967	0.976	0.981	0.986
0.60	0.958	0.971	0.980	0.983	0.988
0.80	0.959	0.972	0.981	0.984	0.988
1.00	0.958	0.974	0.982	0.984	0.988
1.50	0.958	0.976	0.984	0.984	0.988
2.00	0.956	0.978	0.984	0.984	0.988
3.00	0.957	0.979	0.985	0.986	0.988
5.00	0.957	0.980	0.987	0.986	0.990
10.00	0.958	0.981	0.990	0.988	0.992

- Flow rate drained: $Q = S_c \cdot U_c$;
- **Coefficient of contraction** (Table 8);

$$C_c = \frac{S_c}{S} \quad (0.600 \text{ e } 0.640) \rightarrow Q = C_c \cdot S \cdot U_c = C_c \cdot S \cdot C_v \sqrt{2gh} = C_d \cdot S \cdot \sqrt{2gh}$$

Table 8 – Values of C_c for different values of charge and orifices diameters (adapted from Netto, 1998).

Charge, H [m]	Orifices diameters, d [cm]				
	2.0	3.0	4.0	5.0	6.0
0.20	0.685	0.656	0.625	0.621	0.617
0.40	0.681	0.646	0.625	0.619	0.616
0.60	0.676	0.644	0.623	0.618	0.615
0.80	0.673	0.641	0.622	0.617	0.615
1.00	0.670	0.639	0.621	0.617	0.615
1.50	0.666	0.637	0.620	0.617	0.615
2.00	0.665	0.636	0.620	0.617	0.615
3.00	0.663	0.634	0.620	0.616	0.615
5.00	0.663	0.634	0.619	0.616	0.614
10.00	0.662	0.633	0.617	0.615	0.614

- **Coefficient of discharge or exhaust** (Table 9);

$$C_d = C_c \cdot C_v \quad (\text{average practice} = 0.610)$$

Table 9 – Values of C_d for different values of charge and Orifice diameters (adapted from Netto, 1998).

Charge, H [m]	Orifices diameter, d [cm]				
	2.0	3.0	4.0	5.0	6.0
0.20	0.653	0.632	0.609	0.607	0.607
0.40	0.651	0.625	0.610	0.607	0.607
0.60	0.648	0.625	0.610	0.607	0.608
0.80	0.645	0.623	0.610	0.607	0.608
1.00	0.642	0.622	0.610	0.607	0.608
1.50	0.638	0.622	0.610	0.607	0.608
2.00	0.636	0.622	0.610	0.607	0.608
3.00	0.634	0.621	0.611	0.607	0.608
5.00	0.634	0.621	0.611	0.607	0.608
10.00	0.634	0.621	0.611	0.607	0.609

- Theoretical flow (without ΔH).

$$U_c = \sqrt{2gh} \rightarrow \text{Torricelli's Formula}$$

In order to illustrate, **Torricelli's Equation** is a kinematic equation that was found by Evangelista Torricelli; such equation allow to calculate final velocity of a body in rectilinear uniformly variated movement, which means constant acceleration; with this equation it is not necessary to know the interval of time in movement (Ramalho, Nicolau, & Toledo, 2015). This equation can be reduced from the following equations:

$$\text{Movement of an accelerated body} = \begin{cases} s = s_o + v_o t + \frac{at^2}{2}, \text{ related to space} \\ v_f = v_o + at, \text{ related to velocity} \end{cases}$$

Isolating t from the second equation:

$$t = \frac{(v_f - v_o)}{a}$$

And replacing it in the first one, is obtained:

$$\begin{aligned} s - s_o &= v_o \frac{(v_f - v_o)}{a} + \frac{a}{2} \left(\frac{v_f - v_o}{a} \right)^2 \Rightarrow \\ \Rightarrow \Delta s &= \left(\frac{v_f v_o - v_o^2}{a} \right) + \frac{a}{2} \left(\frac{v_f^2 - 2v_f v_o + v_o^2}{a^2} \right) \Rightarrow \end{aligned}$$

$$\begin{aligned}\Rightarrow \Delta s &= \frac{v_f v_o - v_o^2}{a} + \frac{v_f^2 - 2v_f v_o + v_o^2}{2a} \Rightarrow \\ \Rightarrow \frac{2a\Delta s}{2a} &= \frac{2v_f v_o - 2v_o^2}{2a} + \frac{v_f^2 - 2v_f v_o + v_o^2}{2a} \times 2a \Rightarrow \\ \Rightarrow 2a\Delta s &= 2v_f v_o - 2v_o^2 + v_f^2 - 2v_f v_o + v_o^2 \Rightarrow \\ \Rightarrow 2a\Delta s &= -v_o^2 + v_f^2 \Rightarrow \\ \Rightarrow \boxed{v_f^2} &= \boxed{v_o^2 + 2a\Delta s}\end{aligned}$$

Where v_f^2 and v_o^2 represents respectively, final and initial velocities of a body, while Δs represents the distance achieved ("s" comes from Latin *Spatium*, more frequently used "d") and a represents acceleration.

Flow rate drained through orifice of great dimensions (vertical dimensions > 1/3h)

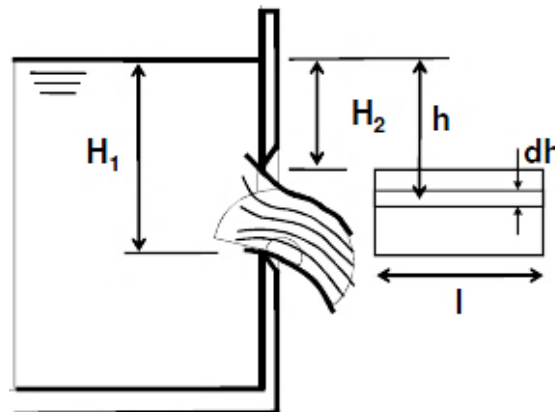


Figure 107 – Flow rate drained through orifices of great dimensions. Rectangular shape (Pinho et al., 2011).

Where:

l is the length of the orifice;

dh is the thickness of the elementary stretch;

h is the height of water above the elementary stretch.

- Elemental flow rate;

$$dQ = C_d \cdot dS \cdot \sqrt{2gh} \rightarrow dQ = C_d \cdot l \cdot \sqrt{2gh} \cdot dh$$

- Total flow rate;

$$Q = \int_{H_2}^{H_1} C_d \cdot l \cdot \sqrt{2gh} \cdot dh \rightarrow Q = \frac{2}{3} C_d l \sqrt{2g} (H_1^{3/2} - H_2^{3/2})$$

Where the area of the orifice is given by:

$$S = l(H_1 - H_2) \Rightarrow l = S/(H_1 - H_2)$$

Then:

$$Q = \frac{2}{3} C_d \frac{S}{(H_1 - H_2)} \sqrt{2g} (H_1^{3/2} - H_2^{3/2}) \Rightarrow Q = \frac{2}{3} C_d S \sqrt{2g} \left(\frac{H_1^{3/2} - H_2^{3/2}}{H_1 - H_2} \right) \Rightarrow Q = C'_d S \sqrt{2gh}$$

- **Coefficient of discharge adjusted, C'_d .**

$$C'_d = x C_d$$

Values of x are founded in tables in functions of d/h , where d is the height of the orifice (DRHGSA, 2007):

Table 10 – Values of correction, x (adapted from DRHGSA, 2007).

Rectangular orifices		Circular orifices	
d/h	x	r/h	x
0.5	0.943	10	0.960
0.5	0.955	0.999	0.962
0.5	0.963	0.99	0.963
0.6	0.966	0.95	0.966
0.7	0.976	0.90	0.970
0.8	0.982	0.85	0.974
0.9	0.986	0.80	0.977
1.0	0.989	0.70	0.983
1.2	0.993	0.60	0.988
1.4	0.995	0.50	0.992
1.6	0.996	0.40	0.995
2	0.997	0.30	0.997
3	0.999	0.20	0.999
10	1	0.10	0.9997

Note: without knowing an exact value of C_d , can be adopted $C'_d = 0.60$ for rectangular or circular orifices with $d \geq 0.30$ m (DRHGSA, 2007).

Consideration of arrival velocity U_0 (Pinho et al., 2011)

- Channels, Orifices of great dimensions: to the static charge above the orifice is added a kinetic charge or energy, $U^2/2g$;
- Rectangular orifice of great dimensions;

$$Q = \frac{2}{3} C_d l \sqrt{2g} \left[\left(H_1 + \frac{U_0^2}{2g} \right)^{3/2} - \left(H_2 + \frac{U_0^2}{2g} \right)^{3/2} \right]$$

- Orifice of small dimensions.

$$Q = C_d S \sqrt{2g \left(h + \frac{U_0^2}{2g} \right)}$$

Orifices totally submerged

The orifice is drowned when the liquid vein flows in a fluid mass, when discharged under water (Figure 108) (DRHGSA, 2007).

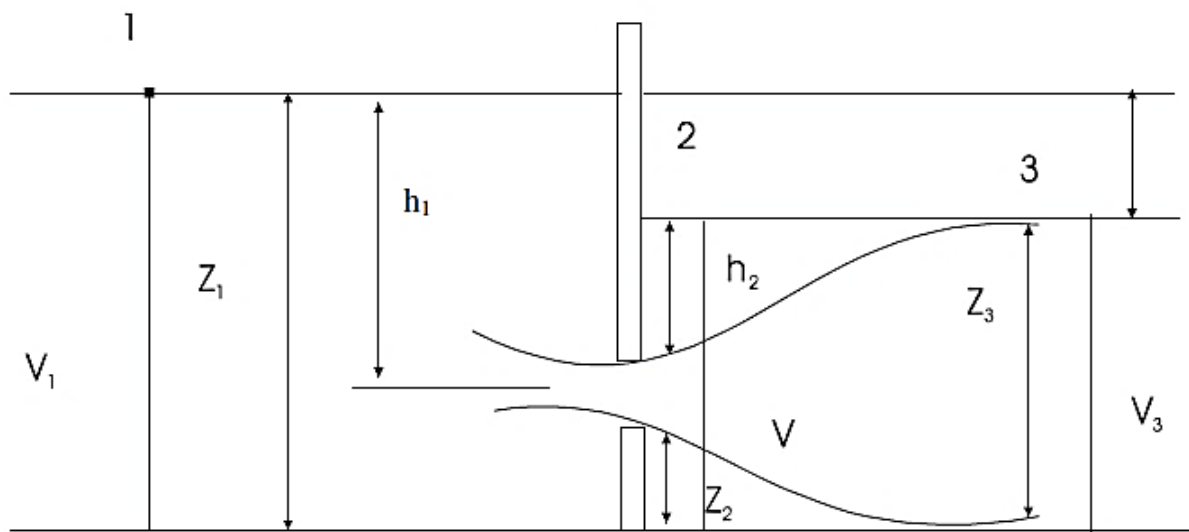


Figure 108 – Totally submerged orifice (DRHGSA, 2007).

- **1st case:** fluids velocity in reservoir is so small or null, that is ignored ($V_1 = V_3 = 0$) (DRHGSA, 2007);

Bernoulli between sections 1 and 2:

$$z_1 + 0 + 0 = z_2 + h_2 + \frac{V^2}{2g} \Rightarrow \frac{V^2}{2g} = z_1 - (z_2 + h_2) \Rightarrow \frac{V^2}{2g} = h$$

$$\therefore V^2 = 2gh \Rightarrow V = \sqrt{2gh}$$

Flow rate is given by:

$$Q = C_{d,s} S \sqrt{2gh}$$

Coefficients for drowned orifices ($C_{d,s}$) are lightly lower than the corresponded to a free discharge, but error is small, when using it. Such coefficients are:

Table 11 – Values of $C_{d,s}$ for drowned orifices (Smith, 1886).

Charge [m]	Orifice dimensions [m]				
	Circular (d) 0.015	Square (a) 0.015	Circular (d) 0.03	Square (a) 0.03	Rectangular (a × b) 0.015x0.03
0.15	0.615	0.619	0.603	0.608	0.623
0.30	0.610	0.614	0.602	0.606	0.622
0.45	0.607	0.612	0.600	0.605	0.621
0.60	0.605	0.610	0.599	0.604	0.620
0.75	0.603	0.608	0.598	0.604	0.619
0.90	0.602	0.607	0.598	0.604	0.618
1.20	0.601	0.606	0.598	0.604	-

- **2nd case**: velocities in upstream and downstream reservoirs cannot be ignored (DRHGSA, 2007).

Again, Bernoulli between sections 1 and 2:

$$z_1 + 0 + \frac{V_1^2}{2g} = z_3 + 0 + \frac{V_3^2}{2g} + h_p$$

But,

$$h_p = \frac{(V - V_3)^2}{2g} \rightarrow \text{Charge loss due to jet expansion}$$

Then:

$$z_1 + \frac{V_1^2}{2g} = z_3 + \frac{V_3^2}{2g} + \frac{(V - V_3)^2}{2g} \Rightarrow z_1 - z_3 + \frac{V_1^2}{2g} - \frac{V_3^2}{2g} = \frac{(V - V_3)^2}{2g} \Rightarrow$$

$$\Rightarrow h + \frac{V_1^2}{2g} - \frac{V_3^2}{2g} = \frac{(V - V_3)^2}{2g} \xrightarrow{\times 2g} (V - V_3)^2 = 2gh + V_1^2 - V_3^2 \Rightarrow$$

$$\Rightarrow V - V_3 = \sqrt{2gh + V_1^2 - V_3^2} \Rightarrow$$

$$\Rightarrow V = V_3 + \sqrt{2gh + V_1^2 - V_3^2} \Rightarrow$$

$$\Rightarrow Q = C_{d,s}S \left(V_3 + \sqrt{2gh + V_1^2 - V_3^2} \right)$$

Orifices partially submerged

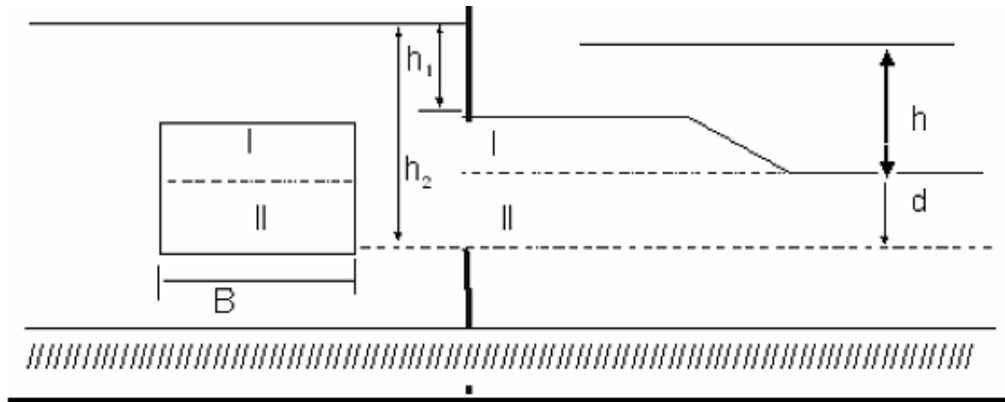


Figure 109 – Orifices partially submerged (DRHGSA, 2007).

A discharge through an orifice partially submerged can be considered as the summation of the charges of an orifice of great dimensions (I) and a drowned orifice (II). With $V_1 = 0$ (DRHGSA, 2007):

$$Q_I = \frac{2}{3} C_d B \sqrt{2g} (h_2^{3/2} - h_1^{3/2})$$

$$Q_{II} = C_{d,s} S \sqrt{2gh} \Rightarrow$$

$$\Rightarrow Q_{II} = C_{d,s} B (h_2 - h) \sqrt{2gh}$$

$$Q = Q_I + Q_{II} \Rightarrow$$

$$\Rightarrow Q = \frac{2}{3} C_d B \sqrt{2g} (h_2^{3/2} - h_1^{3/2}) + C_{d,s} B (h_2 - h) \sqrt{2gh} \Rightarrow$$

$$\Rightarrow Q = B \sqrt{2g} \left[\frac{2}{3} C_d (h_2^{3/2} - h_1^{3/2}) + C_{d,s} (h_2 - h) \sqrt{h} \right]$$

6.1.4 Orifices of thick walls. Additional pipes

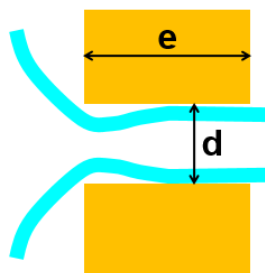


Figure 110 – Orifices of thick walls (Junior L. B., 2005).

Orifices of rounded edges

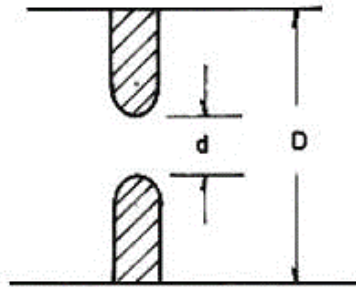


Figure 111 – Orifices of rounded edges (<https://pt.slideshare.net/IsaqueEliasCorreia/instrumentacaobasica2-pdf>).

$$Q = C_d S \sqrt{2gh}, \text{ on what } C_d = 0.98 \neq 1.0 \text{ by friction } \wedge C_c = 1.0$$

Orifices with incomplete Constriction (or contraction)

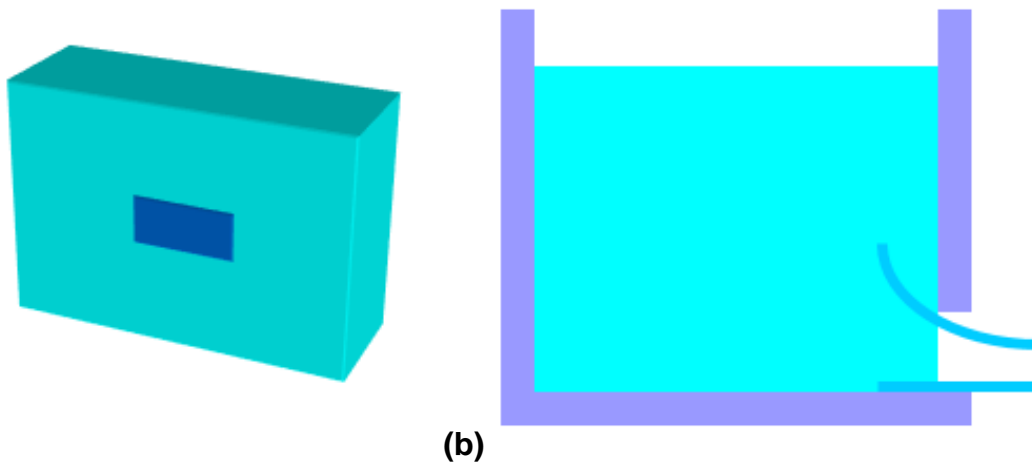


Figure 112 – (a) Full contraction (in all orifices faces); (b) Partial contraction (only at the top) (Junior L. B., 2005).

For rectangular orifices, C_d assume a value of C'_d , by the following form (Junior L. B., 2005):

$$C'_d = C_d (1 + 0.15k), \text{ with } k = \frac{P_{sc}}{P}$$

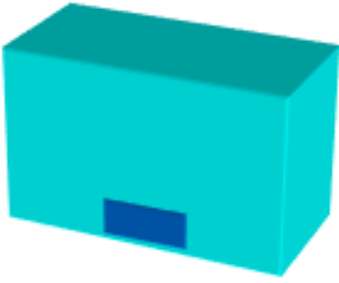
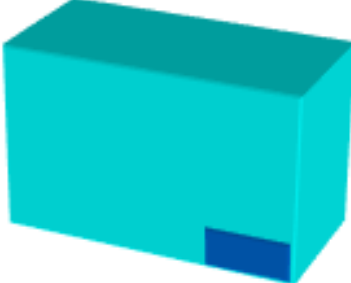
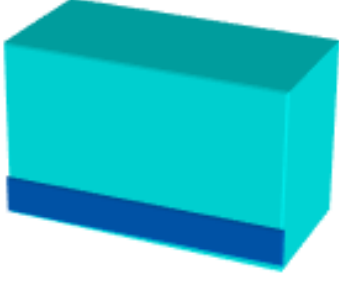
Where:

k is a relation of perimeters;

P_{sc} , P represents respectively, the perimeter of the part where there is suppression of the contraction and the total perimeter of the orifice.

For a rectangular orifice $P = 2(a + b)$, with a and b representing respectively, height and length. So, coefficient k assume next forms:

Table 12 – Relation between perimeters, k for different positions of a rectangular orifice (Junior L. B., 2005).

Middle bottom	Bottom, next to wall	Wide Bottom
		
$k = \frac{b}{2(a + b)}$	$k = \frac{a + b}{2(a + b)}$	$k = \frac{2a + b}{2(a + b)}$

For circular orifices (Junior L. B., 2005):

$$C'_d = C_d(1 + 0.13k)$$

Thus:

- For orifices next to a lateral wall, $k = 0.25$;
- For orifices right at bottom, $k = 0.25$;
- For orifices next to a lateral wall and at bottom, $k = 0.50$;
- For orifices at bottom and confined by both lateral walls, $k = 0.75$.

Additional pipes

Structure made for a water flow with a small charge and length between $5d$ and $1000d$ (Silva, 2014):

- Too short pipe or tube: $5d < L < 100d$;
- Short pipe or tube: $100d < L < 1000d$;
- Long pipe or tube: $L > 1000d$;
- C_d adapted is used and following the law of flows through orifices;
- Formula for long pipes apply if $L > 100d$.

Another classification in circular sections pipes (Pino et al., 2011):

- Cylinder;
- Conics;
- Internal;
- External.

For calculate an approaching of flow rate $Q = C_d S \sqrt{2gh}$ (Silva, 2014):

- Orifices of thin wall: $L/d < 0.5 \rightarrow C_d = 0.61$;
- For openings: $1.5 < L/d < 5 \rightarrow C_d = 0.82$;

- At this point, check the entrance;
- For very short pipes, according to Eytelwein and for cast iron, we have:

Table 13 – Value of C_d according Eytelwein and for very short pipes of cast iron (Silva, 2014).

L/d	C_d
10	0.77
20	0.73
30	0.70
40	0.66
60	0.60

Additional internal pipes - Short pipe addition (Pinho et al., 2011)

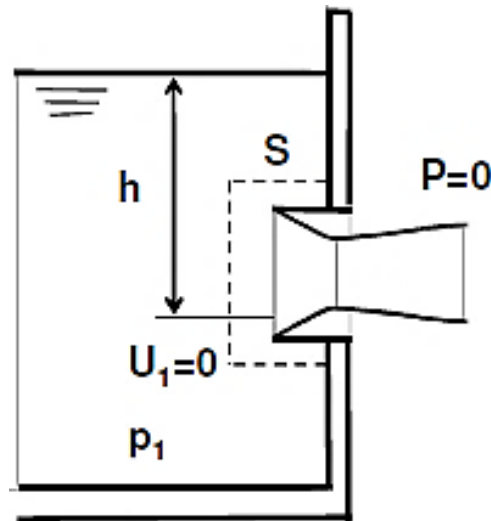


Figure 113 – Short pipe addition (Pinho et al., 2011).

Theorem of Amount of Movement:

$$\rho QU = p_1 S \rightarrow Q = US_c$$

Bernoulli's Theorem:

$$\left(0 + \frac{p_1}{\gamma} + 0\right) - \left(0 + 0 + \frac{U^2}{2g}\right) = 0 \Rightarrow p_1 = \rho \frac{U^2}{2}$$

$$S_c = \frac{S}{2} \Rightarrow Q = \frac{S}{2} \sqrt{2gh} \Rightarrow C_d = \frac{1}{2}$$

Additional internal pipes - Additional internal pipe with adherent liquid vein
(Pinho et al., 2011)

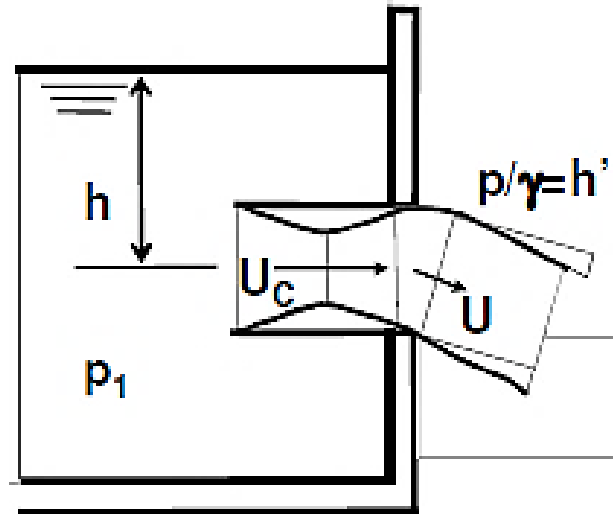


Figure 114 – Additional pipe with adherent liquid vein (Pinho et al., 2011).

Theorem of Amount of Movement:

$$\rho QU = p_1 S, \text{ com } p_1 = \gamma h \wedge Q = US \rightarrow U = \sqrt{gh}$$

$$Q = S\sqrt{gh} = \frac{\sqrt{2}}{2} S\sqrt{2gh} \Rightarrow C_d = \frac{\sqrt{2}}{2}$$

Bernoulli's Theorem ($S_L \rightarrow S_c$):

$$\begin{cases} h = h' + \frac{U_c^2}{2g} \\ h' = h \end{cases}$$

$$p_{abs} = p_a - \gamma h > 0 \Rightarrow h < \frac{p_a}{\gamma}$$

Bernoulli's Theorem ($S_L \rightarrow$ downstream):

$$\begin{cases} h = 0 + \frac{U^2}{2g} + \Delta H \\ \Delta H = \frac{(U_c - U)^2}{2g} \end{cases}$$

$$U = \frac{U_c}{2}$$

Additional external pipes - Additional cylindrical pipe (Pinho et al., 2011)

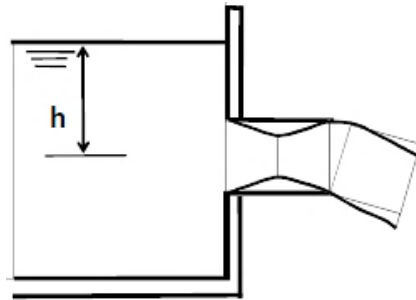


Figure 115 – Additional cylindrical pipe (Pinho et al., 2011).

$$L \geq 1.5\phi$$

$$Q = C_d S \sqrt{2gh}, \text{ with } C_d = 0.82 \text{ (External cylindrical nozzle)}$$

Bernoulli's Theorem ($S_L \rightarrow S_c$):

$$\begin{cases} h = h' + \frac{U_c^2}{2g} \\ h' = h \left[1 - \left(\frac{0.82}{C_c} \right)^2 \right] \end{cases} \xrightarrow{C_c < 0.62} h' > -0.75h$$

Additional external pipes - Additional conical pipe

• Convergent

$$Q = C_d S \sqrt{2gh}, \text{ with } C_d = 0.95$$

Table 14 – C_d for conical converged nozzle (Silva, 2014).

θ (°, degrees)	0	11.5	22.5	45	90
C_d sharp edge	0.97	0.94	0.92	0.85	-
C_d rounded edge	0.97	0.95	0.92	0.88	0.75

• Divergent

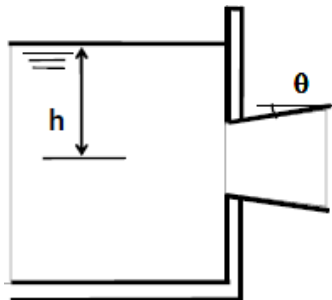


Figure 116 – Additional conical divergent pipe (Pinho et al., 2011).

C_d for conical divergent nozzle (Silva, 2014):

- Sharp edge: $C_d = 1.40$;
- Rounded edge: $C_d = 2.00$;
- Maximum angle for nozzle fulfilling by liquid vein 16° ;
- Maximum flow rate: $L = 9d \wedge \theta = 10^\circ$;
- For $\theta > 7^\circ$, jet the jet stands out and the pipe effects disappears.

6.1.5 Draining time in reservoir

Variable section (Pinho et al., 2011)

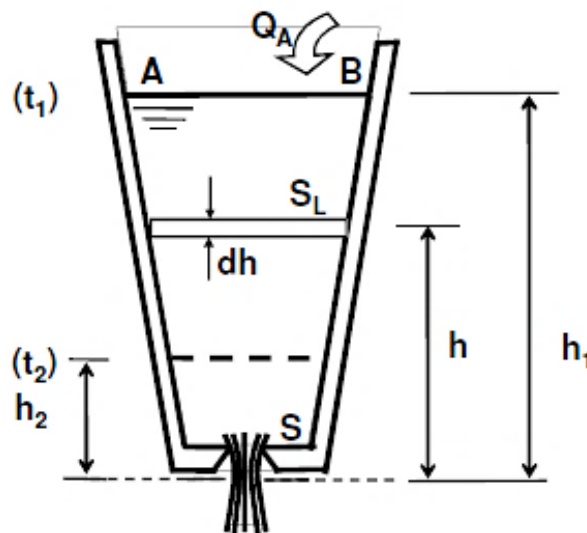


Figure 117 – Draining of a reservoir of variable section (Pinho et al., 2011).

- Charge (h):

$$Q = C_d S \sqrt{gh}$$

- Continuity equation:

$$\begin{aligned} (Q - Q_A) dt &= -S_L dh \Rightarrow \\ \Rightarrow (C_d S \sqrt{2gh} - Q_A) dt &= -S_L \\ t &= - \int_{h_1}^{h_2} \frac{S_L}{(C_d S \sqrt{2gh} - Q_A)} dh \\ \Rightarrow t = t_2 - t_1 &= - \int_{h_2}^{h_1} \frac{S_L}{(C_d S \sqrt{2gh} - Q_A)} dh \end{aligned}$$

Constant section (Pinho et al., 2011)

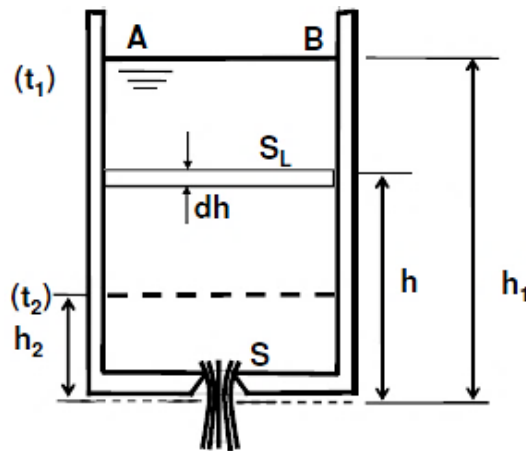


Figure 118 – Draining of a reservoir of constant section (Pinho et al., 2011).

- Considering S_L constant and Q_A null:

$$t = \frac{S_L}{S\sqrt{2g}} \int_{h_2}^{h_1} \frac{1}{C_d\sqrt{h}} dh$$

- Considering also $C_d = \text{cst.}$:

$$t = \frac{S_L}{SC_d\sqrt{2g}} \int_{h_2}^{h_1} \frac{1}{\sqrt{h}} dh \rightarrow t = \frac{2S_L(\sqrt{h_1} - \sqrt{h_2})}{SC_d\sqrt{2g}}$$

- Considering total drain:

$$h_2 = 0 \rightarrow t = \frac{2S_L\sqrt{h_1}}{SC_d\sqrt{2g}} \Rightarrow t = \frac{2V_1}{Q_1}, \text{ com } Q_1 = C_d S \sqrt{2gh_1}$$

6.1.6 Configuration of liquid jets

Phenomenon that occurs to the transversal section of jet that undergoes successive stages, changing its original shape, from a constricted section (Silva, 2014).

A **circular jet** tends to maintain its form along all liquid vein of a jet (Silva, 2014).

A **jet emanating from an elliptical orifice** in the contracted section have an elliptical shape like the orifice. But, while the flows undergo, such section tends to become a circular shape and then back to the elliptical one, so with its mayor axis corresponding with the minor axis of the original section (Silva, 2014).

For **vertical orifices of great dimensions**, due to influence of superficial tensions, occurs an inversion of the liquid vein in case of an orifice of square shape (Pinho et al., 2011):

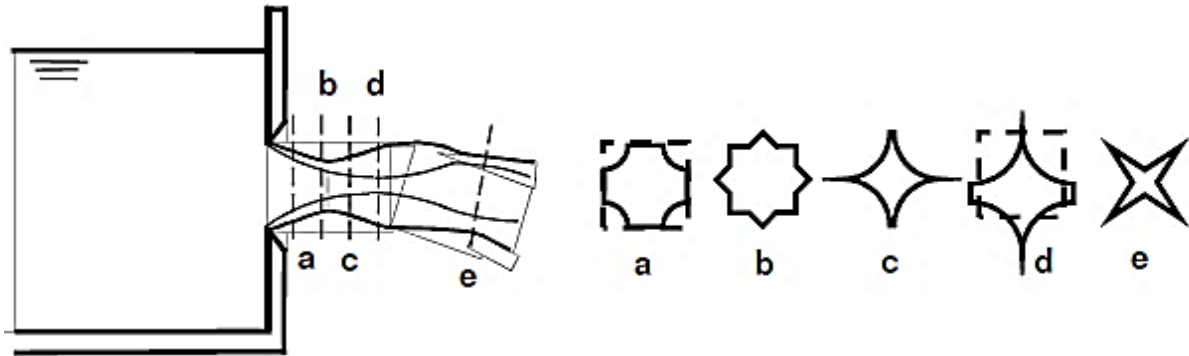


Figure 119 – Inversion of the liquid vein (Pinho et al., 2011).

According to **the longitudinal configuration of a liquid vein** (Pinho et al., 2011):

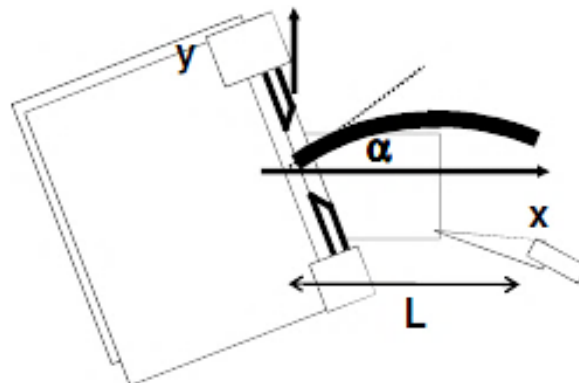


Figure 120 – Configuration of a liquid vein (Pinho et al., 2011).

$$\left\{ \begin{array}{l} \frac{d^2x}{dt^2} \\ \frac{d^2y}{dt^2} \end{array} \right\} \rightarrow \text{simplified formulas} = \left\{ \begin{array}{l} y = x \tan \alpha - \frac{gx^2}{2U^2 \cos^2 \alpha} \\ L = \frac{U^2 \sin(2\alpha)}{g} \end{array} \right.$$

6.2 Flows through spillways

Spillways can be defined as walls, dykes or openings in which a liquids flow, basically are structures formed by an opening in a reservoir wall, where the top edge reaches a liquids free surface, producing a flow through the formed structure (Netto, 1998).

Such term applies for spillways in dams. In hydraulics, spillways or unloaders must be built with a geometric defined shape and its study is made considering it as incomplete orifices, which means, without top edge (Netto, 1998).

Unloaders or spillways (Figure 121) are hydraulics instruments to measure flow rate in natural and artificial water channels, as well as controlling flows in galleries, channels and dams (Netto, 1998).

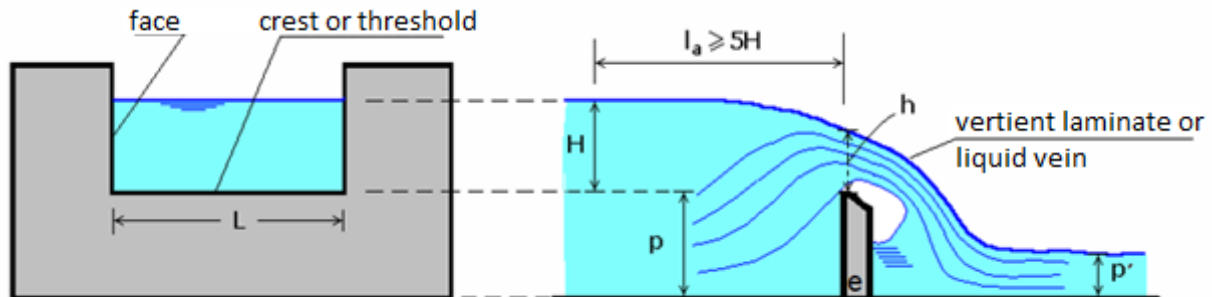


Figure 121 – Scheme of a rectangular unloader or spillway with a free strand blade (Queiroz, 2017).

The horizontal edge is called crest or threshold, and the vertical edge are the faces of the spillway.

The charge of the spillway (H) is the height reached by water, measured from the crest of it. Due to depression (lowering) of the vertient laminate next to the spillway, the charge (H) must be measured at upstream with a distance proximal to $5H$ or greater, where height h correspond to the water height exactly above the crest or threshold. The deepness of the spillway is given by p , and its height at downstream waters is represented by p' , e is its thickness and L its length.

6.2.1 Spillways classification

Many factors can help to classify spillways, as (Queiroz, 2017):

- **Form or shape**
 - Simple: (Rectangular, triangular, trapezoidal, circular, exponential);
 - Composed: (Combined sections – two or more geometric shapes);
- **Crest or threshold**
 - Thin crest (metallic plate or bevelled wood);
 - Thick crest (masonry of stones, bricks or concrete);
- **Relative height of the crest or threshold**
 - Free or complete: ($p > p'$);
 - Drowned or incomplete: ($p < p'$);
- **Relative length of the crest or threshold** (Figure 122)
 - Spillways without lateral contraction ($L = B$);
 - Spillways with a lateral contraction ($L < B$);
 - Spillways with two lateral contractions ($L < B$);

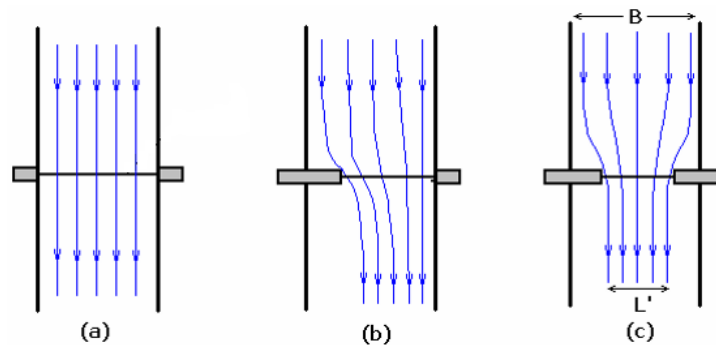


Figure 122 – Spillway (a) without lateral contractions, (b) with one lateral contraction, (c) with two lateral contractions (adapted from Queiroz, 2017).

- **Thickness of the wall**
 - Thin crest or wall: $e \leq 2H/3$ contact of a line between the liquid laminate and the crest;
 - Thick crest or wall: $e > 2H/3$;
- **Liquids laminate shape**
 - Free laminate: with aeration in the internal face, where pressure under such laminate is same as atmospheric;
 - Altered laminate: contracted or adherent;
- **Profile of the crest**
 - Sharp edge;
 - Rounded edge;
- **Position of the spillway (in relation to the current)**
 - Frontal;
 - Oblique;
 - Angular;
 - Lateral;
- **Bottoms profile**
 - Levelled (one level);
 - Stepwise;
- **Normalizations**
 - Standard spillway;
 - Specific spillway.

6.2.2 Influence of the liquid veins shape

When there is no natural incoming air at the space under the liquids laminate, can exists a lower pressure than the atmospheric, inducing a depression or contraction of the liquid vein. Such phenomenon alters the way flow rate is calculate by classic formulas (Queiroz, 2017).

Such phenomenon is normal in spillways without contraction and can occasionally happen in spillways with lateral contraction (Queiroz, 2017).

In those conditions, the liquids laminates are not free anymore, adopting the shape of depress, adherent or drowned laminates (Queiroz, 2017).

When a spillway is used for flow rate measurements, such phenomenon must be avoided (Queiroz, 2017).

The different forms or shape adopted by a liquid vein in a spillway (Queiroz, 2017):

- Free laminates (Figure 123)
 - Pressure over the laminate is equal to atmospheric pressure;
 - An ideal situation for the use of a spillway for flow rate measurements;

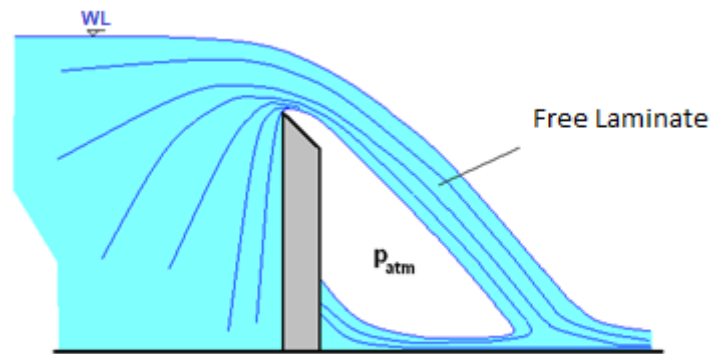


Figure 123 – Free laminate (Queiroz, 2017).

- Depressed laminate (Figure 124)
 - The air is partially dragged by water, inducing a negative pressure under the laminate, which change its shape;

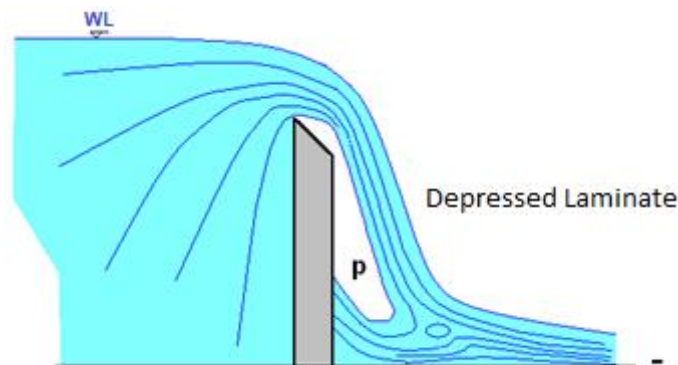


Figure 124 – Depressed laminate (Queiroz, 2017).

- Adherent laminate (Figure 125)
 - The air is totally dragged by water, which push the laminates to stick to the spillway walls. Occurs usually in small flow rate;

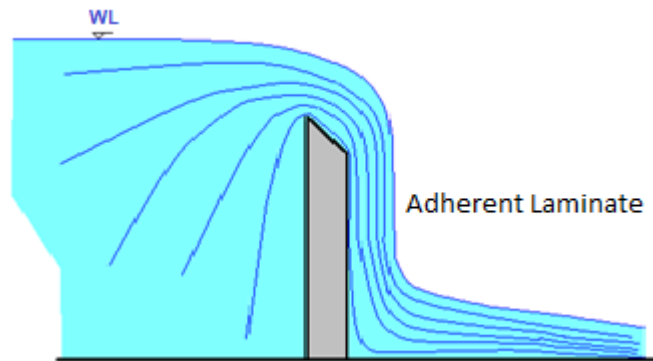
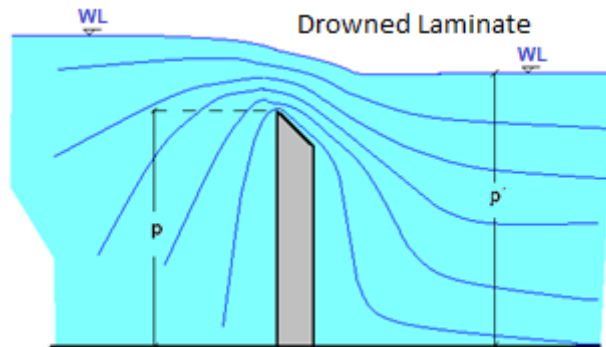


Figure 125 – Adherent laminate (Queiroz, 2017).

- Drowned laminate (Figure 126)
 - Level of the water at downstream is mayor than the crest height;
 - $p > p'$.



6.2.3 Spillway of thin crest or threshold

Spillway of Bazin

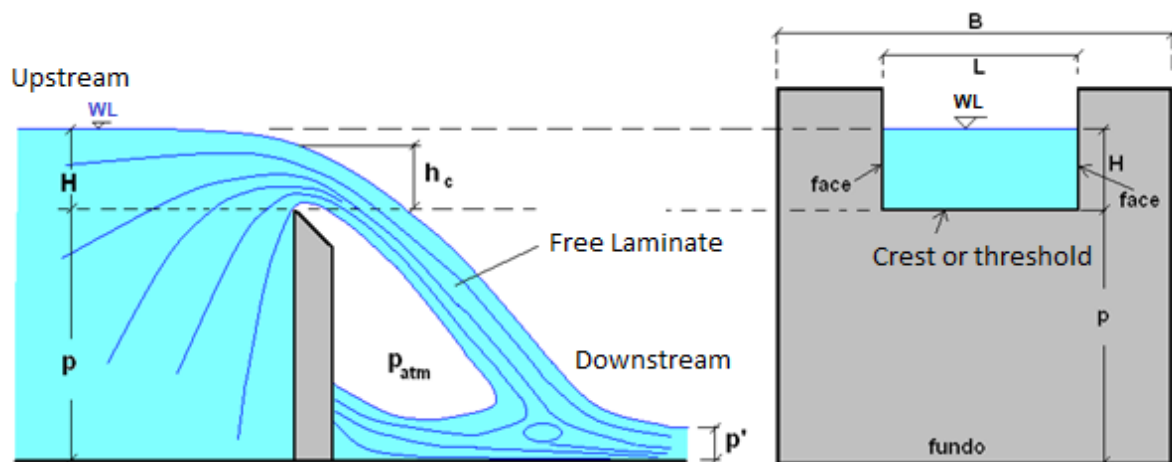


Figure 127 – Square spillway of thin crest or threshold, without lateral contractions and free discharge, or Bazin's spillway (Queiroz, 2017).

The inferior fillets elevate to cross the crest of the spillway. The free surface of the water and the nearby fillets are recessed, with the narrowing of the liquid vein (Queiroz, 2017). In the case of a large orifice:

$$Q = \frac{2}{3} C_d L \sqrt{2g} (h_1^{3/2} - h_2^{3/2})$$

By doing $h_1 = H$ and $h_2 = 0$, the fundamental equation of spillways can be obtained, such equation is also known as Du Buat's formula:

$$Q = \frac{2}{3} C_d L \sqrt{2g} H^{3/2}$$

Doing $\mu = 2/3 C_d$, the flow rate law is obtained:

$$Q = \mu L \sqrt{2g} H^{3/2}$$

Where, for a Bazin's spillway (without lateral contractions):

$$\mu = \left(0.405 + \frac{0.003}{H} \right) \left[1 + 0.55 \left(\frac{H}{H + p} \right)^2 \right]$$

For $0.08 \text{ m} < H < 0.70 \text{ m}$, $0.20 \text{ m} < p < 2.00 \text{ m}$ and $L > 4H$.

When exists a lateral contraction, it is manifested with a decrease of the useful length of the crest causing an overestimation of the flow rate when are used the upper equations. At that case, the length of the spill way is corrected in the formula (Queiroz, 2017).

The corrected length L' , also known as correction of Francis, is given by:

$$L' = L - C'nH$$

Where:

L is the real length of the spillway;

n is the number of contractions;

C' is the factor of contraction;

H is the charge.

Normally C' assume values of (Queiroz, 2017):

- 0.1 for crest and faces with sharp edge;
- 0 for crest and faces with rounded edges.

Note:

1. If $L > 10H$, can be ignored the effects of lateral contraction;
2. The effect of contraction in a vertical plain is consider in the discharge coefficient.

Considering an Approaching Velocity

$V = Q/A \rightarrow$ in the channel that supply the spillway. Kinetic charge (Queiroz, 2017):

$$\alpha \frac{V^2}{2g}$$

When an approaching velocity (V) is not small enough to be ignored, the fully equation that give the flow rate is (Queiroz, 2017):

$$Q = \frac{2}{3} C_d L \sqrt{2g} \left[\left(H + \alpha \frac{V^2}{2g} \right)^{\frac{3}{2}} - \left(\alpha \frac{V^2}{2g} \right)^{\frac{3}{2}} \right]$$

The last expression is known as Weissbach's Formula for flows through rectangular spillways or unloaders (Queiroz, 2017):

- α is the coefficient of Coriolis and vary between 1.0 and 1.66;
- a correction of approaching velocity must be done always, when the area of the channel is inferior to $6HL$.

Another way to consider the approaching velocity is to remember that velocity is:

$$V = \frac{Q}{B(H + p)}$$

And write:

$$Q = \frac{2}{3} C_d L \sqrt{2g} H^{\frac{3}{2}} \left(1 + \frac{3}{2} \alpha \frac{V^2}{2gH} \right)$$

And after some operations to simplify the upper equation, can be write as:

$$Q = \frac{2}{3} C_d L \sqrt{2g} H^{\frac{3}{2}} \left[1 + C_1 \left(\frac{H}{H + p} \right)^2 \right]$$

The upper equation is applicable to a rectangular spillway without constrictions, considering a correction in the approaching velocity (Queiroz, 2017).

Triangle spillway or Unloader

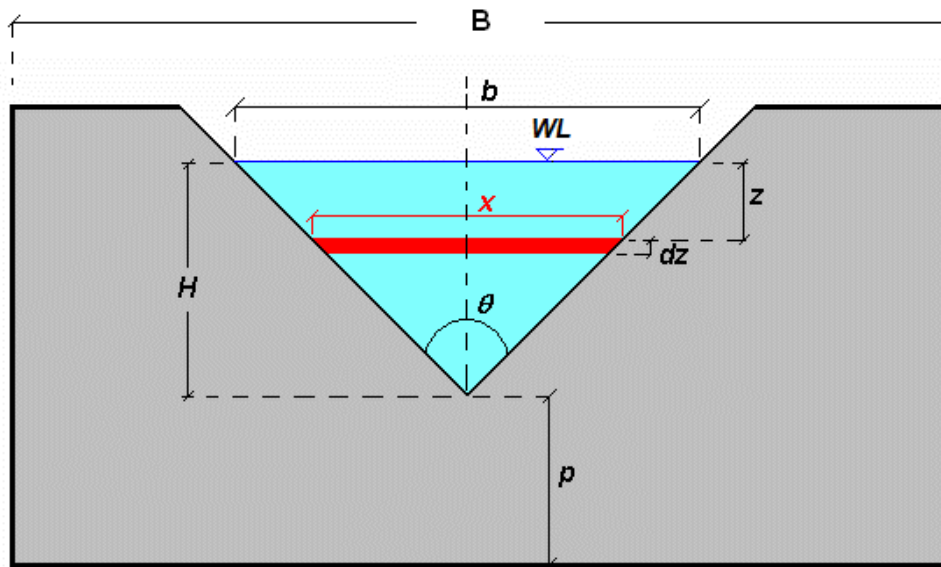


Figure 128 – Triangular discharger (Queiroz, 2017).

Spillway used for measurements of small flow rate ($Q < 30 \text{ l/s}$), having a mayor precision for charges measurements (H) and are built with a steel plate (Queiroz, 2017).

Admitting a horizontal band of elemental height dz and length x , as a small orifice, the flow rate is given by (Queiroz, 2017):

$$dQ = C_d \cdot dA \cdot \sqrt{2gh} \Rightarrow dQ = C_d \sqrt{2gz} \cdot x \cdot dz$$

Following the geometrical relation $b/x = H/(H - z) \rightarrow x = b(1 - z/H)$, for the whole triangular area:

$$Q = \int_0^H dQ = \int_0^H C_d \sqrt{2gz} \cdot b \cdot \left(1 - \frac{z}{H}\right) \cdot dz \Rightarrow Q = \frac{4}{15} C_d \sqrt{2g} b H^{\frac{3}{2}}$$

Also, following the geometrical relation $b = 2H \tan(\theta/2)$, then:

$$Q = \frac{4}{15} C_d \sqrt{2g} 2H \tan\left(\frac{\theta}{2}\right) H^{\frac{3}{2}} \Rightarrow Q = \frac{8}{15} C_d \sqrt{2g} \tan\left(\frac{\theta}{2}\right) H^{\frac{5}{2}}$$

In reality C_d vary with θ and in practice is used an isosceles triangle with a vertical bisector (Queiroz, 2017).

Thomson proposed a spillway with $\theta = 90^\circ$ and a C_d such that:

$$Q = 1.4 H^{5/2}, \text{ with } C_d = 0.593$$

At this case, $0.05 \text{ m} < H < 0.38 \text{ m}$, $p > 3H$ e $B > 6H$; $Q [\text{m}^3/\text{s}]$ and $H [\text{m}]$.

The USBR (1967) proposed a spillway with $\theta = 90^\circ$ and a C_d such that:

$$Q = 1.3424H^{2.48}$$

At such case, recommendations must be followed for p and a length b in function of the channels length where the spillway will be installed (Queiroz, 2017).

The value of θ cannot be too small, because exist an influence of the superficial tension, capillarity and viscosity. Generally, is adopted $\theta > 25^\circ$ (Queiroz, 2017).

Trapezoidal spillway

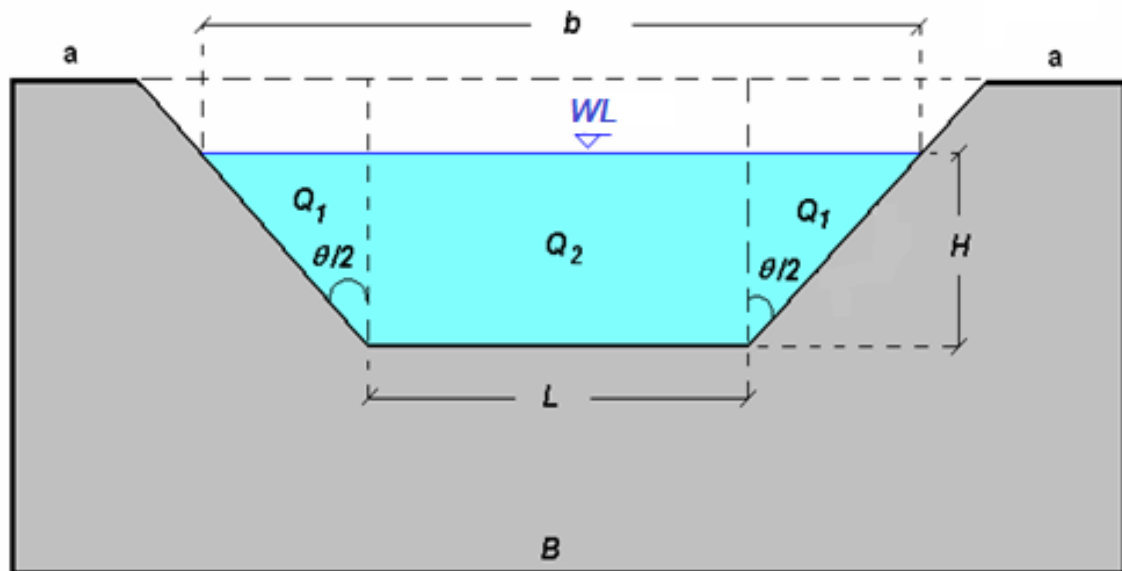


Figure 129 – Trapezoidal spillway (Queiroz, 2017).

It has a trapezoidal shape of lower length L and height H . It is consider as being formed by a rectangular spillway and triangular of angle θ . The trapezoid is used to compensate the reduction of flow rate due to contractions (Queiroz, 2017).

$$Q = Q_2 + 2Q_1 \Rightarrow Q = \frac{2}{3} C_d L \sqrt{2g} H^{\frac{3}{2}} + \frac{8}{15} C_d \sqrt{2g} \tan\left(\frac{\theta}{2}\right) H^{\frac{5}{2}}$$

For this type of spillways can be consider the influence of the approaching velocity by adding $(\alpha \cdot V^2/2g)^{3/2}$ to the value of H (Queiroz, 2017).

Such correction must be done, when the transversal section of the channel is inferior to $6LH$ (Queiroz, 2017).

Trapezoidal spillway (Cipolletti)

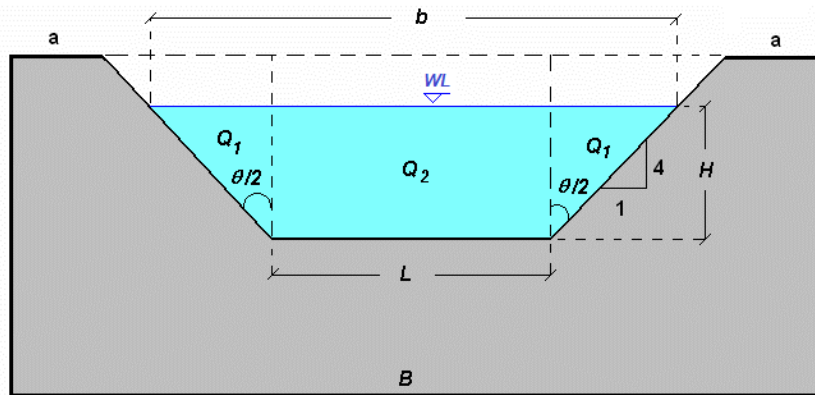


Figure 130 – Trapezoidal spillway (Cipolletti) (Queiroz, 2017).

It is a special type of trapezoidal spillway or unloader, where faces are inclined in 1:4 (h:v), such that $\tan(\theta/2) = 1/4$.

The inclination of 1:4 is made in order to compensate the decrease in length due to lateral contraction, so the equation to be used, is the same as a rectangular spillway of thin wall with two contractions (Queiroz, 2017):

$$Q = \frac{2}{3} C_d (L - 0.1 \cdot 2 \cdot H) \sqrt{2g} H^{3/2} \Rightarrow Q = \frac{2}{3} C_d (L - 0.2 \cdot H) \sqrt{2g} H^{3/2}$$

Cipolletti proposed that $C_d = 0.63$ and $0.08 \text{ m} < H < 0.60 \text{ m}$, $H < L/3$, $p > 3H$, $a > 2H$ and channels length (B) $> 7H$, corresponding to next formula (Queiroz, 2017):

$$Q = 1.861 L H^{3/2}$$

Circular spillway

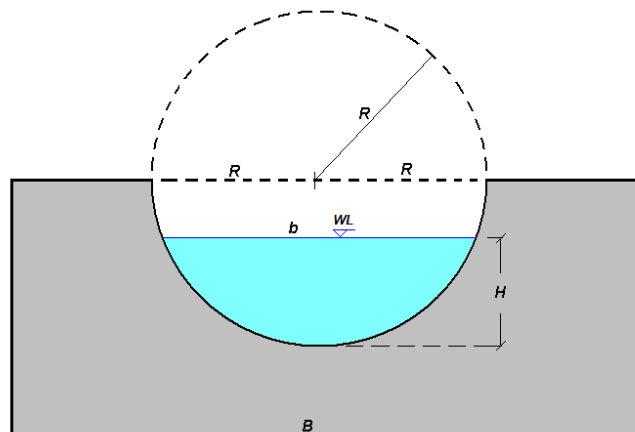


Figure 131 – Circular spillway (Queiroz, 2017).

Spillway used for small flow rate, easy to build and install, without crest levelling, and aired vertient laminate. It is more efficient for small values of H , but is rarely used (Queiroz, 2017).

$$Q = 1.518D^{0.0693}H^{1.807}$$

With Q [m^3/s] and D, H [m].

Vertical pipe spillway of free discharge

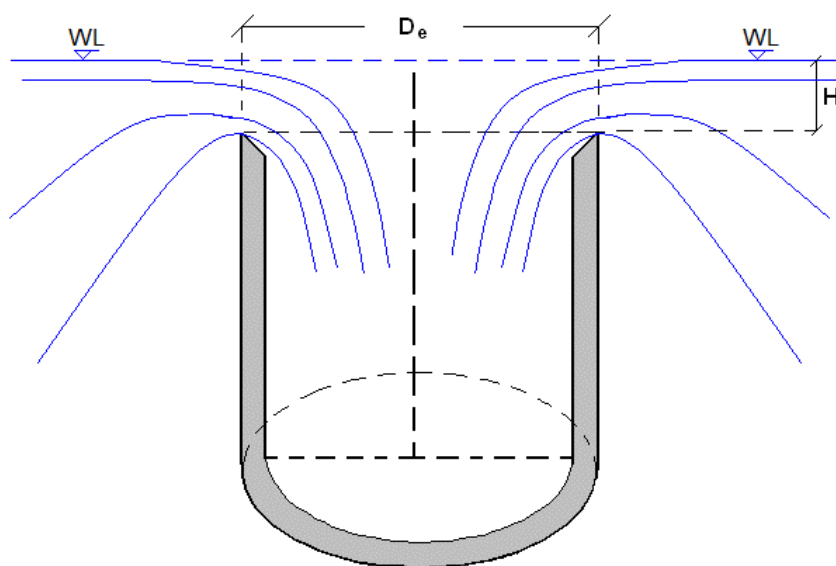


Figure 132 – Vertical pipe spillway of free discharge (Queiroz, 2017).

Formed by a pipe of vertical axis and circular crest, the flows occur in free laminate shape and is largely used in water outlets of dams (Queiroz, 2017).

$$Q = K L H^n, \text{ com } K = \frac{2}{3} C_d \sqrt{2g}$$

With $H < D_e/5$ e $L = \pi D_e$. Normally is adopted $n = 1.42$. The value of K is retired from tables like Table 15 (Queiroz, 2017).

Table 15 – Values of k in function of D_e (adapted from Queiroz, 2017).

D_e [m]	K
0.175	1.435
0.250	1.440
0.350	1.455
0.500	1.465

Inclined spillway

$$\mu_{\theta} = \mu \left(1 - 0.3902 \frac{\theta}{180^{\circ}} \right)$$

Where, θ is the inclination of a spillway or unloader in relation to the vertical. It is adopted a positive signal (+) when inclination is against the stream and negative when is in favour of the stream (Pinho et al., 2011).

6.2.4 Unloader or spillways of thick crest

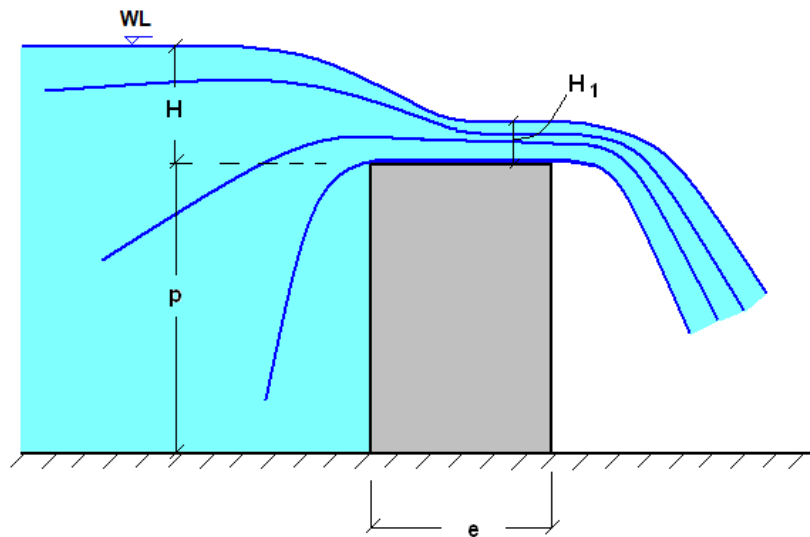


Figure 133 – Rectangular spillway of thick crest (Queiroz, 2017).

The crest must have a thickness enough to both fillets of the fluid stay parallel, which means $e > H/2$ (Queiroz, 2017).

Exists 4 cases involving different thickness bands (Queiroz, 2017):

- Case $H/2 < e < 2H/3$, unstable vein, may or may not stick to crest;
- Case $e < H/2$, equations for spillways of thin wall can be used;
- Case $e > 2H/3$, corrected Bazin's formula must be used for thick crest;

$$Q = \mu' L \sqrt{2g} H^{3/2}, \text{ onde } \mu' = \mu(0.70 + 0.185 \cdot H/e)$$

- Case $e > 3H$, the water surface suffers a contraction or decrease at the beginning of the crest and stay parallel to it.
 - Theoretical flow rate, case the fluid was ideal:

$$Q = 0.385 L \sqrt{2g} H^{3/2} = 1.705 L H^{3/2}$$

- In function of H_1 :

$$Q = 3.133LH_1^{3/2}$$

- According to Lesbros, the real flow rate will be:

$$Q = 0.35L\sqrt{2g}H^{3/2} = 1.55LH^{3/2}$$

6.2.5 Normal crest spillway or unloaders

Spillways of normal crest or threshold are those with an equivalent crest's profile with the internal face of the fluid laminate for a Bazin's spillway.

In many occasions, an overflow spillway of a damn has a crest with curved profile or shape, calculated for a flow rate called "project flow rate", corresponding to a certain charge of project or crest definition (H) (Queiroz, 2017).

There is many types of crest profile or shapes that can be used. The most important are (Queiroz, 2017):

- Creager profile (Figure 134)

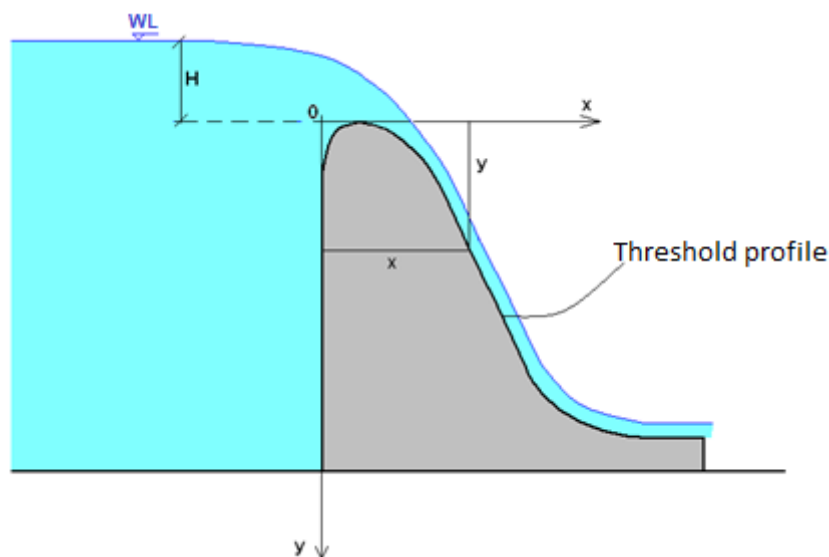


Figure 134– Creager profile (Queiroz, 2017).

- Schemed from a table with coordinates (x,y) of profile (normal crest) relative to $H = 1.0$ m. For $H \neq 1.0$ m, the coordinates of the corresponding profile are multiplied with the value of H ;
- Or schemed from the equation:

$$\frac{y}{H} = 0.47 \left(\frac{x}{H} \right)^{1.8}$$

- Profile Scimeni or WES (EUA) (Figure 135)

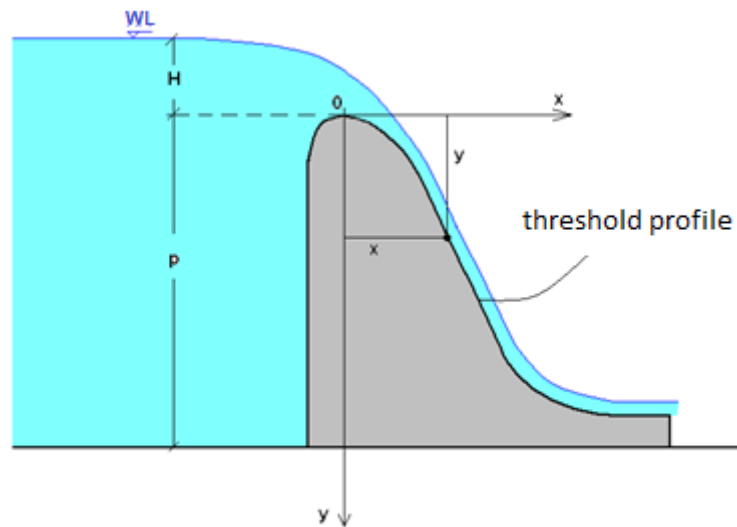


Figure 135 – Profile WES (EUA) (Queiroz, 2017).

- Profile of spillway *WES* (*Waterways Experiment Station*) with parameter of vertical upstream that can be set from equation:

$$\frac{y}{H} = 0.50 \left(\frac{x}{H} \right)^{1.85}$$

And flow rate is calculated by:

$$Q = \mu L \sqrt{2g} H^{3/2}, \text{ with } \mu \text{ calculated of tabulated in function of charge}$$

6.2.6 Cares when using spillways for flow rate measurements

According to E. Trindade Neves, must be used rectangular spillways, preferably without lateral contractions and with (Queiroz, 2017):

- Thin crest or threshold, horizontal and normal to the liquids fillets directions (crest and edge at upstream must be smooth and sharp);
- Distance from the crest until bottom and channels sides must be superior to 2H and at least 20 or 30 cm;
- Spillways walls must be vertical and smooth;
- Free laminate that only touch the crest forming a straight line;
- Avoid laminate dripping: $H > 5 \text{ cm}$;
- H inferior to 60 cm and upstream measure must be at least 5H of crest (ideal between 1.8 m and 5.0 m);
- In upstream must exists a rectilinear stretch of channel capable of regularize the water flow;
- Level of water at downstream must not be close to the crest.

In measurement, all quantities involved in the flow rate determination might have some error that leads to an uncertainty of those measurements. So, for a rectangular spillway or unloader:

$$Q = \mu L \sqrt{2g} H^{3/2} = K L H^{3/2} \Rightarrow \frac{dQ}{dH} = \frac{3}{2} K L H^{1/2} \Rightarrow$$
$$\Rightarrow \frac{dQ}{Q} = \frac{\frac{3}{2} K L H^{1/2} dH}{K L H^{3/2}} \Rightarrow \frac{dQ}{Q} = 1.5 \frac{dH}{H}$$

Where:

dQ/Q represents an error related to flow rate measurement;

dH/H represents an error related to charge measurement.

Which means, an error of 1% in charge measurements due to and error of 1.5% in flow rate measurements, without considering an error at the crests lengths measurements.

CHAPTER 7 - DIMENSIONAL OR DESIGN ANALYSIS

7.1 Introduction

Not always the physical phenomenon that are studied in hydraulics, can be represented by mathematical models, being necessary the construction of physical models in laboratory or in experimental fields (Vasconcelos, 2005).

In these chapter are studied concepts that allow to dimension or design a model in order to study the behaviour of a hydraulic work in project (which is called prototype). And it is instructed to how to relate quantities measured at models with those expected in the prototype (Vasconcelos, 2005).

It is called **scale** of a certain quantity to the relation between a specific model's value and its par of prototypes value (Vasconcelos, 2005).

It is necessary to initially define the geometric scale and in function of those scales of velocity, time, flow rate or rate of flow, pressure, etc. So, in a general way, it is possible to schematize in next form (Vasconcelos, 2005):

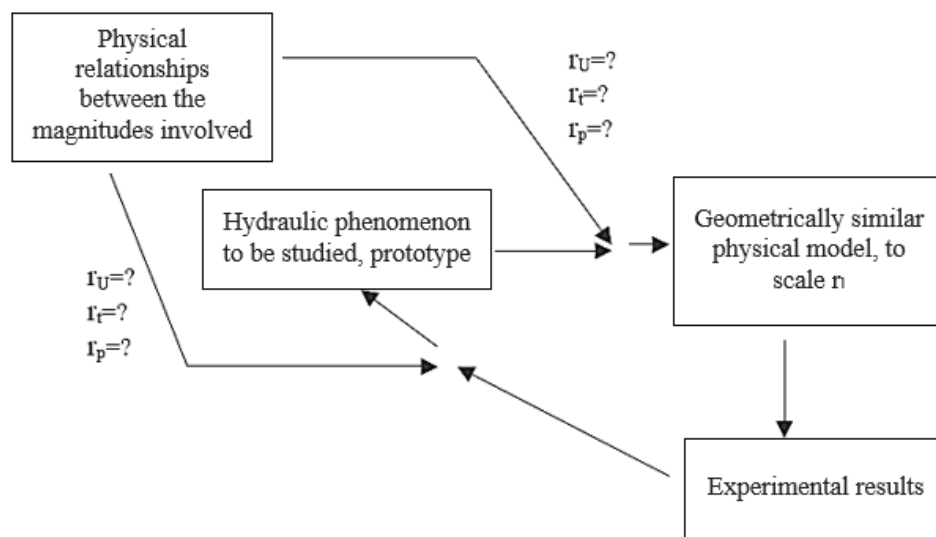


Figure 136 – Study of physical phenomenon's (adapted from Vasconcelos, 2005).

Dimensional or design analysis allows to obtain **physical relations** of a hydraulic phenomenon, starting only from its dimensions (Vasconcelos, 2005). This is a simplification process of a physical problem using dimensional homogeneity in order to reduce the number of variables of analysis. Such process it is particularly useful for (Ignácio & Nóbrega, 2004):

- Represent and interpret experimental data;
- Solve problems that are not possible or too difficult by an analytical solution;
- Establish a phenomenon influence;
- Physical modelling.

7.2 Units and dimensions

Problems in transportation phenomenon involve many variables with different physical meanings. The derivative analytical equations are correct for any unit system (each term of the equation must have same dimensional representation: homogeneity) (Ignácio & Nóbrega, 2004).

Each of those variables represent a magnitude and an associated unit. Units are expressed using only four basic or fundamental quantities, magnitudes or categories (Ignácio & Nóbrega, 2004):

Table 16 – Magnitudes of base and unit of base of the international system (IS) (adapted from Ignácio & Nóbrega, 2004).

Magnitude	Symbol	Dimension	IS Unit
Mass	m	M	kg, kilogram
Distance	l, h, r, x	L	m, meter
Time	t	T	s, second
Temperature	T	Θ	K, kelvin

In addition to the magnitudes of base, exists also derivatives magnitudes or categories:

Table 17 – Examples of derivatives magnitudes or quantities and its units (adapted from Ignácio & Nóbrega, 2004).

Area	Magnitude	Symbol	Dimension	IS Unit
Geometry	Area	A	L^2	m^2
	Volume	V	L^3	m^3
Kinematics	Velocity	U	LT^{-1}	m/s
	Angular Velocity	Ω	T^{-1}	s^{-1}
	Flow rate or rate of flow	Q	L^3T^{-1}	m^3/s
	Flow of mass	M	MT^{-1}	kg/s
Dynamics	Force	F	MLT^{-2}	kg.m/s ²
	Torque	T	ML^2T^{-2}	kg.m ² /s ²
	Energy	E	ML^2T^{-2}	kg.m ² /s ²
	Power	P	ML^2L^{-3}	kg.m ² /s ²
	Pressure	P	$ML^{-1}T^{-2}$	kg/m.s ²
Fluids properties	Density	ρ	ML^{-3}	kg/m ³
	Viscosity	μ	$ML^{-1}T^{-1}$	kg/m.s
	Kinematic Viscosity	ν	L^2T^{-1}	m ² /s
	Superficial tension	σ	MT^{-2}	kg/s ²
	Thermal Conductivity	K	$MLT^{-3}\Theta^{-1}$	kg.m/s ³ .K
	Specific heat	C_p, C_v	$L^2T^{-2}\Theta^{-1}$	m ² /s ² .K

A magnitude or a group of physical magnitudes have a dimension that is represented by a relation of primary magnitudes. If such relation is unitary, the group is called **dimensionless**, which means that has non-dimension (Ignácio & Nóbrega, 2004).

Due to a smaller number of dimensionless groups than physical variables, there is a great reduction in experimental efforts to establish relations between variables (Ignácio & Nóbrega, 2004).

A relation between two dimensionless numbers is given by a function with a unique curve that relate each other (Ignácio & Nóbrega, 2004).

Can be affirmed that the dimensionless groups produce a better approximation to a phenomenon than its own variables (Ignácio & Nóbrega, 2004).

By restricting the experiments conditions, it is possible to obtain data from different geometrical conditions but leading to the same point of the represented curve, this means, that experiments at different scales represents same values for its dimensionless groups. In such conditions, the test or experiments have **similar dynamic** (Ignácio & Nóbrega, 2004).

Problems of engineering (mainly in thermal and fluid areas) are rare to be solved by only applying theoretical analysis, instead it is usual to apply experimental studies (Ignácio & Nóbrega, 2004).

Most of the experimental work is made with the real equipment or with exact replicates. So, most applications in engineering are made based in scales models (Ignácio & Nóbrega, 2004).

7.3 Theorems of Dimensional Analysis

Are usually applied two Theorems, that in Hydraulics, are defined as (Vasconcelos, 2005):

- **Homogeneity Theorem**

All physical relationship must be dimensionally homogeneous. A function $f(x)$ is called homogeneous of grade k if:

$$f(tx) = t^k f(x)$$

Which means, such function when transformed in its variables, results in another function, that is proportional to its original.

Such definition is essential in the treatment of Dimensional Analysis. Besides that, it is fundamental in physics. According to the homogeneity theorem, also called Vaschy-Buckingham's Theorem, says that in all expression, equation or physical formula, the dimension of all terms must be identical (homogeneous equation).

- **Theorem π of Vaschy-Buckingham**

The **theorem π of Vaschy-Buckingham (or theorem of Vaschy-Buckingham)** is the main theorem of dimensional analysis. Establish that, in a physical equation involving several physical dimensional variables n , which are represented by r physical independent and fundamental dimensions, the equation of the process or physical system can be rewritten as an equation of $p = n - r$ dimensionless variables (parameters π), built from original variables up.

This provides a method to calculate groups of dimensionless parameters starting from the given dimensional variables. This is possible even if the equation of the system or process is unknown. Finding dimensionless parameters can simplify a problem or even solved.

This theorem, known as "theorem π " or "theorem of π ", was announced for first time by Aimé Vaschy, in 1892, in an article "About laws of similarity in physics ". Twenty-two years later, was published in 1914 the famous article of Edgar Buckingham: "About physically similar system: illustration of the use of dimensional equations".

All relation dimensionally homogeneous in n physical magnitudes or quantities (Vasconcelos, 2005):

$$F(a_1, a_2, a_3, \dots, a_n) = 0$$

Can be substituted by a relation between $n - p$ (in Hydraulics $p = 3$) dimensionless magnitudes or quantities:

$$\Phi(\pi_1, \pi_2, \pi_3, \dots, \pi_n)$$

Being p the number of independent dimensional quantities that are involved in such phenomenon.

Dimensionless parameters are each one defined by those 3 fundamental magnitudes or quantities (a_k, a_l, a_m) and each of the $n - 3$ remaining magnitudes (Vasconcelos, 2005):

$$\begin{aligned}\pi_1 &= \frac{a_1}{a_k^{x_1} \times a_l^{y_1} \times a_m^{z_1}} \\ \pi_2 &= \frac{a_2}{a_k^{x_2} \times a_l^{y_2} \times a_m^{z_2}} \\ &\vdots \\ \pi_{n-3} &= \frac{a_{n-3}}{a_k^{x_{n-3}} \times a_l^{y_{n-3}} \times a_m^{z_{n-3}}}\end{aligned}$$

In which exponents x_i , y_i and z_i are determined by the conditions of π_i being dimensionless, verifying the **Theorem of Homogeneity**.

Determination of the groups π (6 steps):

- **1st Step** – Make a list of all involved parameters: if not all pertinent parameters are involved, a relation may be obtained, but it will not give a complete solution;
- **2nd Step** – Selection of a set of fundamental dimensions (primary), for example, M, L and T;
- **3rd Step** – Make a second list, where dimensions of all parameters are written in term of primary dimensions;
- **4th Step** – Selection from the last list, several parameters that repeat, equal to the number of primary dimensions, including all primary dimension;
- **5th Step** – Establish dimensional equations combining the selected parameters at step 4, with each of the other parameters in order to form dimensionless sets (it will be $n - m$ equations);
- **6th Step** – Verify in order to ensure dimensionality of each set.

7.3.1 Applications of the Theorem of π to a problem of Fluids Mechanics

According to Vasconcelos (2005),

1st Variables that conditions the phenomenon

- Geometrical characteristics – linear quantities identified by l ;
- Kinematics characteristics – average velocity of flow, U ;
- Dynamical characteristics – variation of pressure, Δp ; gravitational acceleration, \vec{g} ;
- Fluids properties – volumetric mass, ρ ; kinematics viscosity, ν .

Quantities or magnitudes related through a dimensionally homogeneous relationship:

$$F(l, U, \Delta p, \rho, g, \nu)$$

2nd Selection from the magnitudes or quantities, a system of fundamental units, that in hydraulics are traditionally adopted the variables (l, U, ρ)

3rd Define an equation function of dimensionless magnitudes

$$\Phi(\pi_1, \pi_2, \pi_3) = 0$$

With:

$$\pi_1 = \frac{\Delta p}{l^{x_1} \times U^{y_1} \times \rho^{z_1}}$$

$$\pi_2 = \frac{g}{l^{x_2} \times U^{y_2} \times \rho^{z_2}}$$

$$\pi_3 = \frac{v}{l^{x_3} \times U^{y_3} \times \rho^{z_3}}$$

Values x_i , y_i and z_i can be determined by knowing that π_i are dimensionless parameters and the last equations verify the Theorem of Homogeneity. It will be easier if it is supported on a known unit system as for example, the MLT:

Table 18 – Units system MLT (adapted from Vasconcelos, 2005).

Magnitude	Equation of dimensions
l	$M^0 L^1 T^0$
U	$M^0 L^1 T^{-1}$
ρ	$M^1 L^{-3} T^0$
Δp	$M^1 L^{-1} T^{-2}$
g	$M^0 L^1 T^{-2}$
v	$M^0 L^2 T^{-1}$

$$M^0 L^0 T^0 = \frac{M^1 L^{-1} T^{-2}}{(M^0 L^1 T^0)^{x_1} \times (M^0 L^1 T^{-1})^{y_1} \times (M^1 L^{-3} T^0)^{z_1}}$$

$$M^0 L^0 T^0 = \frac{M^0 L^1 T^{-2}}{(M^0 L^1 T^0)^{x_2} \times (M^0 L^1 T^{-1})^{y_2} \times (M^1 L^{-3} T^0)^{z_2}}$$

$$M^0 L^0 T^0 = \frac{M^0 L^2 T^{-1}}{(M^0 L^1 T^0)^{x_3} \times (M^0 L^1 T^{-1})^{y_3} \times (M^1 L^{-3} T^0)^{z_3}}$$

And by applying the Homogeneity Theorem:

$$\text{Relative to } \pi_1: \begin{cases} 1 = 0x_1 + 0y_1 + 1z_1 \\ -1 = 1x_1 + 1y_1 - 3z_1 \\ -2 = 0x_1 - 1y_1 + 0z_1 \end{cases} \Rightarrow \begin{cases} z_1 = 1 \\ x_1 = 0 \\ y_1 = 2 \end{cases} \rightarrow \pi_1 = \frac{\Delta p}{l^0 \times U^2 \times \rho^1} = \frac{\Delta p}{\rho U^2}$$

$$\text{Relative to } \pi_2: \begin{cases} 0 = 0x_2 + 0y_2 + 1z_2 \\ 1 = 1x_2 + 1y_2 - 3z_2 \\ -2 = 0x_2 - 1y_2 + 0z_2 \end{cases} \Rightarrow \begin{cases} z_2 = 0 \\ x_2 = -1 \\ y_2 = 2 \end{cases} \rightarrow \pi_2 = \frac{g}{l^{-1} \times U^2 \times \rho^0} = \frac{gl}{U^2}$$

$$\text{Relative to } \pi_3: \begin{cases} 0 = 0x_3 + 0y_3 + 1z_3 \\ 2 = 1x_3 + 1y_3 - 3z_3 \\ -1 = 0x_3 - 1y_3 + 0z_3 \end{cases} \Rightarrow \begin{cases} z_3 = 0 \\ x_3 = 1 \\ y_3 = 1 \end{cases} \rightarrow \pi_3 = \frac{v}{l^1 \times U^1 \times \rho^0} = \frac{v}{lU}$$

The Theorem of $\pi\pi$ allows to transform a function F, that express a relationship between six magnitudes, at an expression that relates 3 dimensionless magnitudes:

$$\Phi\left(\frac{\Delta p}{\rho U^2}, \frac{gl}{U^2}, \frac{v}{lU}\right) = 0$$

Or, equally:

$$\Phi'\left(\frac{\rho U^2}{\Delta p}, \frac{U^2}{gl}, \frac{lU}{v}\right) = 0$$

Dimensionless parameters determined in this way, shows important properties of the flow, having it owns designations:

- Euler's Number

$$Eu = \frac{\Delta p}{\rho U^2}$$

- Froude's Number

$$Fr = \frac{U^2}{gl} \xrightarrow{l=h} Fr = \frac{U^2}{gh}$$

- Reynolds's Number

$$Re = \frac{Ul}{v} \xrightarrow{l=D} Re = \frac{UD}{v}$$

A function Φ' can be represented in the next way:

$$\Phi'(Eu, Fr, Re) = 0 \quad \text{or} \quad Eu = \Phi''(Fr, Re)$$

The application of the dimensional analysis allows to obtain an expression that represent the hydraulic phenomenon. A function Φ'' can be experimentally or empirically determined.

7.3.2 Physical meaning of the dimensionless parameters

Remembering the form of representation of the involved forces in the last problem, it is possible to relate each of the parameters with forces forms (Table 19) (Vasconcelos, 2005).

Table 19 – Representation of forces in the system (adapted from Vasconcelos, 2005).

Type of force	Representation of forces in the system (l, U, ρ)
Inertial Forces	$F_I = -ma = -\rho l^3 U t^{-1} = -\rho U^2 l^2$
Pressure Forces	$F_p = \Delta p l^2$
Gravitational forces	$F_G = \gamma l^3$
Viscosity forces	$F_v = (\mu U l^{-1}) l^2 = \mu \rho U l$

Comparing the deduced equations for the three dimensionless parameters with a representation of the different forces, it is verified that:

- Euler's number represents a relation between forces of pressure a force of inertia;

$$Eu = \frac{\Delta p}{\rho U^2} = \frac{\Delta p l^2}{\rho U^2 l^2} = \frac{F_p}{F_I}$$

- Froude's number represents a relation between inertial forces and gravitational forces;

$$Fr = \frac{U^2}{gl} = \frac{\rho U^2 l^2}{\rho g l^3} = \frac{F_I}{F_G}$$

- Reynolds's number represents a relation between inertial forces and viscosity forces.

$$Re = \frac{Ul}{\nu} = \frac{\rho Ul^2}{\rho \nu l^2} = \frac{F_I}{F_\nu}$$

CHAPTER 8 - SIMILARITY

8.1 Mechanical and Hydraulics Similarity

Occurs **Mechanics Similarity** between a model and a prototype, geometrically and kinematically, when the main dynamics magnitudes of a physical phenomenon establish the same dynamic scale. When such phenomenon is hydraulic, the mechanical similarity is called **hydraulics similarity** (UEL, 2017).

It is said, that two system are physically similar in a set of magnitudes, if exists a constant relationship between homologous values of such magnitudes in both system (Vasconcelos, 2005).

Physical similarity can be characterized in two different ways (Vasconcelos, 2005):

- Geometrical similarity in which only verify a constant relationship between geometrical magnitudes in a model and its prototype;
- Kinematics similarity in which is verified a constant relationship between geometrical and kinematics magnitudes in a model and its prototype;
- Dynamical similarity in which is verified a constant relationship between geometrical, kinematics and dynamics magnitudes in a model and its prototype.

In a schematic way it can be represented as follows:

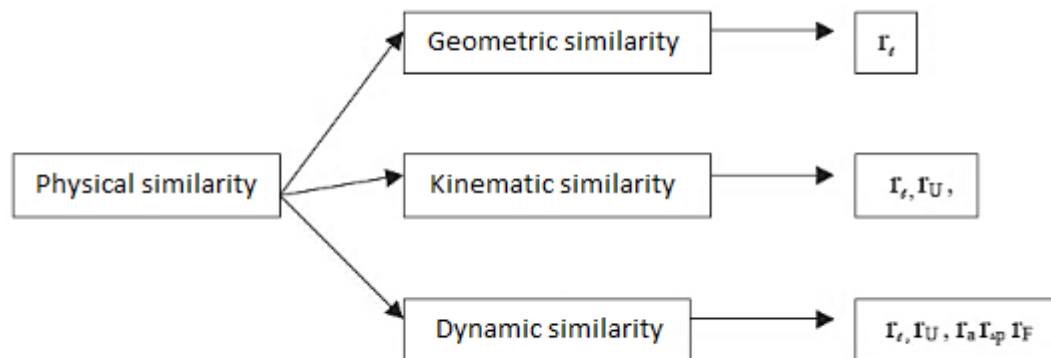


Figure 137 – Schematically representation of physical similarity (adapted from Vasconcelos, 2005).

In Hydraulics, the Theory of Similarity is based in the equality of values of the dimensionless parameters in the model and its prototype (Vasconcelos, 2005).

Not being, however, a compatible equality between all represented parameters of a certain hydraulics phenomenon. Normally it is studied which dimensionless parameter represent at best a certain phenomenon having in count all involved forces, and only after the selection, it is equated in a model and in its prototype. Similarities are designated by the name of the equated parameter (Vasconcelos, 2005).

8.1.1 Euler, Froude and Reynolds's Similarity

Each of those referred similarities will be found based in a geometrical scale and in the equality of the corresponding dimensionless parameter that allows to obtain the values of the scales of the different involved magnitudes (Vasconcelos, 2005). In a schema:

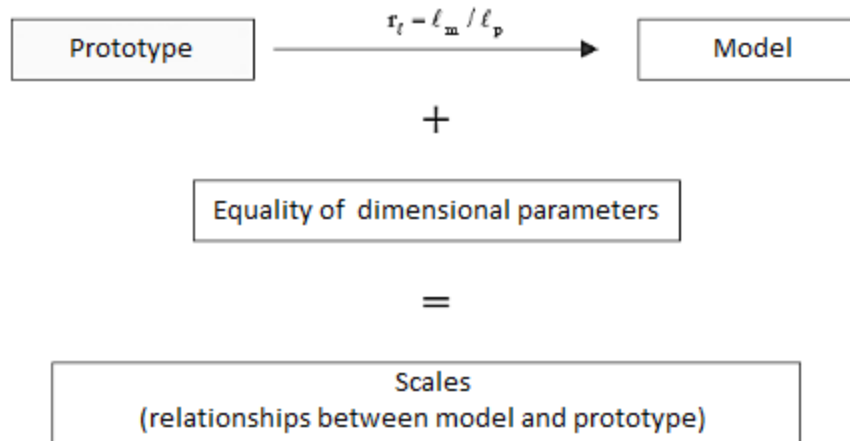


Figure 138 – Similarities (adapted from Vasconcelos, 2005).

It will be represented the scales to verify for the different types of similarity, known as applied geometrical scale. Similarities of Froude and of Reynolds cannot be verified simultaneously if it is applied the same fluid in prototype and in model for the same gravitational acceleration (Vasconcelos, 2005).

However, **Euler's Similarity** is compatible with Reynolds's similarity or with Froude's similarity, because allows to determine the pressures scale from a velocity scale. It is used in situations like a flow where falling pressures is significant, which means, most of kind of flows (Vasconcelos, 2005).

Having a geometrical scale, r_l

Verified: $Eu_m = Eu_p$

Then:

$$\left(\frac{\Delta p}{\rho U^2}\right)_m = \left(\frac{\Delta p}{\rho U^2}\right)_p$$

$$\frac{\Delta p_m}{\rho_m U_m^2} = \frac{\Delta p_p}{\rho_p U_p^2}$$

$$\frac{\Delta p_m}{\Delta p_p} = \frac{\rho_m}{\rho_p} \frac{U_m^2}{U_p^2}$$

$$r_{\Delta p} = r_{\rho} r_U^2$$

For the same liquid: $r_{\rho} = 1$

$$\text{Then: } r_{\Delta p} = r_U^2 \quad \text{or} \quad r_U = r_{\Delta p}^{1/2}$$

Froude's Similarity is applied in situations where exist a predominance of gravitational forces related to viscosity forces, for example: turbulent regimes completely stablished, and flows generated by the weights action (flows in free surface). The effect of viscosity is ignored (Re too-high) (Vasconcelos, 2005).

Having a geometrical scale, r_l

$$\text{Verified: } Fr_m = Fr_p$$

Then:

$$\left(\frac{U^2}{gl} \right)_m = \left(\frac{U^2}{gl} \right)_p$$

$$\frac{U_m^2}{g_m l_m} = \frac{U_p^2}{g_p l_p}$$

$$\frac{U_m^2}{U_p^2} = \frac{g_m l_m}{g_p l_p}$$

$$r_U^2 = r_g r_l$$

For same location: $r_g = 1$

$$\text{Then: } r_U^2 = r_l \quad \text{or} \quad r_U = r_l^{1/2}$$

Reynolds's Similarity is applied in a flow of liquid inside pipes or tubes, since there are no free surfaces, that would determine the action of gravitational forces. flows under pressure and internal flows (Vasconcelos, 2005).

Having a geometrical scale, r_l

$$\text{Verified: } Re_m = Re_p$$

Then:

$$\left(\frac{Ul}{\nu} \right)_m = \left(\frac{Ul}{\nu} \right)_p$$

$$\frac{U_m l_m}{v_m} = \frac{U_p l_p}{v_p}$$

$$\frac{U_m l_m}{U_p l_p} = \frac{v_m}{v_p}$$

$$r_U r_l = r_v$$

For the same liquid: $r_v = 1$

Then: $r_U = r_l^{-1}$

8.1.2 Usual dimensionless parameters

$$\frac{\Delta p}{\rho U^2} = f_1 \left(\frac{U l}{v}, \frac{U^2}{g l}, \frac{U}{c}, \frac{l \omega}{U}, \frac{U^2 \rho l}{\sigma} \right)$$

Table 20 – Usual dimensionless parameters (adapted from NETeF, 2012).

Parameters	Definition	Physics meaning	Importance
Euler's number	$Eu = \frac{\Delta p}{\rho U^2}$	$\frac{\text{Pressure force}}{\text{Inertial force}}$	Flows in which falling pressures are significant, Cavitation
Reynolds's number	$Re = \frac{U l}{v}$	$\frac{\text{Inertial force}}{\text{Viscosity force}}$	Flows influenced by viscosity effects
Froude's number	$Fr = \frac{U^2}{g l}$	$\frac{\text{Inertial force}}{\text{Gravitational Force}}$	Free surface flows
Mach's number	$M = \frac{U}{c}$	$\frac{\text{Inertial forces}}{\text{Compressibility forces}}$	Compressible flows, important for $U > 0.3c$
Strouhal's number	$St = \frac{l \omega}{U}$	$\frac{\text{Centrifugal forces}}{\text{Inertial forces}}$	Non-permanent flow with repetition
Weber's number	$We = \frac{U^2 \rho l}{\sigma}$	$\frac{\text{Inertial forces}}{\text{Superficial tension forces}}$	Flows with free surface, but superficial tension affects the flow.

8.1.3 Similarities to consider in a study of a model

To create a comparative study of similarities between a model and reality, it is necessary that the sets are physically similar (Villa, 2011):

- **Geometric Similarity**
 - Form similarity;
 - The characteristic property of geometrically similar systems is that the ratio between any length or distance measured in the model and its corresponding (in reality) equals to a constant;
 - Such ratio is known as a scale factor;

- **Kinematics Similarity**
 - When two different flows of different geometric scales have the same format of current lines;
 - It is the similarity of the movement, that implies necessarily similarity of distances or lengths (geometrical similarity) and similarity of interval of time;
- **Dynamic Similarity**
 - Is the similarity of forces;
 - Origin of the forces that determines the behaviour of the fluids:
 - Forces due to differences of pressure;
 - Resultant forces of actions of viscosity;
 - Forces due to superficial tension;
 - Elastic forces;
 - Forces of inertia;
 - Forces due to gravitational attraction;
 - Two system are dynamically similar when the absolute values of force, in two equivalents points in such systems, has a fixed ratio.

8.1.4 Similarity in hydraulics turbomachines

According Pinho *et al.* (2011):

- **Parameters** to consider: **H**, **H_o**, **Q**, **p**, **η**, **N** and **D**;
- **Predominant forces**: of inertia and turbulence against gravitational and viscosity forces;
- **Cyclic movement of rotation** → Similarity of Strouhal;

$$St = \frac{l\omega}{U} = \frac{DN}{U}$$

- **Scales of rotation**;
- **Turbines**:

$$\lambda_N = \lambda_p^{-1/2} \lambda_{H_o}^{5/4} \lambda_\eta^{1/2}$$

- **Pumps**:

$$\lambda_N = \lambda_p^{-1/2} \lambda_{H_o}^{5/4} \lambda_\eta^{-1/2}$$

- **Specific rotation of turbines (η_s)** is the velocity or speed of rotation of a turbine geometrically similar, that working with same efficiency as the given turbine, supply a unitary power when a unitary fall act in it;

$$\eta_s = N \frac{p^{1/2}}{H_o^{5/4}} \text{ (rpm)}$$

- **Specific rotation of pumps (η_s)** is the speed or velocity of rotation of a propeller or pump, geometrically like the given one, that gives a unitary flow rate or rate of flow, until a unitary elevation.

$$\eta_s = N \frac{Q^{1/2}}{H_o^{3/4}}$$

8.1.5 Generalities about models

Concepts (UEL, 2017):

- **Prototype** is the project, mechanism or hydraulics work made in real size;
- **Model** is that project, mechanism or hydraulic work at a different scale, usually smaller;
- **Scales** is a relation between homologous magnitudes, of same dimension, between the model and the prototype. Thus, is a dimensionless number. For example: Geometric Scale: $r_l = l_m/l_p$.

Types of models (Pinho et al., 2011):

- **Study of models in hydraulics works** → Similarities like Froude
 - **Spillways or downcomers**;
 - **Dissipation basins**;
- **Study of models geometrically distorted**
 - **Estuaries**;
 - **Naval or Maritime works** → Similarities like Froude;
 - λ_x : scale of horizontal distances;
 - λ_z : scale of vertical distances;
- **Study of model with fixed bottom**;
- **Study of models with movable bottom**
 - Study of solids transportation (erosion in the riverbed or corresponding estuary) → General/Distortional Model.

Problems in engineering (mainly in thermal and fluids areas) are quite difficult to solve by applying exclusively theoretical analysis, so then, is used frequently experimental studies (Ignácio & Nóbrega, 2004).

Most of the experimental work is made with the real equipment or with exact replicas so, most of the applications in engineering are made using scales models (Ignácio & Nóbrega, 2004).

Without planning and some organization, some procedures can (Ignácio & Nóbrega, 2004):

- Waste or consume great intervals of time;
- Not being objective;
- Quite expensive.

The use of scale models leads to (Ignácio & Nóbrega, 2004):

- Economic advantages (time and money);
- Can be used different fluids;
- The results can be extrapolated;
- Can be used reduced or expanded models (depending in convenience).

CHAPTER 9 - FLOWS UNDER PRESSURE

9.1 Generalities

General characteristics of flows (Pinho et al., 2011):

- Permanent and non-permanent flow ;
- Rotational and irrotational flows;
- Laminar and turbulent flows;
- External and internal flows.

Internal flows are also separated depending in **contour conditions** (Pinho et al., 2011):

- **Flows under pressure**: can be found inside pipes, where the fluids in movement occupy completely its transversal section, without external contact (can happen at some isolated points);
- **Free surface flows**: exists always a contact of the liquid stream with an external gas medium, through such “free” surface.

It will be generally studied internal flows, because normally are turbulent (Pinho et al., 2011).

Classification of internal flows respect to **variability of parameters in time** (Pinho et al., 2011):

- **Non-permanent movement**: when at least one variable depends on time.

$$\frac{\partial}{\partial t} \neq 0$$

- **Permanent movement**: when all variables are independent of time.

$$\frac{\partial}{\partial t} = 0$$

- **Varied permanent movement**: if velocity vary along trajectory.

$$\frac{\partial}{\partial t} = 0, \frac{d\vec{v}}{ds} \neq 0$$

- **Uniform permanent movement**: if velocity is constant along trajectory.

$$\frac{\partial}{\partial t} = 0, \frac{d\vec{v}}{ds} = 0$$

General Equation of Resistances Formulas

Resistances Formulas are equations that allows to determine losses of charges or energy, in function of the characteristics of the flow, that it is supposed uniform (Pinho et al., 2011).

Deduction of a general expression:

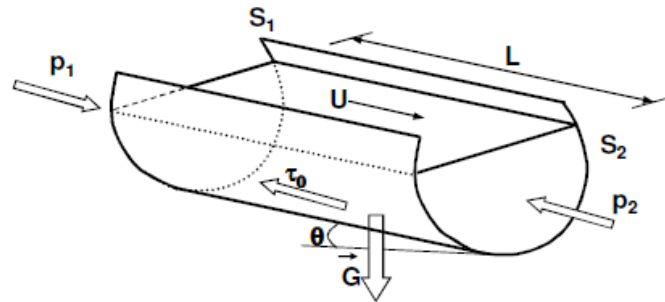


Figure 139 – Circular conduit or pipe (Pinho et al., 2011).

Where:

τ_0 is a tangential tension next to the wall (resistance forces), constant for circular conduit or pipes;

χ is wet perimeter.

Applying the **Theorem of Amount of Movement** to the piece of conduit represented, according to its axis direction:

$$p_1 \cdot S_1 - p_2 \cdot S_2 + G \sin \theta - \tau_0 \cdot \chi \cdot L = 0$$

As $S_1 = S_2 = S \wedge G = \gamma \cdot S \cdot L \wedge \sin \theta = (Z_1 - Z_2)/L$, then:

$$Z_1 + \frac{p_1}{\gamma} - \left(Z_2 + \frac{p_2}{\gamma} \right) = \underbrace{\frac{\tau_0 \cdot \chi \cdot L}{\gamma S}}_{\text{Theo. Bernoulli} \Rightarrow \Delta H}$$

Considering **hydraulics radius (R)**, as the quotient between the wet section (fluids section) and the wet perimeter (fluids perimeter):

$$R = \frac{S}{\chi} \Rightarrow \Delta H = \frac{\tau_0 L}{\gamma S}$$

In **uniform movement**:

$$\Delta H = J \cdot L \Rightarrow J = \frac{\tau_0}{\gamma R} = \frac{U^{*2}}{gR}$$

Where **U^*** is **friction velocity**, defined by:

$$U^* = \sqrt{\tau_0 / \rho}$$

Which is hard to quantify, and also τ_o .

Appealing to dimensional analysis to find a relationship between characteristic parameters of flows (Pinho et al., 2011):

- Geometrical parameters: R ($4R = D$, in circular conduits);
- Rugosity parameters: K_1, K_2, \dots, K_n ;
- Dynamics and kinematics parameters: U ;
- Properties of the fluid: ρ, γ, ν ;
- Tangential tensions next to the wall: τ_o .

By the **Theorem of Vaschy-Buckingham**, using ($4R, U, \rho$) as a fundamental unit system, the equation (Pinho et al., 2011):

$$F(4R, U, \rho, \gamma, \nu, \tau_o, K_1, K_2, \dots, K_n) = 0$$

Transforms into:

$$\varphi\left(\frac{U^2}{4gR}, \frac{4UR}{\nu}, \frac{\rho U^2}{\tau_o}, \frac{K_1}{4R}, \frac{K_2}{4R}, \dots, \frac{K_n}{4R}\right) = 0$$

Which means, that by isolating the dimensionless parameter that relates friction velocity magnitudes and tangential tensions:

$$\frac{\rho U^2}{\tau_o} = \varphi\left(\frac{U^2}{4gR}, \frac{4UR}{\nu}, \frac{K_1}{4R}, \frac{K_2}{4R}, \dots, \frac{K_n}{4R}\right)$$

$$J = \frac{U^2}{\gamma R} \varphi\left(Fr, Re, \frac{\rho U^2}{\tau_o}, \frac{K_1}{4R}, \frac{K_2}{4R}, \dots, \frac{K_n}{4R}\right)$$

$$J = \frac{U^2}{\gamma R} \cdot \frac{1}{8} \lambda \left(Fr, Re, \frac{\rho U^2}{\tau_o}, \frac{K_1}{4R}, \frac{K_2}{4R}, \dots, \frac{K_n}{4R}\right)$$

$$J = \frac{\lambda}{4R} \cdot \frac{U^2}{2g}$$

Where λ is the coefficient of charge losses, or coefficient of resistance.

General expression of constant charges losses (or universal formula) in circular conduits(pipes)

In the case of flows under pressure in circular pipes (Pinho et al., 2011):

$$\lambda = \lambda\left(Fr, Re, \frac{K_1}{4R}, \frac{K_2}{4R}, \dots, \frac{K_n}{4R}\right) \Rightarrow \lambda = \lambda\left(Re, \frac{K_1}{D}, \frac{K_2}{D}, \dots, \frac{K_n}{D}\right)$$

$$J = \frac{\lambda}{D} \cdot \frac{U^2}{2g}$$

9.1.1 Flow establishment

It is said that a flow is established when the average velocity profiles presented are symmetric in relation to the axis of the conduit, and grows starting from the wall until such axis, without changing its shape in its downstream path (Pinho et al., 2011).

It is considered conduits of high length (**L**) (**L** > **100 · D**, where **D** is the diameter of the conduit) and the geometrical characteristics (direction, rugosity, form and dimension of the transversal section) are constants, so it could be considered that (Pinho et al., 2011):

- Pressure distribution in the transversal section is hydrostatic (**b = 1**);
- the **coefficient of Coriolis** is constant along the conduit;
- The loss of charge (**ΔH**) between two sections is proportional to the distance (**L**) between, being constant the unitary loss of charge along the conduit: **J = ΔH/L**.

9.1.2 Rugosity of the tube's walls

Internal surfaces of the conduits have irregularities (**rugosity**), that influence the characteristics of the flow. Becoming necessary to characterize the rugosity in function of the characteristic of the material (Pinho et al., 2011):

- height (dimension of rugosity):
 - **k**: absolute rugosity (Figure 140);



Figure 140 – Absolute rugosity (Pinho et al., 2011).

- **k/D**: relative rugosity;
- form:
 - waves shape (typical in vitreous material);
 - Roughness rugosity (typical of material of crystalline structure);
- distribution of the spatial protuberances.

Artificial rugosity refers to a distribution over a smooth surface of protuberances, as small cubes, parallelepipeds, pyramids, spheres (Pinho et al., 2011).

Artificial rugosity of Nikuradse (Figure 141) is resultant of the collage of sand grains of known granulometry (**ε**) in the internal wall of a tube of glass, being the obtained relative rugosity (**ε/D**) enough to represent totally the rugosity (Pinho et al., 2011).

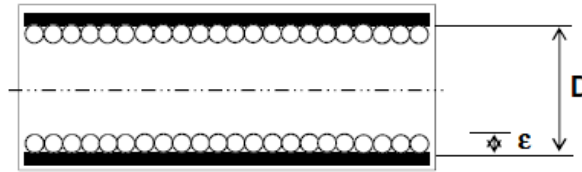


Figure 141 – Artificial rugosity of Nikuradse (Pinho et al., 2011).

9.1.3 Regimes of flows. Experiences of Nikuradse

By using glass tubes of different diameters, combined with different granulometry of sand, Nikuradse had studied different relative rugosities (ϵ/D), in order to determine the expression for the coefficient of resistance, $\lambda = \lambda(Re, \epsilon/D)$ (Pinho et al., 2011):

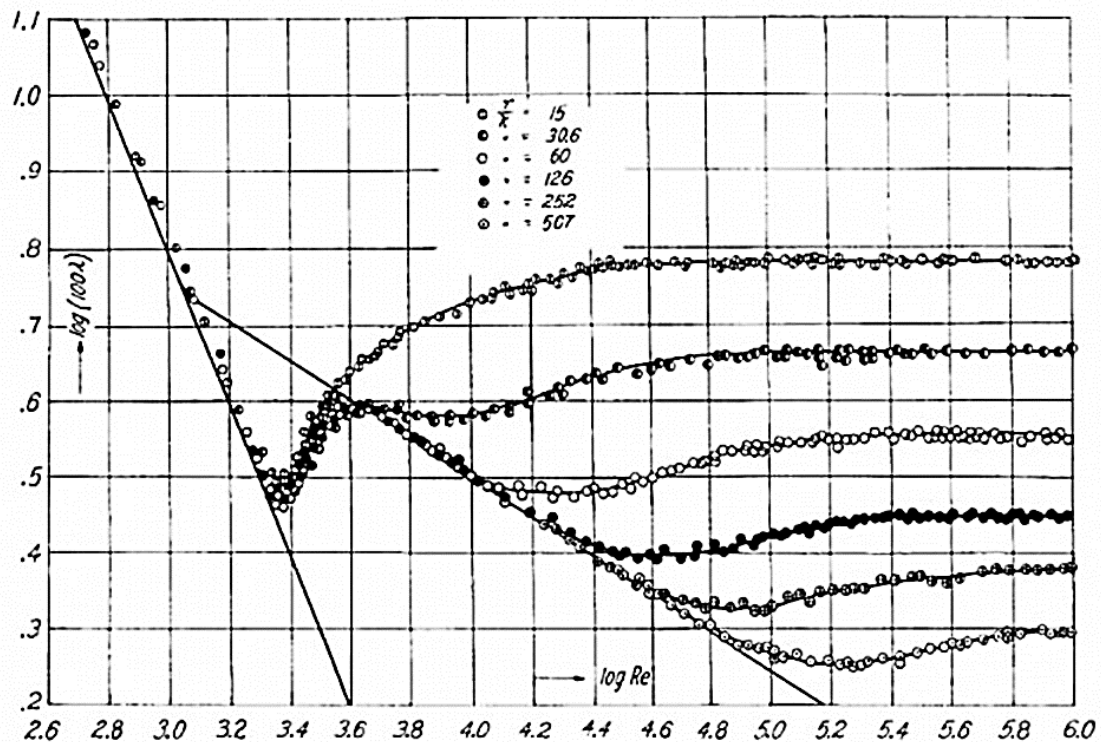


Figure 142 – Experimental results of Nikuradse (Pinho et al., 2011).

Analysis of the results of Nikuradse (Figure 142) allows to identify diverse regimes of flows (Figure 143) in function of the parameters of the number of Reynolds (**Re**) and relative rugosity (ϵ/D) (Pinho et al., 2011):

- I – Laminar regime;
- II – Transition regime laminar/turbulent;
- III – Turbulent regime hydraulically smooth;
- IV – Transition regime smooth/rough;
- V – Turbulent regime hydraulically rough.

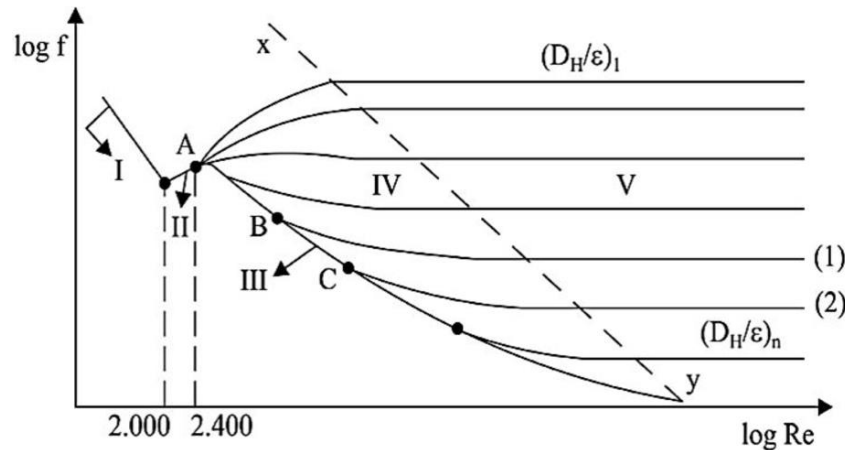


Figure 143 – Flows regimes in conduits (<http://slideplayer.com.br/slide/7750390/#>).

Fundamental regimes in flows under pressure (Pinho et al., 2011):

- Laminar regime, $\lambda = \lambda(Re)$;
- Turbulent regime hydraulically smooth, $\lambda = \lambda(Re)$;
- Transition regime from turbulent hydraulically smooth to turbulent hydraulically rough, $\lambda = \lambda(Re, \varepsilon/D)$;
- Turbulent regime hydraulically rough, $\lambda = \lambda(\varepsilon/D)$.

9.2 Uniform charge losses in flows under pressure

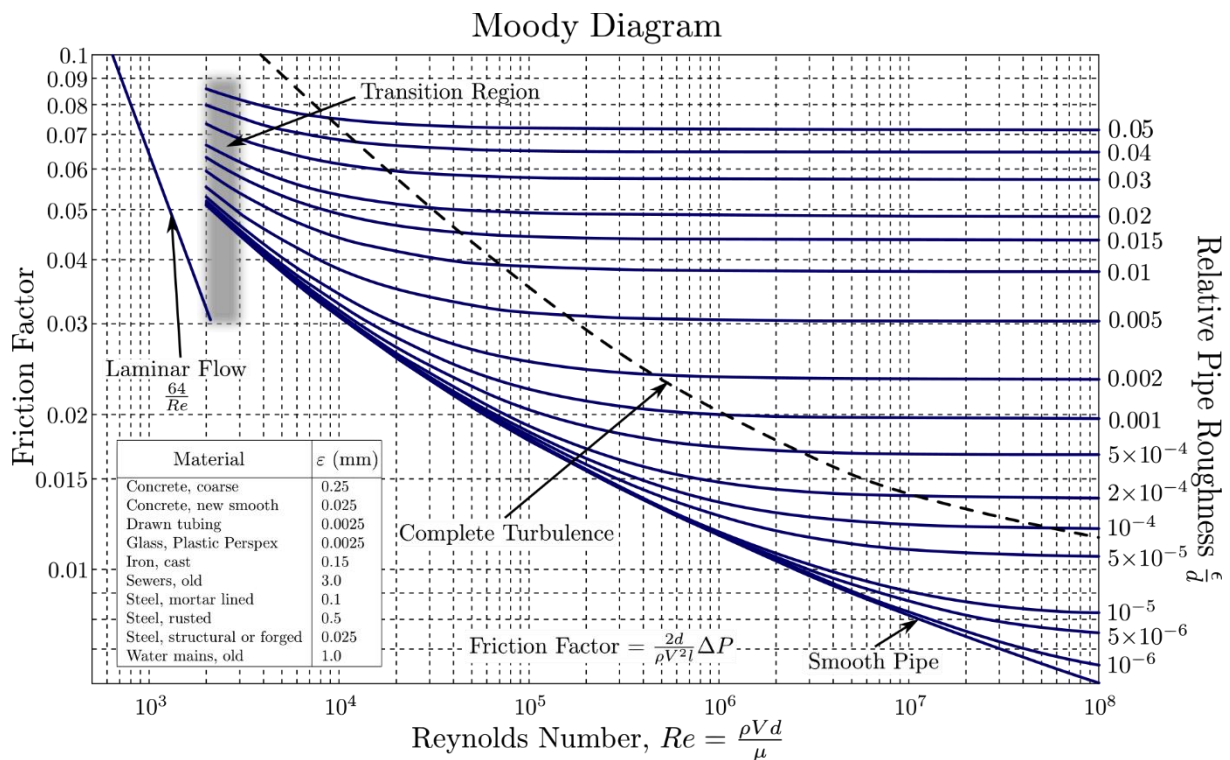


Figure 144 – Moody diagram (source: https://en.wikipedia.org/wiki/Moody_chart#/media/File:Moody_EN.svg).

9.2.1 Charge losses in laminar regime

Poiseuille's formula (Pinho et al., 2011):

$$\lambda = \frac{64}{\text{Re}}$$

9.2.2 Charge losses in turbulent regime hydraulically smooth

Prandtl-Von Karmans formula (Pinho et al., 2011):

$$\frac{1}{\sqrt{\lambda}} = -2 \log \frac{2.51}{\text{Re} \sqrt{\lambda}}$$

9.2.3 Charge losses in turbulent rough regime

Nikuradse's formula (Pinho et al., 2011):

$$\frac{1}{\sqrt{\lambda}} = -2 \log \frac{\varepsilon/D}{3.7}$$

9.2.4 Charge losses in commercial pipes or conduits

Colebrook-White's formula (Pinho et al., 2011):

$$\frac{1}{\sqrt{\lambda}} = -2 \log \left(\frac{k/D}{3.7} + \frac{2.51}{\text{Re} \sqrt{\lambda}} \right)$$

Being **k** the equivalent rugosity of a conduit - a parameter that by replacing **ε** in the established equations for rugosity type Nikuradse's sands grains, leads to the coefficient of charge losses determined for such conduit in turbulent regime hydraulically rough. **Note:** the values of **k** can be found at tables, but differing in its values according to the source, due to the consideration of factors as: variability of the material depending in the manufacturer, considering or not the influence of the joints or the material aging. It is wise to use the most unfavourable values for each pretended use (Pinho et al., 2011).

Application of the Colebrook-White's formulas

Involved parameters (Pinho et al., 2011):

- Conduit diameter (**D**);
- Average velocity of flow (**U(Re)**);

- Equivalent rugosity (**k**);
- Coefficient of resistance or charge losses (**λ**) related with the charge losses per unit of length (**J**), through the **General Expression of the Charge Losses**:

$$J = \frac{\lambda}{D} \frac{U^2}{2g}$$

Types of problems that involves Colebrook-White's formula (Pinho et al., 2011):

1. Determination of the conduit diameter (**D**) (**dimension problem**), when the other parameters are known, or determination of the coefficient of resistance (**λ**) when the other values are known - **implicit problem** - resolution by an iterative method, or by a graphic method;
2. Determination of the equivalent rugosity (**k**), known **λ**, **U** and **D**;

$$k = 3.7D \left(10^{-\frac{\lambda}{2}} - \frac{2.51}{Re\sqrt{\lambda}} \right)$$

3. Determination of the average velocity of flow (**U**), known **J**, **k** and **D**;

$$\begin{cases} J = \frac{\lambda}{D} \frac{U^2}{2g} \\ \frac{1}{\sqrt{\lambda}} = -2 \log \left(\frac{k/D}{3.7} + \frac{2.51}{Re\sqrt{\lambda}} \right) \end{cases} \Rightarrow U = -2\sqrt{2gDJ} \log \left(\frac{k/D}{3.7} + \frac{2.51\nu}{D\sqrt{2gDJ}} \right)$$

4. Calculus of the coefficient of resistance (**λ**):
 - a. Resolution of the Colebrook-White's Formula (**iterative method**);

$$F(\lambda) = \frac{1}{\sqrt{\lambda}} + 2 \log \left(\frac{k/D}{3.7} + \frac{2.51}{Re\sqrt{\lambda}} \right); F(\lambda) = 0$$

- b. Diagram or abacus of Moody (**Graphical method**): input: D, U, k/D → output: λ;
- c. Barr's Formula (Pre-dimensioning);

$$\frac{1}{\sqrt{\lambda}} = -2 \log \left(\frac{k/D}{3.7} + \frac{5.1286}{Re^{0.89}} \right)$$

- d. Darcy-Weisbach's formula;

$$J = \frac{f}{D} \frac{U^2}{2g}$$

- e. Hazen-Williams's formula.

$$J = \frac{10.7}{C_{HW}^{1.852} D^{4.87}} Q^{1.852}$$

9.3 Localized charge losses in flows under pressure

Localized charge losses (accidental, singular or concentrated)

General formula (Pinho et al., 2011):

$$\Delta H_L = K \frac{U^2}{2g}$$

Where:

K is the coefficient of charge losses;

$U^2/2g$ is the kinetic energy.

Where:

$$K = f(\text{Re, contour geometry})$$

Localized charge losses correspond to varied regimes that stablish in pieces of short extension, due to abrupt changes in flows conditions. In such pieces, the charge losses prevail relatively to a continuous charge loss, **corresponding to one discontinuity in the energy line** (Pinho et al., 2011).

9.3.1 Charge losses in an abrupt enlargement

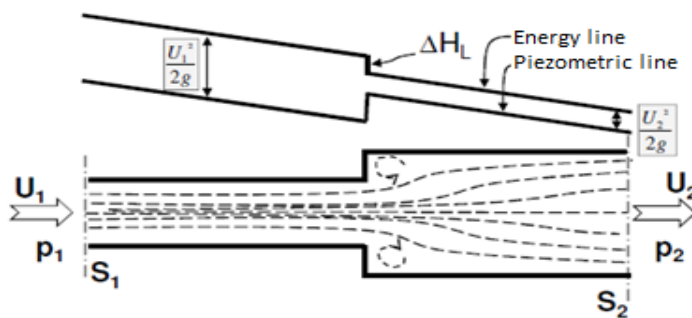


Figure 145 – Charge loss in an abrupt enlargement (Pinho et al., 2011).

Attending to the equation of amount of movement,

$$\rho Q(U_1 - U_2) = p_2 S_2 - p_1 S_1 - p'(S_2 - S_1)$$

Bernoulli's Equation,

$$\frac{p_1}{\gamma} + \frac{U_1^2}{2g} - \left(\frac{p_2}{\gamma} + \frac{U_2^2}{2g} \right) = \Delta H_L$$

Then:

$$\Delta H_L = \left(\frac{U_1 - U_2}{2g} \right)^2 + \left(1 - \frac{S_1}{S_2} \right) \frac{p - p'}{\gamma} = \left(1 - \frac{S_2}{S_1} \right) \frac{U_2^2}{2g} + \left(1 - \frac{S_1}{S_2} \right) \frac{p_1 - p'}{\gamma}$$

As $p_1 - p' = 0$, then:

$$\Delta H_L = \left(1 - \frac{S_2}{S_1} \right) \frac{U_2^2}{2g} \Rightarrow \boxed{\Delta H_L = \left(\frac{U_1 - U_2}{2g} \right)^2} \text{ Formula of Borda}$$

9.3.2 Charge losses in a gradual enlargement

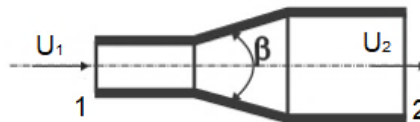


Figure 146 – Gradual enlargement (KSB, 2003).

$$\Delta H_L = \underbrace{\left(1 - \frac{S_2}{S_1} \right)^2}_{\mathbf{K}} \frac{U_2^2}{2g}$$

Table 21 – Value of K in function of the angle β (KSB, 2003).

β	5°	10°	20°	40°	60°	70°	80°	120°
K	0.13	0.17	0.42	0.90	1.10	1.20	1.08	1.05

9.3.3 Charge losses in a passage from a conduit or pipe to a reservoir

Passage with sharp edge

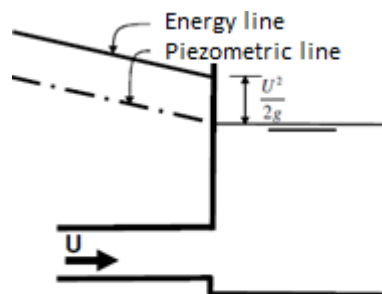


Figure 147 – Passage with sharp edge from a conduit to a reservoir (Pinho et al., 2011).

$$\Delta H_L = \frac{U^2}{2g}$$

Passage with gradual enlargement

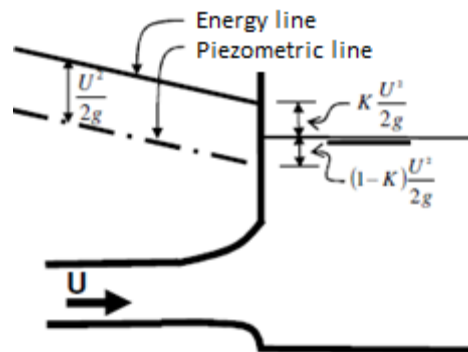


Figure 148 – Passage with gradual enlargement from a conduit to a reservoir (Pinho et al., 2011).

$$\Delta H_L \geq 0.5 \frac{U^2}{2g}$$

9.3.4 Charge losses in an abrupt narrowing or abrupt reduction

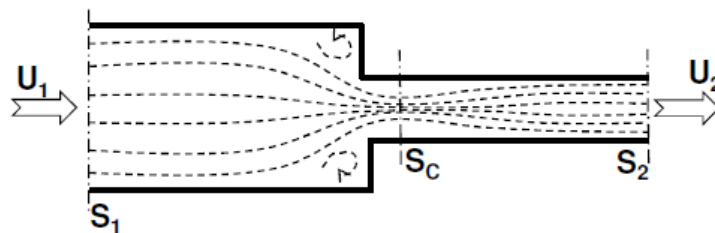


Figure 149 – Abrupt reduction (Pinho et al., 2011).

Evaluating flows:

- Accelerated flow between S_1 and S_C ;
- Delayed flow between S_C and S_2 .

$$\Delta H_L = \underbrace{\left[\left(1 - \frac{S_2}{C_c} \right)^2 + \frac{1}{9} \right]}_K \frac{U_2^2}{2g}$$

Table 22 – Values of K and C_c in function of the sections of input and output, according to Weisbach (Pinho et al., 2011).

S_2/S_1	1.00	0.80	0.60	0.40	0.20	0.10	0.01
$C_c = S_c/S_2$	1.00	0.77	0.70	0.65	0.62	0.61	0.60
K	0.00	0.13	0.22	0.33	0.42	0.45	0.49

9.3.5 Charge losses in a passage from a reservoir to a conduit

Passage with sharp edge

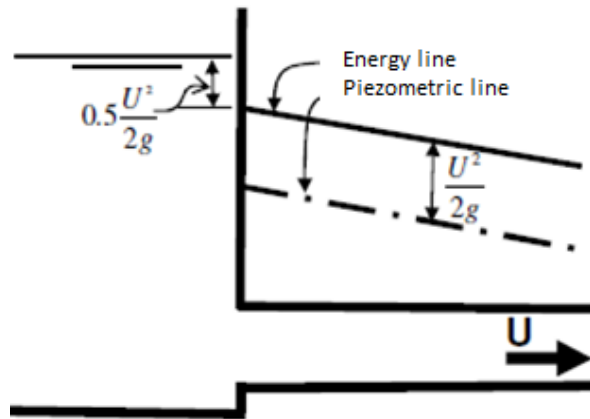


Figure 150 – Passage with sharp edge from a reservoir to a conduit (Pinho et al., 2011).

$$\Delta H_L = 0.5 \frac{U^2}{2g}$$

Passage with gradual reduction

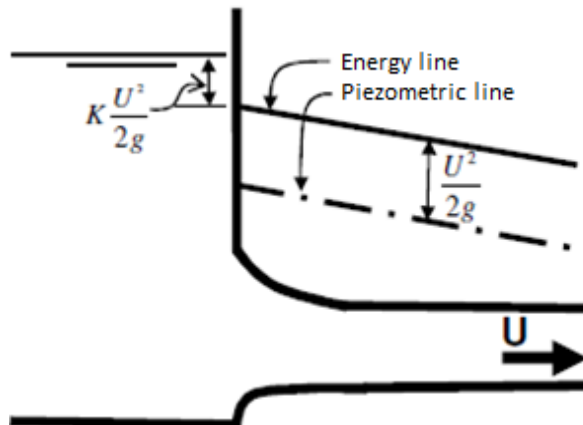


Figure 151 – Passage with gradual reduction from a reservoir to a conduit (Pinho et al., 2011).

$$\Delta H_L \geq 0.05 \frac{U^2}{2g}$$

9.3.6 Charge losses in directions changes

General formula

$$\Delta H_L = K \frac{U^2}{2g}$$

Gradual change of direction

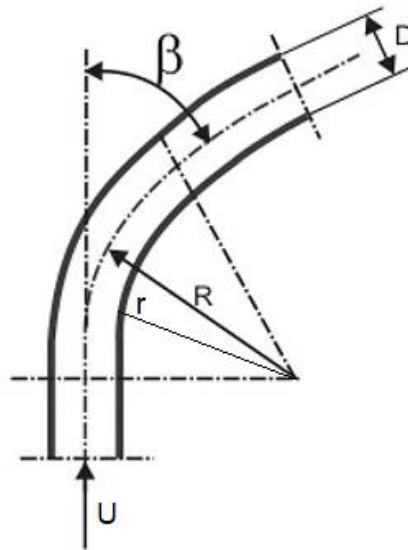


Figure 152 – Gradual change of direction in a tube of circular section (curves) (KSB, 2003).

K is calculated in the next form:

$$K = \beta^\circ/90^\circ \left[0.131 + 1.847 \left(\frac{D}{2R} \right)^{3.5} \right]$$

Abrupt change of direction

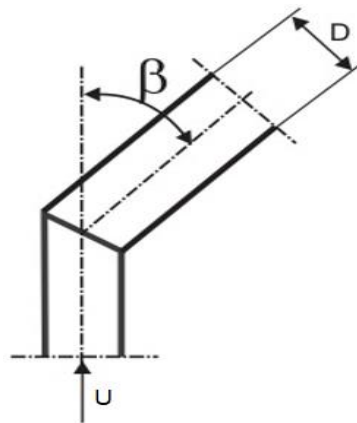


Figure 153 – Abrupt change of direction in a tube of circular section (knee or elbow) (KSB, 2003).

K is calculated in the next form:

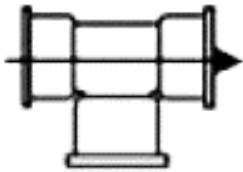
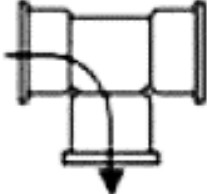
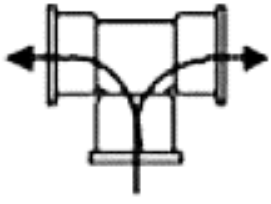
$$K = 0.9457 \sin^2 \frac{\beta}{2} + 2.05 \sin^4 \frac{\beta}{2}$$

In case of a tube being of **rectangular section** where a_0 and b_0 represents respectively, height and length of the parameters **R** and **D** of the last expressions that take next shape:

$$R = r + \frac{b_0}{2} \quad \wedge \quad D = \frac{2a_0b_0}{a_0 + b_0}$$

9.3.7 Charge losses in bifurcation

Table 23 – Equivalent lengths of charge losses in bifurcations, expressed in meters (adapted from <http://hidrossanitariasutfprcm.blogspot.pt/>).

Diameter, D		T 90° Direct Passage	T 90° Lateral output	T 90° Bilateral output
[mm]	[pol]			
13	½	0.3	1.0	1.0
19	¾	0.4	1.4	1.4
25	1	0.5	1.7	1.7
32	1 ¼	0.7	2.3	2.3
38	1 ½	0.9	2.8	2.8
50	2	1.1	3.5	3.5
63	2 ½	1.3	4.3	4.3
75	3	1.6	5.2	5.2
100	4	2.1	6.7	6.7
125	5	2.7	8.4	8.4
150	6	3.4	10.0	10.0
200	8	4.3	13.0	13.0
250	10	5.5	16.0	16.0
300	12	6.1	19.0	19.0
350	14	7.3	22.0	22.0

9.3.8 Charge losses in valves

General formula

$$\Delta H_L = K \frac{U^2}{2g}$$

Flanged, gate, wedge or slide valves

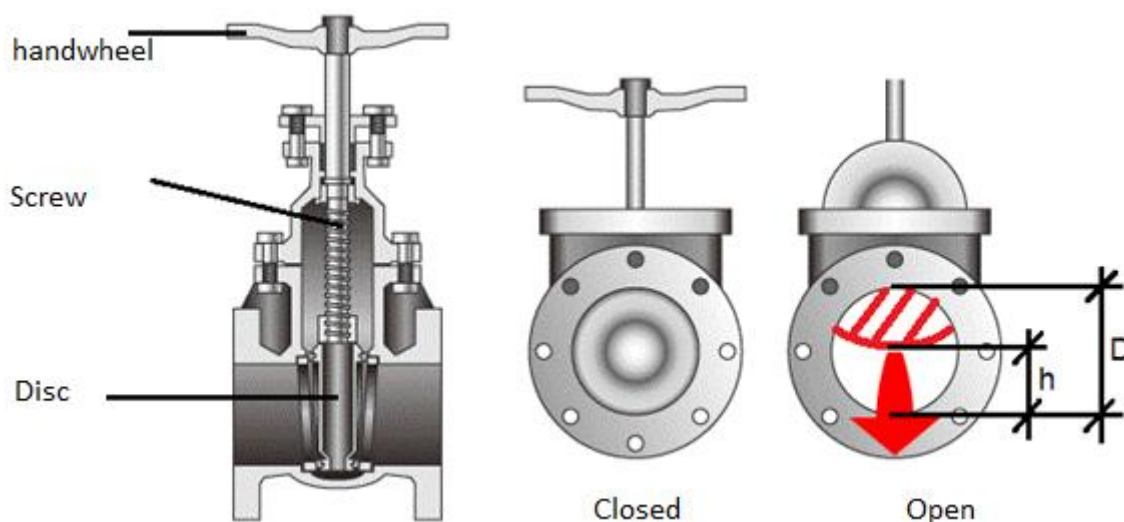


Figure 154 – Gate valve (adapted from <http://www.globalspec.com>).

Table 24 – Values of K in function of the relationship h/D and depending of the sections form (adapted from Pinho et al., 2011).

h/D	0	0.1	0.125	0.2	0.3	0.4	0.5	0.6	0.7	0.8	0.9	1.0
K, \bigcirc	∞	-	97.8	35.0	10.0	4.6	2.06	0.98	0.44	0.17	0.06	0
K, \square	∞	193	-	44.5	17.8	8.12	4.02	2.08	0.95	0.39	0.09	0

Butterfly valves

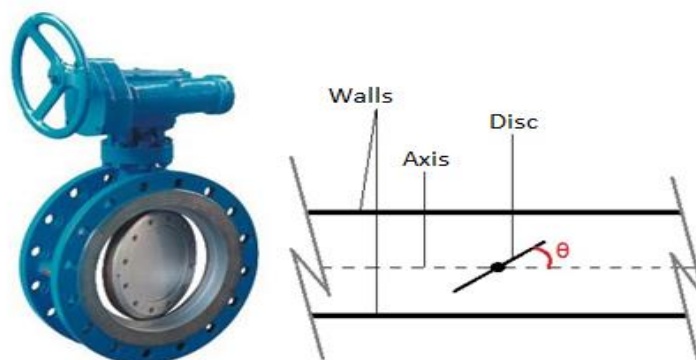


Figure 155 – Butterfly valves (adapted from <http://www.sohanengg.com>).

Table 25 – Values of K in function of θ and depending of the section's forms (adapted from Pinho et al., 2011).

$\theta [^\circ]$	5	10	15	20	25	30	40	50	60	70	80	90
K, \bigcirc	0.24	0.52	0.90	1.54	2.51	3.91	10.8	32.6	118	256	751	∞
K, \square	0.28	0.45	0.77	1.34	2.16	3.54	9.30	24.9	77.4	158	368	∞

Ball or spherical valves

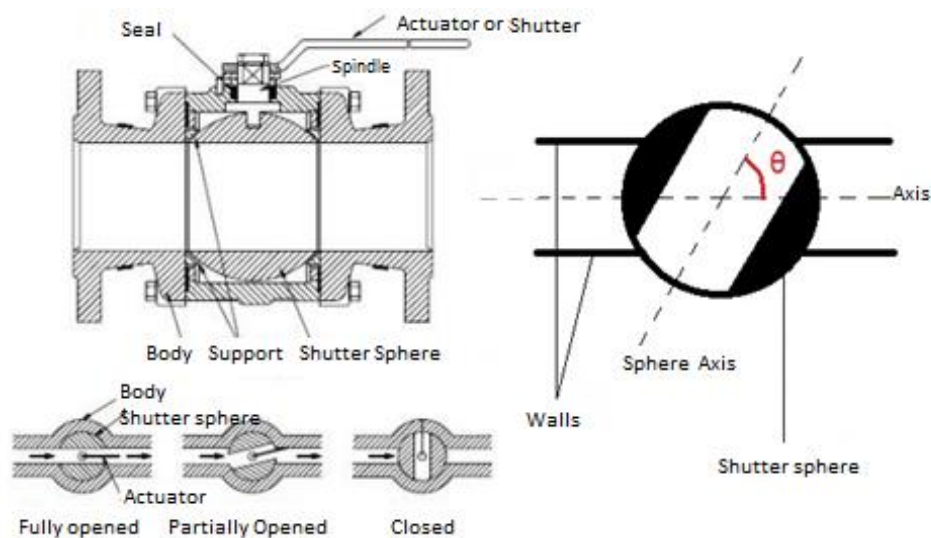


Figure 156 – Spherical valve (adapted from <http://www.histarmar.com.ar> and Pinho et al., 2011).

Table 26 – Values of K in function of θ and depending of the sections form (adapted from Pinho et al., 2011).

θ [°]	5	10	15	20	25	30	40	50	55	60	67	82
K, \bigcirc	0.05	0.31	0.88	1.84	3.45	6.15	20.7	95.3	275	-	∞	-
K, \square	0.05	0.29	0.75	1.56	3.10	5.47	17.3	52.6	-	206	-	∞

Backstop retention valve

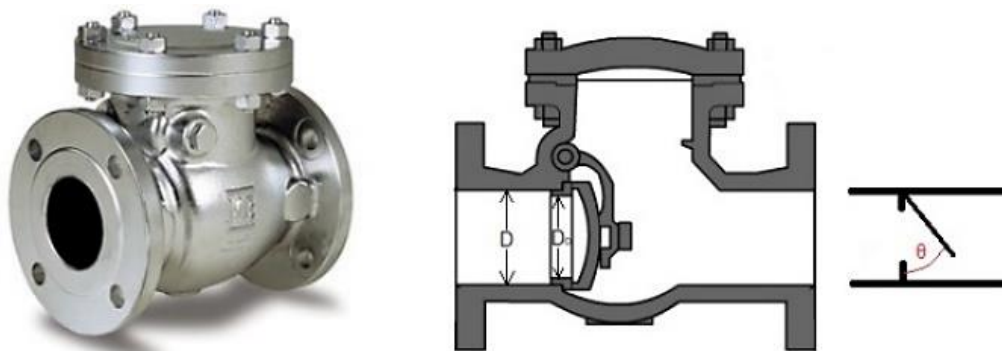


Figure 157 – Backstop retention valve (adapted from <http://www.solucoesindustriais.com.br> and <https://www.unival.com.br>).

Table 27 – Values of K for absolute opening (adapted from Pinho et al., 2011).

D [mm]	40	70	100	200	300	500	700
K	1.3	1.4	1.5	1.9	2.1	2.5	2.9

Table 28 – Values of K in function of the opening angle, for $D_0 = 0,73 D$ (adapted from Pinho et al., 2011).

θ [°]	15	20	25	30	35	40	45	50	55	60	65	70
K	90	62	42	30	20	14	9.5	6.6	4.6	3.2	2.3	1.7

9.3.9 Charge losses in grills

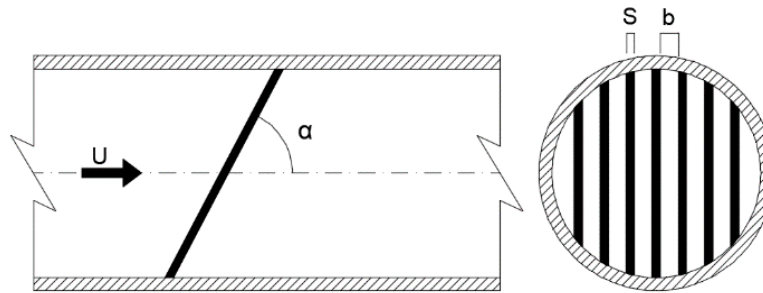


Figure 158 – Grill (adapted from Pinho et al., 2011).

$$\Delta H_L = \underbrace{\beta \left(\frac{S}{b} \right)^{\frac{4}{3}} \sin \alpha}_{\text{K}} \frac{U^2}{2g}$$

Table 29 – Values of β in function of the section profile of the bars (adapted from Pinho et al., 2011).

Section profile of the bars							
Values of β	2.42	1.83	1.67	1.03	0.92	0.76	1.79

9.3.10 Equivalent distance or length to a localized charge loss

Continuous charge losses (Darcy-Weisbach)

$$\Delta H = \frac{\lambda}{D} \frac{U^2}{2g} L$$

For localized charge loss

$$\Delta H_L = K \frac{U^2}{2g} = \frac{\lambda}{D} \frac{U^2}{2g} L_{eq}$$

Where:

$$L_{eq} = \frac{K}{\lambda} D$$

And:

$$L' = L + \sum_{i=1}^n L_{eq,i}$$

9.4 Problems of uniform movement in tubes or pipes

9.4.1 Generalities

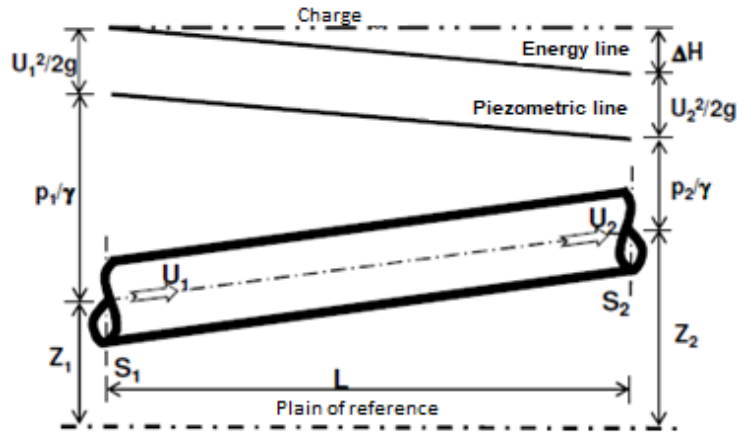


Figure 159 – Schematic representation of a flow inside a tube (Pinho et al., 2011).

Bernoulli's Theorem:

$$E = z + \frac{bp}{\gamma} + \frac{\alpha U^2}{2g} = \text{cst.} \Rightarrow$$

$$\Rightarrow z_1 + \frac{p_1}{\gamma} + \frac{U_1^2}{2g} = z_2 + \frac{p_2}{\gamma} + \frac{U_2^2}{2g} = \Delta H \Rightarrow$$

$$\Rightarrow \Delta H = h_f + \sum \Delta H_L$$

Where:

$$\sum \Delta H_L = \sum_{i=1}^n L_{eq,i}$$

And according to **Darcy-Weisbach** formulation, h_f is defined as:

$$h_f = f \frac{L}{D} \frac{U^2}{2g} \quad \text{or} \quad h_f = KQ^2, \quad \text{where } f = f\left(\text{Re}, \frac{e}{D}\right)$$

According to **Hazen-Williams**, h_f take next form:

$$h_f = \frac{10.7L}{C_{HW}^{1.852} D^{4.87}} Q^{1.852} \quad \text{or} \quad h_f = KQ^{1.852}, \quad \text{where } C_{HW} = f(\text{material}, D)$$

9.4.2 Types of problems

When the **magnitudes to determine** are (Pinho et al., 2011):

- **Flow rate (Q);**
- **Conduit diameter (D);**
- **Velocity (U);**
- **Continuous charge losses (J).**

The **available equations** for the resolutions of these problems involving such parameters are (Pinho et al., 2011):

- **Continuity, $Q = AU$;**
- **Resistance, $DJ = \varphi(U)$.**

So, it is possible to define **3 types of problems** (Pinho et al., 2011):

- **Type I**, where **D** and **Q** are given, to **determine J**;
- **Type II**, where **D** and **J** are given, to **determine Q**;
- **Type III**, where **Q** and **J** are given, to **determine D**.

9.4.3 Determination of the piezometric elevations when flow rate and diameters are known

At these situations we have (Pinho et al., 2011):

- **Problems type I**
 - Given: Q, D;
- Equations to use:
 - Continuity $\rightarrow U$;
 - Resistance $\rightarrow J$;
- Objective:
 - Piezometric line;
 - Piezometric heights or elevations;
 - Pressures at different sections of the conduit or pipe.

9.4.4 Determination of the flow rate when diameters and charge losses are known

- **Problem Type II** (Pinho et al., 2011)
 - Given: D, J;
- Equation to use:
 - Rough turbulent flow
 - Resistance $\rightarrow Q = \pi \sqrt{g/8\lambda} \sqrt{\Delta H/L'} D^5$
 - Hydraulically smooth flow (iterative process):

- 1st step: Resistance $\rightarrow Q = \pi \sqrt{g/8\lambda} \sqrt{\Delta H/L'} D^5$. Consider L_{eq} valid for a turbulent regime and λ arbitrary;
- 2nd step: Resistance $\rightarrow Q = \pi \sqrt{g/8\lambda} \sqrt{JD^5}$. By the obtained value of Q , proceed to calculate charge losses and the respectively coefficient λ , where $J = (\Delta H - \sum_{i=1}^n \Delta H_{L_i})/L$;
- Objective:
 - Flow rate in conduit.

9.4.5 Determination of the diameters when flow rate and charge losses are known

- **Problems Type III** (Pinho et al., 2011)
 - Given: Q, J ;
- Equations to use (iterative process):
 - 1st step: Resistance $\rightarrow D = [(8\lambda Q^2 L')/(g\pi^2 J)]^{1/5}$. Consider L_{eq} valid for a turbulent regime and λ arbitrary;
 - 2nd step: Resistance $\rightarrow D = [(8\lambda Q^2)/(g\pi^2 J)]^{1/5}$. With an obtained value of D , proceed to calculate charge losses and a new value of λ , where $J = (\Delta H - \sum_{i=1}^n \Delta H_{L_i})/L$;
- Objective:
 - Diameter of the conduit.

Note: in practice, this kind of problem of hydraulic dimensioning of a tube is conditioned by the diameters of the market stock, being normally adopted the minor diameter that satisfies piezometric conditions and required velocities (Pinho et al., 2011).

9.4.6 Position of the conduits depending on the piezometric line

1st Case: Conduit under the effective piezometric line in its complete extension

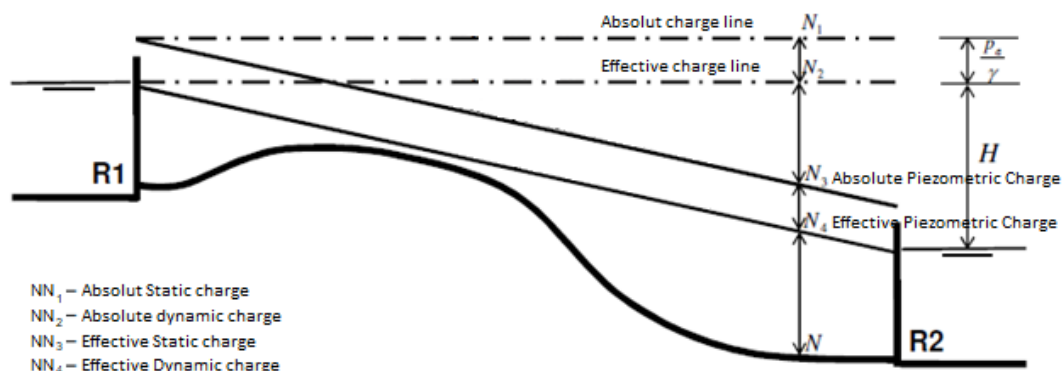


Figure 160 – Conduit under the effective piezometric line in its complete extension (Pinho et al., 2011).

At such situation, it is verified (Pinho et al., 2011):

- Positive effective pressure at all points in conduit;
- Optimal position for flow.

2nd Case: Conduit above the effective piezometric line (at CD) while the absolute piezometric line stays under

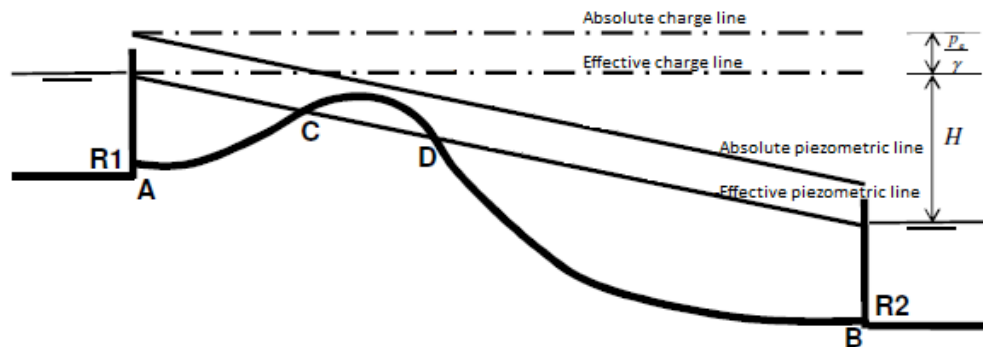


Figure 161 – Conduit above the effective piezometric line (at CD), but below the absolute piezometric line (Pinho et al., 2011).

At such situation, it is verified (Pinho et al., 2011):

- In the piece **CD**, exists air bags, reducing flow rate;
- In the piece **DB**, occurs an intermittent or partial operation;
- It is advised not to use suction cups or suckers in piece **CD**;
- Use of different diameter in **AC** and **DB**;
- If the depression is high enough, the **liquid steam tension** can be raised, unleashing a **cavitation effect**.

3rd Case: Conduit coinciding with the effective piezometric line in its complete extension

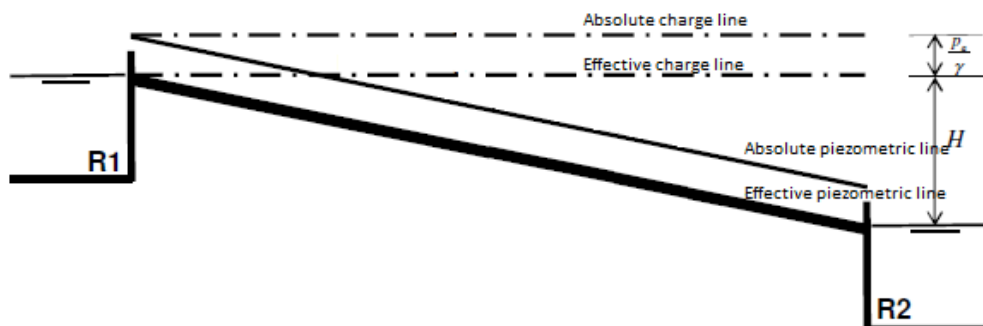


Figure 162 – Conduit coinciding with the effective piezometric line in its complete extension (Pinho et al., 2011).

At such situation, it is verified (Pinho et al., 2011):

- Every single point is at atmospheric pressure. The conduit works as a channel.

4th Case: The conduit crosses the effective charge line (at CD), staying under the absolute piezometric line

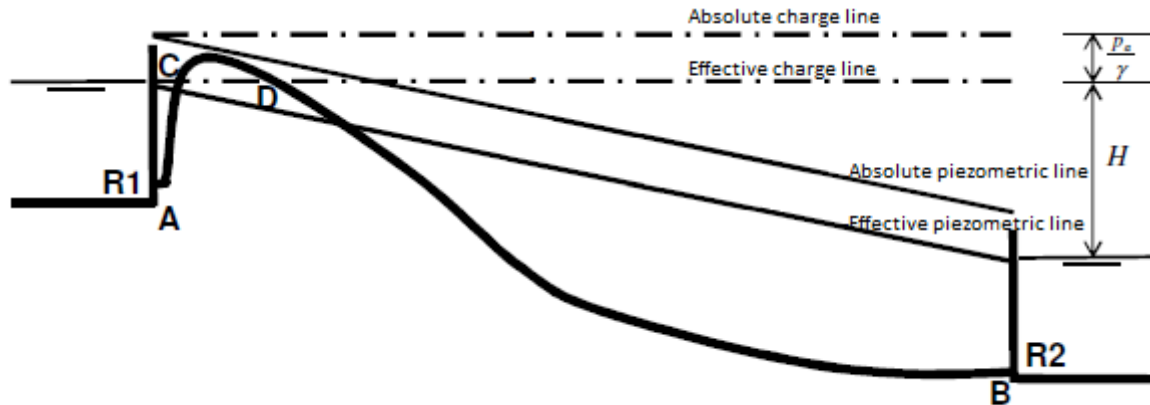


Figure 163 – The conduit crosses the effective charge line (in CD), staying under the absolute piezometric line (Pinho et al., 2011).

At such situation, it is verified (Pinho et al., 2011):

- It is a **siphon** working in precarious conditions;
- The flow can only be established, **necessarily**, after suction (priming) of the siphon.

5th Case: Conduit cross the absolute piezometric line (at CD), but does not achieve the effective charge line

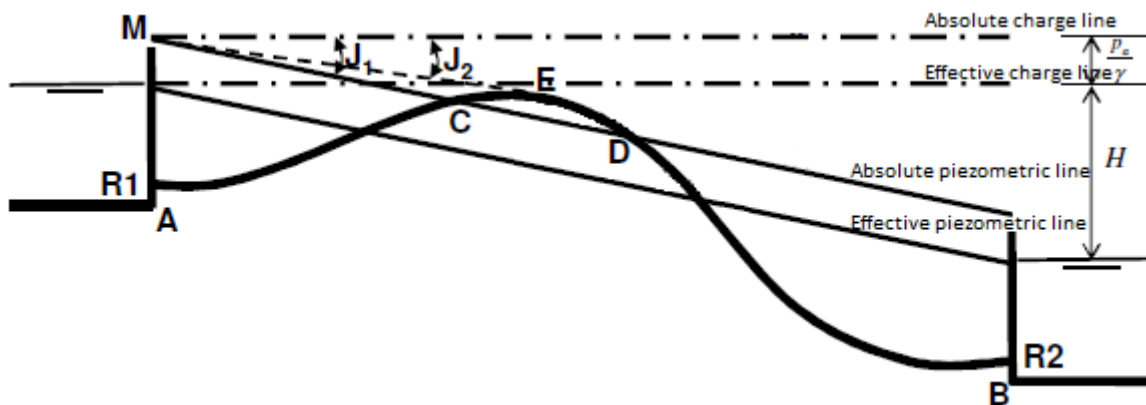


Figure 164 – The conduit crosses the absolute piezometric line (at CD) but does not achieve the effective charge line (Pinho et al., 2011).

At this situation, it is verified (Pinho et al., 2011):

- The absolute pressure between **CD** would be negative (which does not have any physical possibility);
- The absolute piezometric line would suffer a displacement to **ME**, decreasing its declination from **J₁** to **J₂**. Starting from **D**, has the same inclination as **J₁**;

- Between **E** and **D**, the absolute piezometric line coincide with conduit, where pressure is theoretically zero, verifying in practice a flow with a partial completion of the section and having some intermittences due to liquids steam release and dissolved air.

6th Case: Conduit cross the absolute piezometric line and overpass the effective charge line

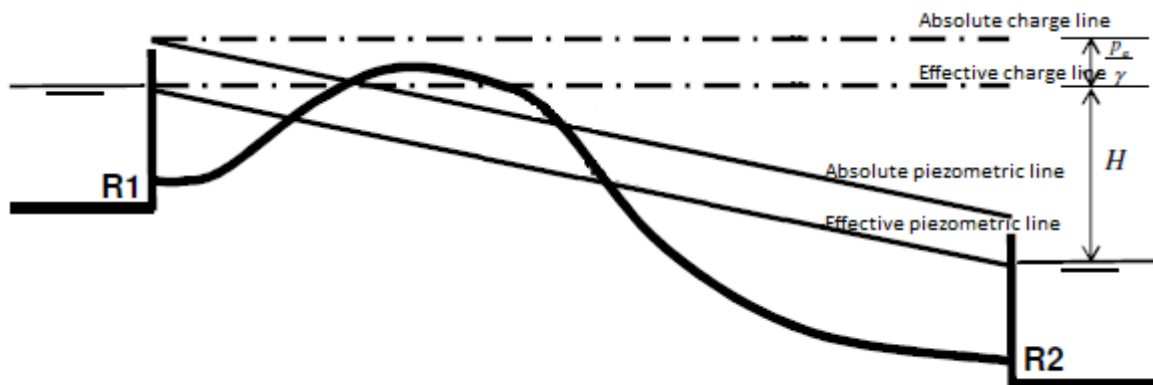


Figure 165 – The conduit crosses the absolute piezometric line and overpass the effective charge line (Pinho et al., 2011).

At such situation, it is verified (Pinho et al., 2011):

- As the conduit overpass the free surface of the reservoir **R1**, it is necessary to induce the flow by siphoning;
- The characteristic of the operativity of the flows are identical to the 5th Case. However, it is verified, that the section is partially filled and with accented irregularities for a mayor extension of conduit;
- Must be noticed the impossibility of stablishing a regime of flow if the conduit or pipe would have a section over the height of the absolute charge line, unless exists an external stimulator (mechanical elevation).

Dispositive to avoid depressions in pipes or conduits

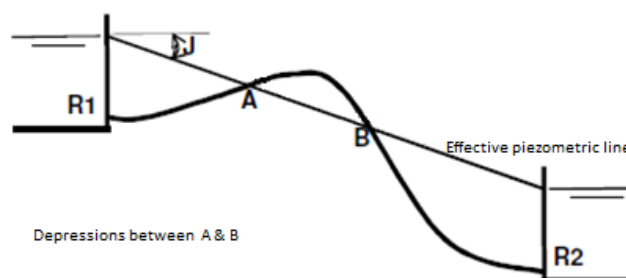


Figure 166 – Condition of maximum transportation (Pinho et al., 2011).

In order to avoid depression between A and B at the upper figure, next methods must be adopted (Pinho et al., 2011):

- Reservoir at constant level (**R**);

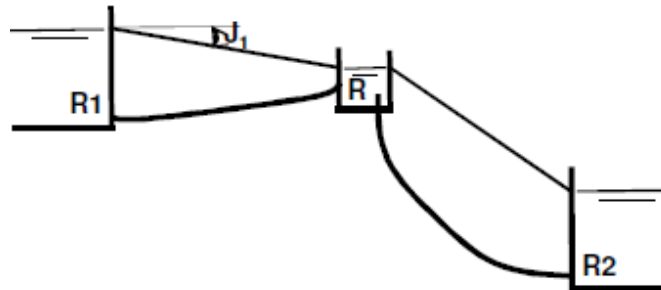


Figure 167 – Reservoir at constant level.

- Partially open valve (**V**).

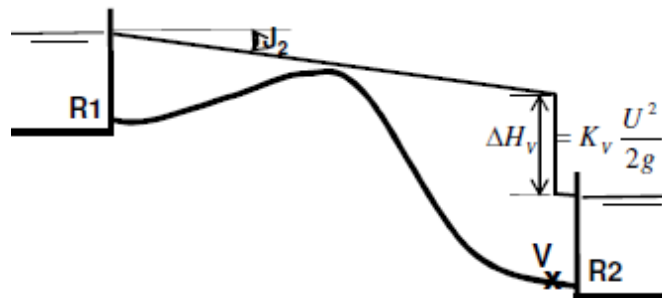


Figure 168 – Partially open valve.

9.4.7 Conduits supplied by both extremes

1st Case: Operation from R1 to R2 reservoir

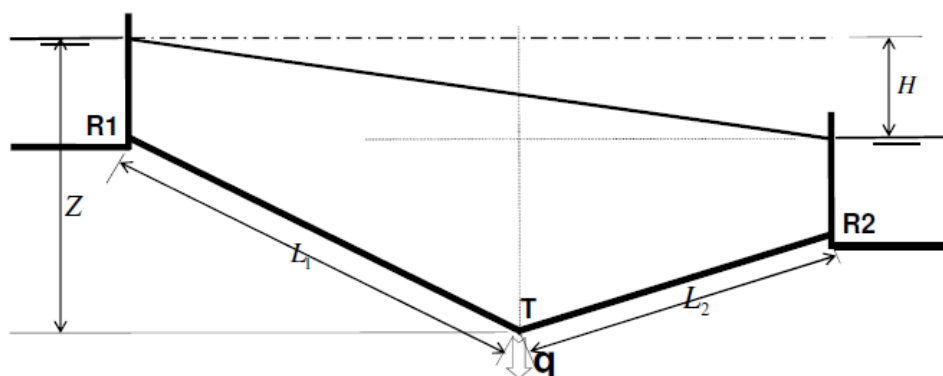


Figure 169 – Operation from R1 to R2 reservoir (Pinho et al., 2011).

The charge loss (**h_f**) is calculated by next formula:

$$h_f = K \frac{Q^2}{D^5} (L_1 + L_2), \text{ with } K = f \frac{8}{\pi^2 g}$$

And the resultant flow rate (Q):

$$Q = \sqrt{\frac{HD^5}{K(L_1 + L_2)}}$$

2nd Case: Operation with a T bifurcation, flow rate q and piezometric at $T > R2$

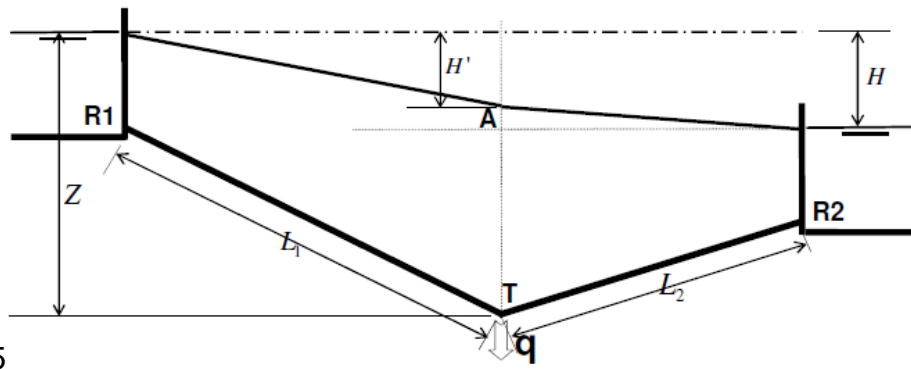


Figure 170 – Operation with a T bifurcation, flow rate q and piezometric $T > R2$ (Pinho et al., 2011).

At this situation, **R1** supplies simultaneously **T** and **R2**. Q_{R1} is calculated as:

$$Q_{R1} = q_T + q_{R2} = \sqrt{\frac{H'D^5}{KL_1}} + \sqrt{\frac{(H - H')D^5}{KL_2}}$$

3rd Case: Operation with T bifurcation, flow rate q and piezometric at $T = R2$

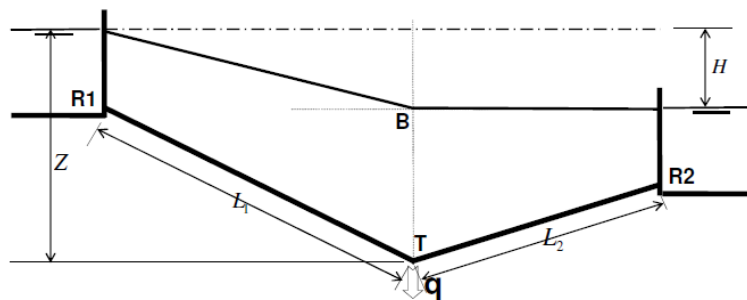


Figure 171 – Operation with a T bifurcation, flow rate q and piezometric line in $T = R2$ (Pinho et al., 2011).

At such situation, **R1** supplies **T**. Q_{R1} is calculated as:

$$Q_{R1} = q_T = \sqrt{\frac{HD^5}{KL_1}}$$

4th Case: Operation with a T bifurcation, flow rate q and piezometric at $T < R2$

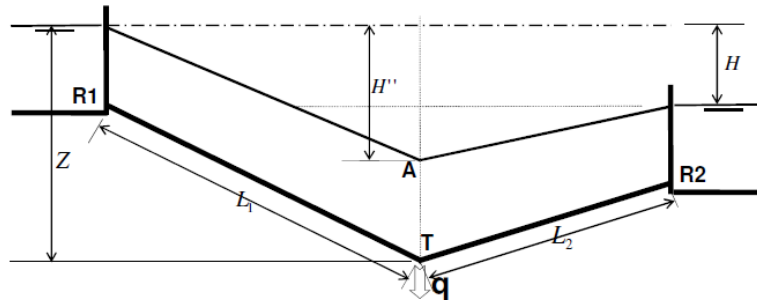


Figure 172 – Operation with a T bifurcation, flow rate q and piezometric at $T < R2$ (Pinho et al., 2011).

At such situation, **R1** and **R2** supplies simultaneously **T**. Q_T is calculated as:

$$Q_T = q_{R1} + q_{R2} = \sqrt{\frac{H'' D^5}{KL_1}} + \sqrt{\frac{(H'' - H) D^5}{KL_2}}$$

5th Case: Operation with a T bifurcation, flow rate q and piezometric at $T = T$ (effective pressure = 0, Maximum flow rate at T)

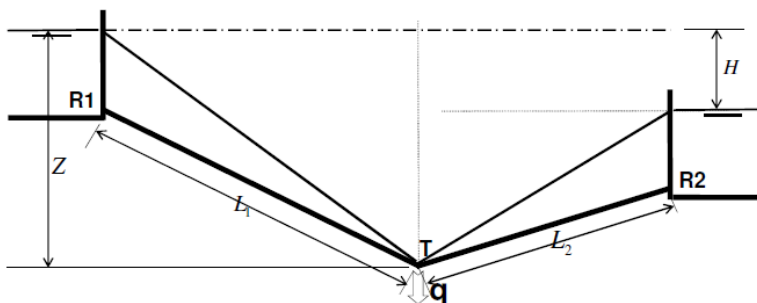


Figure 173 – Operation with a T bifurcation, flow rate q and piezometric at $T = T$ (Pinho et al., 2011).

At such situation, **R1** and **R2** supplies simultaneously **T**. Q_T is calculated as:

$$Q_T = q_{R1} + q_{R2} = \sqrt{\frac{Z D^5}{KL_1}} + \sqrt{\frac{(Z - H) D^5}{KL_2}}$$

9.4.8 Dimensioning of gravitational conduits

The types of problems presented at this situation, by knowing **flow rate** (Q) to determine the **economical diameter** (D_{econ}), can be solved through solutions that focus in piezometric elevations or in flows velocities (Pinho et al., 2011):

Solution A

Determine the minimal **D**, in order to (Pinho et al., 2011):

- **V_{max}** admissible must not be exceeded;
- The piezometric elevations are satisfied.

Table 30 – Velocities and maximum flow rate recommended for asbestos cement (Pinho et al., 2011).

D [mm]	50	60	80	100	125	150	175	200	>200
V _{max} [m/s]	0.60	0.70	0.75	0.75	0.80	0.80	0.90	0.90	1.00
Q _{max} [L/s]	1.2	2.0	3.8	5.9	9.8	14.1	21.6	28.3	-

Solution B

The minimal piezometric inclination is fixed and by the resistance's equation **D** is calculated (Pinho et al., 2011):

- Darcy-Weisbach:

$$D = \sqrt[5]{\frac{8\lambda Q^2}{g\pi^2 J}}$$

- Hazen-Williams:

$$D = \sqrt[4.87]{\frac{10.7Q^{1.852}}{C_{HW}^{1.852} J}}$$

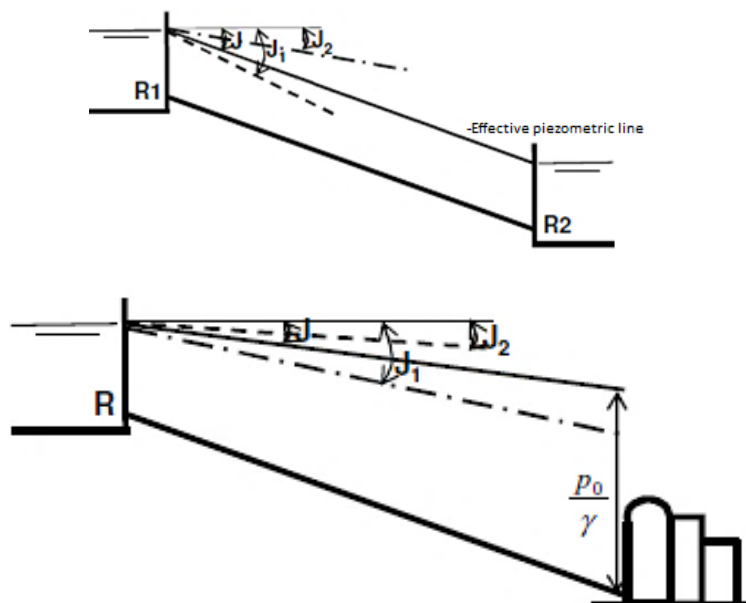


Figure 174 – Examples of application (Pinho et al., 2011).

9.5 Dimensioning of elevatory pipes or conduits

9.5.1 Generalities

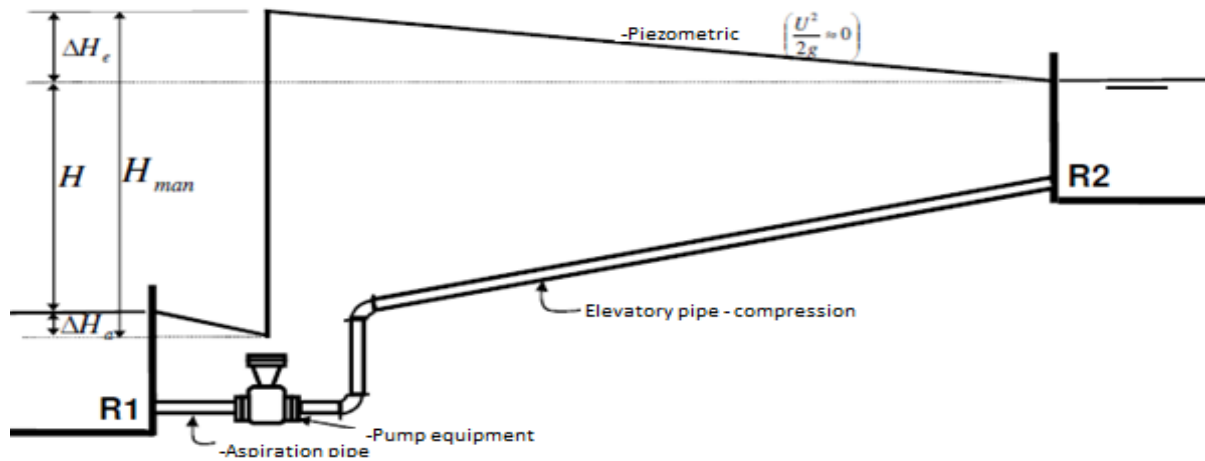


Figure 175 – Example of an elevatory pipe or conduit (Pinho et al., 2011).

Pumps effective power

$$P = \frac{\rho g Q H}{\eta} \text{ (W)}$$

Consumed energy in elevation

$$E = P t \text{ (W.h)}$$

9.5.2 Economical and resources considerations

The **costs of an elevatory pipe** includes the **investment costs** (Figure 176) and the **operating costs** (Figure 177) (Pinho et al., 2011).



Figure 176 – Investment costs (initial costs) (Pinho et al., 2011).

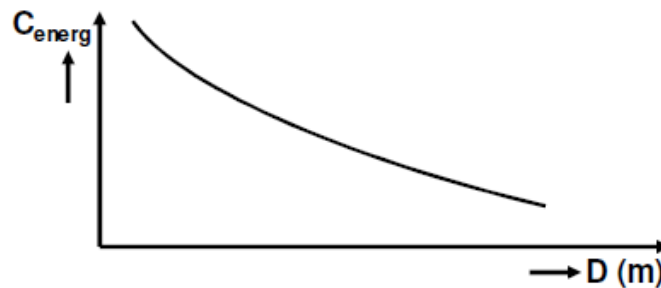


Figure 177 – Operating costs (annual costs, most significant: energy cost) (Pinho et al., 2011).

Note: discussion refer to 1 m of pipe (Pinho et al., 2011).

9.5.3 Expenses structure

Initial expenses (C_1)

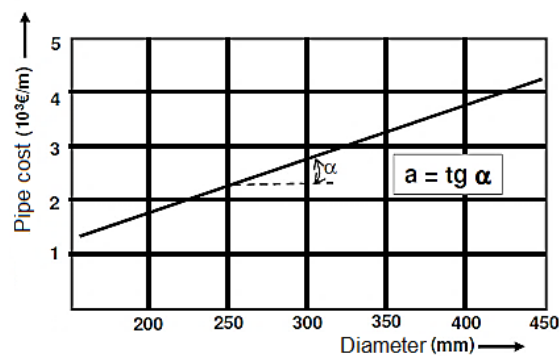


Figure 178 – Initial costs or expenses (C_1) (Pinho et al., 2011).

$$C_1 = a \cdot D \text{ [€/m]}$$

Where:

a is a constant scale factor [€/m/m];

D is the diameter of the pipe or conduit [m].

Annual expenses or cost of energy (C_2)

Power:

$$P = \underbrace{\gamma Q H}_{P_1} + \underbrace{\gamma Q \Delta H}_{P_2}, \text{ with } \Delta H = \begin{cases} \Delta H_a + \Delta H_e, & \text{if } \sum \Delta H_L \neq 0 \\ h_f, & \text{if } \sum \Delta H_L = 0 \end{cases}$$

Where:

P_2 is independent of D ;

$P_2 = f(D) \rightarrow$ increase when D decrease \rightarrow A discussion focus on P_2 .

On that way, there are different situations that can be identified (Pinho et al., 2011):

- To elevate $1 \text{ m}^3/\text{s}$ to a height of 1 meter, it is necessary
 - $P_2 = 9800 \cdot h_f [\text{W}]$;
- To elevate $1 \text{ m}^3/\text{h}$ to a height of 1 meter, it is necessary
 - $P_2 = 2.72 \cdot h_f [\text{W}]$;
- To elevate $1 \text{ m}^3/\text{h} \cdot \text{year}$ to a height of 1 meter, it is necessary **energy**
 - $E_2 = (8760 \text{ h/ano})(2.72 \cdot h_f \times 10^{-3}) [\text{kW} \cdot \text{h/ano}]$;
- To elevate $1 \text{ m}^3/\text{h} \cdot \text{year}$ to a height of 1 meter, exist an expense of **energy**
 - $C_2 = 23.8 \cdot h_f \cdot e [\text{€/year} \cdot \text{m}]$;
- If it is elevated a $Q \text{ m}^3/\text{h} \cdot \text{year}$ with an efficiency of η
 - $C_2 = 23.8 \cdot Q \cdot h_f \cdot \frac{e}{\eta} [\text{€/year} \cdot \text{m}]$.

Where:

h_f is the charge loss $[\text{m/m}]$;

e are the energy costs $[\text{€/kW} \cdot \text{h}]$;

η is the efficiency of the elevatory group (motor-pump).

Applying the equation of Darcy-Weisbach to determine h_f and considering (Pinho et al., 2011):

$$\begin{cases} Q = 500 - 10000 \text{ m}^3/\text{h}, K = 1 \text{ mm}, T = 10^\circ\text{C} \\ f = 0.018 - 0.025 \text{ (taking } f_{\text{ave}} = 0.021), g = 9.81 \text{ m/s}^2 = 1.27 \times 10^8 \text{ m/h}^2 \end{cases}$$

$$h_f = 0.021 \frac{8}{\pi^2 (1.27 \times 10^8)} \frac{Q^2}{D^5} = 1.34 \times 10^{-10} \frac{Q^2}{D^5}$$

And:

$$C_2 = 32 \times 10^{-10} \frac{e}{\eta} \frac{Q^3}{D^5} (\text{€/m} \cdot \text{year})$$

9.5.4 Calculus of the economical diameter

Constant consumption of water

Considering **constant expenses of energy** along the project horizon (Pinho et al., 2011):

$$\text{Annual Cost} \rightarrow C_{\text{total}} = C_1 + C_2 = \beta a D + 32 \times 10^{-10} \frac{e}{\eta} \frac{Q^3}{D^5} (\text{€/m} \cdot \text{year})$$

Where, β is the annual rate of interest.

C_{total} will be minimum for:

$$\frac{\partial C_{\text{total}}}{\partial D} = 0, \text{ where: } \frac{\partial C_{\text{total}}}{\partial D} = \beta a - 160 \times 10^{-10} \frac{e Q^3}{\eta D^6}$$

And:

$$D = 0.05 \cdot \sqrt{Q} \cdot \sqrt[6]{e/\eta a \beta} \text{ (m)}$$

Where:

$$U_{\text{opt}} = 0.14 \cdot \sqrt[3]{\eta a \beta / e} \text{ (m/s)}$$

Linear increase of water consumes

Considering an **increase in energy prices**, **based in an actual value**, is obtained (Pinho et al., 2011):

- Energy costs of the year **1**:

$$C_{2_1} = 32 \times 10^{-10} \frac{e}{\eta D^5} Q_1^3 (1 + \gamma)$$

Being γ the rate of increase of energy expenses.

- Cost of energy by the end of the year **n**:

$$C_{2_n} = 32 \times 10^{-10} \frac{e}{\eta D^5} Q_n^3 (1 + \gamma), \text{ with } Q_n = (1 + \alpha) Q_0$$

Being α the rate of annual increase of consume.

Then, the general formula will be:

$$C_{2_n} = 32 \times 10^{-10} \frac{e}{\eta D^5} Q_0^3 (1 + \gamma)^n (1 + \alpha)^3 \text{ (€/m.year)}$$

Having in count the diagram of **Monetary-time flows** (Pinho et al., 2011):

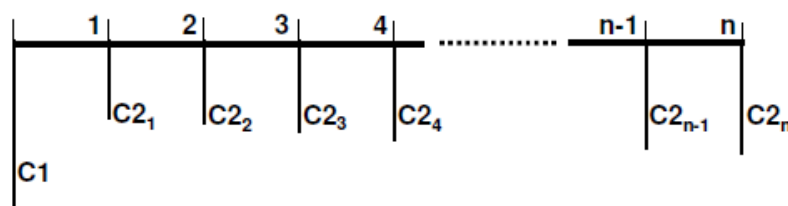


Figure 179 – Monetary-time flows diagrams (Pinho et al., 2011).

$$VC_{total} = C_1 + \frac{C_2}{(1 + \beta)} + \frac{C_2}{(1 + \beta)^2} + \frac{C_2}{(1 + \beta)^3} + \dots + \frac{C_2}{(1 + \beta)^n}$$

Or:

$$VC_{total} = aD + 32 \times 10^{-10} \frac{eQ_0^3}{\eta D^5} \left[\frac{(1 + \gamma)(1 + \alpha)^3}{(1 + \beta)} + \frac{(1 + \gamma)(1 + 2\alpha)^3}{(1 + \beta)^2} + \dots + \frac{(1 + \gamma)(1 + n\alpha)^3}{(1 + \beta)^n} \right]$$

Obtaining (Pinho et al., 2011):

$$VC_{total} = aD + 32 \times 10^{-10} \frac{eQ_0^3}{\eta D^5} \delta \text{ (€/m . year)}$$

$$\text{where: } \delta = \left[\frac{(1 + \gamma)(1 + \alpha)^3}{(1 + \beta)} + \frac{(1 + \gamma)(1 + 2\alpha)^3}{(1 + \beta)^2} + \dots + \frac{(1 + \gamma)(1 + n\alpha)^3}{(1 + \beta)^n} \right]$$

$$\text{where: } \delta = f(\alpha, \beta, \gamma)$$

VC_{total} will be minimum for (Pinho et al., 2011):

$$\frac{\partial VC_{total}}{\partial D} = 0, \text{ where: } \frac{\partial VC_{total}}{\partial D} = \beta - 160 \times 10^{-10} \frac{e Q_0^3}{\eta D^6} \delta = 0$$

where:

$$U_{opt} = 0.14 \cdot \sqrt[3]{a\eta/e\delta} \text{ (m/s)}$$

Exponential increase of water consumption

Considering bases similar to the linear increase, is obtained (Pinho et al., 2011):

$$U_{opt} = 0.14 \cdot \sqrt[3]{a\eta/e\delta'} \text{ (m/s)}$$

Where:

$$Q_n = (1 + \alpha)^n Q_0$$

It is obtained:

$$\delta' = \left[\frac{(1 + \gamma)(1 + \alpha)^3}{(1 + \beta)} + \frac{(1 + \gamma)(1 + \alpha)^6}{(1 + \beta)^2} + \dots + \frac{(1 + \gamma)(1 + \alpha)^{3n}}{(1 + \beta)^n} \right]$$

$$\text{where: } \delta = f(\alpha, \beta, \gamma)$$

9.5.5 Influence of consume during the year

Great variation of the consume along a year

Relationship between energy (E) and flow rate (Q) is given by (Pinho et al., 2011):

$$E = f(Q)^3 \text{ (cubic function)}$$

To elevate Q_{med} in one day, it is necessary less energy than E_{med} (Pinho et al., 2011):

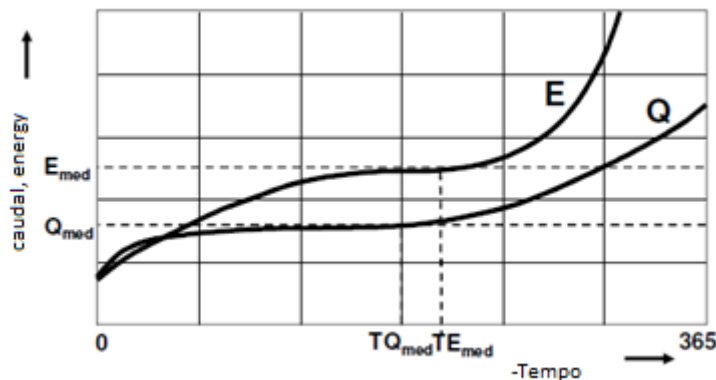


Figure 180 – Flow rate/energy in function of time (Pinho et al., 2011).

The value of E_{med} will not produce Q_{med} , instead Q_{ideal} :

$$Q_{ideal} = \sqrt[3]{\frac{1}{T} \int_0^T [Q(t)]^3 dt}$$

For:

$$Q_{ideal} = (1.20, 1.26) Q_{med}$$

Choosing:

$$Q_{ideal} = 1.26 Q_{med}$$

$$\begin{cases} U_{opt} = 0.11 \cdot \sqrt[3]{a\eta/e\delta} \text{ [m/s]}, \text{ For a linear increase of consume} \\ U_{opt} = 0.11 \cdot \sqrt[3]{a\eta/e\delta'} \text{ [m/s]}, \text{ For a exponential increase of consume} \end{cases}$$

9.5.6 Formulas for an approximated dimensioning

Formula of Bresse

$$D = 1.5\sqrt{Q}, \text{ with } D \text{ [m]}; Q \text{ [m}^3/\text{s]}$$

Formula of Dacach

$$D = 0.9Q^{0.45}, \text{ with } D \text{ [m]}; Q \text{ [m}^3/\text{s]}$$

9.5.7 Dimensioning of the conduit's walls

The dimensioning of the conduit's walls related to **service pressure** in which the pipes or conduit are submitted (σ_s) (Pinho et al., 2011).

$$e = \frac{pD}{2\sigma_s}, \text{ with } p < \sigma_s$$

Where:

e is the thickness of the conduit [m];

p is the pressure in the conduit [N/m^2];

D is the diameter of the conduit [m];

σ_s is the service tension of the conduit material [N/m^2].

Note: pressure to consider in dimensioning must be **static** or **dynamic**, in agreement with the project's circumstances (Pinho et al., 2011).



Figure 181 – Example of an application (Pinho et al., 2011).

9.6 Problems in uniform movement by a group of pipes or conduits

9.6.1 Conduits in serial connection

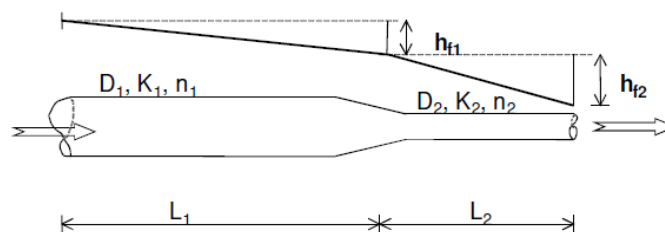


Figure 182 – Conduits in serial connection (Pinho et al., 2011).

With:

$$h_f = KQ^n$$

$$h_{fe} = \sum h_{fi} \quad \text{or} \quad K_e Q_e^{n_e} = K_1 Q_1^{n_1} + K_2 Q_2^{n_2} + \dots = \sum K_i Q_i^{n_i}$$

$$\text{for } n_i = n_j, \forall ij$$

$$K_e = K_1 + K_2 + \dots + K_n = \sum K_i$$

9.6.2 Conduits in parallel

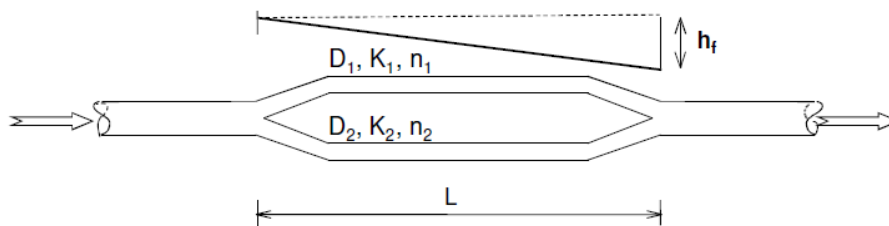


Figure 183 – Conduits in parallel (Pinho et al., 2011).

$$h_{fe} = h_{f1} = h_{f2} = h_{f3} = \dots = h_{fn}$$

$$Q_e = Q_1 + Q_2 + \dots = \sum Q_i, \text{ as } Q = \left(\frac{h_f}{K}\right)^{1/n}$$

$$\left(\frac{h_f}{K_e}\right)^{1/n_e} = \left(\frac{h_f}{K_1}\right)^{1/n_1} + \left(\frac{h_f}{K_2}\right)^{1/n_2} + \dots = \sum \left(\frac{h_f}{K_i}\right)^{1/n_i}$$

$$\text{for } n_i = n_j, \forall ij$$

$$\left(\frac{1}{K_e}\right)^{1/n_e} = \left(\frac{1}{K_1}\right)^{1/n_1} + \left(\frac{1}{K_2}\right)^{1/n_2} + \dots = \sum \left(\frac{1}{K_i}\right)^{1/n_i}$$

9.6.3 Node of conduits

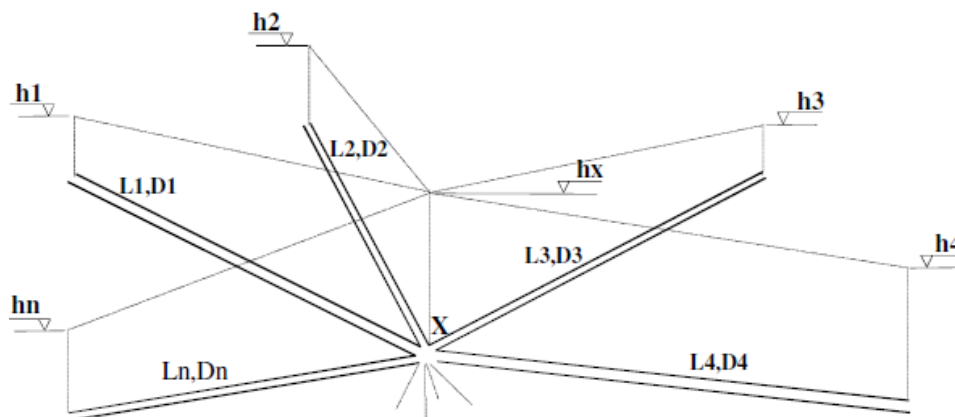


Figure 184 – Nodes of conduits (Pinho et al., 2011).

When the piezometric elevation in extremes is known, it is possible to determine the flow rate of each pipe or conduit (Pinho et al., 2011).

Usually the direction of flow is not evident or known, so any solution must include such determination (Pinho et al., 2011).

9.6.4 Web of pipes or conduits. Equation system

Charge losses

Localized losses due to singularities in flows (Pinho et al., 2011):

- Curves;
- Custom appliances;
- Valves;
- Pipes of different diameters;
- Etc.

Use of an **equivalent tube** with same **D** and equivalent length **ΔL** , such that **$h_f = \Delta L$** (Pinho et al., 2011).

Formula of Darcy-Weisbach:

$$h_f = f \frac{L U^2}{D 2g} \Rightarrow L = \frac{h_f D 2g}{f U^2} \therefore \Delta L = \frac{K_L D}{f}$$

$$K_e = \frac{a(L + \sum \Delta L)}{2gDA^2}$$

Formula of Hazen-Williams:

$$h_f = \frac{10.7L}{C_{HW}^{1.852} D^{4.87}} Q^{1.852} \therefore \Delta L = 0.00773 K_L Q^{0.148} C_{HW}^{1.852} D^{0.8703}$$

$$K_e = \frac{10.7(L + \sum \Delta L)}{C_{HW}^{1.852} D^{4.87}}$$

Equations in Q (Unknowns: Flow rate in pipes)

Flow analysis in pipeline networks are based in two laws (Pinho et al., 2011):

- **Law of Continuity:** Equations in **Nodes**

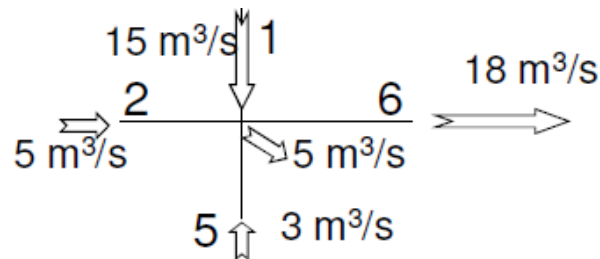


Figure 185 – Equations in Nodes (Pinho et al., 2011).

$$\sum Q_i = 0 \Rightarrow \left(\sum Q_i \right)_{\text{out}} - \left(\sum Q_i \right)_{\text{in}} = C \Rightarrow Q_6 - Q_1 - Q_2 - Q_5 = -5 \Rightarrow \\ \Rightarrow 18 - 15 - 5 - 3 = -5$$

In a system with J nodes: $(J - 1)$ Independent linear equations in Q .

- **Law of energy:** Equations in the **Meshes**

$$\sum h_{fi} = 0$$

$$\left\{ \begin{array}{l} \sum_{I=1}^I h_{fi} = 0 \\ \sum_{II=1}^{II} h_{fi} = 0 \\ \vdots \\ \sum_{L=1}^L h_{fi} = 0 \end{array} \right\} \Rightarrow \left\{ \begin{array}{l} \sum_{I=1}^I K_I Q_I^{n_I} = 0 \\ \vdots \\ \sum_{L=1}^L K_L Q_L^{n_L} = 0 \end{array} \right. \quad \text{with } h_f = KQ^n$$

In a system with L meshes (not overlapping) (natural): L independent non-linear equation in Q .

Concluding, in a system with J nodes and L natural meshes and N pipes, must satisfies the equation (Pinho et al., 2011):

$$N = (J - 1) + L$$

Notes (Pinho et al., 2011):

- If all external inputs or outputs were **unknown**, are necessary J equations in the independent nodes;
- The number of independent equations is equal to the number of unknowns (Q in N pipes);
- $J - 1$ equations of continuity are **linear**;
- L equations of energy (meshes) are **non-linear**.

An application example:

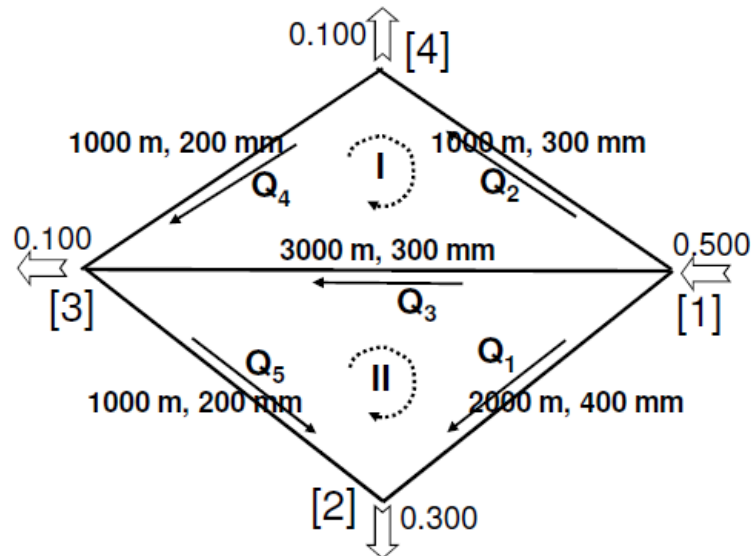


Figure 186 – Application examples of equations in Q (Pinho et al., 2011).

$$\left. \begin{array}{l} K_1 = 22 \\ K_2 = 53 \\ K_3 = 22 \\ K_4 = 53 \\ K_5 = 22 \end{array} \right\} \text{constants obtained from Hazen – William's formula}$$

The level of the represented mesh:

- N^o of pipes, **N = 5**;
- N^o of nodes, **J = 4**;
- N^o of meshes, **L = 2**.

$$\left\{ \begin{array}{l} J - 1 = 3 \text{ independent equations of continuity (linear)} \\ L = 2 \text{ energy equations (natural meshes) (non-linear)} \end{array} \right.$$

$$\text{J - 1 continuity} \left\{ \begin{array}{l} Q_1 + Q_2 + Q_3 = 0.500 \quad (1) \\ -Q_1 - Q_5 = -0.300 \quad (2) \\ -Q_3 - Q_4 + Q_5 = -0.100 \quad (3) \end{array} \right.$$

$$\text{L energy} \left\{ \begin{array}{l} -446Q_4^{1.852} - 53Q_2^{1.852} + 159Q_3^{1.852} = 0 \quad (4) \text{ (I)} \\ 22Q_1^{1.852} - 446Q_5^{1.852} - 159Q_3^{1.852} = 0 \quad (5) \text{ (II)} \end{array} \right.$$

$$Q_1 = 0.276; Q_2 = 0.132; Q_3 = 0.093; Q_4 = 0.032; Q_5 = 0.024$$

Knowing $H_i \rightarrow H_j$

Equations in **H** (Unknowns: Pressures/Piezometric elevations in nodes)

Analysis of the pressure in networks of conduits based in the **Law of Continuity** in **Nodes** (Pinho et al., 2011).

Being:

$$Q_{ij} = \left(\frac{h_{fij}}{K_{ij}} \right)^{1/n_{ij}} = \left(\frac{H_i - H_j}{K_{ij}} \right)^{1/n_{ij}}$$

Then, the equation of continuity in nodes will be:

$$\left[\sum \left(\frac{H_i - H_j}{K_{ij}} \right)^{1/n_{ij}} \right]_{\text{out}} - \left[\sum \left(\frac{H_i - H_j}{K_{ij}} \right)^{1/n_{ij}} \right]_{\text{in}} = C$$

Concluding, the problem is reduced to the resolution of a system of $(J - 1)$ non-linear equations (Pinho et al., 2011).

Following an example of application:

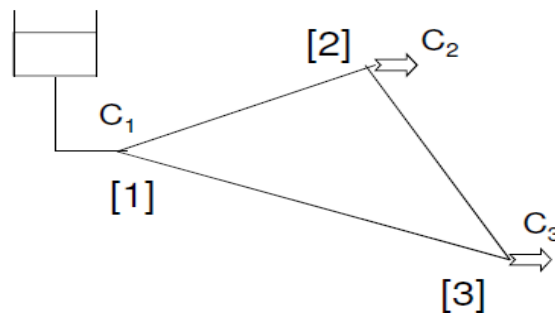


Figure 187 – Example of application of equations in H (Pinho et al., 2011).

H_1 is known and **$J - 1 = 2$** .

$$\begin{cases} Q_{12} + Q_{13} = C_1 (= C_2 + C_3) \\ -Q_{12} + Q_{23} = -C_2 \end{cases}, \text{ ou}$$

$$\begin{cases} \left(\frac{H_1 - H_2}{K_{12}} \right)^{1/n_{12}} + \left(\frac{H_1 - H_3}{K_{13}} \right)^{1/n_{13}} = C_2 + C_3 \\ - \left(\frac{H_1 - H_2}{K_{12}} \right)^{1/n_{12}} + \left(\frac{H_2 - H_3}{K_{23}} \right)^{1/n_{23}} = -C_2 \end{cases}$$

Equations in ΔQ (Unknowns: Correction of flow rate)

Analysis of the flow rate is made by an interactive solving of system of **L** natural equations, estimating flow rate in pipes, satisfying the **Law of Continuity** in the various **Nodes** (Pinho et al., 2011).

Concluding, the problem is reduced to the resolution of a system of **L** equations **non-linear** (energy) (Pinho et al., 2011).

Note: $N = (J - 1) + L > J - 1 > L$

For the resolution of this kind of problems, next method is adopted (Pinho et al., 2011):

1. Define a system of flow rate **Q_0** , that satisfies the equation of continuity in $J - 1$ nodes (also in node J);
2. Solving **L** equations of energy (mesh), the estimated flow rate does not satisfy **$\sum h_{fi} = 0$** ;
3. Adjusting the values of the estimated flow rate **Q_{0i}** with **ΔQ_L** in each mesh, will tend to **$\sum h_{fi} \rightarrow 0$** .

$$\begin{cases} \sum_i^I K_i (Q_{0i} + \Delta \vec{Q}_1)^{n_i} = 0, \text{ (charge losses in mesh I)} \\ \sum_i^{II} K_i (Q_{0i} + \Delta \vec{Q}_2)^{n_i} = 0, \text{ (charge losses in mesh II)} \\ \sum_i^L K_i (Q_{0i} + \Delta \vec{Q}_L)^{n_i} = 0, \text{ (Charge losses in mesh L)} \end{cases}$$

Following an example of application:

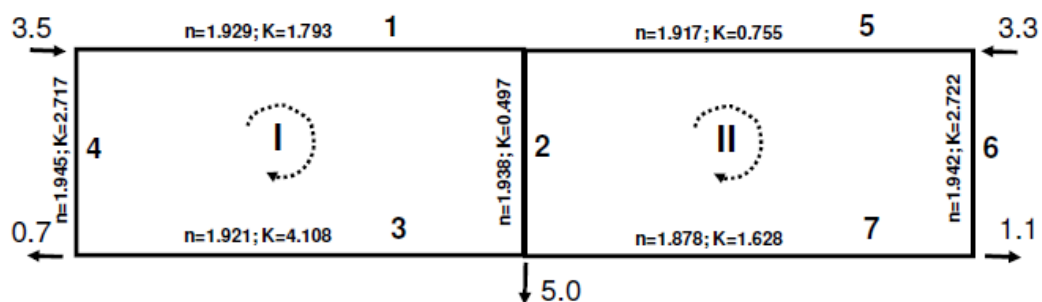


Figure 188 – Example of application in equations in ΔQ (Pinho et al., 2011).

$$Q_{01} = 1.75; Q_{02} = 3.55; Q_{03} = 1.05; Q_{04} = 1.75; Q_{05} = 1.80; Q_{06} = 1.75; Q_{07} = 1.80$$

L = 2 equations of energy (natural meshes) (non-linear):

$$\begin{cases} F_1 = 1.793(1.75 + \Delta Q_1)^{1.929} + 0.497(3.55 + \Delta Q_1 - \Delta Q_2)^{1.938} - 4.108(1.05 - \Delta Q_1)^{1.921} - 2.717(1.75 - \Delta Q_1)^{1.945} = 0 \\ F_2 = -0.755(1.80 + \Delta Q_2)^{1.917} + 2.722(1.5 + \Delta Q_2)^{1.942} + 1.628(0.4 + \Delta Q_2)^{1.878} - 0.497(3.55 - \Delta Q_2 + \Delta Q_1)^{1.938} = 0 \end{cases}$$

Obtaining:

$$\Delta Q_1 \wedge \Delta Q_2 \Rightarrow Q_i \Rightarrow h_i \Rightarrow H_i$$

Equations in ΔH (Unknowns: Corrections of pressures)

Process similar to the equations in ΔQ , by estimating of H in nodes, for which must be verified the continuity equations. The error of each mesh (ΔH) must be consider in the next iteration (Pinho et al., 2011).

9.6.5 Networks of pipes. Meshes

Linear theory method

- Computational methods, Complex systems
- Equations in Q with $N = (J - 1) + L$ equations

Newton-Raphson method

- Computational methods, Complex systems
- Equations at H with $(J - 1)$ equations
- Equations at ΔQ with L equations
- Equations at ΔH with L equations

Hardy-Cross method

- Computational methods
- Manual calculation, Simple systems
- Equations at ΔQ with L equations
- Equations at ΔH with L equations

Figure 189 – Method to solve problems involving meshes (adapted from Pinho et al., 2011).

Method of Hardy-Cross

Form the presented methods, we will focus in this method, due to the viability to hand calculation (Pinho et al., 2011).

Iterative method of Newton-Raphson:

$$x^{m+1} = x^m - \frac{F(x^m)}{\frac{dF^m}{dx}}$$

Method of Cross (applying the method of Newton-Raphson to the function ΔQ_e):

$$\left. \begin{aligned} \Delta Q_i^{m+1} &= \Delta Q_i^m - \frac{F_i^m}{\frac{dF_i^m}{d(\Delta Q_i)}} \\ F_i &= \sum K_i Q_i^{n_i} \Rightarrow \frac{dF_i}{d(\Delta Q_i)} = \sum n_i K_i Q_i^{n_i-1} \end{aligned} \right\} \Delta Q = - \frac{\sum K_i Q_i^{n_i}}{\sum |n_i K_i Q_i^{n_i-1}|}$$

Formula of Darcy-Weisbach

$$\Delta Q = - \frac{\sum K_i Q_i^2}{2 \sum |K_i Q_i|} = - \frac{\sum (h_f)_i}{2 \sum |(h_f/Q)_i|}$$

Formula of Hazen-Williams

$$\Delta Q = - \frac{\sum (K_{HW})_i Q_i^{1.852}}{1.852 \sum |(K_{HW})_i Q_i^{0.852}|} = - \frac{\sum (h_f)_i}{1.852 \sum |(h_f/Q)_i|}$$

Following an application example:

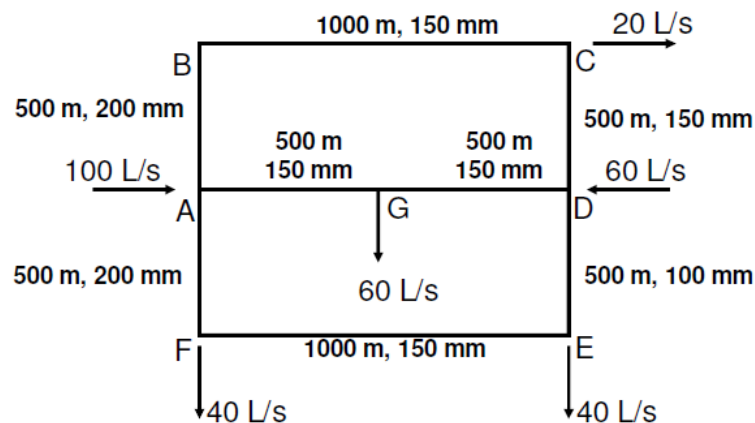


Figure 190 – Example of application of the method Hardy-Cross (Pinho et al., 2011).

1st step: arbitrary values for the flow rate of the pipes are assumed while satisfying the continuity equation for each node.

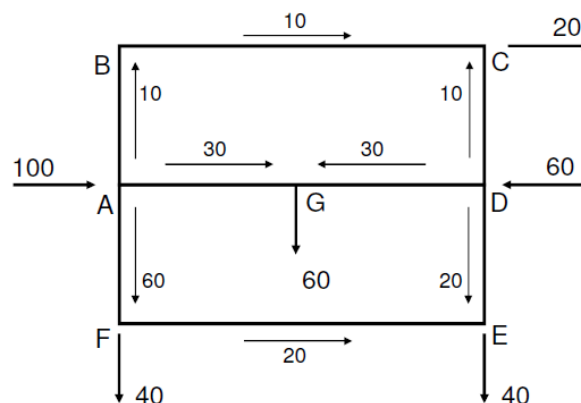


Figure 191 – Arbitration of flow rate (Pinho et al., 2011).

2nd step: successively calculate for the different mesh, the correction of Flow rate ΔQ_i , correcting the flow rate in the common tubes or pipes of the different meshes **consistently**. Can be presented a calculus schema as follows, until $\Delta Q_m \approx 0$ (Pinho et al., 2011):

Table 31 – Resume of the calculations (adapted from Pinho et al., 2011).

Section	L	D	K_{HW}	$K_{HWi} = \frac{10.7L}{C_{HWi}^{1.852} D_i^{4.87}}$			$h_{fi} = K_{HWi} Q_i^{1.852}$			$\Delta Q = -\frac{\sum(h_f)_i}{1.852 \sum (h_f/Q)_i }$	
				1 st iteration			2 nd iteration			Final iteration	
				Q [L/s]	h_f	$\frac{h_f}{Q}$	Q [L/s]	h_f	$\frac{h_f}{Q}$	Q [L/s]	h_f
A-B	500	200	1438	10	0.28	28	9.19	0.24	26	7	0.15
B-C	1000	150	11673	10	2.31	231	9.19	1.97	215	7	1.19
C-D	500	150	5837	-10	-1.15	115	-10.81	-1.33	123	-13	1.88
D-G	500	150	5837	30	8.83	294	32.02	9.96	311	31	9.38
G-A	500	150	5837	-30	-8.83	294	-27.98	-7.76	277	-29	8.29
				$\Sigma =$	1.44	963	$\Sigma =$	3.08	953		
				$\Delta Q =$	-8.1E-04		$\Delta Q =$	-1.75E-03			
A-G	500	150	5837	30	8.83	294	27.98	7.76	277	29	8.29
G-D	500	150	5837	-30	-8.83	294	-32.02	-9.96	311	-31	9.38
D-E	500	100	42046	20	30.01	1500	17.17	22.62	1317	16	19.85
E-F	1000	150	11673	-20	-8.33	417	-22.83	-10.64	466	-24	11.68
F-A	500	200	1438	-60	-7.85	131	-62.83	-8.55	136	-64	8.85
				$\Sigma =$	13.83	2636	$\Sigma =$	1.23	2508		
				$\Delta Q =$	-2.83E-03		$\Delta Q =$	-2.64E-04			

3rd step: determination of the pressures in nodes of the network.

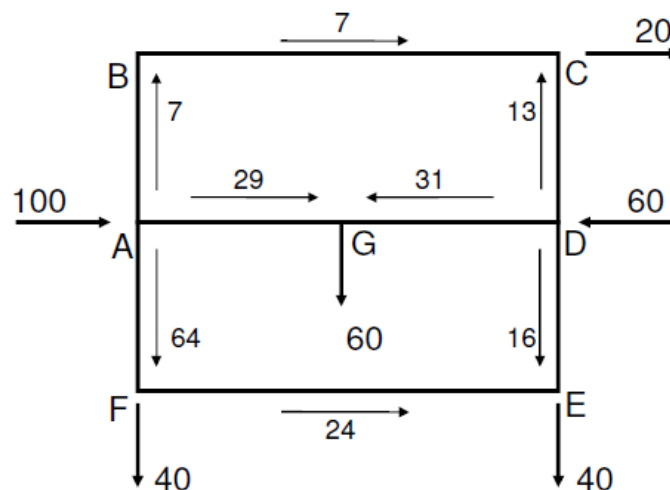


Figure 192 – Determination of the pressures in nodes of the network (Pinho et al., 2011).

Table 32 – Pressures in network nodes (Pinho et al., 2011).

Node		A	B	C	D	E	F	G
Pressure*	[m]	58.85	58.70	57.51	59.39	39.54	50.00	51.78
	[kPa]	588.5	587.0	575.1	593.9	395.4	500.0	517.8

*1 kPa = 10⁻¹ m

9.6.6 Networks of pipes or conduits. Dispositive of control of pressures and flow rate in networks

Devices that conditions **Q** and **Piezometric Elevations** (Pinho et al., 2011):

- Reservoirs;
- Retention Valves;
- Hydraulic Pumps;
- Orifices;
- Reduction of Pressures Valves.

Reservoirs

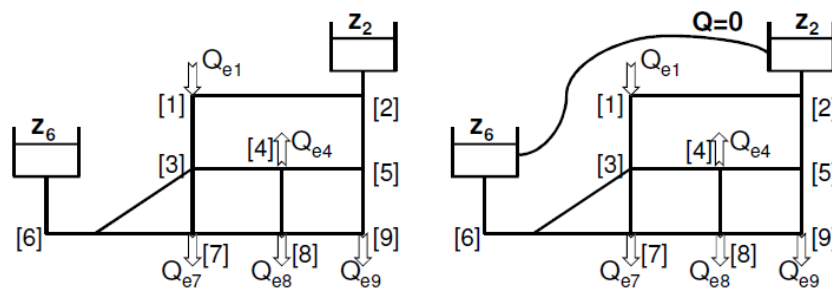


Figure 193 – Reservoir of control of pressures and flow rate (Pinho et al., 2011).

At such situation: (Pinho et al., 2011):

- Equations in **H** and **ΔH**
 - Piezometric Elevation (**Z**) defined in nodes;
- Equations in **Q** and **DQ**
 - 1 Reservoir: Piezometric Elevation defined in one node;
 - More than 1 Reservoir: Creation of a **virtual mesh**, starting from **virtual pipes** with **$Q_i = 0$** .

Retention Valves

The **retention valves** (Figure 194) are valves that allows flows in only one direction, and its close automatically if the direction change (Pinho et al., 2011).

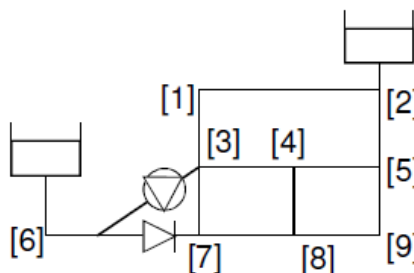


Figure 194 – Retention valve (Pinho et al., 2011).

Mathematical Treatment (Pinho et al., 2011):

- Start the calculus ignoring valves;
- In successive iteration it is verified if:
 - Downstream pressure > Upstream: the tube is eliminated from the next iteration;
 - Downstream pressure < Upstream: the tube is considered in the next iteration as if no exists a retention valve;
- The operation conditions must be verified in all iterations, being possible to modify at different time in the convergence process.

Hydraulic pumps

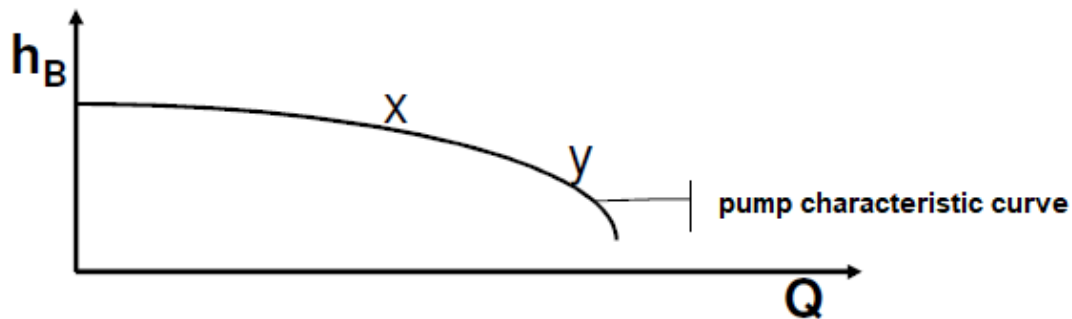


Figure 195 – Characteristic curve of the pump (Pinho et al., 2011).

Mathematical treatment (Pinho et al., 2011):

- Characteristic curve of the pump (quadratic):
 - $h_B = AQ^2 + BQ + H_0$, with A, B, H_0 constants taken from the characteristic curve with $A < 0$;
- Trying to adjust the exponential equation:
 - $h_B = \chi Q^{-\delta}$, with $\delta \approx 0.5$;
- As $\delta \neq 2$ (Formula of Resistance), do next variables changes:
 - $G = Q + B/A$;
- them:
 - $h_B = AG^2 + h_0$, with $h_0 = H_0 - B^2/(4A)$.

Valves for pressure reduction (VPR)

Being:

H_i the piezometric elevation in node i ;

H_j the piezometric elevation in node j ;

H_R the piezometric elevation corresponding to the regulation of the valve;

H_C the piezometric elevation calculated in the section that contains the VPR.

Different modes of VPR operations (Pinho et al., 2011):

- $H_C > H_R \wedge H_i > H_j$, downstream pressure of VPR $H_C = H_R$, normal situation;

- $H_C < H_R \wedge H_i > H_j$, **VPR** does not work and acts as any singularity with a localized charge loss;
- $H_i < H_j$, **VPR** gets closed working as a retention valve and $Q_{ij} = 0$.

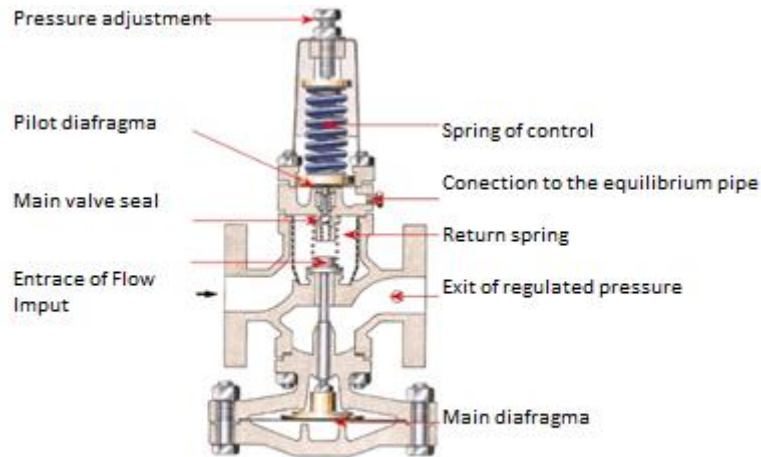


Figure 196 – Pressure reduction valve (<http://www.vaportec.com.br>).

Following an example of application:

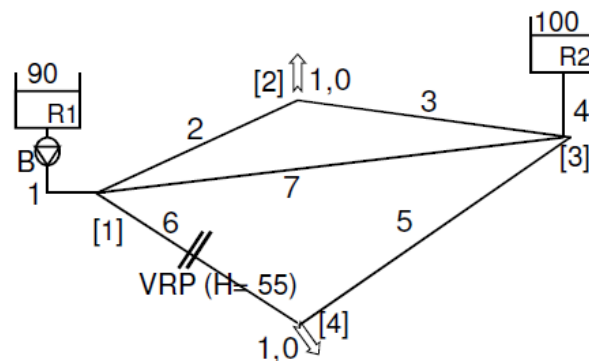


Figure 197 – Example of a network of pipes with regulating devices (Pinho et al., 2011).

Resolution of equations in terms of **Q** (Pinho et al., 2011):

- **J** Eq. of Continuity in nodes:
$$\begin{cases} -Q_1 + Q_2 + Q_6 + Q_7 = 0 \\ -Q_2 - Q_3 = -1 \\ Q_3 - Q_4 + Q_5 - Q_7 = 0 \\ -Q_5 - Q_6 = -1 \end{cases};$$
- Eq. Real Mesh: $-K_2 Q_2^{n_2} + K_3 Q_3^{n_3} + K_7 Q_7^{n_7} = 0$;
- Eq. Virtual Mesh-Res.: $-K_4 Q_4^{n_4} + K_7 Q_7^{n_7} + K_1 Q_1^{n_1} + A_1 G_1^2 = 100 - 90 - h_{01}$;
- Eq. of Transformation: $G_1 - Q_1 = (B/2A)_1$;
- Eq. Virtual Mesh-VPR: $-K_6 Q_6^{n_6} + K_5 Q_5^{n_5} + K_4 Q_4^{n_4} = 55 - 100$;
- **Note:** $\sum K_i Q_i^{n_i} \pm \sum h_B = \Delta H$;
- **Nº of equations:** **7** (+1 for a solution of the linear equation of the pump).

9.7 Varied movement in conduits

9.7.1 Charge losses in a varied movement

Consider a tube with route distribution (Pinho et al., 2011):

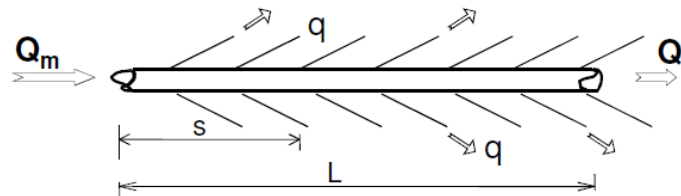


Figure 198 – Pipe with route distribution (Pinho et al., 2011).

$$q = \frac{Q_m - Q_j}{L} \quad \text{or} \quad Q_m = Q_j + qL$$

$$Q(s) = Q_m - qs \quad \text{or} \quad Q(s) = Q_j + q(L - s)$$

Where:

q is the unitary flow rate of the route [L/s.m];

qL is the flow rate of the route [L/s].

Considering only (Pinho et al., 2011):

- $\Delta h = h_f (\sum h_L = 0)$;
- $D = \text{cst.}$;
- Rough Turbulent Regime (f independent of Re).

Then:

$$H_m - H_j = \frac{8f}{\pi^2 g D^5} \int_0^L [Q_j + q(L - s)]^2 ds$$

Integrating:

$$H_m - H_j = \frac{8f}{\pi^2 g D^5} \left(Q_j^2 + Q_j qL + \frac{1}{3} q^2 L^2 \right)$$

Considering a uniform flow with same total charge losses between **m** and **j**, with a corresponding equivalent flow rate (Q_e), will be (Pinho et al., 2011):

$$H_m - H_j = \frac{8f Q_e^2}{\pi^2 g D^5}$$

$$Q_e = \sqrt{Q_j^2 + Q_j qL + \frac{1}{3} q^2 L^2}$$

Transforming a problem of Varied Regime into a problem of Uniform Regime (Pinho et al., 2011).

Conclusions about charge losses ($h_f = H_m - H_j$) (Pinho et al., 2011):

- The piezometric line is a parabola;
- In the pipes with route services ($Q_j = 0$), h_f is a **1/3** of the height that could exists in a uniform movement for **$Q = qL$ ($= Q_m$ at this case).**

As Q_e is non-linear and considering (Pinho et al., 2011):

$$\left(Q_j + \frac{qL}{2}\right)^2 < Q_e^2 < \left(Q_j + \frac{qL}{\sqrt{3}}\right)^2$$

Bresse proposed:

$$Q_e = Q_j + 0.55qL$$

For the analysis of a branched network, without verifying continuity in nodes, can be write (Pinho et al., 2011):

$$\left| \sum_K (Q_{ki})_j \right| + Q_{ei} = \left| \sum_I (Q_{li})_m \right|$$

9.7.2 Problems of varied movement in conduits

Considering the following example of application:

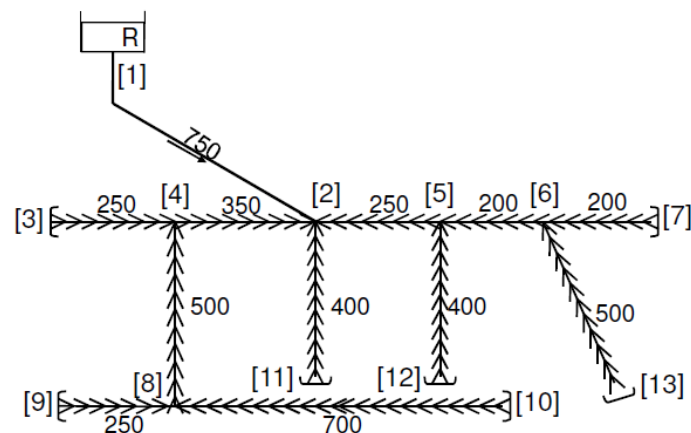


Figure 199 – Example of a problem involving varied movement in conduits (Pinho et al., 2011).

$$Q_p = 8 \text{ L/s}$$

$$q = \frac{Q_p}{\sum L_{ij}} = \frac{8}{4000} = 0.002 \text{ L/s.m}$$

Table 33 – Calculus of flow rate (adapted from Pinho et al., 2011).

Conduit	L	Q [L/s]			
	[m]	Upstream	Route	Downstream	Equivalent
1-2	750	8.00	0.00	8.00	8.00
2-4	350	4.10	0.70	3.40	3.79
4-3	250	0.50	0.50	0.00	0.28
4-8	500	2.90	1.00	1.90	2.45
8-9	250	0.50	0.50	0.00	0.28
8-10	700	1.40	1.40	0.00	0.77
2-11	400	0.80	0.80	0.00	0.44
2-5	250	3.10	0.50	2.60	2.88
5-12	400	0.80	0.80	0.00	0.44
5-6	200	1.80	0.40	1.40	1.62
6-7	200	0.40	0.40	0.00	0.22
6-13	500	1.00	1.00	0.00	0.55

CHAPTER 10 - PERMANENT FLOW IN CONDUITS CONDITIONED BY HYDRAULIC MACHINES

10.1 Hydraulics Turbines

In order to understand the concept of **turbine**, it is necessary to understand the concept of **turbomachines**: machines that transfer energy between a flowing fluid and an impeller or rotor, by the dynamic action of a group of blades that rotate continuously with the rotor (Mata-Lima, 2010). **Note**: the **helix from propeller** (aircraft or naval), that are made to create a propulsion force, are also classified as turbomachines (Mata-Lima, 2010).

So, a **turbine**, a motive turbomachine which extract energy from the fluid and supply energy to an external by a rotative axis or transmission axis. Ex.: **Hydraulics turbines**, from steam to gas, winds farms (Mata-Lima, 2010).

The **hydraulics turbines installed in a hydroelectrical central** allows the conversion of flows energy into mechanical rotation (potential energy and kinetic energy of the fluid to exclusively kinetic energy of the rotator), which will be converted to electrical energy by a generator (Cruz, 2006). The energy conversion in turbine is based in the conservation of energy principles and the amount of movement (angular) (Cruz, 2006).

10.1.1 Characteristic of operation

Types of turbines

Action turbines (of Impulsion) are tangential turbines, **actioned by water at atmospheric pressure**, like in the case of a **Pelton turbine** (Figure 200) (Braga, 2014):

- So, such turbine operates at atmospheric pressure. It is constituted by a wheel and one or more injectors, that transform the pressure energy in to kinetics energy. As soon as the jets of water hits the blades of the impeller, generate an impulsion producing movement;
- There can be from one to six injectors (although the normal minimum is two);
- The injectors have a **needle** that allows to regulate the water, decreasing the flow rate when necessary. It also has a **deflector** that can deviate the direction of the jet (such deflector usually points directly to the wheel extremity);
- It is more useful for big useful falls;
- Operate with major rotation velocities of the rotor axis;
- Can operate with a wide gamma of flow rate, without losing efficiency;
- It can suffer erosion when waters are not well clean or have detritus, due to the force of impact of the jet, that makes the detritus or sand works as a lime;
- Such kind of turbines helps to avoid high pressures.

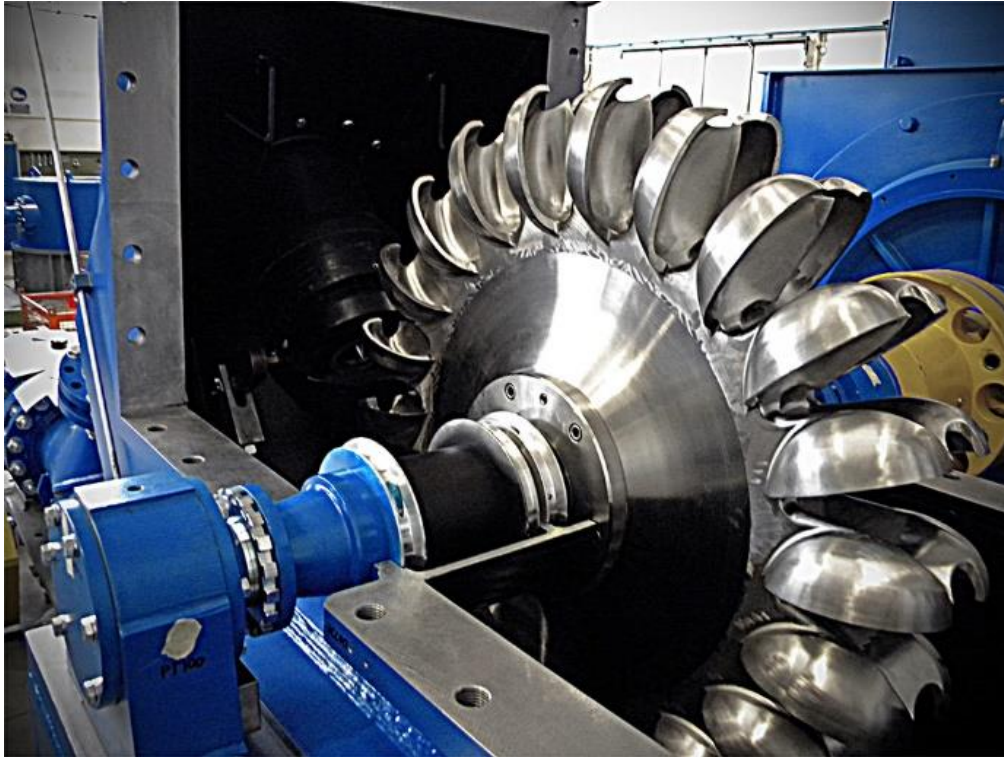


Figure 200 – Pelton Turbine (<https://www.zeco.it>).

Reactions Turbines refers to radial turbines, axial and mixed (or diagonals), that works in conditions of **flows under pressure** (Braga, 2014).

Radial Turbomachines usually the stream lines inside the impeller are majorly located in perpendicular planes to the rotation axis, as in the case of the **Francis turbine** (Figure 201) (Braga, 2014):

- The radials turbines work with an outcoming flow of water. The water under pressure comes in through a spiral pipe of decreasing transversal section, being deviated by a set of static blades of the distributor to a central rotor. The water crosses the lateral wall of the rotor, pushing the set of blades of the impeller and then spill out through the base with reduced velocity and pressure;
- It was created by Jean-Victor Poncelet in 1820 and improved by the north American engineer James Francis in 1849;
- The statics blades can be adjusted;
- Are the most used due to its flexibility and efficiency;
- Operates with falls from 10 until 650 m, with a velocity of 80 to 1000 rpm;
- It is not necessary a big structure for it as in a Pelton Turbine, which means lower expenses in concreting and excavation;
- The diffusor usually has a decreasing section to promote energy recovering from kinetics and pressure energy;
- The flow rate is greater as major are the guidelines opening.



Figure 201 – Francis Turbine (<https://hydrotu.en.ec21.com>).

Axial Turbomachines the stream line are located approximately in cylindrical surfaces of revolution, and the radial component of velocity is relatively small, like in the case of a **Kaplan turbine** (Figure 202 and Figure 203) (Braga, 2014):

- An axial turbine, according to the fluid's movement in relation of the respective wheel or impeller. It is like a propeller of a ship (helix), which have a system of blades servo-controllable by and hydraulic system of oil under pressure connected to a servo motor;
- It was created by the Austrian engineer Victor Kaplan that, starting from theoretical and experimental studies, create a new type of turbine of helix, that allows to change or vary the pitch of the rotor blades and of the distributor;
- Applied in small falls (till 50 m) and in great volumes of water;
- The action of the blades made by a pumping system located outside of the turbine and united to the blades of the distributor, so that depending in the distributor opening, correspond to a declination value of the rotor blades;
- Are highly efficient (until 94%).



Figure 202 – Kaplan Turbine (<https://www.zeco.it>).



Figure 203 – Kaplan Turbine (bulb) (<https://www.zeco.it>).

Mixed Turbomachines the stream lines in the wheel are approximately in surfaces of revolution that are far away from the other cases. As an example, **Dériaz turbine** (Figure 204) (Braga, 2014):

- His name is given in honour to the inventor, a swiss engineer;
- Such turbines are similar to Kaplan and Francis; thus, the blades of the rotor are articulated and can vary its angle of inclination due to a mechanism;
- This kind of turbine is usually used in systems, that needs to recover water at an upstream reservoir, when it is not producing power. Giving the name in some cases of Turbine-pump.



Figure 204 – Dériaz Turbine (<http://www.directindustry.com/>).

10.1.2 Operation of integrated turbines at installations

Consider Figure 205 which shows a hydraulic circuit between two reservoirs, composed by a pipe or conduit and a **singularity (T)**, where occurs an **abrupt hydraulics charge variation (ΔE)** (Cruz, 2006).

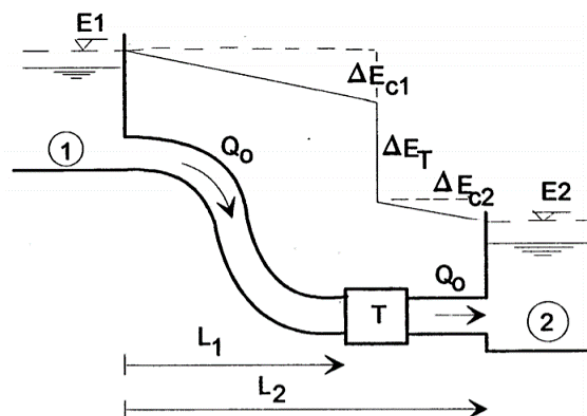


Figure 205 – The loss of charge ΔE_T at a singularity that can be converted in a useful fall at a turbine (Cruz, 2006).

When the energy lines are known in upstream and downstream sections, as well as the continuous and localized loss charges along the pipe or conduit, between section 1 and the singularity T, and between it and the section 2, then the principle of energy conversion (Bernoulli's theorem) allows to deduce next equation (Cruz, 2006):

$$E_1 - \sum_{i=1}^N \Delta E_{c1} - \Delta E_{c2} - \Delta E_T = E_2$$

Where:

E_1, E_2 represents the hydraulics charges in sections 1 and 2;

ΔE_1 is the localized charge losses along the pipe;

$\Delta E_{c1}, \Delta E_{c2}$ represents the continuous charge losses along the pipe;

ΔE_T is the charge loss of the singularity T.

The **hydraulic charge** is defined by (Cruz, 2006):

$$E = \frac{P}{\gamma} + z + \frac{v^2}{2g}$$

At such situation, the **charge loss (ΔE_T)** depends of **differential of elevations ($E_1 - E_2$)**, between the upstream and downstream reservoirs and the total charge losses along the pipe (Cruz, 2006):

$$\Delta E_T = E_1 - E_2 - \Delta E_{c1} - \Delta E_{c2} - \sum_{i=1}^N \Delta E_{l1}$$

When the **flow rate in permanent regime (Q_o)** is known, the **power dissipated in singularity (T)** is the next one (Cruz, 2006):

$$P_T = \gamma Q_o \Delta E_T$$

being γ the volumetric weight of the liquid. Such power is completely transformed in outcoming heat or temperature variation of the liquid (Cruz, 2006).

In order to exploit such power in a mechanical useful form for energy conversion to produce electrical energy, it is necessary to make the flows power transfer its energy to a rotating mechanism that constitute a resistance. Then, by replacing the dissipating singularity (**T**) by an adequate turbomachine (with a wheel in an axis), the acting hydraulic binary will allow the desire transfer of power with minimal losses in the machine. Such **losses** will be **characterized by the turbine efficiency (η_T)** (Cruz, 2006).

Then, the power supplied by the turbine is (Cruz, 2006):

$$P_T = \eta_T \gamma Q_o H_U$$

Being **H_U** , the variation of hydraulic charge between the upstream and downstream section of the turbine (Figure 206) (Cruz, 2006).

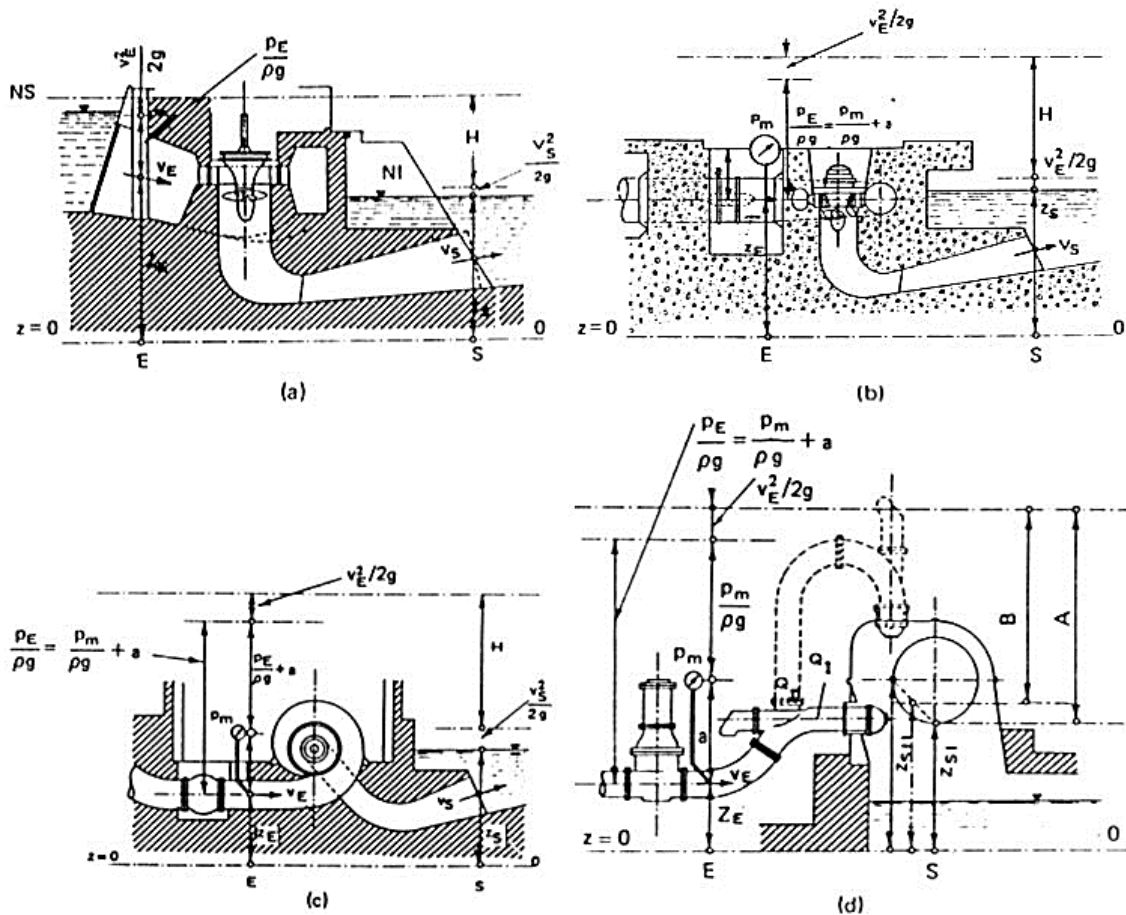


Figure 206 – Examples of the definition of useful falls H in Kaplan (a), Francis (b), of horizontal axis (c) and Pelton (d) turbines (Cruz, 2006).

Theorems and equations of Euler

The hydraulic binary acting in the turbine wheel can be calculated from the principle of conservation of amount of angular movement (**Theorem of Euler of moments**). Basic hypothesis (Figure 207) (Cruz, 2006):

- The fluid behaves as incompressible;
- The distribution of velocities at the input and output of the impeller or wheel is uniform.

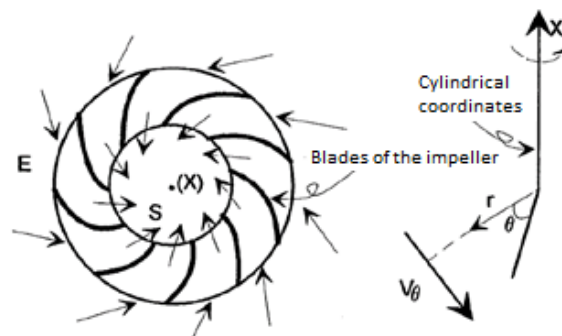


Figure 207 – Euler Theorem applied to a control volume contained in an impeller/wheel of a turbine (Cruz, 2006).

By assuming the plain of the impeller or wheel is in a plain YZ and the axis of rotation has a direction XX, the application of the principle of conservation of the amount of angular movement according X, in cylindrical coordinates, leads to (Cruz, 2006):

$$T_{Xi} = \frac{\check{Z}}{\check{Z}t} \int_{Vc} \rho \omega_X dV - \rho Q V_{\theta E} r_E + \rho Q V_{\theta S} r_S$$

or

$$-T = \int_{Vc} \frac{\check{Z} V_{\theta}}{\check{Z}t} r dV - \rho Q V_{\theta E} r_E + \rho Q V_{\theta S} r_S$$

Where:

T_{Xi} is a generic acting binary with an axis respect X;

T the hydraulic binary acting in the impeller or wheel;

r_E, r_S are the radius of the circumferences at input and output of the wheel or impeller (the indices of E and S indicate the input and output).

In **permanent regime** is obtained (Cruz, 2006):

$$T = \rho Q (V_{\theta E} r_E - V_{\theta S} r_S)$$

It is usual to use next designations:

$$V_{\theta E} = V_1 \cos \alpha_1$$

$$V_{\theta S} = V_2 \cos \alpha_2$$

$$r_E = r_1$$

$$r_S = r_2$$

Obtaining the next general equation for the acting binary in the impeller:

$$T = \rho Q (V_1 r_1 \cos \alpha_1 - V_2 r_2 \cos \alpha_2)$$

Where:

T is the hydraulic binary acting in the impeller or wheel [Nm];

ρ is the volumetric mass of the liquid [kg/m³] - (for water, = 1000 kg/m³);

Q is the flow rate of the turbine [m³/s];

V_1, V_2 is the velocity (absolute) of flow, respectively in the input and output of the wheel or impeller [m/s];

r_1, r_2 is the radius of the impeller (wheel), with center in the group axis, respectively in the input and output of the flow [m];

α_1, α_2 is the angle between the absolute velocities of flow with peripheral velocity of the wheel at input and output of it.

Remember that the **hydraulic charge transferred by the flow to the impeller or wheel**, or **useful fall of the wheel** (H_{UR}), corresponding to the energy per unit of liquid weight, then the power transferred to the wheel by the flow obey the next expression (Cruz, 2006):

$$T\omega = \rho g Q H_{UR}$$

Where:

ω is the angular velocity of the wheel or impeller [rad/s];

g is gravitational acceleration (9.8 [m/s²]);

H_{UR} is the useful fall in the wheel or impeller [m].

And by following next relations valid for a rigid body in rotation around an axis (Cruz, 2006):

$$\begin{cases} \omega r_1 = c_1 \\ \omega r_2 = c_2 \end{cases}$$

It is obtained next expression (**1st Form of Euler's Equation**) for the useful fall of the wheel (Cruz, 2006):

$$H_{UR} = \frac{V_1 C_1 \cos \alpha_1 - V_2 C_2 \cos \alpha_2}{g}$$

The Theorem of Euler is applied to a volume of control with an angular velocity ω , being valid next vectorial relations (Cruz, 2006):

$$\vec{V} = \vec{C} + \vec{W} \rightarrow \text{General vectorial expression}$$

Where:

\vec{V} is the absolute velocity of flow;

\vec{C} if the peripheral velocity of the wheel;

\vec{W} is the relative velocity of flow.

A general vectorial expression, when applied at the input and output of the wheel, can be characterized geometrically by triangles of velocities (Figure 208) (Cruz, 2006).

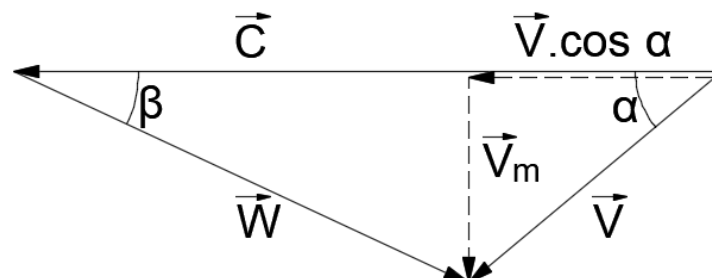


Figure 208 – Triangle of velocities (adapted from Cruz, 2006).

Based in those triangles, next identities can be written:

$$V \sin \alpha = W \sin \beta \equiv V_m$$

$$V \cos \alpha = C + V \cos \beta$$

Being β the angle of relative velocity \vec{W} with the velocity \vec{C} .

Are also valid next identities:

$$V_m^2 = V^2 - V^2 \cos^2 \alpha$$

$$V_m^2 = W^2 - (C - V \cos \alpha)^2$$

And by replacing,

$$V^2 - V^2 \cos^2 \alpha = W^2 - C^2 - V^2 \cos^2 \alpha + 2CV \cos \alpha$$

Where:

$$CV \cos \alpha = \frac{V^2 + C^2 - W^2}{2}$$

Applying the last equation to the triangles of the input and output:

$$C_1 V_1 \cos \alpha_1 = \frac{V_1^2 + C_1^2 - W_1^2}{2}$$

$$C_2 V_2 \cos \alpha_2 = \frac{V_2^2 + C_2^2 - W_2^2}{2}$$

And by also introducing the expression of useful fall (H_{UR}) it is obtained the **2nd Form of Euler's Equation** (Cruz, 2006):

$$H_{UR} = \frac{V_1^2 - V_2^2}{2g} + \frac{C_1^2 - C_2^2}{2g} + \frac{W_2^2 - W_1^2}{2g}$$

The useful fall in the impeller (wheel), can be decomposed in the next terms (Cruz, 2006):

$$\frac{V_1^2 - V_2^2}{2g} = \text{Component of kinetic transfer;}$$

$$\frac{C_1^2 - C_2^2}{2g} + \frac{W_2^2 - W_1^2}{2g} = \text{Component of static transference or pressure component;}$$

$$\frac{C_1^2 - C_2^2}{2g} = \text{Resultant component of the centrifugal effects.}$$

The relative importance of each component of H_{UR} depends on the **type of turbine** (Cruz, 2006). **Example:** in action turbines (Pelton) only exists the first component (Cruz, 2006).

Hydraulic efficiency

When the hydraulic charge variation between the input and the output sections of the turbine, the useful fall in the turbine of H_U , the **hydraulic efficiency (η_H)** is defined in the next form (Cruz, 2006):

$$\eta_H = \frac{H_{UR}}{H_U}$$

The useful fall (H_U) is obtained by hydraulic calculations of circuit dimensioning. The local of the sections of input (E) and output (S) of the turbine for the calculus of H_U is defined by international standards (check an example at Figure 206 for Kaplan, Francis, of horizontal and vertical axis, and Pelton turbines) (Cruz, 2006).

The hydraulic efficiency represents the internal hydraulics losses (resistance in solid walls, turbulence, impact in blades) (Cruz, 2006).

In the case of Pelton turbines with a vertical axis or a horizontal axis, with an injector, the useful drop is calculated based on the jet axis dimension (Cruz, 2006):

$$H_{U1} = \frac{P_E}{\gamma} + \frac{V_E^2}{2g} + Z_E - Z_S$$

In case of the Pelton's turbines of horizontal axis with two injectors, the useful fall is calculated following the next expression that ponders the elevation differences of the points where contact of the jets with the blades of the impellers take place (check Figure 206) (Cruz, 2006):

$$H_{U2} = \frac{Q_I}{Q_I + Q_{II}} (Z_E + a - Z_{SI}) + \frac{Q_{II}}{Q_I + Q_{II}} (Z_E + a - Z_{SII}) + \frac{P_m}{\gamma} + \frac{V_E^2}{2g}$$

Having in count the 1st form of Euler's equation, it is obtained the following expression for hydraulic efficiency (Cruz, 2006):

$$\eta_H = \frac{V_1 C_1 \cos \alpha_1 - V_2 C_2 \cos \alpha_2}{g H_U}$$

The designer of the turbine must maximize η_H . The typical values of η_H are in the order of 0.90 to 0.96 (Cruz, 2006).

Example: for turbines of Pelton (action turbines) is possible to deduce an analytical expression for hydraulic efficiency (Cruz, 2006):

- **Useful fall in the wheel**
 - 2nd form of Euler's Equation

$$(1): H_{UR} = \frac{V_1^2 - V_2^2}{2g}$$

Attending to $C_1 = C_2 = C$, it is concluded that:

$$\frac{W_2^2 - W_1^2}{2g} = 0 \wedge W_2 = W_1 = W$$

- 1st form of the Euler's Equation

$$H_{UR} = \frac{C}{g} (V_1 \cos \alpha_1 - V_2 \cos \alpha_2)$$

Attending to $\alpha_1 = 0$ and $V_1 = C_1 + W_1$,

$$V_1^2 = C_1^2 + W_1^2 + 2C_1W_1$$

$$V_2^2 = C_2^2 + W_2^2 - 2C_2W_2 \cos \beta$$

And knowing that $C_1 = C_2 = C$ and $W_1 = W_2 = W$,

$$V_1^2 - V_2^2 = 2CW(1 + \cos \beta)$$

And replacing in (1):

$$H_{UR} = \frac{CW}{g} (1 + \cos \beta)$$

- **Hydraulic efficiency**

$$\eta_H = \frac{H_{UR}}{H_U} = \frac{2CW(1 + \cos \beta)}{V_1^2}$$

Assuming that:

$$V_1 = \sqrt{2gH_U} \wedge W = V_1 - C$$

It is obtained:

$$\eta_H = 2 \left[\frac{C}{V_1} - \left(\frac{C}{V_1} \right)^2 \right] (1 + \cos \beta)$$

Being the hydraulic efficiency of the Pelton's turbine maximal for $C/V_1 = 0.5$ (peripheral velocity for the impeller or wheel = 0.5 of the fluid's jets velocity):

$$\eta_H = 0,5(1 + \cos \beta)$$

Total efficiency

The total efficiency of a turbine involves hydraulics losses and other related resultant power losses of (Cruz, 2006):

- **Volumetric losses** or flow rate losses ($\eta_V = 0.98$ a 0.995);
- **Mechanical friction losses** (in rollers), ($\eta_m \geq 0.98$);
- **Losses by air resistances** (η_r).

The total efficiency will be:

$$\eta_T = \eta_H \eta_V \eta_m \eta_r$$

The maximum value of η_T , for optimal conditions or for better efficiency, (flow rate, drop or fall and rotation velocity fixed) depends in the type of turbine. The value of efficiency can vary for different values of useful fall, flow rate, power and rotation velocity (examples in Figure 209, Figure 210 and Figure 211) (Cruz, 2006).

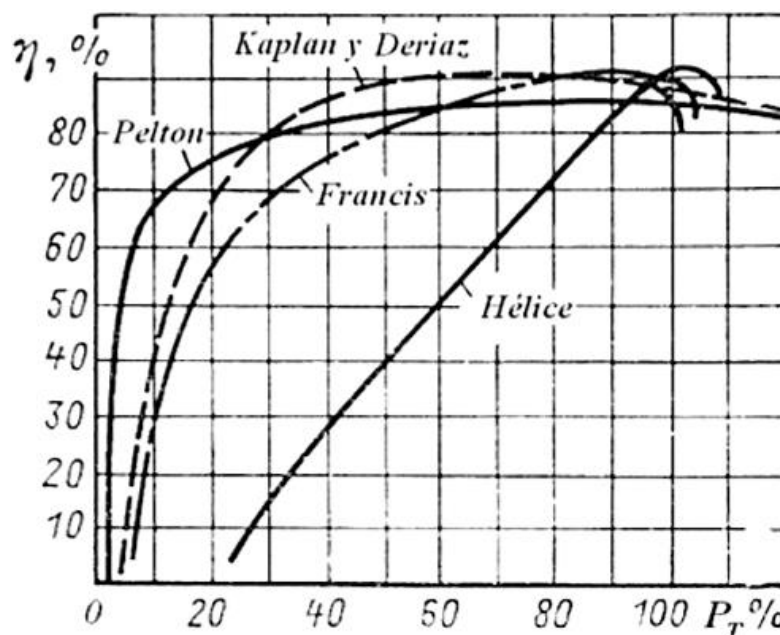


Figure 209 – Efficiency versus power (https://pt.slideshare.net/buti_81/hidraulica-turbinas).

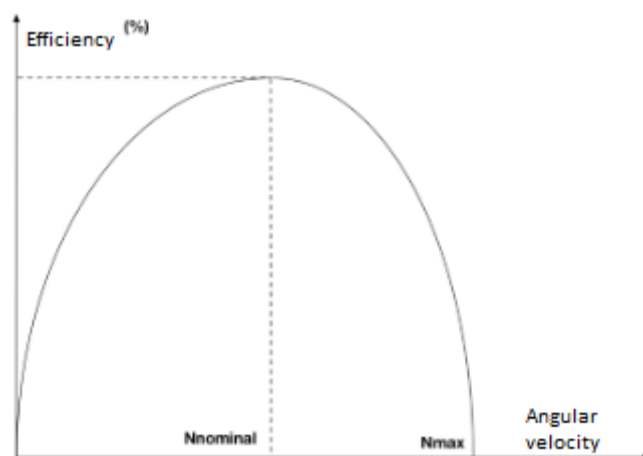


Figure 210 – Variation of efficiency with rotation velocity (<http://www.antonioquilherme.web.br.com>).

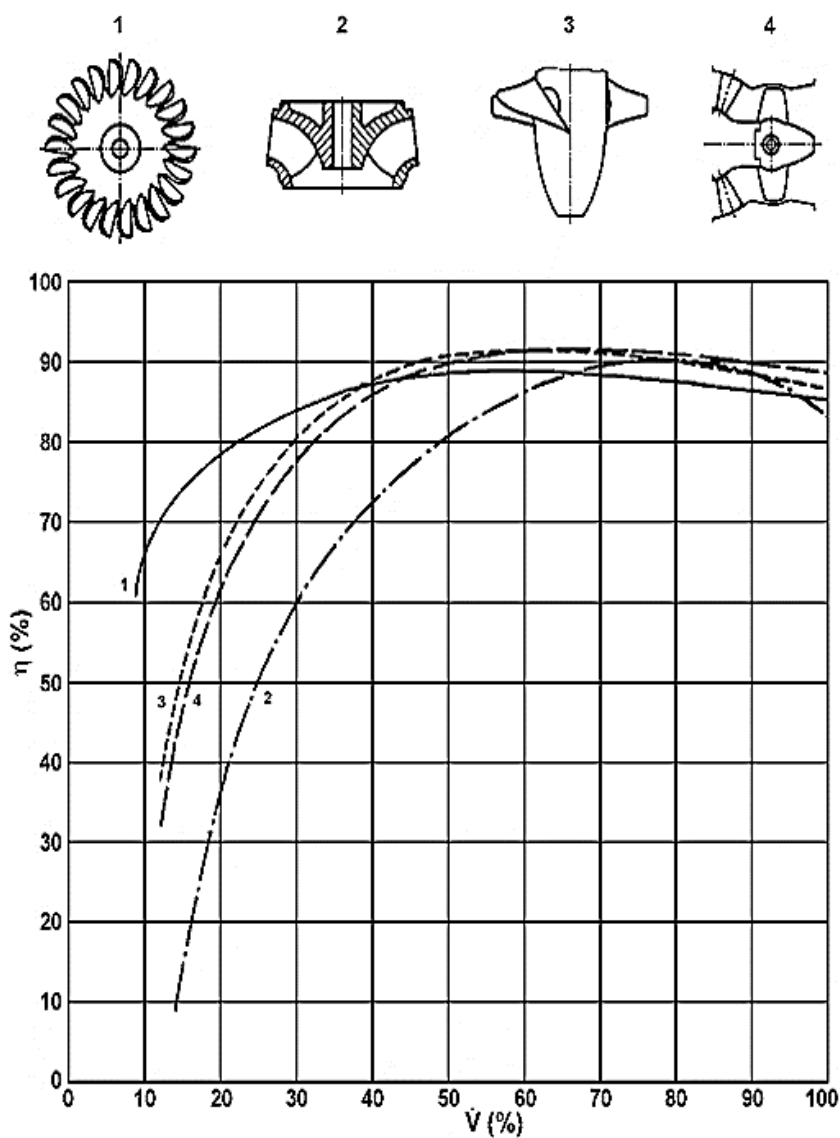


Figure 211 – Efficiency/flow rate for turbines: (1) Pelton, (2) Francis, (3) Kaplan, (4) Bulb (Cruz, 2006).

In design or planning studies (economic analysis and optimization of exploit) of hydroelectric uses, the variation of efficiency must be considered. The efficiency conditions the operation of a turbine: under a certain limit, the turbine must not work (Cruz, 2006).

The global efficiency of the central includes turbines, generators, transformers and connections to web efficiency (Cruz, 2006).

Grade of reaction of turbines

Designed as **grades of reaction of turbines**, to the ratio between the static component of H_{UR} and the value of H_{UR} (Cruz, 2006):

$$\varepsilon = \frac{\frac{C_1^2 - C_2^2}{2g} + \frac{W_2^2 - W_1^2}{2g}}{\frac{V_1^2 - V_2^2}{2g} + \frac{C_1^2 - C_2^2}{2g} + \frac{W_2^2 - W_1^2}{2g}}$$

Applying the Bernoulli's Theorem between the input and the output sections of the impeller or wheel, it is obtained:

$$H_{UR} = \frac{V_1^2 - V_2^2}{2g} + Z_1 - Z_2 + \frac{P_1 - P_2}{\gamma}$$

Being $Z_1 - Z_2$ the difference between the elevations of those two sections. Assuming that $Z_1 = Z_2$, the grade of reaction can be calculated in the following form:

$$\varepsilon = \frac{\frac{P_1 - P_2}{\gamma}}{H_{UR}}$$

and considering that $P_2 < P_1$,

$$\varepsilon = \frac{\frac{P_1}{\gamma}}{H_{UR}}$$

In the action's turbines, the flow in inputs and outputs of the impeller are under atmospheric pressure (relative pressures):

$$\frac{P_1}{\gamma} = \frac{P_2}{\gamma} = \frac{P_{atm}}{\gamma} = 0$$

Where the grade of reaction is null. It happens in Pelton and Cross-Flow turbines.

In turbine of reaction, the flow crosses the impeller with pressure and the grade of reaction is not null. It happens in Francis, Kaplan and Helices turbines (Cruz, 2006).

Admitting that the upstream charge of the impeller or wheel is practically null,

$$H_{UR} \cong \frac{V_1^2}{2g} + \frac{P_1}{\gamma}$$

Where:

$$H_{UR} \cong \frac{V_1^2}{2g} + \epsilon H_{UR} \quad \text{ou} \quad V_1 \cong \sqrt{2g(1 - \epsilon)H_{UR}}$$

In turbines of action like Pelton type, following the definition of H_{UR} ,

$$H_{UR} = \frac{V_1^2 - V_2^2}{2g}$$

And $\epsilon = 0$, where:

$$V_1 \cong \sqrt{2gH_{UR}}$$

In turbines of reactions (ex.: Francis turbines) the acting binary in the impeller (wheel) is the result of the variation of direction of the flows when cross the wheel and the action of the pressure. In order to modify such direction, the impeller must react with hydrodynamics forces along the blades. By reaction, the blades are under equal forces in the opposite direction. The binary of those forces according to the axis of the turbine correspond to the acting hydraulic binary (Cruz, 2006).

Similarity of turbines

Specific number of rotations

According to the theory of dynamic similarity, for two turbines geometrically similar is valid next relationship (Cruz, 2006):

$$(1): \frac{n}{n'} = \left(\frac{P}{P'}\right)^{\frac{1}{2}} \left(\frac{H'_U}{H_U}\right)^{\frac{5}{4}}$$

Where:

n, n' represents rotation velocities;

P, P' is the power of the turbine;

H_U, H'_U is the useful fall.

The specific number of rotations of the turbine is defined by (Cruz, 2006):

$$n_s = \frac{P^{1/2}}{H_U^{5/4}}$$

Which correspond to consider in (1) the following values (Cruz, 2006):

$$n' = n_s; P' = 1; H'_U = 1$$

The useful fall (H_U) correspond to the useful fall of the best efficiencies and P to the maximal power based in such fall. The value of n_s is going to depend on the adopted units (Cruz, 2006):

$$n_s[\text{m, CV}] = 1.17 \cdot n_s[\text{m, kW}] = 4.45 \cdot n_s[\text{ft, HP}]$$

Each value of n_s represents a set of similar impellers (turbines) and it is a fundamental parameter in the representation and dimensioning of turbines (Cruz, 2006).

In case of a Pelton turbine with N injectors, the specific number can be obtained in the next form (Cruz, 2006):

$$n_s = n \frac{(NP_i)^{1/2}}{H_U^{5/4}} = \sqrt{N} \cdot n_{si}$$

being P_i the power of a turbine per injector and n_{si} is the specific number according to one injector.

In turbines with multiples impellers or wheels (M wheels), the specific number is defined in the following form (Cruz, 2006):

$$n_s = \sqrt{M} \cdot n_{si}$$

being n_{si} the specific number referent to each wheel or impeller.

Specific velocities

The specific velocities are defined by the relations between real velocities (V , W and C), the input and output of the impeller or wheel and the velocity given by the expression $\sqrt{2gH_u}$ (Cruz, 2006):

$$\text{For } i = 1, 2: v_i = \frac{V_i}{\sqrt{2gH_u}}; c_i = \frac{C_i}{\sqrt{2gH_u}}; w_i = \frac{W_i}{\sqrt{2gH_u}}$$

Then, the hydraulic efficiency of the turbine can be expressed as:

$$\eta_H = 2(v_1 c_1 \cos \alpha_1 - v_2 c_2 \cos \alpha_2)$$

To improve η_H to its point of optimal operation, the angle α_2 must be equal or close to 90° and (Cruz, 2006):

$$\eta_H = 2v_1 c_1 \cos \alpha_1$$

Turbines can be classified as slowly or fast depending to the value of c_1 according to $v_1 \cos \alpha_1$ (Cruz, 2006):

- **Slow turbine:** $c_1 < v_1 \cos \alpha_1$;
- **Normal turbine:** $c_1 = v_1 \cos \alpha_1$;
- **Fast turbine:** $c_1 > v_1 \cos \alpha_1$.

In turbines of action (Pelton turbines), v_1 has a value proximal to a unit, and by admitting $\alpha_1 = 0$ and $\eta_H = 1$, the minimal value of c_1 will be 0.5 (Cruz, 2006).

Other used parameters

Relative velocity [m, rpm] is the specific velocity c for c' transformed in n [rpm] (Cruz, 2006):

$$k_U \text{ or } k_u (\text{when english units are used}) = \frac{Dn}{60\sqrt{2gH_u}}$$

Unit velocity [m, rpm] is a velocity in rpm of a turbine of unit diameter working for a unitary useful fall (Cruz, 2006).

$$n_{11} = \frac{Dn}{\sqrt{H_u}}$$

Unit flow rate [m³/s, m] is the flow rate of a turbine with unit diameter that operates with a unitary useful fall (Cruz, 2006).

$$q_{11} = \frac{Q}{D^2\sqrt{H_u}}$$

Unit power [kW, m] is the power of turbine with a unit diameter and unitary useful fall (Cruz, 2006).

$$\rho_{11} = \frac{P}{D^2H_u^{1.5}}$$

Rotation velocity

In permanent regime, the turbines adapted directly to a **synchronous** generator rotate at **a velocity compatible with the web frequency and the number of pairs of generator poles**. Then, the **number of rotations per minute (n)** of a turbine that actions a generator/alternator is related with the number of pairs of poles of it (**P**) and with the frequency of the electrical web (**f**) by the following expression (Cruz, 2006):

$$n = \frac{60f}{P}$$

In Portugal, $f = 50$ Hz. The value of **n** vary in general between about 70 and 1500 rpm.

In order to exploit micro hydraulic power plants, it is convenient to reduce the dimension of the structures in civil construction and in equipment in order to reduce costs. Then, it is convenient to have high rotation velocities of at least 500 rpm (Cruz, 2006).

In some installation are used between a turbine and a generator, **velocities variators** in order to have a more affordable solution (smaller and faster generators) (Cruz, 2006).

If the central is connected to an isolated web, the frequency in the electrical web must be maintained by the respective turbines, which implies an efficient **velocity regulation**, in order to minimize the frequency variation in transition regimes (Cruz, 2006).

In case of a central of small hydroelectrical exploitation to supply an interconnected web, which have an installed power higher (at least ten times) than the central, it is possible to use an asynchronous generator, allowing to a have a rotation velocity of the turbine higher than the synchronous velocity mentioned before. A central hydroelectric supplied with asynchronous generator can be connected to isolated webs (Cruz, 2006).

For special situations it is possible to use synchronous generators of variable velocity (Cruz, 2006):

- Generators with the possibility of changing the number of pairs of poles (machines of incremental velocity) in which the possible velocities are for example, two;
- Generators with adjustable velocity in continuous mode between a minimal and a maximal value.

Such generators are more expensive but are indicated in cases where the falls vary periodically higher and lower of the value of useful falls of best efficiency, being particularly indicated for reversible groups (turbines-pumps). As a practical rule, the increase of produced energy will be in the order of $\pm 10\%$ of the percentual variation of

the useful fall higher and lower of the average fall or the fall of best efficiency (Cruz, 2006).

Cavitation in turbines

Cavitation is defined as the formation of vacuum bubbles in the liquid mass in flow, or around of a body displacing in a liquid, at some moment, when local pressure tends to be close of the steam pressure of the liquid and the liquid particles move apart from the boundary surfaces (adapted from the definition of *US Department of Interior*). These last conditions correspond to an insufficiency of the resultant forces of pressure to overcome the forces of inertia of the particles in flows and to push them to follows the boundary surfaces. Such vacuum bubbles or emptiness tends to be filled with released steam or vapor or gases. The interconnected factors that lead to cavitation are high velocities, low pressures and abrupt variations in boundaries (Cruz, 2006).

The haulage of those steam bubbles followed by its respective collapse next o solid walls produce an attack in such boundary surfaces, leading to a loss of material and the erosion of it. In turbomachines, such phenomenon causes also an efficiency reduction, vibration and noise (Cruz, 2006).

In turbines of reaction, the output or exit pressure of the impeller is small but velocity is quite high, forming conditions for such phenomenon (Cruz, 2006). Consider next figure:

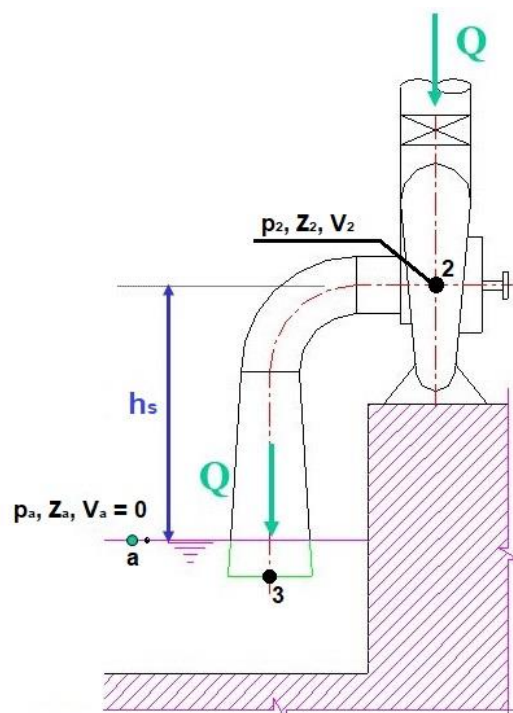


Figure 212 – Schema of a diffuser of a turbine of reaction and definition of aspiration height (adapted from <http://slideplayer.com.br/slide/1473748/>).

According to the Bernoulli's Theorem:

$$\frac{P_2}{\gamma} + \frac{V_2^2}{2g} + Z_2 = \frac{P_3}{\gamma} + \frac{V_3^2}{2g} + Z_3 + \Delta H_{2-3}$$

Being ΔH_{2-3} the total charge loss between the points 2 and 3, respectively at the exit or output of the impeller and the free surface at downstream (refund) (Cruz, 2006).

Considering that:

$$V_2 = C_V \sqrt{2gH_U} = K_2 \sqrt{H_U} \wedge V_3 = \frac{A_2 K_2}{A_3} = \frac{A_2 K_2 \sqrt{H_U}}{A_3} = K_3 \sqrt{H_U}$$

In which ΔH_{2-3} is the summation of localized and continuous charge losses,

$$\Delta H_{2-3} = \Delta H_L + \Delta H_C = \sum_L K_L \frac{V^2}{2g} + \frac{fLV^2}{2g} = K_{2-3} \frac{H_U}{2g}$$

It is obtained:

$$\left[\frac{K_2^2}{2g} - \frac{K_3^2}{2g} - \frac{K_{2-3}^2}{2g} \right] H_U = \frac{P_3 - P_2}{\gamma} + Z_3 - Z_2$$

A free surface $P_3/\gamma = P_{atm}/\gamma = h_b$ (**barometric local height**, which depends in the local altitude, Table 34) and, when occurs cavitation, $P_2/\gamma = P_v/\gamma = h_v$ (**height of water evaporation**, which is in function of temperature, Table 35) (Cruz, 2006).

Table 34 – Barometric height in function of the local elevation (adapted from Cruz, 2006).

Elevation [m]	h_b [m]
0	10.351
500	9.751
1000	9.180
1500	8.637
2000	8.120
3000	7.160
4000	6.295

Table 35 – Height of water evaporation in function of temperature (adapted from Cruz, 2006).

T [°C]	h_v [m]
5	0.089
10	0.125
15	0.174
20	0.239
25	0.324

Assigning h_s (**aspiration height**) as the difference between the elevation ($Z_2 - Z_3$) in the central, then (Cruz, 2006):

$$\frac{K_2^2}{2g} - \frac{K_3^2}{2g} - \frac{K_{2-3}^2}{2g} = \frac{h_b - h_V - h_s}{H_U} = \sigma_C$$

Being σ_C designed by **coefficient of cavitation in the central**.

Assigning $h_{s,max}$ as the maxima value for aspiration height, in which start cavitation effect in turbines for determined conditions of operation (flow rate, fall and grade of distributor opening) (Cruz, 2006):

$$\frac{h_b - h_V - h_{s,max}}{H_U} = \sigma_T$$

Being σ_T assigned as **coefficient of cavitation of a turbine** or **coefficient of Thoma**, which is equal to the value of (Cruz, 2006):

$$\frac{K_2^2}{2g} - \frac{K_3^2}{2g} - \frac{K_{2-3}^2}{2g}$$

In considered limit conditions of cavitation.

To avoid such undesirable effect in a turbine, it must be verified next inequality (Cruz, 2006):

$$\sigma_C > \sigma_T$$

In a limit case,

$$\sigma_C = \sigma_T$$

And,

$$h_b - h_V - h_{s,max} = \sigma_T H_U$$

Where:

$$h_{s,max} = h_b - h_V - \sigma_T H_U$$

Note: in order to use such equation must have in mind the point of the section of reference of the wheel or impeller in order to obtain $h_{s,max}$ (Cruz, 2006).

So, to avoid cavitation,

$$h_s \leq h_{s,max}$$

Each set or family of turbines geometrically similar, operating in conditions of dynamic similarity has the same value of σ_T . The coefficient of Thoma is in function of n_s : **as higher is n_s , higher is σ_T** (Table 36) (Cruz, 2006).

Table 36 – Coefficient Thoma in function of n_s (adapted from <http://slideplayer.es/slide/4161770/>).

n_s	50	100	150	200	250	300	350	400	500	600	700	800
σ_T	0.04	0.05	0.08	0.13	0.22	0.31	0.45	0.6	0.7	0.9	1.5	2.1
Type of turbine	Slow Francis	Slow Francis	Normal Francis	Normal Francis	Fast Francis	Fast Francis	Extra Francis	Extra Francis	Helix and Kaplan			

The values of σ_T are obtained experimentally by the manufacturer and depends in operation conditions of the turbine (Cruz, 2006).

In order to determine $h_{s,max}$ of the turbines, it is necessary to define the point of operation of it to stablish fixed limits conditions of h_s . **Example:** fall of best efficiency, at fully opening and level of the river corresponding to a turbinate flow rate (Cruz, 2006).

10.1.3 Selection of adequate turbines for an installation

The designer must select the types of turbines adequate for the studied case. Such process is based in project experience and recent technical information. To help in such selection can be used some graphics and figures supplied by manufacturers of turbines, by manuals or by specialists (Figure 213 and Figure 214) (Cruz, 2006).

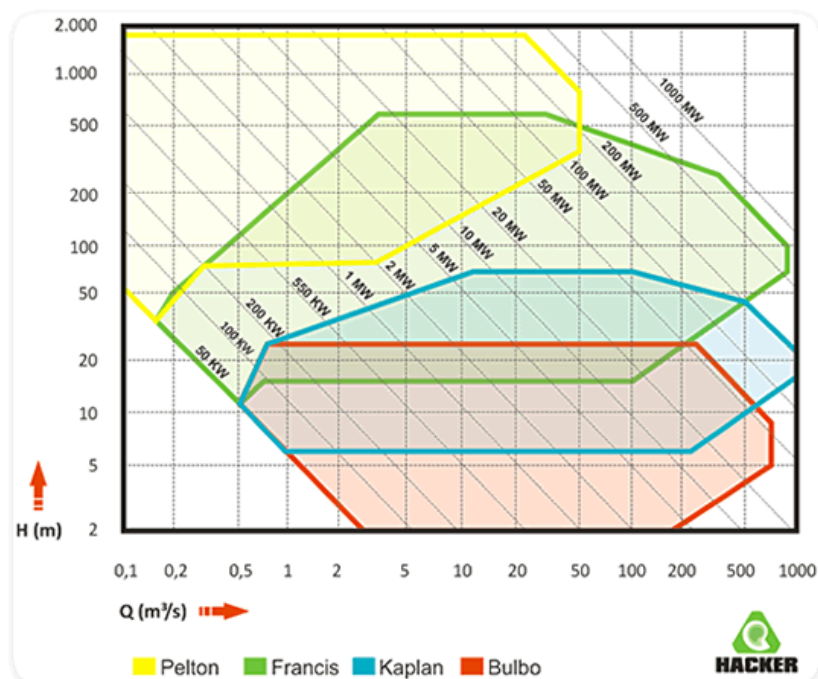


Figure 213 – Graphic with a typical field of application of the three types of turbines (www.hacker.ind.br).

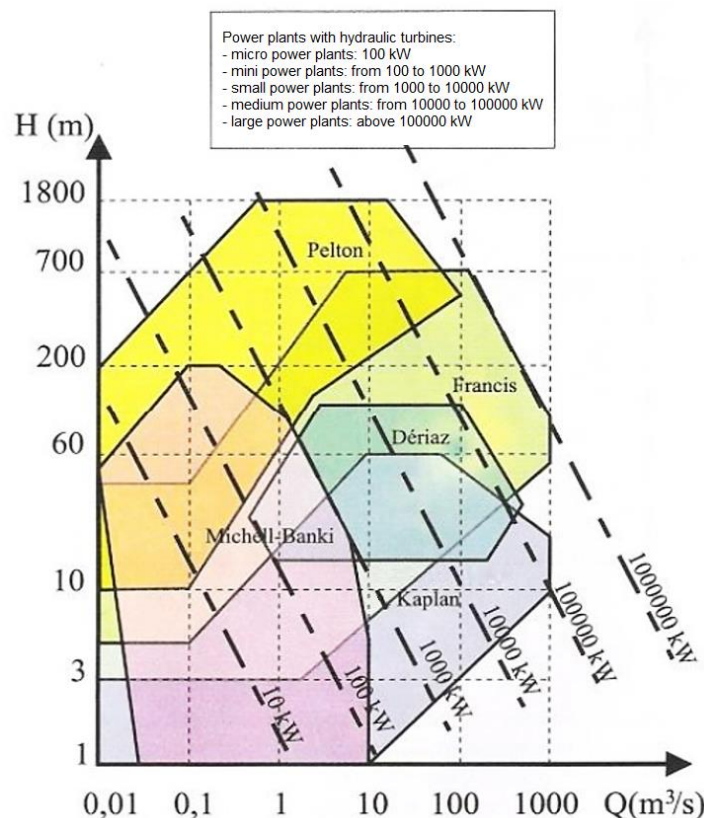


Figure 214 – Field of application of turbines (Filho, 2015).

General rule is the primary selection of the type of turbine that is more efficient based in the fall and the turbined flow rate (Table 37) (Cruz, 2006).

Table 37 – Primary selection of the type of turbine, function of the fall and turbined flow rate (adapted from Cruz, 2006).

Parameters	Type of Turbine
High falls (and lower flow rate)	Turbine of Pelton
Average falls	Turbine of Francis
Low falls (and high flow rate)	Turbine of Kaplan

For each type of turbine is adequate for certain conditions of operability. Consider the case of a **Pelton turbine** as an example (Cruz, 2006).

What would happen if we use a Pelton turbine to operate a quite lows fall?

- The most compacted machine (with an injector) would have a certain value of n_s^* and must obey to an optimized relationship of impeller or wheel diameter and jet diameter, being $D_R = 9D_j$;
- For a certain flow rate (Q) and power (P) are valid the following equations:

$$P = \eta \gamma Q H_U$$

$$Q = S_j \sqrt{2gH_U}$$

$$S_j = \pi \frac{D_j^2}{4}$$

- Then, for a certain power, the jet diameter increases as the falls decrease, at the same time, the impeller diameter also increases ($D_R = 9D_j$);
- Maintaining $n_s = n_s^*$ is the power, the decrease of H_U leads to a decrease of rotation velocity of the impeller (n).

Conclusion: if the Pelton turbine were used for low falls, it would have excessively large diameters (dimensions) and to low rotation velocities, demanding generator with a huge number of pairs of poles (big and expensive): at a too low velocity it would be quite hard to regulate and control the installation set or group. Thus, the application of such turbine at too low falls would not be affordable or sustainable, which means non-efficiency. (Cruz, 2006).

10.2 Hydraulic pumps

A **Pump** is a turbomachine which supplies energy to the fluid flow, based in external energy (electrical or motorize) to give power to a motor, that supplies angular movement to a propeller by an axis, and such propeller transfer the energy to the fluid. As an example, apart from pumps are compressors and fans (Mata-Lima, 2010).

10.2.1 Operation Description

Types of pumps

Summary description

Pump are essentially constituted by (Pinho et al., 2011):

- Impeller;
- Pumps body:
 - Supports of rollers of the impeller;
 - Orientation of the fluid inside the machine.

Apart from that, the body of the pump includes **aspirations pipes** (at upstream) and **compression pipes** (at downstream) (Pinho et al., 2011).

Axial pumps

The available energy in the axis of transmission (from a motor) is transmitted to a fluid by a helix of vertical axis. The fluid is propelled to a pipe slightly divergent with shape of a smooth curve, allowing the exit of the fluid from the propulsor chamber (where ends the axis and the propulsor silo) (Figure 215) (Pinho et al., 2011).

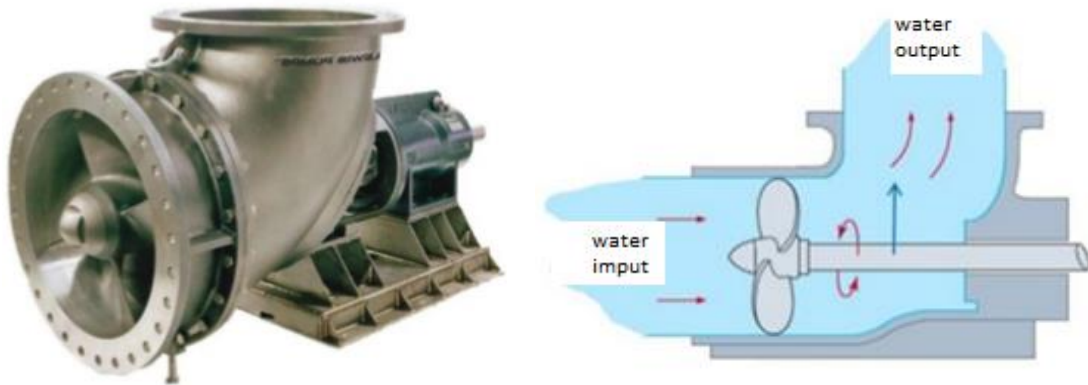


Figure 215 – Axial pump (Universidade Federal do ABC, 2013).

Centrifugal pumps

Machines of axial or mix operation. Exists different types depending on (Pinho et al., 2011):

- Design of the impeller or propeller (Figure 216) - the impeller is made by a core or nucleus where all blades are symmetrically fixed;



Figure 216 – Example of a closed impeller (a), partially open (b) and open (propeller) (c) (<http://hidromachinesudeg.blogspot.pt/2016/02/componentes-de-bombas-y-turbinas.html>).

- Trajectory of the fluid
 - Radial Flow Pumps (Figure 217) - the entrance of the fluid is by an axial input and exit by a radial output at the periphery of the impeller;



Figure 217 – Radial flow pump (sectional cut) (<http://www.tecpa.es>).

- Mixed Flow Pumps (Figure 218) - the entrance of the fluid is by an axial input while exits by an intermedium axial and radial output;



Figure 218 – Mix flow pump (<http://xylemappliedwater.pt>).

- Design of the pumps body
 - Volute Pump (Figure 219) - around of the impeller exists a volute that keeps constant the flows output velocity;



Figure 219 – Volute pump of duplex aspiration (www.sulzer.com).

- Diffusor Pump (Figure 220) - of concentric constant section with the impeller, supplied with fixed blades that guide the flow and reduce fluids velocity;

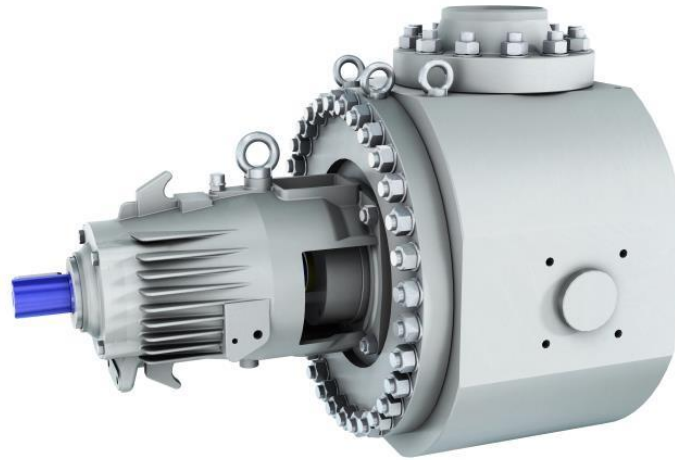


Figure 220 – Pumps of simple staging of horizontal diffuser style (www.sulzer.com).

- Number of cells
 - Monocellular or single cell (Figure 221);



Figure 221 – Single cell pump (<http://www.bombaszeda.com>).

- Multiple cells pump or “floor pump” (Figure 222).



Figure 222 – Multicellular pumps (<http://www.efafllu.pt>).

Denominations and main formulas for pumping systems

Denominations, units

Table 38 – Denominations /Basic units (adapted from Pinho et al., 2011).

Denomination	Notations	Practical unit	Coherent unit
Flow rate	Q	m ³ /h	m ³ /s
Total height (Charge)	H	m	m
Value NPSH	NPSH	m	m
Capacity of aspiration	S	m ³ /h	m ³ /s
Input power	P	kW	Nm/s
Pumps efficiency	η	-	-
Rotation velocity	n	rpm	rps
Pressure	P	bar	N/m ²
Specific mass	ρ	kg/dm ³	kg/m ³
Flows velocity	v	m/s	m/s
Gravity	g	m/s ²	m/s ²
Subscribed:	d	output zone of the pump	
	s	input zone of the pump	
	a	output zone of the system	
	e	input Zone of the system	

Flow rate

The different flow rate denominations are (Pinho et al., 2011):

- Nominal flow rate (Q_N): flow rate for which the pump is designed;
- Optimal flow rate (Q_{opt}): flow rate at optimal efficiency;
- Minimum flow rate (Q_{min}): minimal flow rate allowed;
- Maximum flow rate (Q_{max}): maximal flow rate allowed.

Height of total elevation (total charge)

The **Total height (H) of a pump** is the mechanical work transmitted by the pump to the pumped fluid per unit of liquid weight (Pinho et al., 2011).

The different heights denominations are (Pinho et al., 2011):

- Nominal height (H_N): total height of operation;
- Optimal height (H_{opt}): total height at an optimal efficiency;
- H_0 height in vacuum (H_0): total height of operation at vacuum ($Q = 0$).

Total energy = Position energy + Pressure energy + Kinetics energy:

$$E = Z + \frac{p}{\rho g} + \frac{v^2}{2g}$$

Total height of the flow (H) is composed by (Pinho et al., 2011):

- $Z_d - Z_s$, difference of **altitude** (weight) between the upstream and downstream pipes (pipes of impulsion and aspiration);
- $p_d - p_s/\rho g$, differences of **pressure** of liquids between the upstream and downstream pipe;
- $v_d^2 - v_s^2/2g$, differences of **kinetics energy** of the liquid between the upstream and downstream pipe.

Then, **H** is:

$$H = (Z_d - Z_s) + \frac{p_d - p_s}{\rho g} + \frac{v_d^2 - v_s^2}{2g}$$

An application example (Pinho et al., 2011):

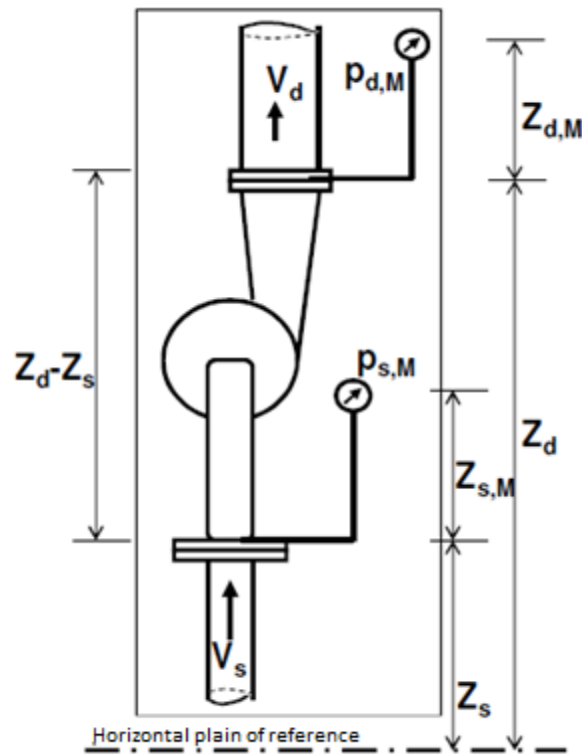


Figure 223 – Application example (determination of H) (Pinho et al., 2011).

Given data:

- DN_s 50 ($A_s = 0.00196 \text{ m}^2$);
- DN_d 65 ($A_d = 0.00332 \text{ m}^2$);
- Liquid: cold water, $\rho = 1000 \text{ kg/m}^3$;
- $Z_d - Z_s = 0.3 \text{ m}$; $Z_{d,M} = 1.0 \text{ m}$; $Z_{s,M} = 0.5 \text{ m}$;
- $Q_N = 50 \text{ m}^3/\text{h} = 0.0139 \text{ m}^3/\text{s}$.

Pressure at pumps upstream section or pipes:

$$p_s = p_{s,M} \pm \rho g Z_{s,M}$$

Pressure at pumps downstream section:

$$p_d = p_{d,M} \pm \rho g Z_{d,M}$$

In case of circuits with air measurements, $Z_{s,M}$ and $Z_{d,M}$ can be ignored due to $\rho_{ar} \ll \rho_{liquido}$.

$$p_{d,M} = 4.9 \text{ bar} = 490000 \text{ N/m}^2$$

$$p_{s,M} = -0.25 \text{ bar} = -25000 \text{ N/m}^2$$

$$\begin{aligned} \frac{p_d - p_s}{\rho g} + (Z_d - Z_s) &= \frac{p_{d,M} - p_{s,M}}{\rho g} + (Z_{d,M} - Z_{s,M}) = \\ &= \frac{490000 \text{ N/m}^2 - (-25000 \text{ N/m}^2)}{1000 \text{ kg/m}^3 \cdot 9.81 \text{ m/s}^2} + (1 \text{ m} - 0.5 \text{ m}) = \\ &= 52.5 \text{ m} + (1 \text{ m} - 0.5 \text{ m}) = 53 \text{ m} \end{aligned}$$

$$v_d = \frac{Q_N}{A_d} = \frac{0.0139 \text{ m}^3/\text{s}}{0.00196 \text{ m}^2} = 7.1 \text{ m/s}$$

$$v_s = \frac{Q_N}{A_s} = \frac{0.0139 \text{ m}^3/\text{s}}{0.00332 \text{ m}^2} = 4.2 \text{ m/s}$$

$$\frac{v_d^2 - v_s^2}{2g} = \frac{(7.1 \text{ m/s})^2 - (4.2 \text{ m/s})^2}{2 \cdot 9.81 \text{ m/s}^2} = 1.7 \text{ m}$$

$$\therefore \text{Total Height (H)} = 54.7 \text{ m}$$

Total height H_A of the system

It is the total energy introduced by the pump, necessary to maintain the flow rate (Q) in the system (Pinho et al., 2011).

$$H_A = \underbrace{(Z_a - Z_e) + \frac{p_a - p_e}{\rho g}}_{\text{static component independent of the flow}} + \underbrace{\frac{v_a^2 - v_e^2}{2g}}_{\text{dynamic component dependent of the caudal}} + H_V$$

An application example (Pinho et al., 2011):

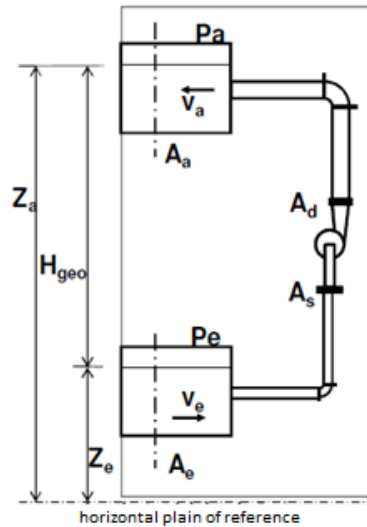


Figure 224 – Ascending pumping between reservoirs (Pinho et al., 2011).

Given data:

- Liquid: cold water; $\rho = 1000 \text{ kg/m}^3$;
- $H_{\text{geo}} = Z_a - Z_e = 43 \text{ m}$;
- $Q_N = 50 \text{ m}^3/\text{h} = 0.0139 \text{ m}^3/\text{s}$;
- $A_a = 0.14 \text{ m}^2$; $V_a = 0.1 \text{ m}^2/\text{s}$;
- $A_e = 0.35 \text{ m}^2$; $V_e = 0.04 \text{ m}^2/\text{s}$.

$$\frac{p_a - p_e}{\rho g} = 0 \wedge \frac{v_a^2 - v_e^2}{2g} = 0.00043 \text{ m} \approx 0$$

$H_{V_s} = 2.0 \text{ m}$: losses in charge e due to friction in aspiration pipes and localized losses at reservoir exit or output.

$H_{V_d} = 8.9 \text{ m}$: losses of charge due to friction in compression pipes and localized losses in reservoir entrance or input.

$$\therefore H_A = 43 + 0 + 0 + (2 + 8.9) = 53.9 \text{ m}$$

Cavitation, NPSH

If the **static pressure** of a fluid lows until an associated steam or vapor pressure at a certain temperature, as for example, an increase of absolute velocity or changes in piezometric heights ($Z_a - Z_e$), forming **steam bubbles** localized in the liquid mass. Such bubbles are transported at any other point by the flow and then suddenly explode if static pressure rise again to superior values of steam or vapor pressure (Pinho et al., 2011).

This production and sudden destruction of filled cavities of steam gives the designation of **cavitation** (Pinho et al., 2011).

In pumps, **cavitation** can occur due to local reduction of pressure at entrance of the impeller channels because of an increase of flows velocity at that point (Pinho et al., 2011).

Cavitation has the following effects (Pinho et al., 2011):

- Erosion of the material (pumps and pipes);
- Reduction of total height;
- Reduction of pump efficiency;
- Increase of vibration and noise;
- Modification of the operation characteristics.

In order to **avoid** or **limit cavitation** in pumps must be configured a reserve **in static pressure** related to the **steam tension** of the liquid in the impellers. The difference between absolute static pressure (measured in meters) and the steam or vapor tension of the liquid (in meters) is designated by **Net Positive Suction Head (NPSH)** and is measured in meters (Pinho et al., 2011).

NPSH required by a pump

The **NPSH required by a pump** ($NPSH_{req}$) is the minimal value, where the total height in a plain of reference for NPSH, must exceed the vapor tension of the pumped liquid, in order to guarantee a correct operation of the pump without cavitation, at a **nominal rotation velocity** (n_N), at a **nominal height** (H_N) and a **nominal flow rate** (Q_N) of design (Pinho et al., 2011).

The **plain of reference for a NPSH value** (Figure 225) is defined by a horizontal plain that pass through the circle that is determined by the most extreme points of the main curvature of the impeller blades or laminates (Pinho et al., 2011).

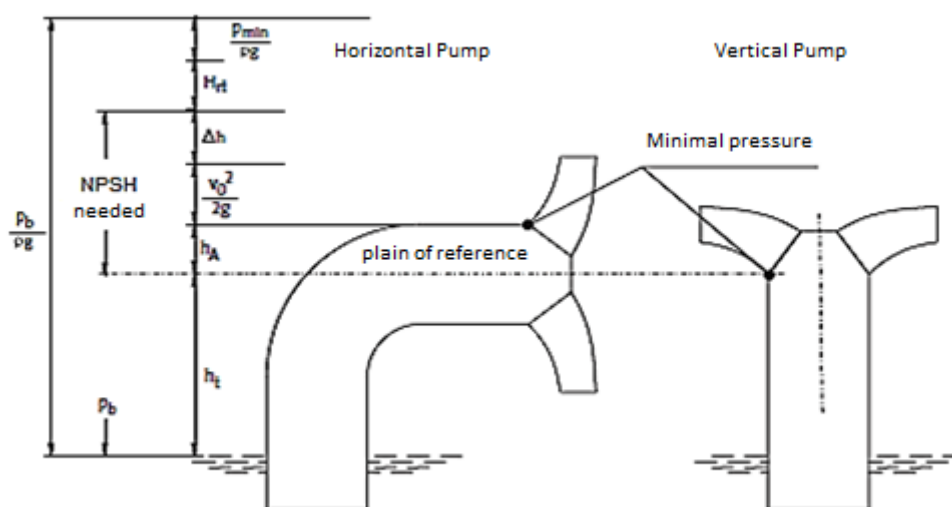


Figure 225 – Plain of reference for NPSH (adapted from <http://www.nuevainingenieria.com/tag/cavitacion/>).

NPSH available at an installation

The **NPSH available at some installation** ($NPSH_{dis}$) is the difference between **total height** (static pressure height+ Kinetic pressure) and **Steam or vapor pressure height** referred to a plain of reference for NPSH value (Pinho et al., 2011).

$$NPSH_{dis} = \frac{p_s + p_b}{\rho g} + \frac{v_s^2}{2g} - \frac{p_D}{\rho g} + Z'_s$$

Z'_s is the difference between the center of the input section of the pump and the plain of reference for NPSH value:

- > 0 , when the plain of reference for NPSH value is under the input section;
- < 0 , when the plain of reference for NPSH value is above the input section;
- $= 0$, when both level overlap.

In case of an **elevated pump**,

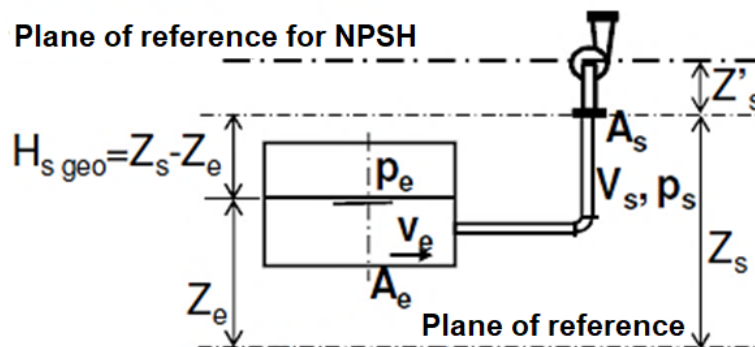


Figure 226 – Elevated pump (Pinho et al., 2011).

NPSH is determined as:

$$H_{s\ geo} = Z_s - Z_e$$

By the Bernoulli's Theorem,

$$\begin{aligned} \frac{p_s + p_b}{\rho g} + \frac{v_s^2}{2g} &= \frac{p_e + p_b}{\rho g} + \frac{v_e^2}{2g} - H_{s\ geo} - H_{V\ s} \Rightarrow \\ \Rightarrow NPSH &= \frac{p_e + p_b - p_D}{\rho g} + \frac{v_e^2}{2g} - H_{s\ geo} - H_{V\ s} + Z'_s \end{aligned}$$

In case of a free surface $\Rightarrow p_e = 0 \Rightarrow$

$$\Rightarrow NPSH = \frac{p_b - p_D}{\rho g} + \frac{v_e^2}{2g} - H_{s\ geo} - H_{V\ s} + Z'_s$$

In case of a **pump in charge**,

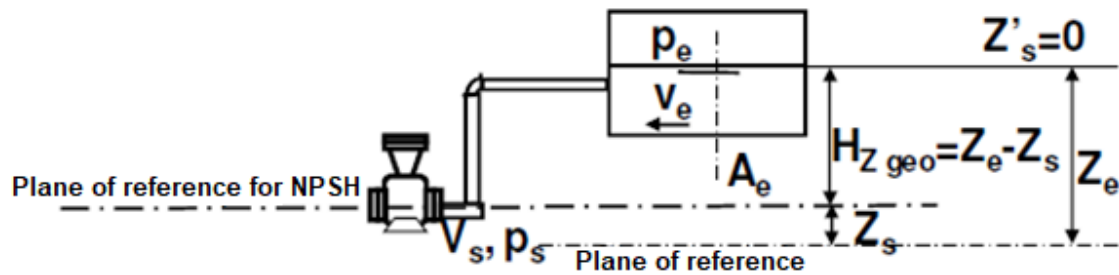


Figure 227 – Pump in charge (Pinho et al., 2011).

$$H_{Z\text{ geo}} = -H_{s\text{ geo}} = Z_e - Z_s$$

$$\text{NPSH} = \frac{p_e + p_b - p_D}{\rho g} + \frac{v_e^2}{2g} - H_{Z\text{ geo}} - H_{V\text{ s}} + Z'_s$$

In case of a free surface $\Rightarrow p_e = 0 \Rightarrow$

$$\Rightarrow \text{NPSH} = \frac{p_b - p_D}{\rho g} + \frac{v_e^2}{2g} - H_{Z\text{ geo}} - H_{V\text{ s}} + Z'_s$$

In practice $\frac{v^2}{2g} \cong 0$, so it is frequently omitted

For a **safety operation** of the pump, **$\text{NPSH}_{\text{dis}} \geq \text{NPSH}_{\text{req}}$** and in **conditions of safety**, **$\text{NPSH}_{\text{dis}} \geq \text{NPSH}_{\text{req}} + 0.5 \text{ m (aprox.)}$** (Pinho et al., 2011).

Power, Efficiency

The **Power of the Pump (P_Q)** is the useful energy transferred to the fluid (Pinho et al., 2011).

$$P_Q = \rho g Q H \text{ (W)}$$

The **Absorbed Power (P)** is the energy received by the motor of the pump (Pinho et al., 2011).

$$P > P_Q, \text{ due to losses in pump}$$

Others important definitions of power includes include (Pinho et al., 2011):

- Nominal power (**P_N**): required power for **Q_N , H_N , n_N** ;
- Optimal power (**P_{opt}**): required power at optimal efficiency;
- Power in vacuum (**P_o**): required power for $Q = 0$.

Efficiency/performance of the pump (η) is the reason between a hydraulic power transmitted by the pump and the power absorbed in the spindle (Pinho et al., 2011).

$$\eta = P_Q/P$$

Specific velocity (n_q)

For a certain value of **Q** and **H** can be obtained by pumps with impeller of different forms, **depending of its specific velocity**. Such variable (n_q) defines a characteristic value of the impeller form (Pinho et al., 2011).

The **specific velocity** is defined as the rotation velocity of an impeller geometrically similar in all its components and it was designed in order to produce an elevation height of **1 m for a flow rate of 1 m³/s** (Pinho et al., 2011). By the similarity laws,

$$n_q = n \frac{(Q/Q_q)^{1/2}}{(H/H_q)^{3/4}} \text{ [rpm]}$$

$$Q[\text{m}^3/\text{s}]; H[\text{m}]$$

The **specific velocity** refers to (Pinho et al., 2011):

- Data of service at an optimal efficiency point of the impeller;
- Data of service at a single stage in multicellular pumps;
- Data of service at a side of an impeller, in case of impeller with two entrances or inputs.

$$\text{For } Q = 1 \text{ m}^3/\text{s} \wedge H = 1 \text{ m} \rightarrow$$

$$\rightarrow n_q = n \frac{Q_{\text{opt}}^{1/2}}{H_{\text{opt}}^{3/4}} \text{ [rpm]}$$

$$Q_{\text{opt}}[\text{m}^3/\text{s}]; H_{\text{opt}}[\text{m}]$$

The **form of the impeller** of a pump, which means, the **specific velocity**, has a great importance in the pump efficiency (Figure 228) (Pinho et al., 2011).

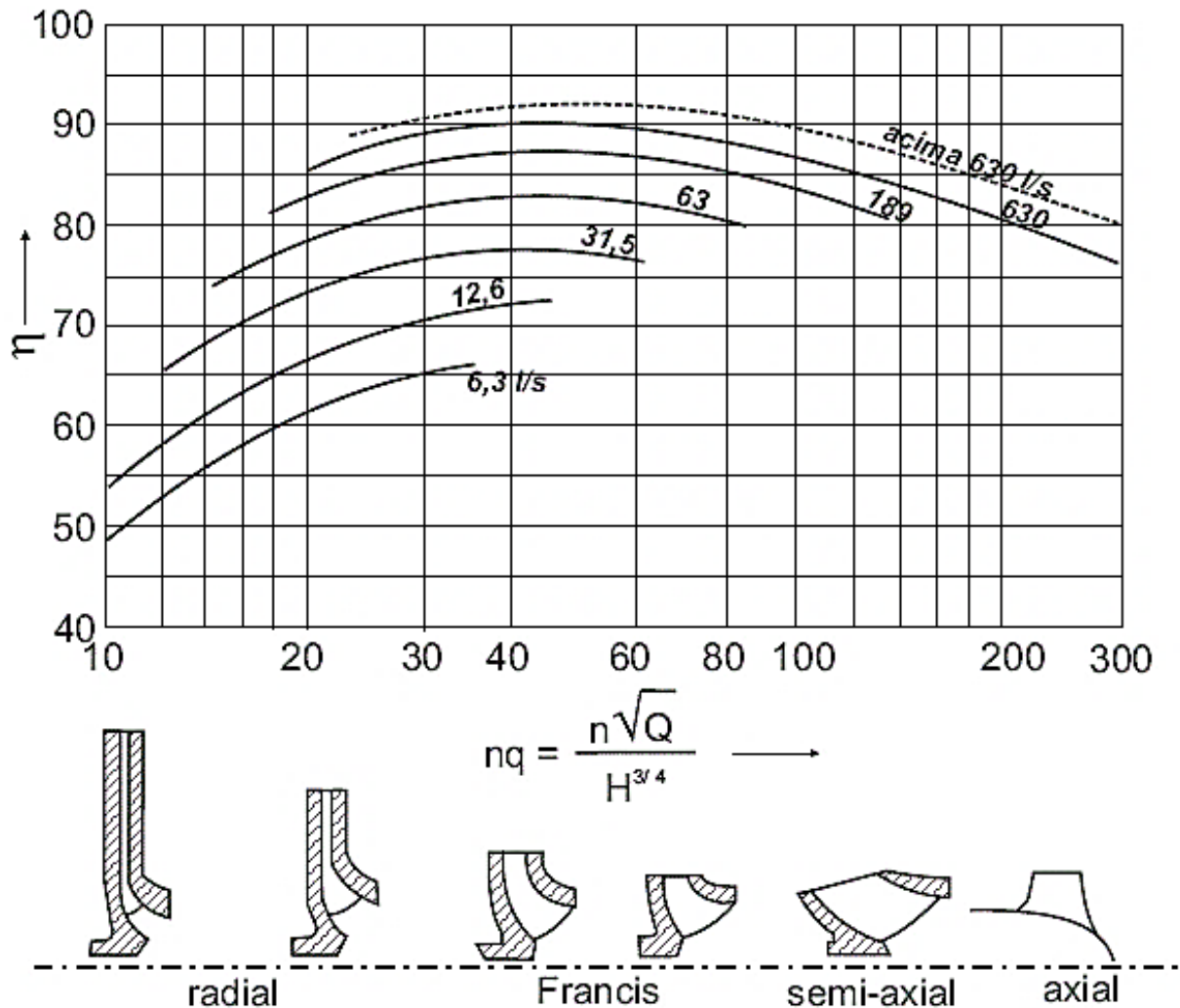


Figure 228 – Relation between specific velocity in some impellers, efficiency and flow rate (Escola da Vida, 2018).

10.2.2 Operation of pumps integrated to an installation

Characteristic curves

Characteristic curves of pumps

For a certain pump with a specific **rotation velocity**, a height (H), an absorbed power (P), an efficiency (η) and a value of NPSH are function of Q. The relationship between those magnitudes is represented by **characteristic curves of a pump** (Figure 229 and Figure 230) (Pinho et al., 2011).

Therefore, such curve represents the operational hydraulics conditions of the machine working at a certain rotation (revolutions per unit of time).

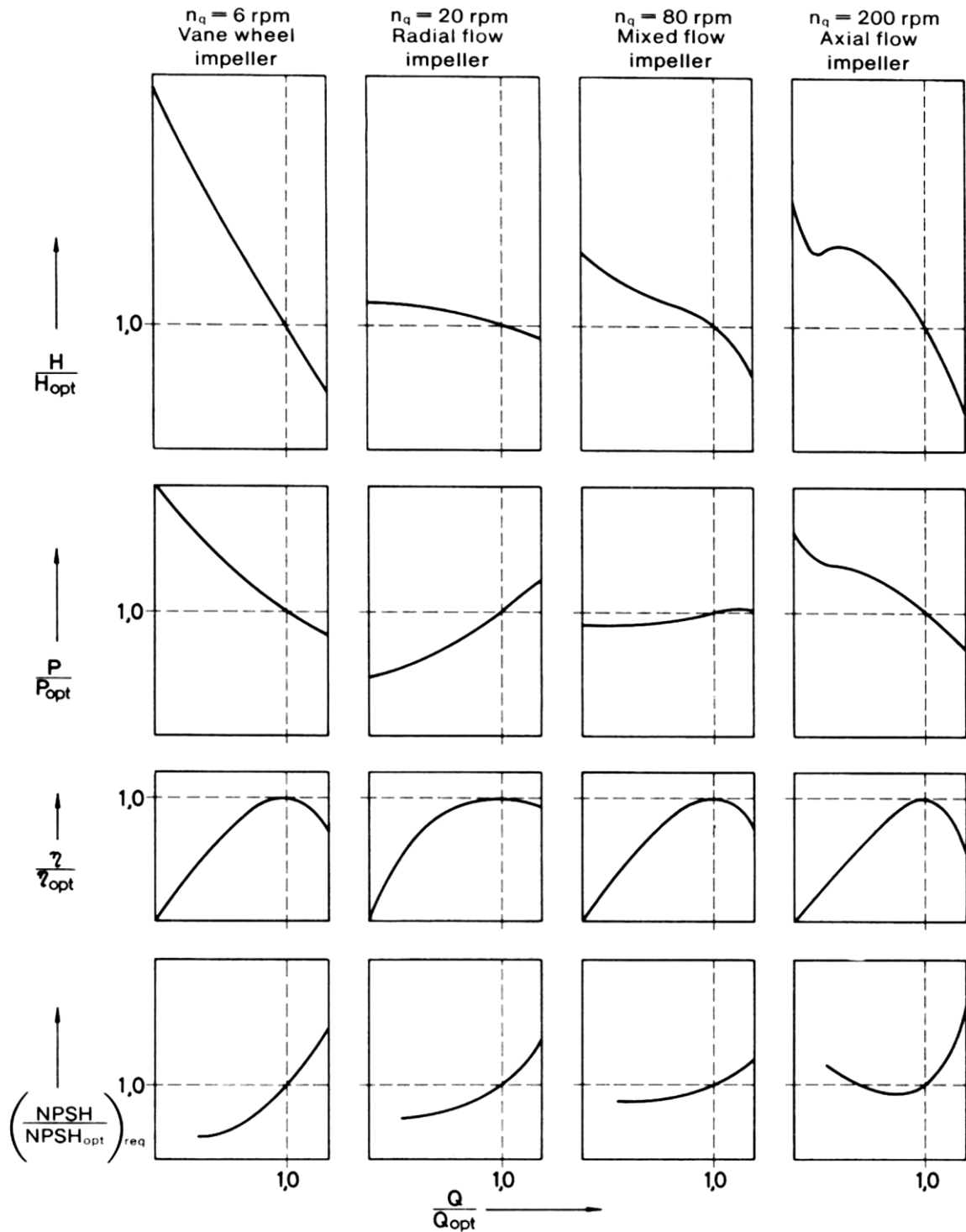


Figure 229 – Influence of the specific velocity in form of the characteristic curves of a pump (adapted from Pinho et al., 2011).

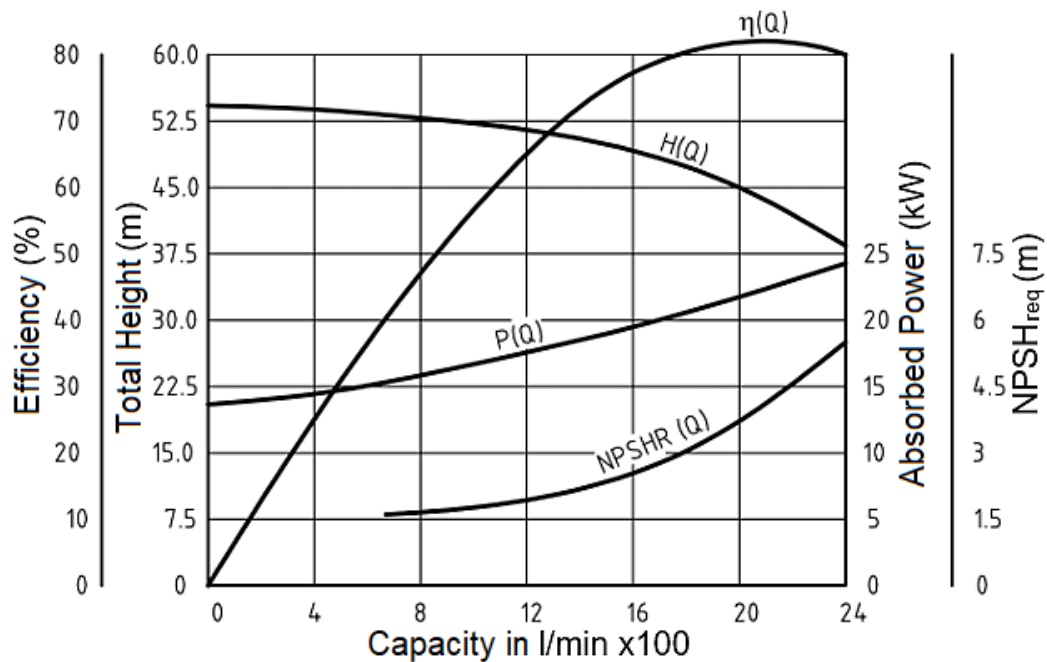


Figure 230 – Characteristic curves of a pump (adapted from Area Mecânica, 2011).

Characteristic curves of installations

It is called by **characteristic curve of an installation** (Figure 231) the graphical of the difference and inclination of the charge line at the exit and entrance of the pump with flow rate flowed at the same installation (Pinho et al., 2011).

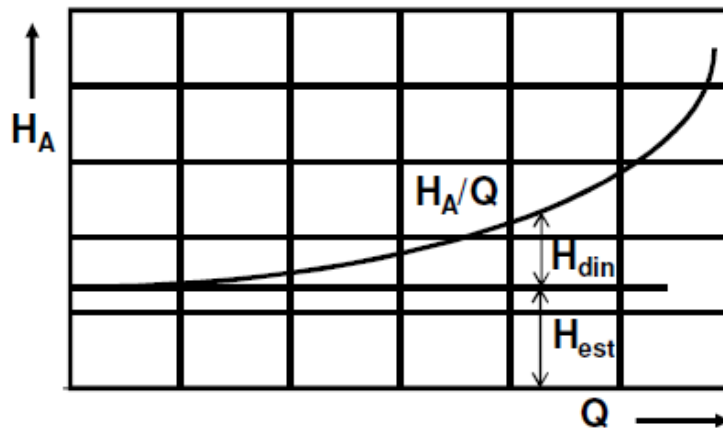


Figure 231 – Example of a characteristic curve of an installation (Pinho et al., 2011).

$$H = f(Q^2)$$

$$H_{\text{est}} = H_{\text{geo}} + \frac{p_a - p_e}{\rho g}$$

$$H_{\text{din}} = H_V + \frac{v_a^2 - v_e^2}{2g}$$

As an application example (Pinho et al., 2011):

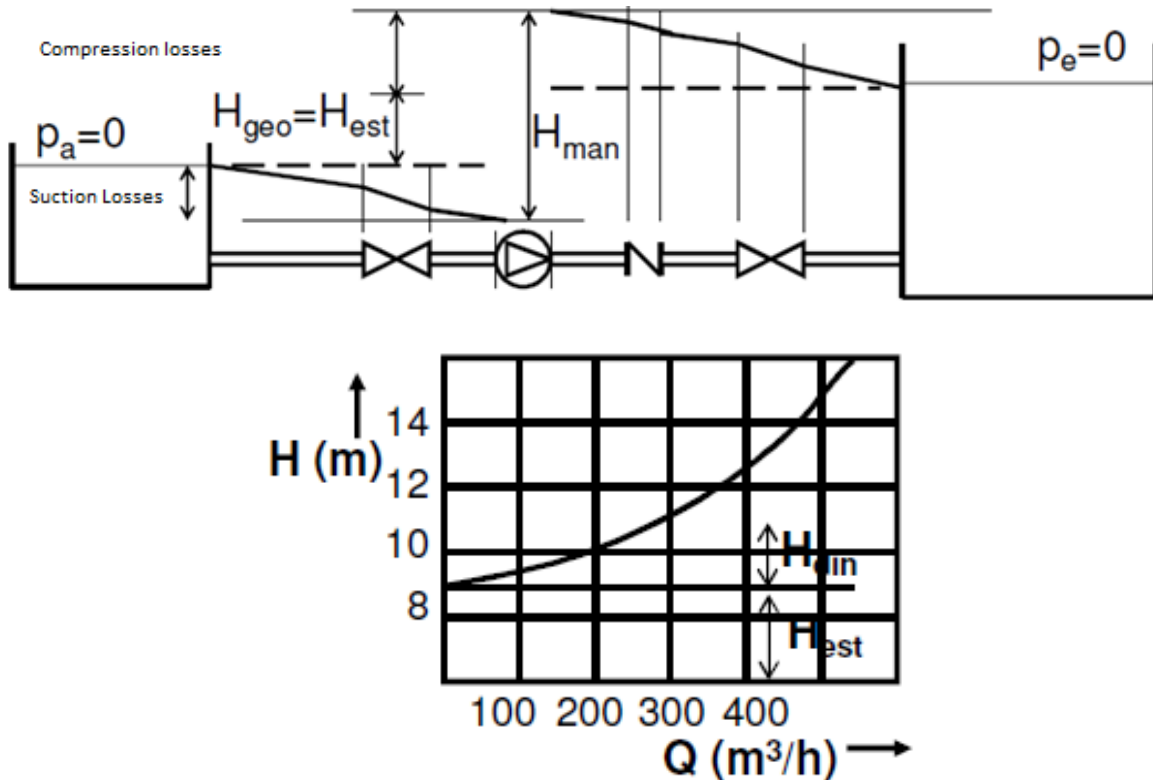


Figure 232 – Example of application of the concept of an installation characteristic curve (Pinho et al., 2011).

For: $Q = 350 \text{ m}^3/\text{h} \wedge H_{\text{est}} = 9.0 \text{ m}$

$$\begin{array}{rcl}
 \sum H_{L \text{ asp}} & = & 0.18 \text{ m} \\
 \sum H_{L \text{ comp}} & = & 0.78 \text{ m} \\
 H_f & = & 1.94 \text{ m} \\
 \hline
 H_{\text{din}} & = & 2.90 \text{ m}
 \end{array}$$

Point of operation of a pump

It is a representative point of the characteristics of operation of a pump, when it is integrated at some installation, which means, a point where the characteristic curve (H/Q) intersects the characteristic curve of an installation (H_A/Q) (Pinho et al., 2011).

Such point determines the flow rate (Q) that can be impelled by the pump to the installation. It also determines (Pinho et al., 2011):

- Absorbed power (P);
- Efficiency (η);
- Required NPSH value ($NPSH_{\text{req}}$).

Being necessary to verify $NPSH_{dis} \geq NPSH_{req}$ (Pinho et al., 2011).

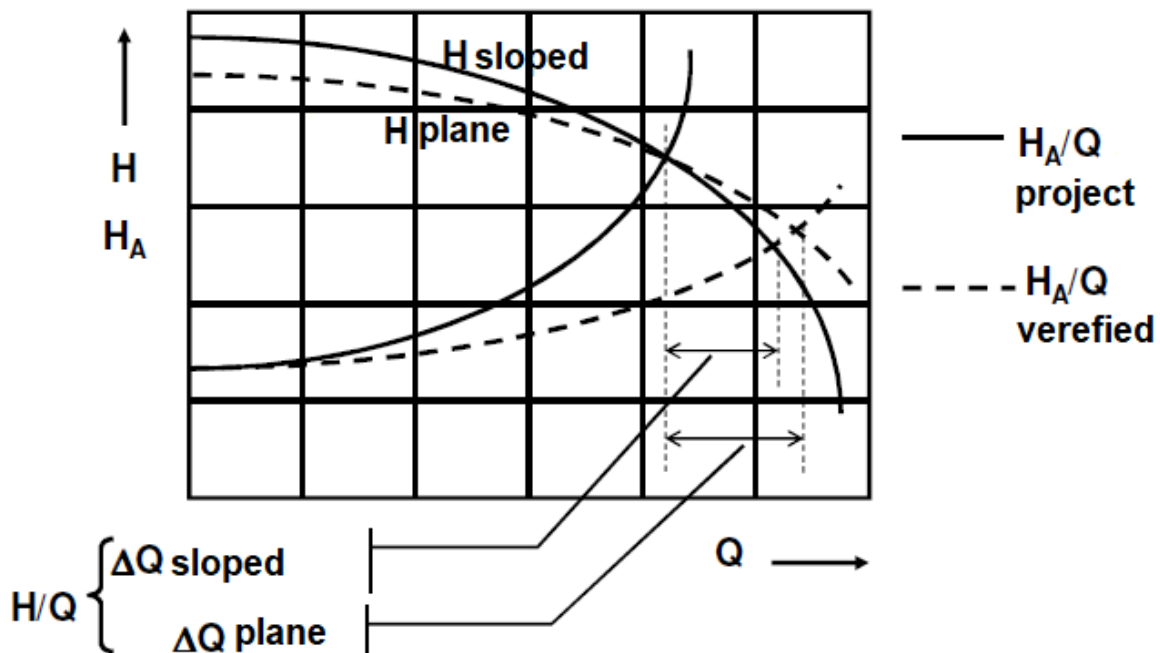


Figure 233 – Variation of a flow rate due to a deviation produced by the change of operation conditions (Pinho et al., 2011).

Configuration of a pump operation to operation requirements

Possible actions to implement in order to adapt the pumps operation to requirements (Pinho et al., 2011):

- **Change of installations characteristics (curve H_A/Q)**
 - Adjustment of flow rate admission (check valve);
 - Use of a “Bypass” (control of flow rate diversion);
- **Change of pumps characteristics (curve H/Q)**
 - Variation of rotation velocity of the impeller (control of velocity);
 - Change of the impeller diameter;
 - Variation of the flow orientation blade angles at upstream input of the impeller (pre-rotation);
 - Reduction of the flow rate that flow through the impeller by controlling cavitation (self-check, control by cavitation);
 - Scraping the outcoming edges of the impeller blades.

Adjustment and control of the flow rate admission

When the pumps are controlled by this system, the charge losses in the system increase, being H_{din} greater in virtue of the control valve setting (Figure 234) (Pinho et al., 2011).

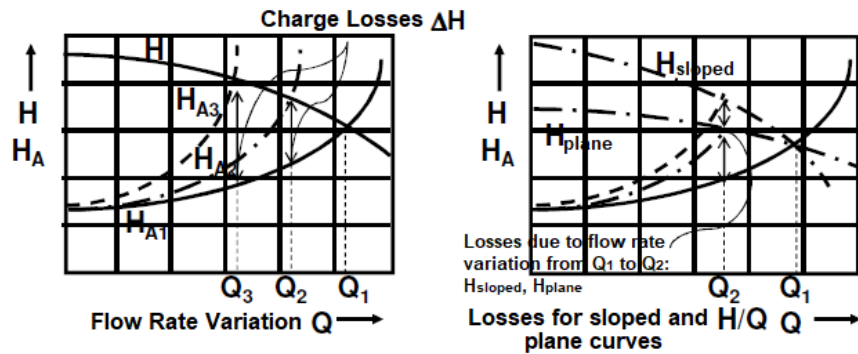


Figure 234 – Regulation of the flow rate admission (Pinho et al., 2011).

The adjustment must be applied at downstream of the pump. If it is applied at upstream, the $NPSH_{disp}$ will be reduced, a then cavitation must be prevented.

Use of “Bypass”

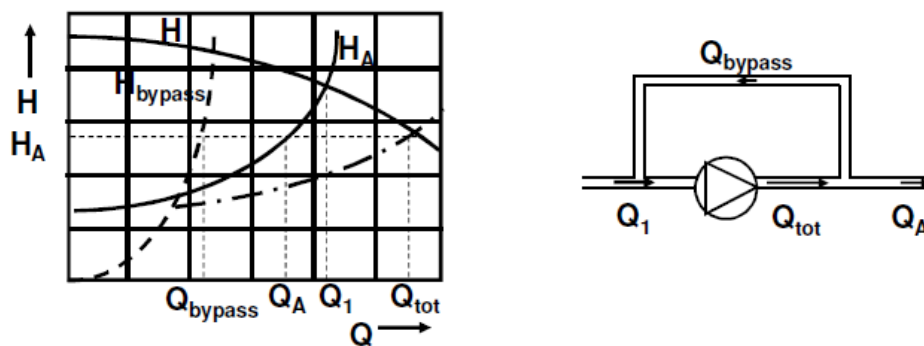


Figure 235 – Use of a “Bypass” (Pinho et al., 2011).

$$Q_{tot} = Q_{bypass} + Q_A$$

$$Q: Q_1 \rightarrow Q_{tot}$$

Flow rate efectively pumped (liquid): $Q_1 \rightarrow Q_A$

Variation of rotation velocity of the impeller

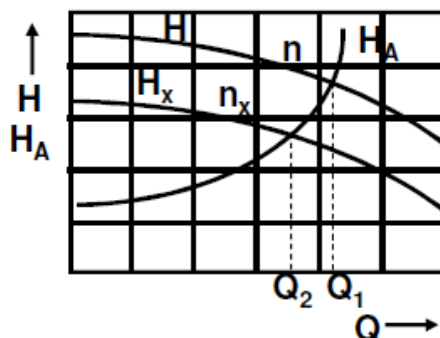


Figure 236 – Variation of the rotation velocity of the impeller (Pinho et al., 2011).

By Similarity Laws (Pinho et al., 2011):

$$\frac{Q_X}{Q} = \frac{n_X}{n}; \frac{H_X}{H} = \left(\frac{n_X}{n}\right)^2$$

For small changes:

$$\left(\frac{\Delta n}{n} \leq 0,2\right) \rightarrow \eta \cong \text{cst.}$$

For big changes:

$$\eta_X \cong 1 - (1 - \eta) \left(\frac{n}{n_X}\right)^{0,1}$$

$$\frac{P_X}{P} \cong \frac{\eta}{\eta_X} \left(\frac{n_X}{n}\right)^3$$

Changing the impeller diameter (reduction)

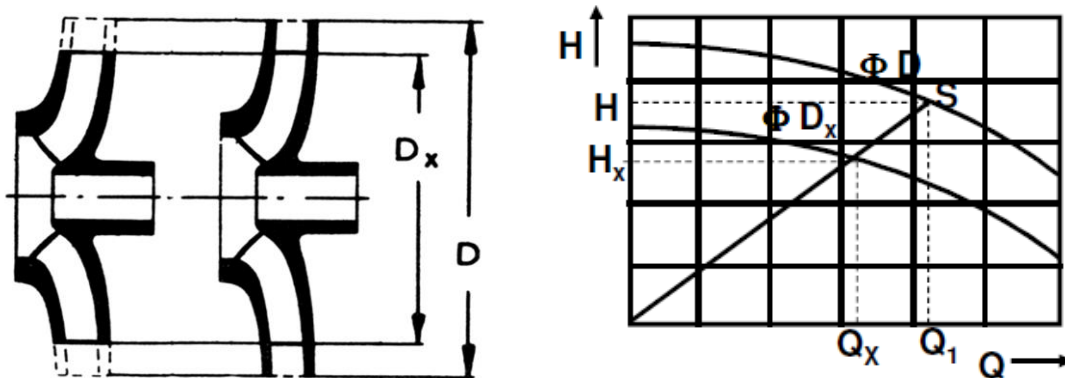


Figure 237 – Change of the impeller diameter (reduction) (Pinho et al., 2011).

$$\frac{Q_X}{Q} = \left(\frac{D_X}{D}\right)^2; \frac{H_X}{H} = \left(\frac{D_X}{D}\right)^2$$

By characteristic curves, it is possible to define **D_X** (Pinho et al., 2011):

1. Draw a line passing at the point ($Q = 0, H = 0$) and the operational point (S);
2. Using the values of Q and H of that point, the diameter (D_X) can be obtained from:

$$D_X \cong D \sqrt{\frac{Q_X}{Q}} \quad \text{or} \quad D_X \cong D \sqrt{\frac{H_X}{H}}$$

Such relations can be applied to small reductions of diameter. For great reductions of diameters, it is recommended to apply variation in stages (Pinho et al., 2011).

In order to avoid such actions of reduction in normal conditions of operation, the manufacturers already supply curves of H/Q , P/Q , η/Q for an original diameter and for a series of values D_x (Pinho et al., 2011).

Operation of pumps in pipes webs

Pipes or conduit of branched compression

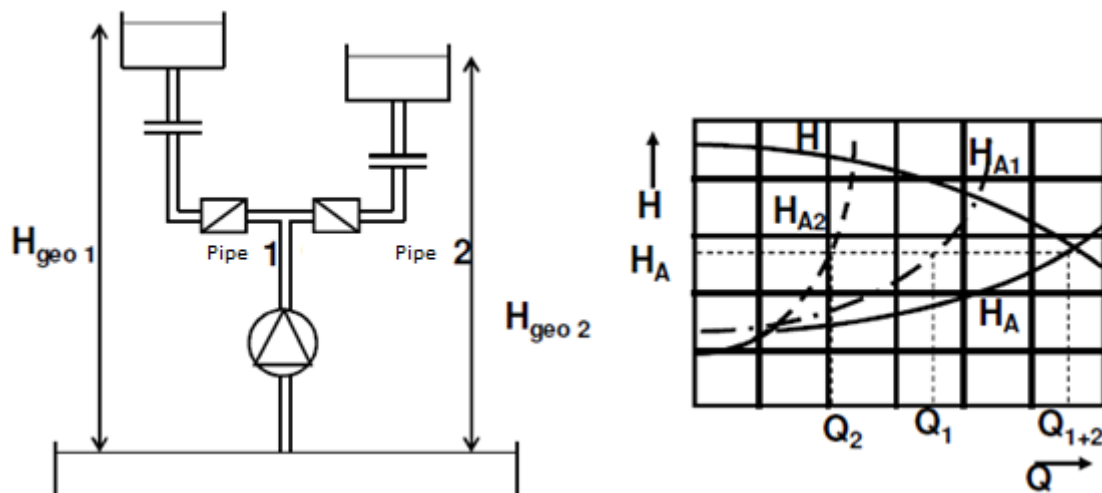


Figure 238 – Pipes or conduits of branched compression (Pinho et al., 2011).

If H_{est} were different, it must be set a retention valve to avoid draining of one reservoir after pumps shutdown (Pinho et al., 2011).

Operation of parallel pumps with common pipes

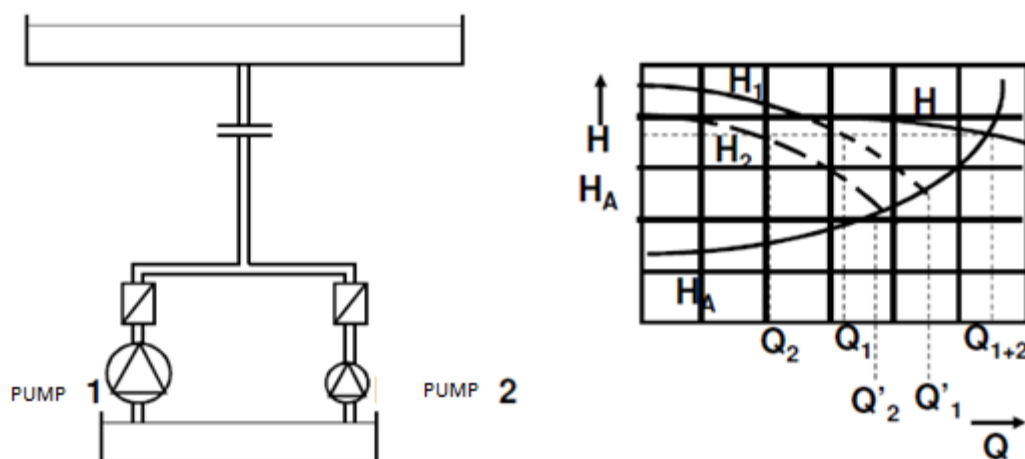


Figure 239 – Operation of parallel pumps with common pipe (Pinho et al., 2011).

A common curve (H/Q) is obtained by adding both flow rate (Q_1 and Q_2) of each pump for the same elevation height. **Note:** $Q'_1 > Q_1 \wedge Q'_2 > Q_2$ (Pinho et al., 2011).

Operation of pumps in serial connection at same pipes

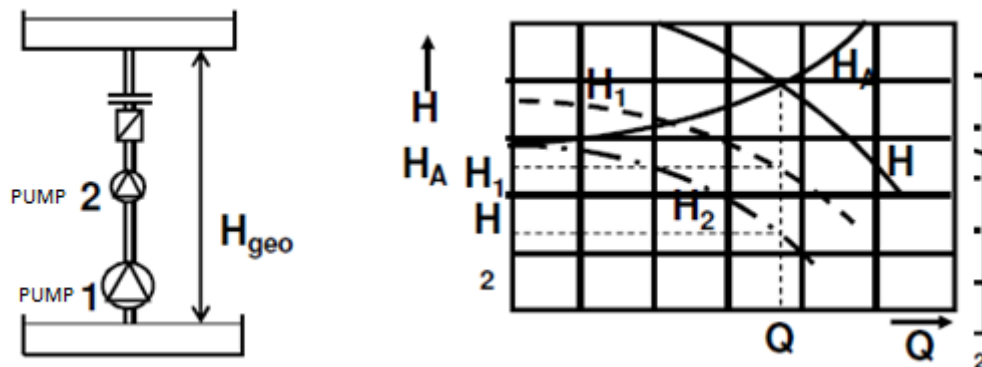


Figure 240 – Operation of pumps in serial connection at same pipes (Pinho et al., 2011).

A common curve (H/Q) is obtained considering the **total elevation height as the summation of all elevations heights** (H_1 and H_2) of each pump for the same **flow rate** (Pinho et al., 2011).

It is the principle of conceptions of multicellular pumps (stage pumps), which possess multiple impellers in series, at same axis, allowing to achieve **higher elevations heights** (Pinho et al., 2011).

In case of different pumps, the implanted order must ensure that the **lower NPSH value** are set first in the series, or in an increasing order (Pinho et al., 2011).

10.2.3 Selection of adequate pumps at some installation

The selection of a pump adequate for a certain installation must consider next aspects (Mata-Lima, 2010):

- The fields/domains of application of centrifugal pumps, axial and mixed (Figure 241):
 - Centrifugal pumps - Residential installations, boilers feeding, deep well, of process, chemical, re-circulation, petrochemical, sewers, effluents, fire-systems, condensing systems, etc.;
 - Axial pumps - Continuous circulation of corrosive/abrasive, abrasive pulps of brine of procedure wastes, process of evaporation and re-crystallization (brines, see water), salt factories, diverse chemicals factory, treatment and regenerations plants;
 - Mixed pumps - it is an intermediate case between radial and axial pumps, according trajectory or even its application domain;

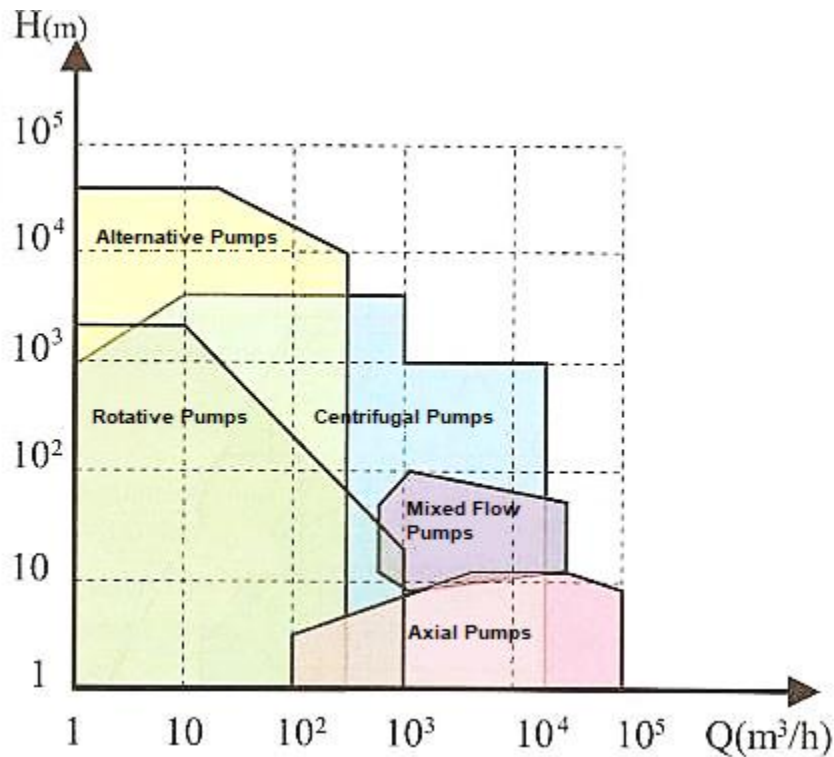


Figure 241 – Field of pump application (Henn, 2006).

- Specific number of rotations;
- Diagram of pump operation (hill diagram, Figure 242);

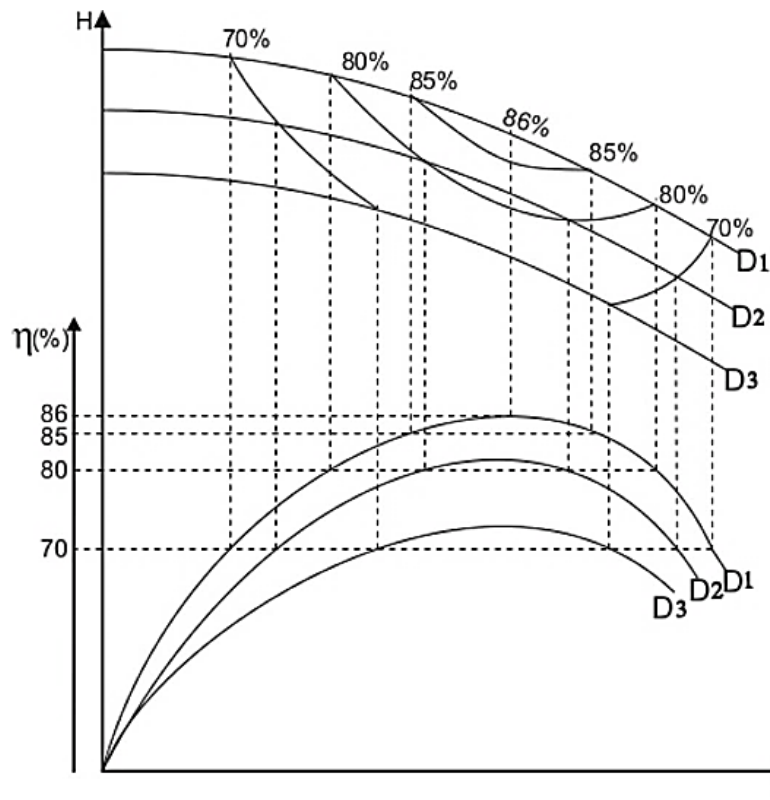


Figure 242 – Example of a hill diagram (<http://www.escoladavida.eng.br/mecfluquimica/aulasfei/ccb.htm>).

- Mosaic of pump uses (Figure 243). After defining flow rate, the total elevation height and rotation velocity, can be use a mosaic of pumps uses to pre-select a pump;

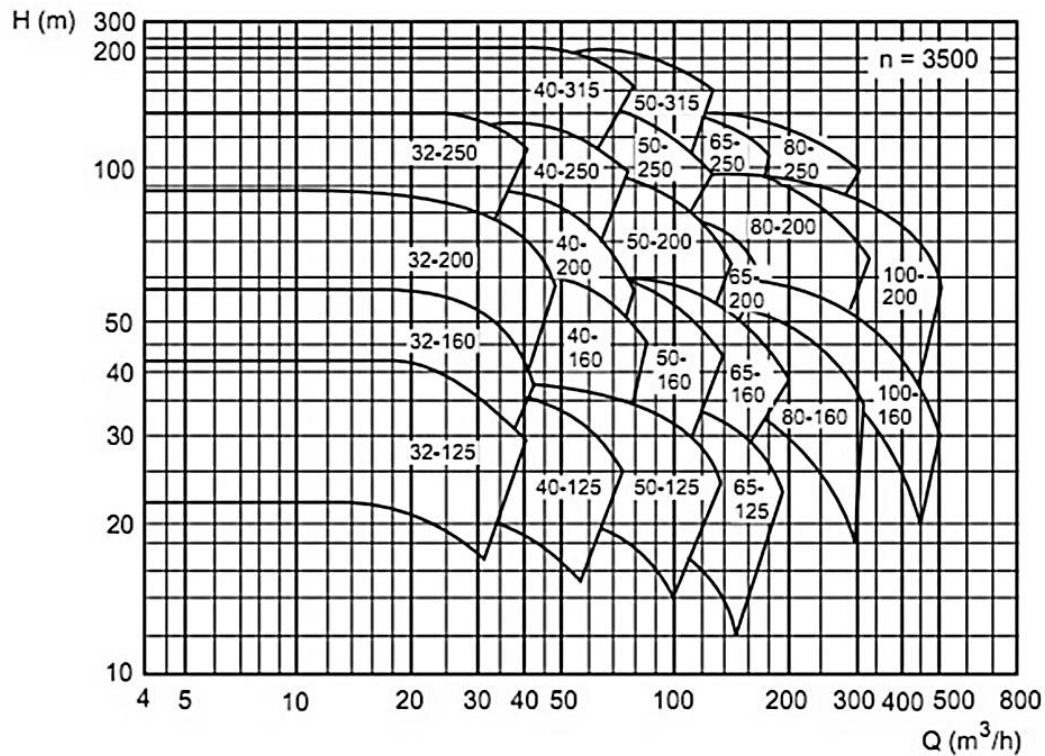


Figure 243 – Example of mosaics of pumps uses, to pre-selection of a pump (adapted from *Catálogo das Bombas KSB*).

- But final decision of the pump and its impeller diameter is based in the hill diagram of the pre-selected pump.

The last-mentioned details, that now a days is supplied by pumps catalogues. In case of doubt, the manufacturer must be contacted to obtain more information (Mata-Lima, 2010).

CHAPTER 11 - FLOWS WITH A FREE SURFACE

11.1 Generalities

Flows with a free surface are a liquid flow that is partially confined by solid walls, and a surface contacting the atmosphere or other gas (Figure 244).



Figure 244 – Levada das 25 Fontes, Calheta. Channel (solid walls); Water (with a free surface) (Origin: Autor).

Application:

- Irrigation;
- Draining Systems;
- Sewers (Residual and Pluvial);
- Water Supply;
- Hydroelectrical Exploitation.

Branch of Study:

- Permanent Movement (Uniform, Varied);
- Fixed beds.

11.1.1 Flows Classifications

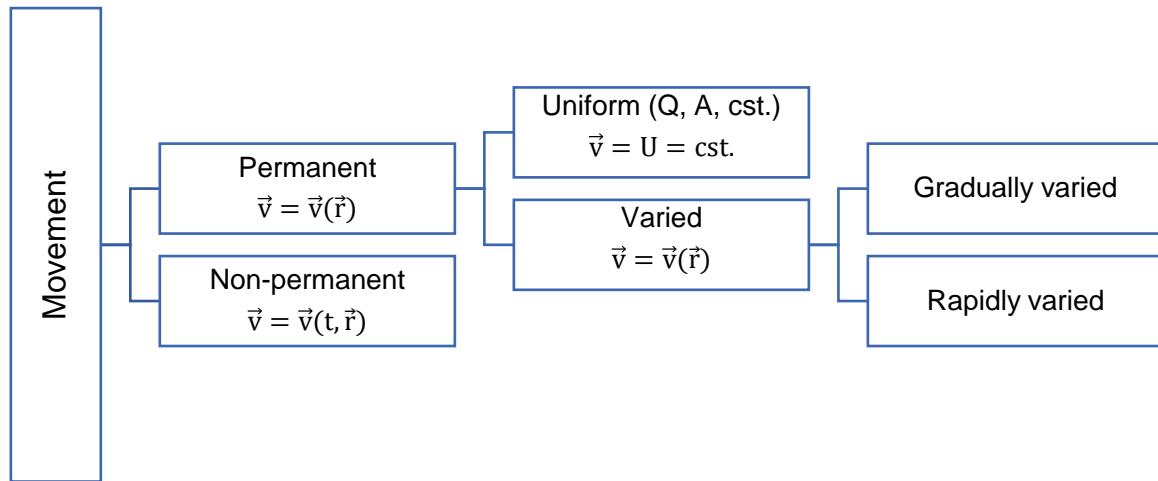


Figure 245 – Classification of flows.

Uniform Movement:

- Section (A) and flow rate (Q) constants;
- Free surface parallel to the bottom (due to $A = \text{cst.}$);
- Can be found in prismatic channels (or cylindrical);
- The channel is inclined in flows orientation (Bottom // Piezometric // Energy Line);
- Wet or sunken section: section of flow limited by the free surface and by the channel section under such free surface plain (F.S.).

Varied Permanent Movement:

- The average velocity (U) is not constant;
- It is verified a constant flow rate (Q) and variable area (A), or variable flow rate (Q) and variable area (A);
- With a constant flow rate (Q) and prismatic section, such movement will tend to become a uniform movement when is quite separated from any singularity.

Permanent Movement Gradually Varied:

- The fillets stay straight;
- The velocities are approximately normal at straight sections;
- The distribution of pressures is hydrostatics;
- Backwater's Curve - Longitudinal profile of the free surface of a permanent flow gradually varied. Such study includes:
 - Backwater in prismatic channels with constant flow rate;
 - Backwater in prismatic channels with variable flow rate in space;

- Backwater in non-prismatic channels with constant flow rate;
- Backwater in non-prismatic channels with variable flow rate in space.

Permanent Movement Rapidly Varied:

- The fillets have an appreciable curvature;
- Non-hydrostatic distribution of pressure;
- It is found at small sections of the channel, frequently associated to zone of regime gradually varied.

Non-Permanent Movement:

- Variation of the section (A) and flow rate (Q);
- Can be highly or gradually varied.

11.1.2 Types of channels



Natural Channels (Caldeirão Verde, Santana)

- The hydraulic properties are difficult to define due to their irregularity;
- Empirical hypotheses are frequently used;
- Must be supported by knowledge of hydrology, geomorphology, sediment transport;
- Examples: Torrents, Rivers and Creack, Estuary Mouth, Free Surface Underground Flows (Fluvial Hydraulics).



Artificial Channels (João Gomes and Santa Luzia river mouth, Funchal)

- The application of hydraulic theories leads to results that can be considered satisfactory considering what happens in practice;
- Examples: Navigation, Irrigation, Drainage, Collectors.

Figure 246 – Types of channels (Origin: author).

11.1.3 Geometry of a channel

The **Section of the channel** is normal to the current lines (straight section in linear flows), while the **vertical section of the channel** is the section in a vertical plain that contains a point located at the lowest elevation in the section (Figure 247).

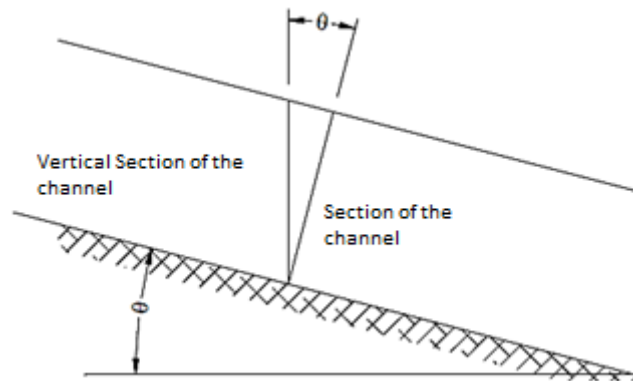


Figure 247 – Representation of the type of channel section (adapted from Costa & Lança, 2011).

Note: when θ is small, the vertical section coincides with the channel section.

Natural Channels (irregular sections):

- Parabolic or Trapezoidal;
- Minor Bed (normal flow rates);
- Mayor Bed (floods flow rates).

Artificial Channels (regular sections):

- Trapezoidal (common in open channels at terrain);
- Rectangular (stable margins);
- Triangular (ditches);
- Circular (collectors);
- Others (collectors of great dimensions).

Geometrical Characteristics of the Longitudinal Profile

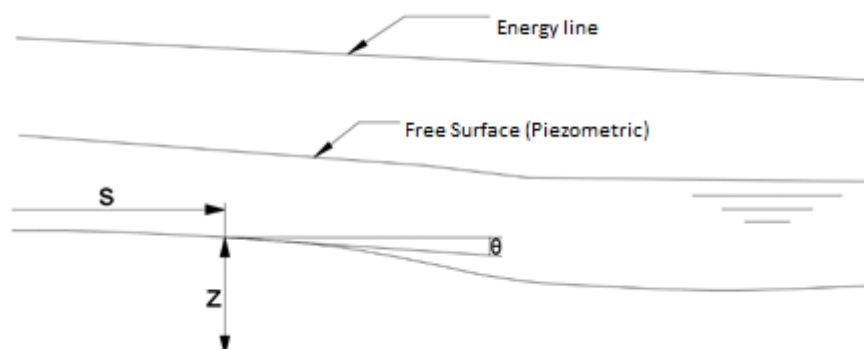


Figure 248 – Representation of the geometrical characteristics in a longitudinal profile.

Note: i – Slope of the channel; $i = \tan \theta$; $\sin \theta = -\frac{\partial z}{\partial s}$.

Geometrical Characteristics of Plain Sections

The properties of a section in a flow can be completely defined by the geometry of the channel section and by the flow deepness (Figure 249 and Figure 250).

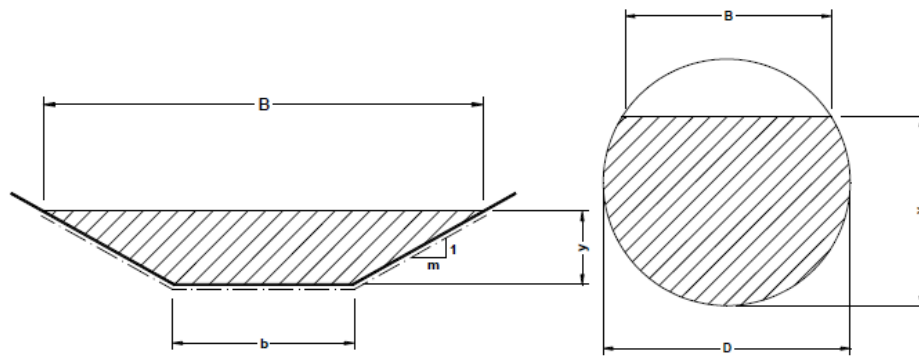


Figure 249 – Representation of the geometric characteristics in a plain section (Costa & Lança, 2011).

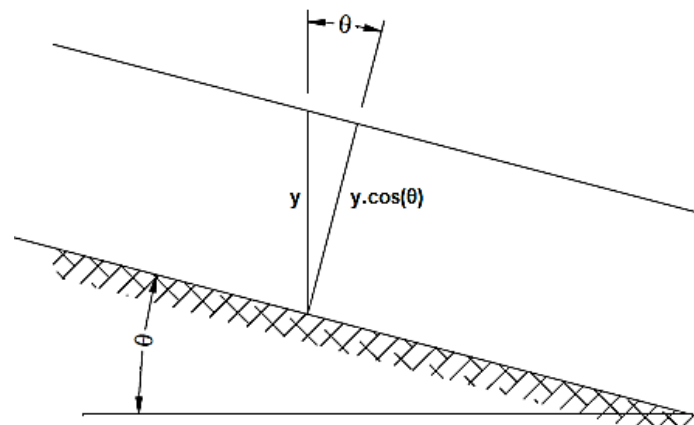


Figure 250 – Water heights and slope of the section (adapted from Costa & Lança, 2011).

About the last two figures, it is defined:

- **Superficial width of the flow** is indicated by **b**;
- **The area of the transversal section (S)** is the area of the section normal to the fillets;
- **Sunken or wet perimeter (X)** is the development of the curve according to the contact of the liquid with the solid walls of the section;
- **Hydraulics ray or ratio (R)** is the ratio between the area of the transversal section (wet area) and the sunken or wet perimeter:

$$R = \frac{S}{X}$$

- **The deepness of water height in the section ($y \cos \theta$)** is the distance measured in the channel section according to the line with major slope between the free surface and the bottom;
- **The deepness or water height in the channel (y)** is the vertical distance between the bottom in the section and the considered free surface;
- **The average deepness or hydraulic deepness (y_m)** is the ratio between the transversal section and the superficial width:

$$y_m = \frac{S}{b}$$

Relations between the geometrical characteristics of the rectangular sections

Channels of Rectangular Section:

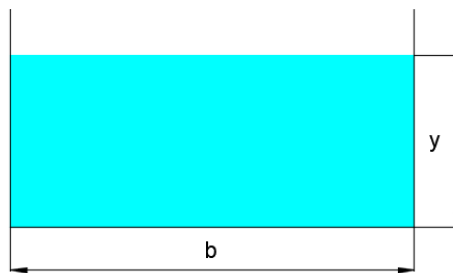


Figure 251 – Rectangular section of the channel.

$$S = by$$

$$X = b + 2y$$

$$y_m = y$$

$$R = \frac{y}{1 + 2\frac{y}{b}}; \text{ With } b \gg y, \frac{y}{b} \rightarrow 0 \rightarrow R \cong y$$

Channels of Trapezoidal Section:

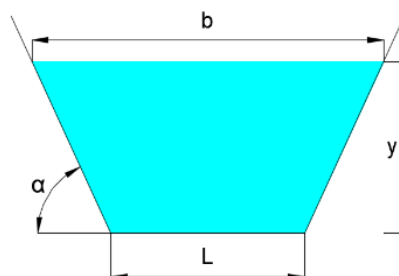


Figure 252 – Channel of trapezoidal section.

$$b = L + \frac{2y}{\tan \alpha}$$

$$S = \left(L + \frac{y}{\tan \alpha} \right) y$$

$$X = L + \frac{2y}{\tan \alpha} \sqrt{\tan^2 \alpha + 1}$$

$$y_m = \frac{L \tan \alpha + y}{L \tan \alpha + 2y} y$$

$$R = \frac{L \tan \alpha + y}{L \tan \alpha + 2y \sqrt{\tan^2 \alpha + 1}} y$$

Circular Section of the Channel:

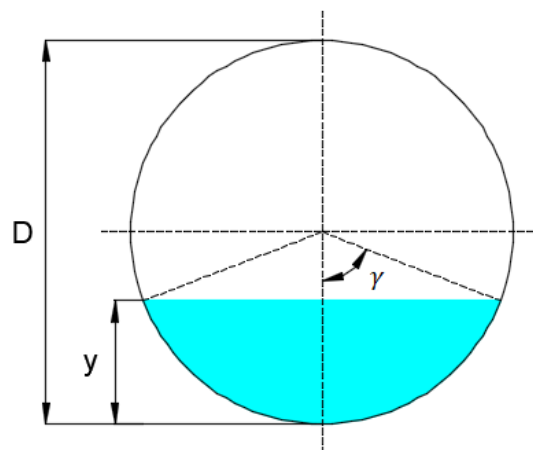


Figure 253 – Circular section of the channel.

$$b = D \sin \gamma \text{ (} \gamma \text{ in radians)}$$

$$y = \frac{D}{2} (1 - \cos \gamma)$$

$$S = \frac{\pi D^2}{4} \frac{2\gamma}{2\pi} - b \frac{D}{4} = \frac{D}{4} (D\gamma - b \cos \gamma) = \frac{D^2}{4} (\gamma - \sin \gamma \cos \gamma) = \frac{D^2}{8} [2\gamma - \sin(2\gamma)]$$

$$X = Dy$$

$$y_m = D \frac{2\gamma - \sin(2\gamma)}{8 \sin(\gamma)}$$

$$R = D \frac{2\gamma - \sin(2\gamma)}{8\gamma} \text{ or, for a full filled section, } R = \frac{D}{4}$$

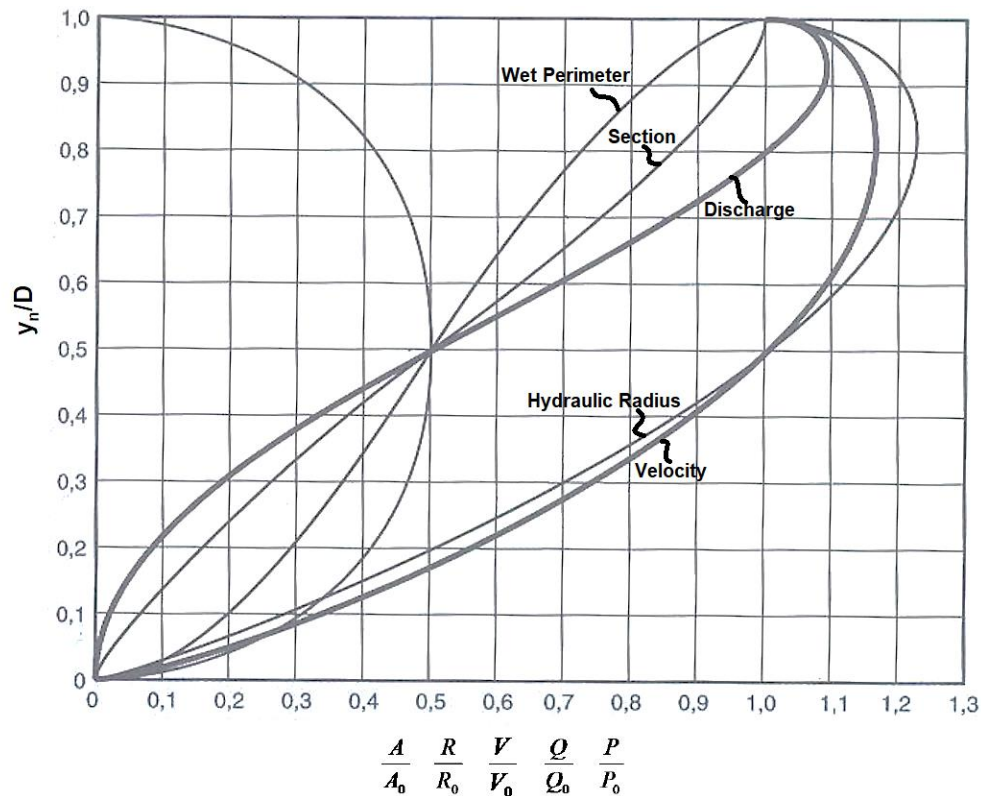


Figure 254 – Channel's circular section (geometrical relations) (adapted from Netto, 1998).

Note: Geometric elements in dimensionless coordinates referred to D and the corresponding values of a full filled section.

Relations between the geometrical characteristics of irregular sections

Graphical relations between characteristic parameters (P):

It is measured or calculated after the measurements, the values of P_i corresponding to different value of y_i . Example:

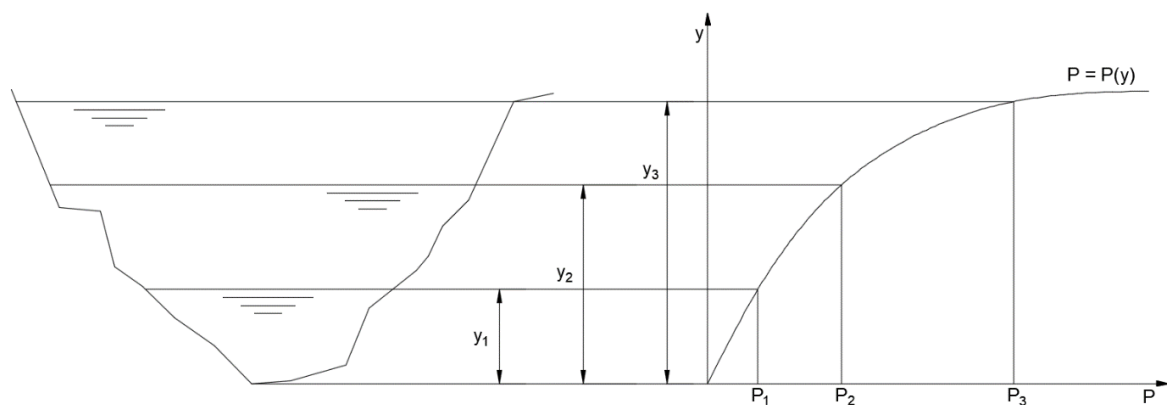


Figure 255 – Irregular section of the channels (graphical relationship).

Use of complex numerical relations in computers for lower beds of natural channels by the monomial form:

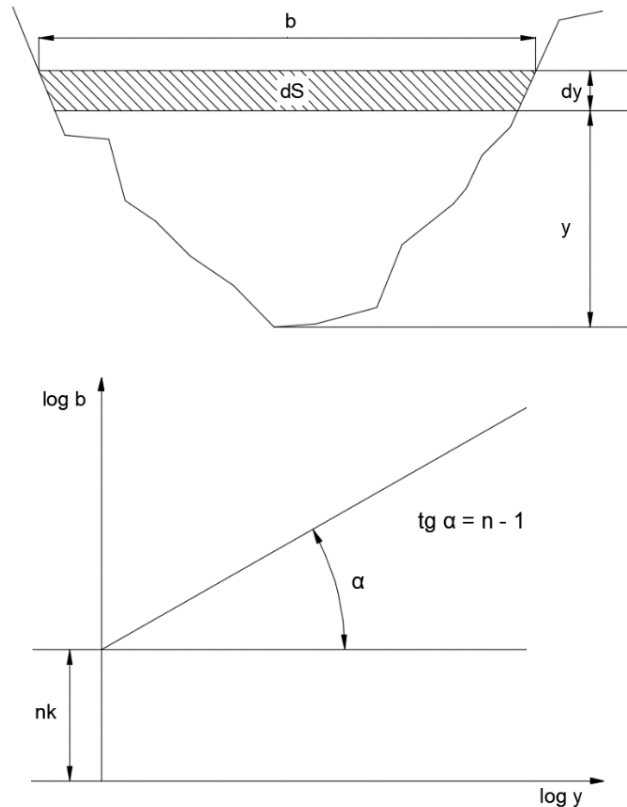


Figure 256 – Irregular section of the channel (relationship through a monomial form).

$$S = ky^n$$

Where k, n are parameters depending in the section configuration.

$$b = \frac{dS}{dy}$$

By connecting the last formula with $S = ky^n$, it is obtained:

$$b = Kny^{n-1}$$

$$\log b = \log nK + (n - 1) \log y$$

In order to obtain **n** and **k**, it is enough to have the corresponding values of **b** and **y** and obtain in a logarithmic scale a line with angular coefficient of **n – 1** value and ordered at origin in **nk**.

11.2 Applications of the Bernoulli's theorem to Flow with free surface

11.2.1 Expression of the Bernoulli's theorem

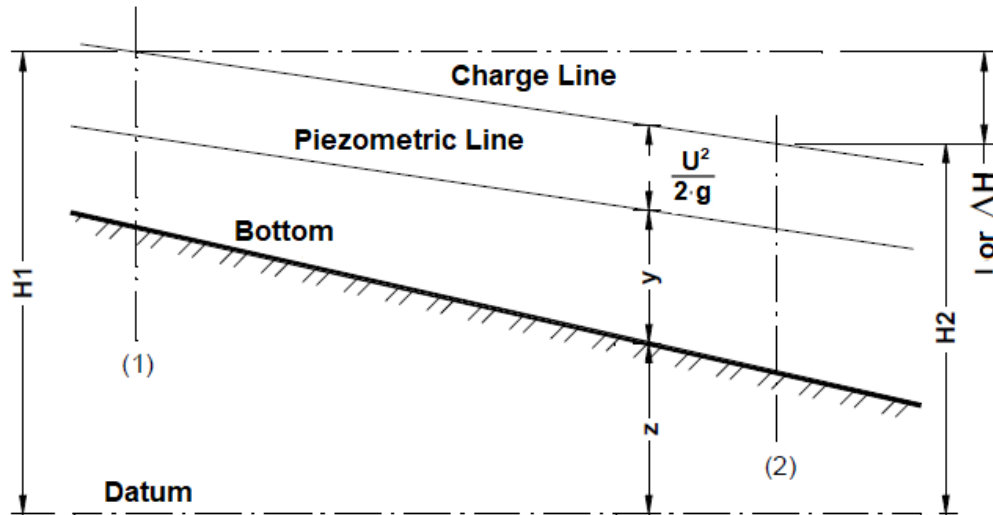


Figure 257 – Representation for deduction of Bernoulli's Theorem simplification (Costa & Lança, 2011).

$$\frac{\partial}{\partial s} \left(z + \lambda y + \frac{\alpha U^2}{2g} \right) = -\frac{1}{g} \frac{\partial}{\partial t} (\alpha U) + \frac{\partial H}{\partial s}$$

Where:

- $\lambda = \beta \cos \theta$ is the coefficient of the pressure distribution;
- β is the Jaeger coefficient (Centrifugal Forces);
- α is the coefficient of kinetic energy;
- α' is the coefficient of amount of movement.

At such case the following simplifications are applied:

- Hydrostatic distribution of pressure in the transversal section;

$$\beta = 1 \Rightarrow \frac{\partial}{\partial s} \left(z + y \cos \theta + \frac{\alpha U^2}{2g} \right) = -\frac{1}{g} \frac{\partial}{\partial t} (\alpha U) + \frac{\partial H}{\partial s}$$

- Permanent movement:
 - Hydrostatic distribution of pressure (linear flows);

$$z_1 + y_1 \cos \theta_1 + \frac{\alpha_1 U_1^2}{2g} - \left(z_2 + y_2 \cos \theta_2 + \frac{\alpha_2 U_2^2}{2g} \right) = \Delta H$$

- Non-hydrostatic distribution of pressure.

$$z_1 + \beta_1 y_1 \cos \theta_1 + \frac{\alpha_1 U_1^2}{2g} - \left(z_2 + \beta_2 y_2 \cos \theta_2 + \frac{\alpha_2 U_2^2}{2g} \right) = \Delta H$$

11.2.2 Distribution of pressure in the transversal section

Refers to the pressure measured by the height achieved by the column of water at a piezometric tube installed at a certain section perpendicular to fillets.

Rectilinear Flows

Different to the flows under pressure, where the pressure is considered constant in the transversal section of the conduit or pipe, but in case of flows with free surface exists a great variation of the pressure according to the deepness. It is considered that the distribution of pressure in the section obey the Stevin's law (hydrostatic pressure) and its acceleration component (Centrifugal force, $F_c = 0$) (Soares, 2011).

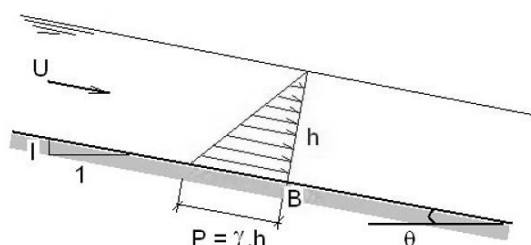


Figure 258 – Distribution of pressures in the transversal section, rectilinear flow (Soares, 2011).

For $I < 10\%$ consider pressure approximately equal to the hydrostatics ($P = \gamma h$).

For $I > 10\%$ must be consider the angle of slope, which means, pseudo-hydrostatic pressure ($P = \gamma h \cos^2 \theta$) (Soares, 2011).

Non-Rectilinear Flows

In a case where the curvature of the current line in vertical orientation is significant, as in the case of the spillways, showing a curved flow, which have changes in the hydrostatical distribution of pressures forcing to use a factor of correction to determine the flow pressure (Soares, 2011).

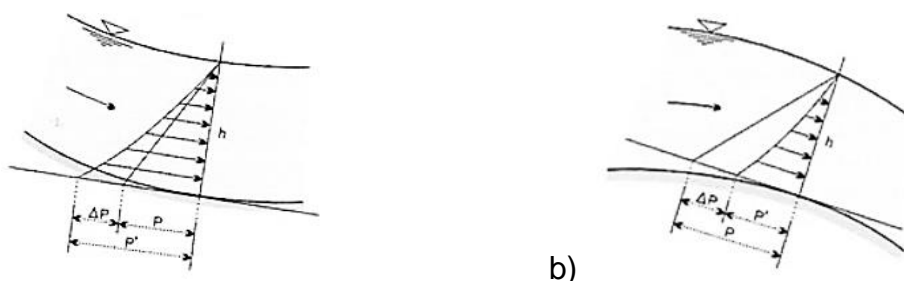


Figure 259 – Distribution of pressures in the cross-section, concave (a) and convex flow (b) (Soares, 2011).

In concave flows is observed an additional pressure (ΔP), $P' = P + \Delta P$. And in the convex flows is observed a sub pressure (ΔP) or reduction of pressure in comparison to the static pressure, $P' = P - \Delta P$. ΔP it is determined using the following expression (Soares, 2011):

$$\Delta P = \frac{\gamma h}{g} \cdot \frac{U^2}{r}$$

Where:

P' is the resultant corrected pressure;

P is the hydrostatic pressure;

γ is the specific weight of the water;

g is the gravitational acceleration;

U is the average velocity or speed of the flow;

r is the curvature radius of the fluid.

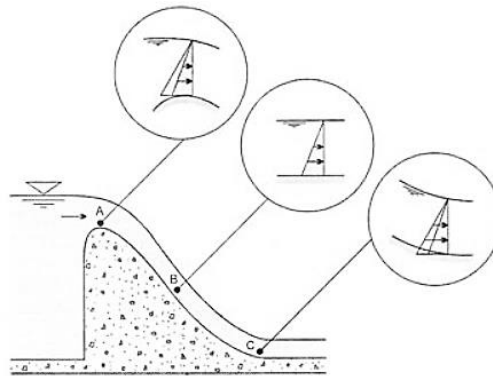


Figure 260 – Example of a non-rectilinear flow, spillway (Soares, 2011).

11.2.3 Distribution of velocity in the transversal section

The velocities of the varied liquid fillets at a cross-section of a channel are affected by:

- **Influence of the Walls** (Friction-Retardant Action);
- **Free Surface** (Superficial Tension and Air Resistance).

The velocity is major in the fillets most distant from the walls and bottom of the channel. The curves, geometric place of the point with same velocity are called Isotactics (Figure 261).

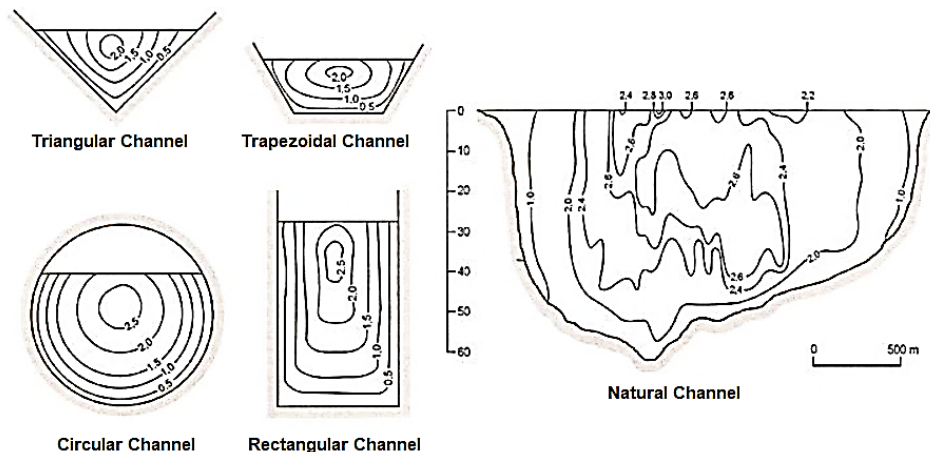


Figure 261 – Isotactics curves for different sections (adapted from Soares, 2011).

Distribution of velocities at a transversal section

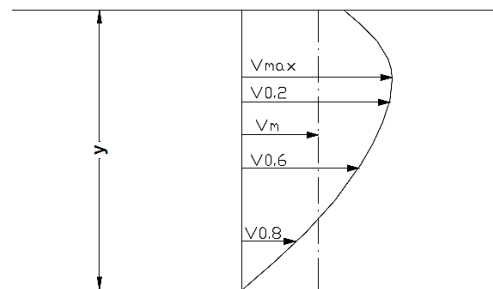


Figure 262 – Distribution of velocities (Costa & Lança, 2011).

The maximum velocity (v_{max}) at a vertical transversal section has values between $0.05y$ and $0.25y$ (Costa & Lança, 2011).

The average velocity (v_m) which is used in the flow rate calculus, it is the average of the velocity at deepness $0.20y$ and $0.80y$, which means, the velocity at deepness $0.6y$ ($v_{0.6}$). However, exists scientist that consider as more accurate the average of the deepness (Costa & Lança, 2011):

$$v_m = (v_{0.2} + v_{0.8} + 2v_{0.6})/4$$

Distribution of flow rate at a transversal section

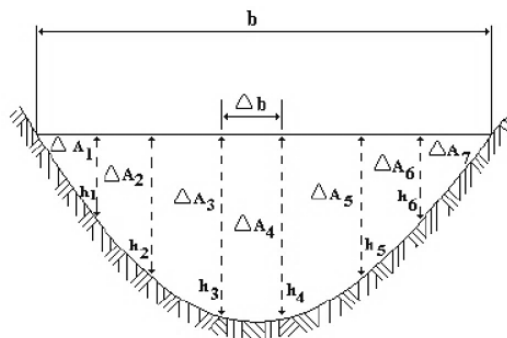


Figure 263 – Distribution of flow rate (http://www.escoladavida.eng.br/mecflubasica/aula2_unidade3.htm).

By deducing the average velocities and by using the next equation,

$$Q = \sum v_i \cdot A_i$$

it is possible to determine the flow rate in flows with free surface as for example, in rivers. To show how to apply such application, consider a transversal section of a river represented in the Figure 263, where the flow rate is calculated by:

$$Q = \sum_{i=1}^n v_i \cdot \Delta A_i$$

The equation applicated to such figure, results in:

$$Q = \left(v_1 \cdot \frac{h_1 \cdot \Delta b}{2} \right) + \left(\frac{v_1 + v_2}{2} \cdot \frac{h_1 + h_2}{2} \cdot \Delta b \right) + \left(\frac{v_2 + v_3}{2} \cdot \frac{h_2 + h_3}{2} \cdot \Delta b \right) + \left(\frac{v_3 + v_4}{2} \cdot \frac{h_3 + h_4}{2} \cdot \Delta b \right) + \left(\frac{v_4 + v_5}{2} \cdot \frac{h_4 + h_5}{2} \cdot \Delta b \right) + \left(\frac{v_5 + v_6}{2} \cdot \frac{h_5 + h_6}{2} \cdot \Delta b \right) + \left(v_6 \cdot \frac{h_6 \cdot \Delta b}{2} \right)$$

11.2.4 Energy losses. Resistance formulas

General expression of the resistance formulas:

$$h_f = \Delta H = f \frac{L}{4R} \frac{U^2}{2g}$$

$$f = f \left(\frac{4UR}{v}, \frac{U^2}{4gR}, \frac{k_1}{4R}, \frac{k_2}{4R}, \dots, \frac{k_n}{4R} \right)$$

Laminar regime:

$$f = \frac{C_1}{Re}, \text{ with } Re = \frac{4UR}{v}$$

Turbulent regime (more usual). Empiric formulas (Chézy, Manning-Strickler)

A – Formulas of Chézy type:

$$U = \sqrt{8g/f} \sqrt{R(\Delta H/L)}$$

$$\text{With } C = \sqrt{8g/f} \rightarrow U = C \sqrt{R(\Delta H/L)}$$

$$\text{With } J = \Delta H/L \rightarrow U = C \sqrt{RJ}$$

Uniform Regime:

$$U = C \sqrt{R \sin \theta}$$

With a small θ :

$$U = C \sqrt{Ri}$$

Where, i is the slope of the bottom.

Bazin Formula:

$$C = \frac{87\sqrt{R}}{C_B + \sqrt{R}}$$

Where C_B is in function on the type of channel walls (Table 39).

Table 39 – Values of C_B in function of the type of channel walls.

Nature of the Walls	$C_B [m^{1/2}]$
Channels of smooth concrete	0.06
Channels of not-straightened concrete or well-regular masonry	0.16
Channels of well regular soil or regular masonry	0.45
Channels of irregular soil or irregular masonry	0.85
Channels of irregular soil with vegetation, regular water courses in rocks beds	1.30
Channels in soils with vegetation at bottom and walls or water courses with pebble	1.75

Kutter Formula:

$$C = \frac{100\sqrt{R}}{C_K + \sqrt{R}}$$

Where C_K is in function of the nature or type of channels walls (Table 40);

Table 40 – Values of C_K in function of the nature or type of walls.

Nature of the Walls	$C_K [m^{1/2}]$
Channels of smooth concrete with semi-circular section	0.12
Channels of smooth concrete with rectangular section	0.15
Channels of well-regular masonry	0.25
Channels of ordinary masonry	0.35
Channels of irregular masonry	0.55
Channels of regular soil without vegetation	1.25-1.50
Channels of barely care soil with vegetation	1.75-2.00

Ganguillet-Kutter Formula:

$$C = \frac{23 + \frac{0.00155}{J} + \frac{1}{n}}{1 + \left(23 + \frac{0.00155}{J}\right) \frac{n}{\sqrt{R}}}$$

Where $n = 1/K$, being K the coefficient of the formula of Manning-Strickler.

Formula of Thijssse:

Table 41 – Formulas of Thijssse for C , in function of the flow's regime.

Regime	Formula
Smooth	$C = 18 \log 3Re/C$
Rough	$C = 18 \log 12R/K$
Transitional	$C = -18 \log(C/3Re + K/12R)$

Formula of Powell:

Table 42 – Formulas of Powell for C , in function of the flow's regime.

Regime	Formula
Smooth	$C = 23 \log \frac{3.3Re}{C}$
Rough	$C = 23 \log \frac{R}{K}$
Transition	$C = -23 \log \left(\frac{C}{3.3Re} + \frac{K}{R} \right)$

Table 43 – Values of K in function of the material.

Nature	K [mm]
Channels of smooth concrete	0.06
Channels of not straightened concrete	0.30
Channels of straight and uniform soil	13
Channels of soil, drayed	33

Formula of Crump:

$$C = -\sqrt{32g} \log \left(\frac{0.0676K}{R} + \frac{0.222v}{R\sqrt{gR}} \right)$$

B – Formulas of Manning-Strickler:

$$U = KR^{2/3}J^{1/2}$$

$$\text{For channels with small slope : } U = KR^{2/3}i^{1/2}$$

Where K depends in the nature or type of walls, independently of the flow's conditions (in pressure or channel).

Table 44 – Values of K in function of the nature of the walls.

Nature	$K [m^{1/3}s^{-1}]$
Channels of walls coated with smooth mortar	100-90
Channels of smooth concrete	80
Channels of ordinary masonry	70
Channels of irregular soil, rough concrete or degraded masonry	60
Channels of irregular soil, with few vegetation or regular water courses in rock beds	50
Channels of degraded soil or water courses of pebble	40

C – Application of the resistance formulas to heterogeneous or complex sections:

The presented formulas are only valid for simple sections where tangential tensions are constants along the wet or sunken perimeter.

Composed Section:

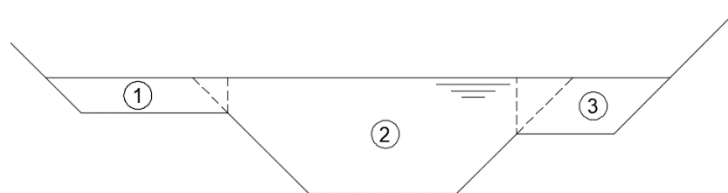


Figure 264 – Composed section.

Chézy's formula application:

$$Q = (C_1 S_1 \sqrt{R_1} + C_2 S_2 \sqrt{R_2} + \dots + C_n S_n \sqrt{R_n}) \sqrt{J}$$

Manning-Strickler's formula application:

$$Q = (K_1 S_1 R_1^{2/3} + K_2 S_2 R_2^{2/3} + \dots + K_n S_n R_n^{2/3}) \sqrt{J}$$

Heterogenous Section (different rugosities along the wet perimeter or sunken perimeter):

$$\chi = \sum_i \chi_i$$

Where χ_i represents parts of wet perimeter with different rugosities.

Using Chézy's formula:

$$J = \frac{U^2}{C^2 R} \rightarrow J = \frac{U^2}{S} \frac{\chi}{C^2}$$

If the coefficient of Bazin are used, for each part χ_l with coefficient C_{Bl} :

$$C_l = \frac{87\sqrt{R}}{C_{Bl} + \sqrt{R}}$$

For all the channel section:

$$J = \frac{U^2}{S} \sum_l \frac{\chi_l}{C_l^2} \text{ ou } C = \sqrt{\chi / \sum_l \frac{\chi_l}{C_l^2}}$$

Using the formula of Manning-Strickler:

The value of K is calculated by the formula of Einstein:

$$K = \left[\chi / \sum_l \frac{\chi_l}{K_l^{2/3}} \right]^{2/3}$$

Being K_l the coefficient of the formula of Manning-Strickler corresponding to a rugosity of a part with length χ_l .

11.2.5 Specific Energy

Specific Energy is the flows energy per unit of liquids weight referred to the bottom of the channel.

From Bernoulli's Theorem, it is obtained:

$$E = \beta y \cos \theta + \frac{\alpha U^2}{2g}$$

The expression of Bernoulli, turns into:

$$\frac{\partial}{\partial s} (z + E) = -\frac{1}{g} \frac{\partial}{\partial t} (\alpha' U) - J$$

Being $J = -\frac{\partial H}{\partial s}$ the energy losses per unit of length.

For descending channels (positive slope):

$$\frac{\partial z}{\partial s} = -\sin \theta$$

Where:

$$\frac{\partial E}{\partial s} = -\frac{1}{g} \frac{\partial}{\partial t} (\alpha' U) + \sin \theta - J$$

is the variation of the specific energy along the channel.

For permanent movement:

$$\frac{\partial E}{\partial s} = \sin \theta - J$$

For channels of small slope:

$$\sin \theta \cong \tan \theta = i$$

where i correspond to the channels slope.

The slope of the energy line is also small, and:

$$J \cong I_e$$

Where I_e correspond to the slope of the energy line.

For small slopes and hydrostatical pressures:

$$E = y + \frac{\alpha U^2}{2g}$$

11.2.6 Surfaces of energy

Definition of Specific Energy:

$$E = \beta y \cos \theta + \frac{\alpha U^2}{2g}$$

And being $Q = U \cdot S$, then:

$$E = \beta y \cos \theta + \frac{\alpha Q^2}{2gS^2}$$

So, defining:

$$\varphi(Q, E, y, s) = 0$$

As **hypersurface** in a space of four dimensions (Q, E, y, s) being s a function of y at a certain section. Fixed a certain section, the parameter s remains fixed, showing its influence through to β and α .

In case of a curvature of the liquid fillets being poorly accentuated, consider a hydrostatic distribution of pressure:

$$E = \beta y \cos \theta + \frac{\alpha Q^2}{2gS^2} \text{ or } F = (Q, E, y) = 0$$

Which represents and space of three dimensions (Q, E, y) representing an **energy surface** (Figure 265).

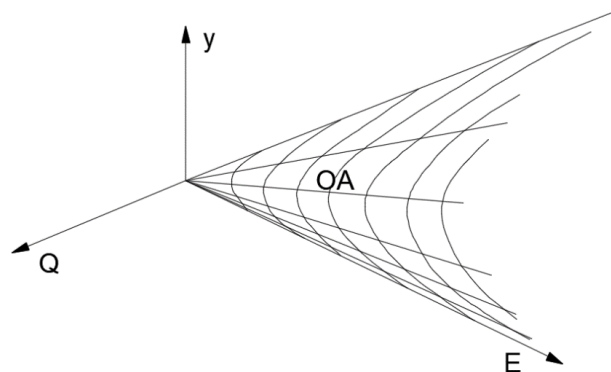


Figure 265 – Energy surface.

Where **OA** represents a uniform flow, where the parameters Q , E and y do not change, at a certain channel.

For $Q = \text{cte.}$ And $E = \text{cte.}$, are develop to types of curves of interest:

Variation of specific energy with the water height ($Q = Q_0 \text{ cte.}$):

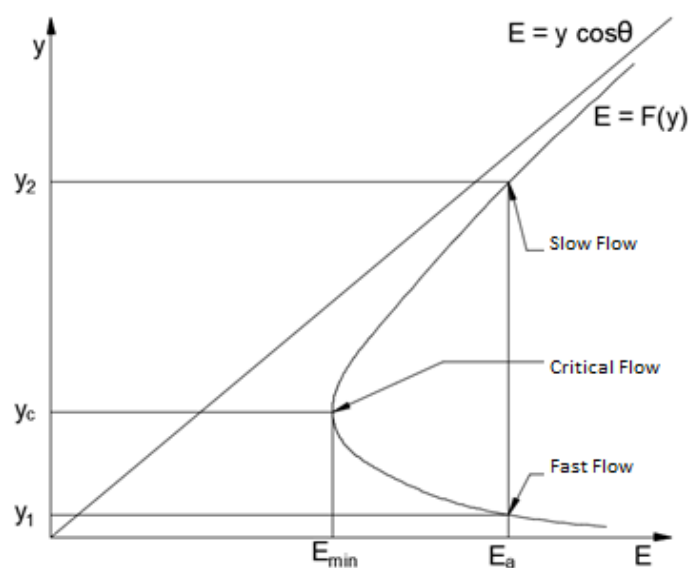


Figure 266 – Curve of energy variation with the water height.

As assíntotas da curva são $y = 0$ e $E = y \cos \theta$.

Variation of the flow rate with the water height ($E = E_0$ cte.):

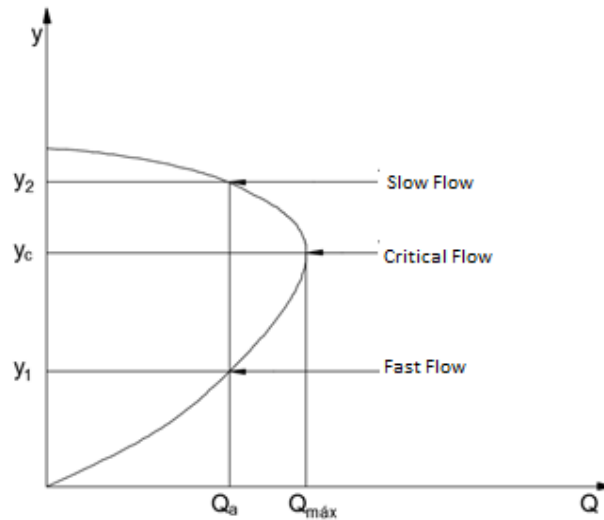


Figure 267 – Curve of flow rate variation with the water height.

$$Q = S\sqrt{2g(E_0 - y \cos \theta)}$$

11.2.7 Critical values

The **Critical Regime** is defined based in the variation laws of the water height: with E being $Q = \text{cte.}$; with Q being $E = \text{cte.}$.

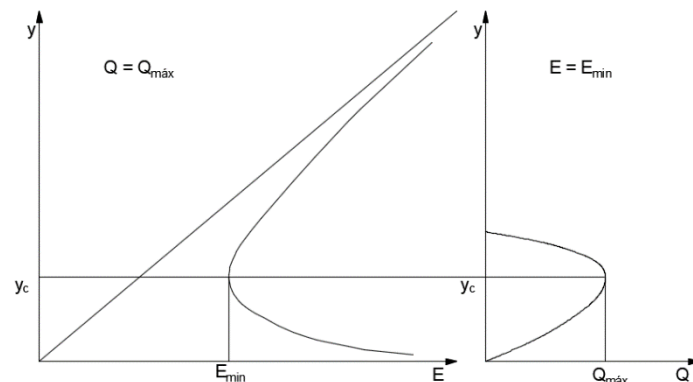


Figure 268 – Curve of flow rate and energy variation with the water height.

Critical values:

In critical regime:

$$\frac{Q}{\sqrt{g \cos \theta}} = S_c \sqrt{y_{mc} / \alpha_c}$$

In a simple way, for small slopes $\cos \theta = 1$; $\alpha = 1$:

$$\frac{Q}{\sqrt{g}} = S_c \sqrt{y_{mc}} \text{ or } \sqrt{g y_{mc}} = \frac{Q}{S_c} = U_c$$

Determination of the critical height:

By determining $Q/\sqrt{g \cos \theta}$ and $S\sqrt{y_m/\alpha}$

For $\alpha = 1$ and a regular section:

The equation is solved in **y** determining the **critical height**.

For channels of irregular section:

Graphical method: $S\sqrt{y_m/\alpha}$ in function of y : $\Psi(y) = S\sqrt{y_m/\alpha}$

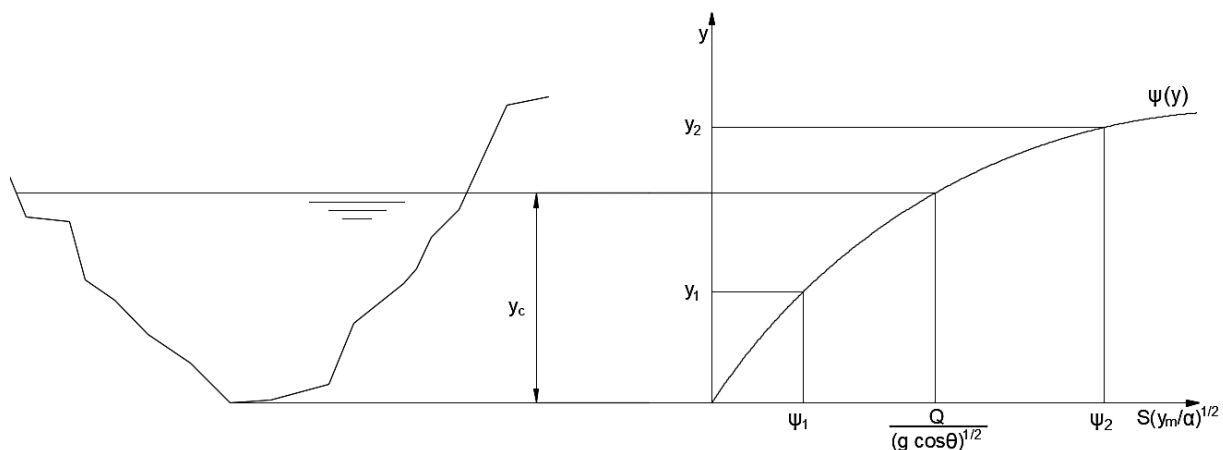


Figure 269 – Graphical method for the irregular section.

For channels of irregular section, where it is not possible to establish an analytical relationship between the parameters:

Numerical method that consists in determine a regression law adequate for pairs of values of **y** and capacity of transportation $\Psi(y)$. For example:

Newton's Method – Finding the zeros of a function:

$$\Psi(y) = \bar{\Psi}(y) - \frac{Q}{\sqrt{g \cos \theta}}$$

11.3 Application of theorem of amount of movement to flows of free surface

11.3.1 Principles and definitions

Amount of movement:

- Discreet medium:

$$\vec{P} = \sum_{i=1}^M m_i \vec{v}_i$$

- Continuous medium:

$$\vec{P} = \int_V \rho \vec{v} dV$$

Theorem of Amount of Movement:

If the total mass of the system,

$$m = \sum_{i=1}^M m_i = \text{cst.} \frac{d\vec{P}}{dt} = \sum_{i=1}^n \vec{F}_i$$

The derivative respect time of the amount of movement of a system of particles is equal to the summation of the external forces applied to such system.

General expression of the Theorem of Amount of Movement:

$$\int_S \rho \vec{v} (\vec{v} \cdot \vec{n}) dS = - \int_V \frac{\partial}{\partial t} (\rho \vec{v}) dV + \int_V \rho \vec{G} dV + \int_S \vec{T} dS$$

Where:

$\vec{M} = d\vec{P}/dt = \int_S \rho \vec{v} (\vec{v} \cdot \vec{n}) dS$, represents the **quantity of movement flowed through the surface of control (S)** per unit of time, and $\vec{M} = \vec{M}_1 - \vec{M}_2$, shows the differences between the amount of movement that leaves or abandon the system (M_1) and the amount of movement that comes or enters the system (M_2) in a considered volume, per unit of time;

$\vec{I} = \int_V \frac{\partial}{\partial t} (\rho \vec{v}) dV$, represents the **integral of the local density of the mass flow**. It is equal to the main vector of the inertial local forces system when it is an incompressible fluid and is null for a permanent flow;

$\int_V \rho \vec{G} dV$, represents the **main vector of mass forces** that acts over the contained fluid inside the surface of control;

$\int_S \vec{T} dS$, represents the **resultant of the tensions acting along the surface of control**, by the surrounding fluid or by solid walls in contact with such fluid.

11.3.2 Total amount of movement. Specific force

Consider permanent flows (or non-permanent with a slow variation of magnitudes in time),

$$\int_V \frac{\partial}{\partial t} (\rho \vec{v}) dV = 0$$

Then:

$$\int_S \rho \vec{v} (\vec{v} | \vec{n}) dS = \int_V \rho \vec{G} dV + \int_S \vec{T} dS$$

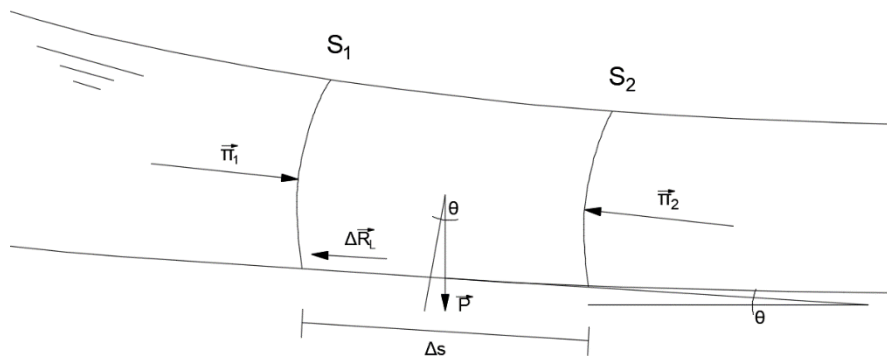


Figure 270 – Theorem of amount of movement in the direction of flow.

Applying the theorem of amount of movement, with an expression projected in the direction of the flow (considering Δs as straight line and Δs small):

$$\left[\int_S \rho \vec{v} (\vec{v} | \vec{n}) dS \right]_S = -\alpha'_1 \rho Q_1 U_1 + \alpha'_2 \rho Q_2 U_2 = -\alpha'_1 \rho \frac{Q_1^2}{S_1} + \alpha'_2 \rho \frac{Q_2^2}{S_2}$$

$$\left[\int_V \rho \vec{G} dV \right]_S = P \sin \theta = \gamma S \sin \theta \Delta s$$

Where:

S is the average of S_1 and S_2 ;

x_1 and x_2 are the projections of the pressure forces applied in S_1 and S_2 .

$$\left[\int_S \vec{T} dS \right]_S = \pi_1 - \pi_2 - \Delta R_L$$

Where, ΔR_L is the projection of the resultant forces (normal and tangential) applied in the bed of the channel.

Then:

$$-\alpha'_1 \rho Q_1 U_1 + \alpha'_2 \rho Q_2 U_2 = \gamma S \sin \theta \Delta S + \pi_1 - \pi_2 - \Delta R_L$$

or

$$\Delta M = M_2 - M_1 = \gamma S \sin \theta \Delta S - \Delta R_L$$

Where:

$$M = \pi + \alpha' \rho \frac{Q^2}{S}$$

Assigning **M** to the **total Quantity of Amount of Movement or Total Impulsion**.

For any kind of distribution of pressures in the section of the channel (ΔM , variation of the total amount of movement between S_1 and S_2) is equal to the resultant weight with the resistance's forces applied in an elemental length (ΔS).

Dividing **M** by the specific weight of the fluid (γ), it is obtained:

$$F = \frac{M}{\gamma} = \frac{\pi}{\gamma} + \frac{\alpha' Q^2}{g S}$$

Assigning **F** as the **Specific Force or Specific Impulsion**.

By doing:

$$\frac{\Delta M}{\Delta S} = \gamma S \sin \theta - \frac{\Delta R_L}{\Delta S}$$

Or with $\Delta S \rightarrow 0$:

$$\frac{dM}{dS} = \gamma S \sin \theta - \frac{dR_L}{dS}$$

Expression that shows the variation of the total impulsion along the flow.

$$\Delta R_L = \tau_0 \chi \Delta S$$

$$\frac{\Delta M}{\Delta S} = \gamma S \sin \theta - \tau_0 \chi$$

Where,

$$\frac{dM}{dS} = \gamma S \left(\sin \theta - \frac{\tau_0}{\gamma R} \right)$$

For a uniform movement $\tau_0 = \gamma R J$ and attending to $J = \sin \theta$,

$$\frac{dM}{dS} = 0 \text{ or } M = \text{cst.}$$

By confirming again that, for a uniform movement, the sectioned values (as **M**) have constants values.

For a hydrostatic distribution of pressures, the impulsion π in a plain section has a value of:

$$\pi = \gamma S \eta \cos \theta$$

Where η represents deepness, measured according to line of major slope of the section, which have the respective gravity center under the free surface.

Thus:

Total Quantity of Movement:

$$M = \gamma \left(S \eta \cos \theta + \frac{\alpha' Q^2}{g S} \right)$$

The expression represents as line of the total quantity of movement.

Specific Force:

$$F = S \eta \cos \theta + \frac{\alpha' Q^2}{g S}$$

11.3.3 Surfaces of total quantity of movement

In an identical way to the already developed for surfaces of energy and considering only flows of hydrostatical distribution of pressures, can be defined an equation of the type:

$$f(Q, M, y) = 0$$

Since the geometry of the channel is known (η and S can be related with y). Considering a space of three dimensions (Q, M, y), the equations represents a surface, which is dominated as **surface of Total Quantity of Movement**.

Variation of the Total Quantity of Movement with the water height ($Q = Q_0$ cte.):

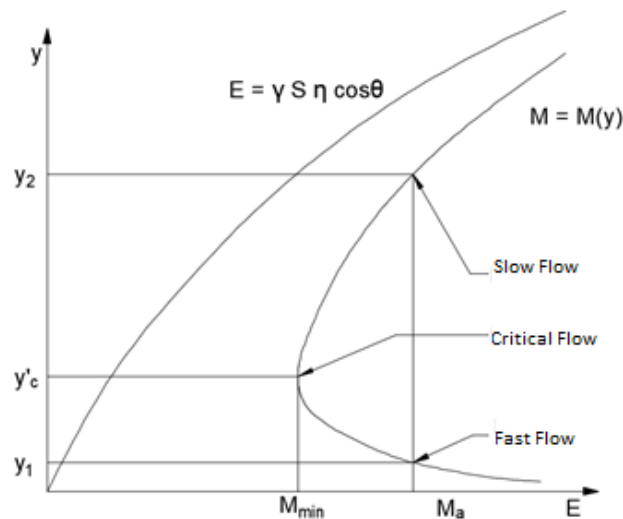


Figure 271 – Variation of the Total Quantity of Movement with the water height ($Q = Q_0$ cst.).

$$M = y \left(S \eta \cos \theta + \frac{\alpha' Q_0^2}{g S} \right)$$

The asymptotes of the curve are $y = 0$ and $M = \gamma S \eta \cos \theta$.

Variation of the flow rate with the water height ($M = M_0$ cte.):

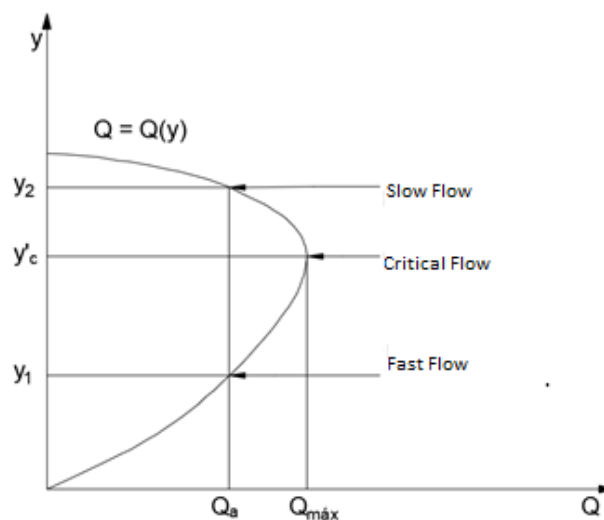


Figure 272 – Variation of the flow rate with the water height ($M = M_0$ cst.).

$$Q = \sqrt{\frac{M_0 S}{\alpha' \rho} - \frac{g S^2 \eta \cos \theta}{\alpha'}}$$

In the same way as in the case of the specific energy can demonstrate that the critical height (y_c') obtained through a curve of total impulsion coincide with the one obtained through the flow rate curve.

$$f(Q_{\max}, M, y) = 0$$

$$f(Q, M_{\min}, y) = 0$$

$$\frac{dM}{dy} = -\frac{\frac{\partial f}{\partial y}}{\frac{\partial f}{\partial M}} = 0 \wedge \frac{dQ}{dy} = -\frac{\frac{\partial f}{\partial y}}{\frac{\partial f}{\partial Q}} = 0$$

Boundaries conditions, that verify simultaneously for:

$$\frac{df}{dy} = 0$$

11.3.4 Relation between the total amount of movement and the specific energy

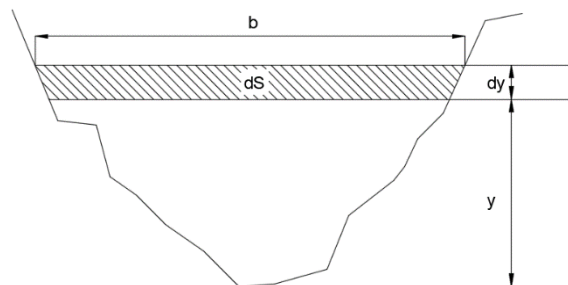


Figure 273 – Relationship between the Total Amount of Movement and the specific energy.

Considering:

- Specific Energy

$$E = y \cos \theta + \frac{\alpha Q^2}{2g S^2}$$

- Linear Flows

$$\frac{\partial E}{\partial y} = \cos \theta - \frac{\alpha Q^2}{g S^3} \frac{dS}{dy}$$

- Total Quantity or Amount of Movement

$$M = \gamma \left(S\eta \cos \theta + \frac{\alpha' Q^2}{g S} \right)$$

- Linear Flows

$$\frac{\partial M}{\partial y} = \gamma \left[\cos \theta \frac{\partial}{\partial y} (S\eta) - \frac{\alpha' Q^2}{g S^2} \frac{dS}{dy} \right]$$

Where $b = dS/dy$. Knowing that $S\eta$ represents the static moment,

$$d(S\eta) = \left[S(\eta + dy) + b \frac{(dy)^2}{2} \right] - S\eta = Sdy + b \frac{(dy)^2}{2} \rightarrow d(S\eta) = Sdy \rightarrow \frac{d}{dy} (S\eta) = S$$

$$\frac{\partial E}{\partial y} = \cos \theta - \frac{\alpha b Q^2}{g S^3} \quad (1); \quad \frac{\partial M}{\partial y} = \gamma S \left[\cos \theta - \frac{\alpha' b Q^2}{g S^3} \right] \quad (2)$$

Where:

$$\frac{\partial M}{\partial E} = \gamma S \frac{\cos \theta - \frac{\alpha b Q^2}{g S^3}}{\cos \theta - \frac{\alpha' b Q^2}{g S^3}}$$

Being $\alpha \cong \alpha' \cong 1$, then $\partial M / \partial E = \gamma S$. Thus, **M** increase when **E** increase (are proportional); if **y(S)** were the increasing equation of **E** (Slow regimes), **M** vary faster with **E**.

Critical values:

The boundaries conditions of **E** and **M** relatively to **y** is obtained by equating to zero the expressions (1) and (2):

$$(1): \frac{\alpha_c b_c Q^2}{g S_c^3} = \cos \theta; (2): \frac{\alpha'_c b_c Q^2}{g S_c^3} = \cos \theta$$

Where:

c affects defined critical magnitudes based in considerations of the specific energy;
c' affects magnitudes based in considerations of the Total Quantity of Movement.

When:

- $y_c \neq y_{c'}$, normally present proximal values;
- $y_c = y_{c'}$, it is verified when $\alpha \cong \alpha' \cong 1$.

11.4 Uniform regime in channels

11.4.1 Conditions of establishment of uniform regime in channels

Variation of the specific energy along a channel:

$$\frac{\partial E}{\partial S} = \sin \theta - J$$

In **uniform flow** $E = \text{cte.}$, where:

$$J = \sin \theta$$

Conclusion:

- The energy line is parallel to the bottom;
- The water height (**y**) is constant, where a free surface is also parallel to the bottom and such energy line;
- The uniform flow is only possible for prismatic channels of uniform rugosity;
- Although is quite difficult to happen in real cases, in many practical appliances is used its mathematical developing to solve problems with a small oscillation to such equilibrium regime.

11.4.2 Normal height

It is called **normal height** (or normal deepness or uniform deepness) is the height of the water in prismatic channels of known **geometrical section**, **slope** e **uniform rugosity** in which a certain flow rate flow (y_n). Other normal elements are:

- Normal section, S_n ;
- Normal wet or sunken perimeter, χ_n ;
- Normal hydraulic ray or ratio, R_n ;
- Normal superficial length, b_n ;
- Normal specific energy, E_n .

Determination of a normal height:

Using a resistance formula (Ex. Chézy):

$$Q = CS\sqrt{R \sin \theta}$$

By calling the sectional magnitude $CS\sqrt{R} \rightarrow$ capacity of transportation, we have:

$$\frac{Q}{\sqrt{\sin \theta}} = C_n S_n \sqrt{R_n} \rightarrow (\text{Chézy})$$

$$\frac{Q}{\sqrt{\sin \theta}} = K_n S_n R_n^{2/3} \rightarrow (\text{Manning} - \text{Strickler})$$

The calculation of the normal height is done starting from the law of capacity transportation variation with the water deepness, by seeking for the normal value that equals $Q/\sqrt{\sin \theta}$.

Graphical method:

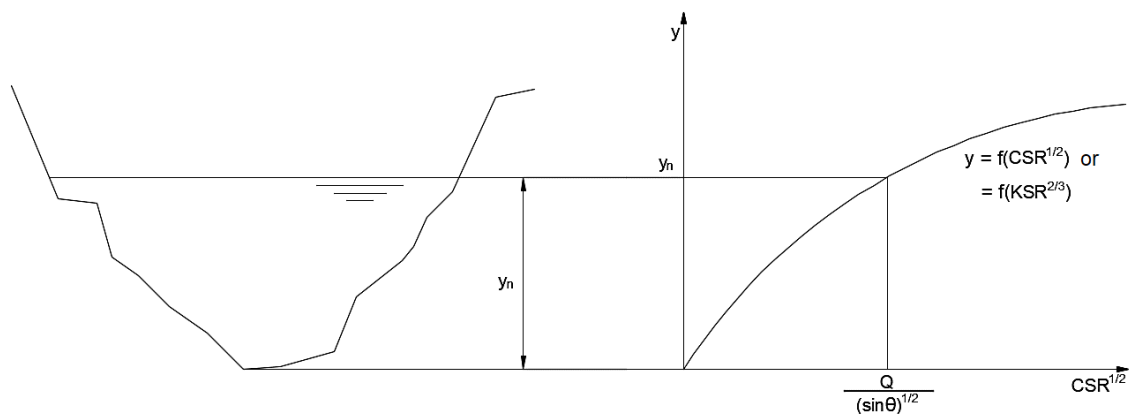


Figure 274 – Determination of the normal height by the graphical method.

Numerical method (Iterative method – Newton):

Determination of the zeros of a function:

$$\Phi(y) = \bar{\varphi}(y) - \frac{Q}{\sqrt{\sin \theta}} \rightarrow \text{General expression}$$

$$\Phi(y) = \frac{87SR}{C_B + \sqrt{R}} - \frac{Q}{\sqrt{\sin \theta}} \rightarrow (\text{Chézy} - \text{Bazin})$$

$$\Phi(y) = KSR^{2/3} - \frac{Q}{\sqrt{\sin \theta}} \rightarrow (\text{Manning} - \text{Strickler})$$

Rectangular section (using Chézy – Bazin):

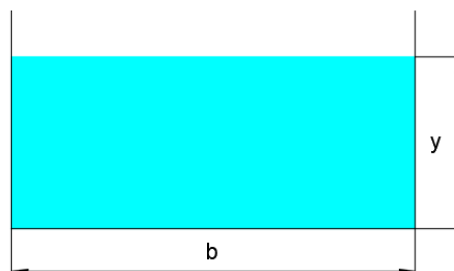


Figure 275 – Rectangular section.

$$\Phi(y) = \frac{\frac{87b^2y^2}{b+2y}}{C_B + \sqrt{\frac{by}{b+2y}}} - \frac{Q}{\sqrt{\sin \theta}}$$

Trapezoidal section (Using Chézy-Bazin):

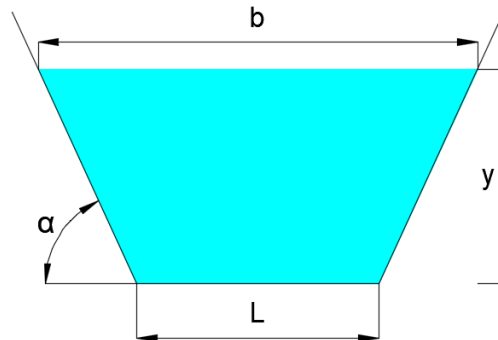


Figure 276 – Trapezoidal section.

$$\Phi(y) = \frac{87 \left(L + \frac{y}{m}\right)^2 \frac{y^2}{\left(L + \frac{2y}{m} \sqrt{m^2 + 1}\right)}}{C_B + \sqrt{\frac{mL + y}{mL + 2y \sqrt{m^2 + 1}}} y} - \frac{Q}{\sqrt{\sin \theta}}, \text{ with } m = \tan \alpha$$

Circular section (Using Manning-Strickler):

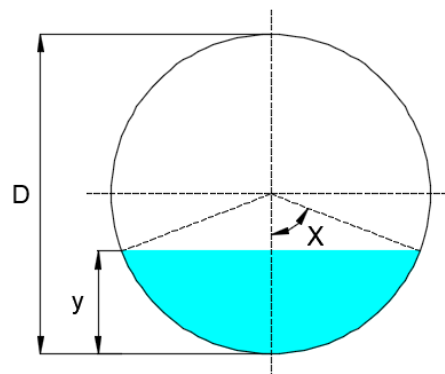


Figure 277 – Circular section.

$$\Phi(y) = \frac{K}{32} \left\{ \frac{D^8 [2X - \sin(2X)]^5}{X^2} \right\}^{1/3} - \frac{Q}{\sqrt{\sin \theta}}$$

For a circular section with same values of flow rate, slopes, geometry and rugosity of the channel, it can occur to have two different water heights.

11.4.3 Section of maximum flow rate

Rectangular section:

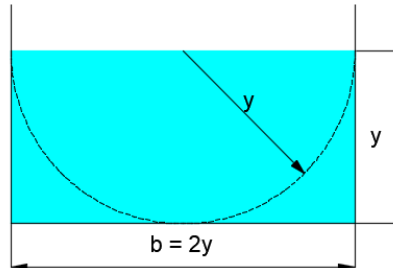


Figure 278 – Rectangular section.

$$\chi = \frac{S}{y} + 2y$$

Condition of χ_{\min} ,

$$\frac{d\chi}{dy} = -\frac{S}{y^2} + 2 = 0 \rightarrow b = 2y$$

Trapezoidal section:

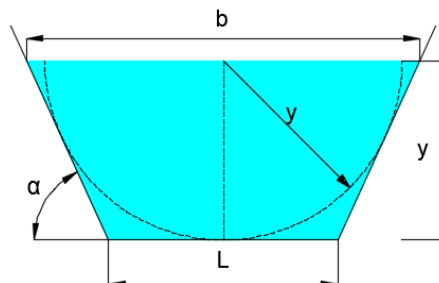


Figure 279 – Trapezoidal section.

$$m = \tan \alpha$$

$$\chi = L + \frac{2y}{m} \sqrt{m^2 + 1} \wedge S = \left(L + \frac{y}{m}\right) y \Rightarrow \chi = \frac{S}{y} + \frac{2y}{m} \left(\sqrt{m^2 + 1} + \frac{1}{2}\right)$$

Condition of χ_{\min} ,

$$\frac{d\chi}{dy} = -\frac{S}{y^2} + \frac{2}{m} \left(\sqrt{m^2 + 1} - \frac{1}{2}\right) = 0 \Rightarrow L = \frac{2y}{m} \left(\sqrt{m^2 + 1} - 1\right)$$

It is about a section that circumscribes an arch of a circumference of radius y centered at a medium point of the free surface.

$$S = \frac{2y^2}{m} \left(\sqrt{m^2 + 1} - \frac{1}{2} \right)$$

$$\chi = \frac{2y}{m} (2\sqrt{m^2 + 1} - 1)$$

$$R = \frac{y}{2}, (\text{independent of } m)$$

Can be verified from this expression its vigour for rectangular sections.

Normally the problem to determine is a set for a certain rugosity, slope and transversal section area, sections form of minimum resistance and maximum flow rate. But do not confuse with the most affordable or economical - f(excavation, type of coatings material, etc.).

By the expression of Manning-Strickler:

$$Q = K_0 S_0 R^{\frac{2}{3}} (\sin \theta_0)^{\frac{1}{2}}$$

With K_0 , S_0 , θ_0 given at a certain problem, the flow rate will be maximal when the hydraulic ray or ratio is maximal ($R = S_0/\chi$) \rightarrow when the wet or sunken perimeter is minimal (χ).

Semi-circular section:

It is the most advantageable section for a certain area.

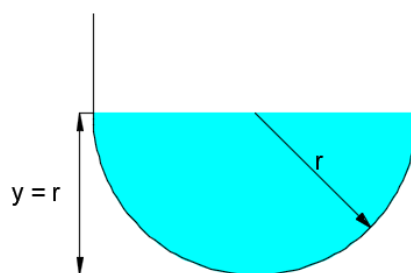


Figure 280 – Semi-circular section.

$$S = \frac{\pi r^2}{2}$$

$$\chi = \pi r$$

$$R = \frac{r}{2} = \frac{y}{2}$$

11.4.4 Problems of uniform movement in channels

The precision of the formulas is lower than those ones used in the calculus and design of flows under pressure. Some causes are (Simões, 2011):

1. Great number of problems with varied types and forms of channels, with a different wet section, affecting the charge losses;
2. Difficulty to assume a correct value for walls rugosity and channels bottom;
3. The proposed formulas were deduced for channels of small dimensions, being any increase of turbulence a perturbation for the channel performance and consequently leads to poor quality results.

Main problems in projects (Netto, 1998):

1. The project of the channel can have complex conditions that demands sensibility from the designer and support from experimental data. The project of great importance works must be executed with a specialist support;
2. Knowing that the uniform channels and uniform flows do not exists in practice, the solutions will be always an approximation, but justifying rounding in calculation for more than 3 significant algorithms;
3. For channels of great slope or inclination, it is recommended to verify the conditions for a critical flow;
4. In channels or gutters of small extension, it is not justifying the use of practical formulas for deepness or flow rate determination.

11.4.5 Critical uniform regime

The critical flow in an open channel or covered channel with a water free surface is characterized by some conditions (Fletcher & Grace, 1972):

- The specific energy is a minimum for a certain discharge;
- The discharge is a maximum for a certain specific energy;
- The specific force is a minimum for a certain discharge;
- The velocity in terms of static pressure (*velocity head*) is equal to half-hydraulic deepness in a channel of small slope;
- The number of Froude is equal to 1.0;
- The velocity of flow in a channel of small slope is equal to the celerity of small gravity waves in shallow waters.

If a critical regime of flow exists in all the project, the flow in the channels is a critical flow, and the slope of such channel is a critical slope (i_c). An inclination lower than i_c will cause a sub-critical regime, and a major inclination will cause a super-critical regime. A flow close to a critical regime can be unstable. In project, if the deepness is proximal to critical or critical, the form or slope must be changed to achieve a stable hydraulic state.

The critical velocity (U_c) can be calculated from the critical hydraulic deepness (y_c). For a rectangular canal or channel, the flow deepness is equal to the hydraulic deepness ($y_n = y_c$), thus, the critical velocity is:

$$U_c = \sqrt{gy_c}$$

11.5 Permanent regime gradually varied in channels or channels

11.5.1 Theoretical equations of movement gradually varied in channels

Flow in which the deepness varies gradually along the channel:

Equation of energy:

$$\frac{dE}{dS} = \sin \theta - J \wedge E = y \cos \theta + \frac{\alpha Q^2}{2gS^2} \text{ (Specific Energy)}$$

$$\frac{dE}{dS} = \cos \theta \frac{dy}{dS} - y \sin \theta \frac{d\theta}{dS} + \frac{Q^2}{2gS^2} \frac{d\alpha}{dS} + \frac{\alpha Q}{gS^2} \frac{dQ}{dS} - \frac{\alpha Q^2}{gS^3} \frac{dS}{dS}$$

As:

$$\frac{dS}{dS} = \frac{\partial S}{\partial S} + b \frac{dy}{dS} \wedge Fr = \frac{\alpha b Q^2}{gS^3 \cos \theta}$$

Then:

$$\frac{\alpha Q^2}{gS^3} \frac{dS}{dS} = \frac{\alpha Q^2}{gS^3} \frac{\partial S}{\partial S} + \frac{\alpha Q^2}{gS^3} b \frac{dy}{dS}$$

Knowing that:

$$\frac{Fr}{\cos \theta} = \frac{\alpha b Q^2}{gS^3}$$

Follows:

$$\frac{dy}{dS} = \frac{\sin \theta - J}{(1 - Fr) \cos \theta} - \frac{\frac{\alpha Q}{gS^2} \frac{dQ}{dS}}{(1 - Fr) \cos \theta} + \frac{\frac{\alpha Q^2}{gS^3} \frac{\partial S}{\partial S} - \frac{Q^2}{2gS^2} \frac{d\alpha}{dS} + y \sin \theta \frac{d\theta}{dS}}{(1 - Fr) \cos \theta}$$

In prismatic channels ($\theta = \text{cst.}$ and $\partial S / \partial S = 0$), with constant flow rate ($Q = \text{cst.}$ and $\partial S / \partial S \approx 0$ $\partial \alpha / \partial s \approx 0$):

$$\frac{dy}{dS} = \frac{\sin \theta - J}{(1 - Fr) \cos \theta}$$

11.5.2 Backwater in prismatic channels with constant flow rate

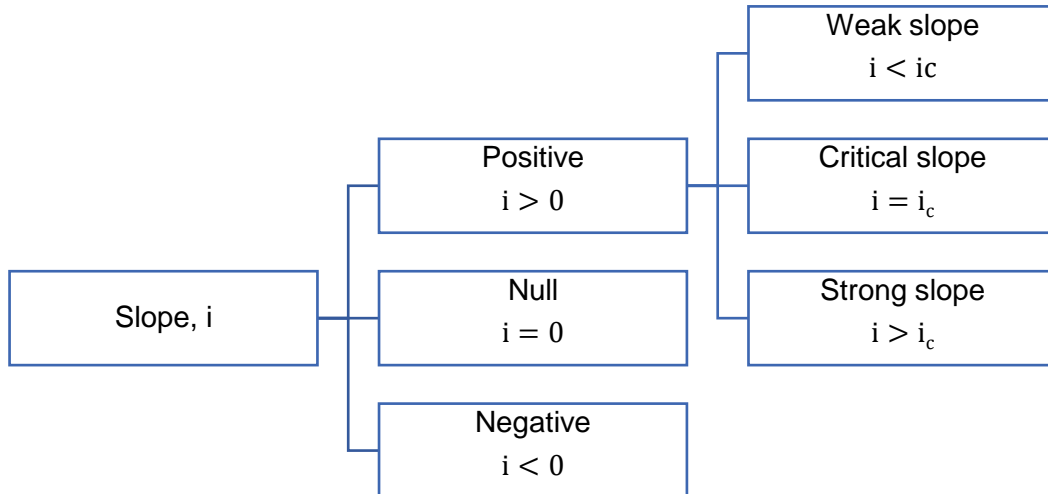


Figure 281 – Slope.

Values of $\sin \theta - J$:

For a uniform regime in which the same channel would flow the flow rate Q :

$$Q = K S_n R_n^{2/3} (\sin \theta)^{1/2} \rightarrow \sin \theta = \frac{Q^2}{K^2 S_n^2 R_n^{4/3}}$$

For a tangent uniform regime (virtual uniform movement in which the section flows the same flow rate in a prismatic channel with the same reaction):

$$J = \frac{Q^2}{K^2 S^2 R^{4/3}}$$

Table 45 – Values of $(\sin \theta - J)$.

$\sin \theta - J = \frac{Q^2}{K^2} \left(\frac{1}{S_n^2 R_n^{4/3}} - \frac{1}{S^2 R^{4/3}} \right)$	
y (Varied Regime)	$\sin \theta - J$
$y > y_n$	> 0
$y = y_n$	$= 0$
$y < y_n$	< 0

Values of $(1 - Fr) \cos \theta$:

Table 46 – Values of $[(1 - Fr) \cos \theta]$.

y (Varied Regime)	Fr	$(1 - Fr) \cos \theta$
$y > y_c$	< 1	> 0
$y = y_c$	$= 1$	$= 0$
$y < y_c$	> 1	< 0

Then:

$y = y_n \Rightarrow dy/dS = 0 \Rightarrow y = \text{cst.}$, then the slope of the free surface \approx Bottom slope;

$y = y_c \Rightarrow dy/dS = \infty \Rightarrow$ Non-hydrostatic distribution of pressures; The equation is not valid.

Backwater curves in channels of weak slope, $i < i_c \wedge y_n > y_c$:

A channel of weak slope exists when its inclination is lower than the critical. At such situation may exists three configurations of backwater curves, presented in Table 47, which graphical representations are show in Figure 282.

Table 47 – Discretization of backwater curves in channels of weak slope.

y	$(1 - Fr) \cos \theta$	$\sin \theta - J$	dy/dS	Backwater Curve
$y > y_n$	> 0	> 0	> 0	I1, Elevating R.C
$y_c < y < y_n$	> 0	< 0	< 0	I2, Lowering R.C
$y < y_c$	< 0	< 0	> 0	I3

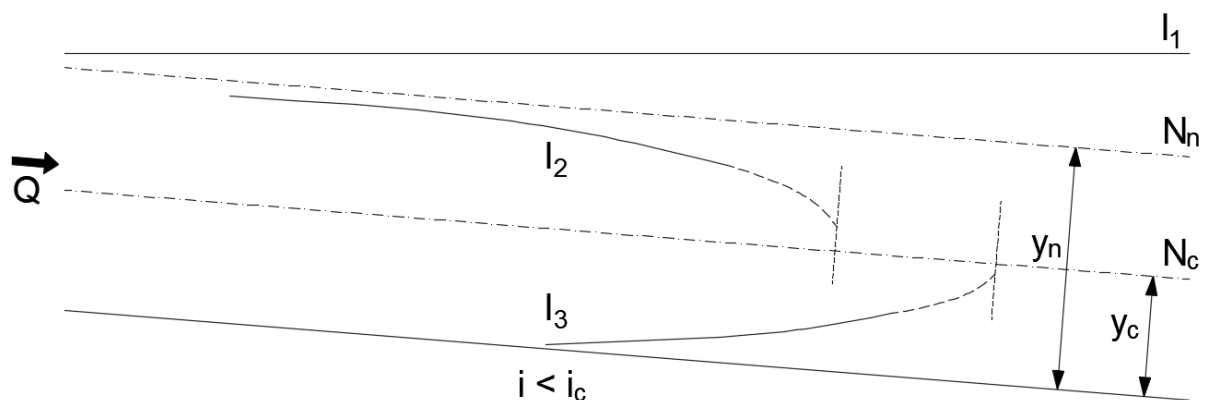


Figure 282 – Backwater curve in channels of weak slope (adapted from Barbosa, 1982).

Thereby in a prismatic channel of weak slope with constant flow rate might occur three different backwater curves, generally called I1, I2 and I3 (Barbosa, 1982).

The curve I1 is an elevating RC, so the water height increases as the coordinate S do. Such curve tends to the normal level at upstream and tends to horizontal at

downstream due to the water height tends to infinity, so consequently, the number of Freud and the energy losses per unit of length tends to zero, which is a horizontal asymptote.

The curve I2 is usually called as lowering RC. Such curve tends to the bottom at downstream, due to $dy/dS < 0$, which means, the curve tends to the critical level; and at upstream tends to the normal height of the flow.

Finally, the curve I3 is characterized by an increase of the water height as the coordinate S increase, tending to the critical height.

Backwater curves in channels of critical slope, $i = i_c \wedge y_n = y_c$:

In channels of critical slope, Figure 283, due to the coincidence of the normal height and the critical height, it can occur only two types of configurations for such curves, the first one when the water height of the regime is superior and when is lower than the critical.

The curves C1 and C3 are characterized by an increase of water deepness as S increase, so being the curve C1 start from the critical height and suffers an increase, while the curve C3 achieve a maximal height with values proximal to normal and critical height (because at such situation, both values coincide).

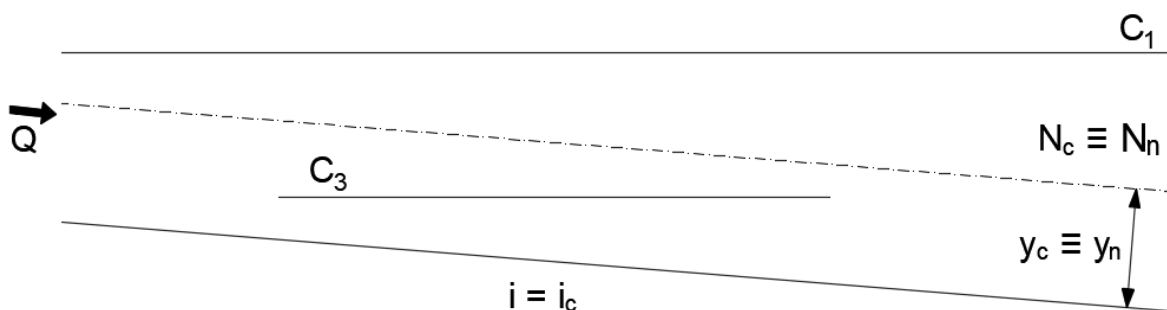


Figure 283 – Backwater curves in channels of critical slope or inclination (adapted from Barbosa, 1982).

$$\frac{dy}{dS} = \frac{\sin \theta - J}{(1 - Fr) \cos \theta} = \tan \theta \frac{1 - \frac{J}{\sin \theta}}{1 - Fr}$$

Using the formula of Chézy:

$$\frac{dy}{dS} = \tan \theta \frac{1 - \frac{S_n^2 R_n C_n^2}{S^2 R C^2}}{1 - \frac{\alpha b Q^2}{g \cos \theta S^3}}$$

$$\text{Fr} = \frac{\alpha b_c Q^2}{g \cos \theta S_c^3} = 1 \Rightarrow \frac{\alpha Q^2}{g \cos \theta} = \frac{S_c^3}{b_c} \text{ (In critical regime)}$$

$$\frac{\alpha b Q^2}{g \cos \theta S^3} = \frac{b S_c^3}{b_c S^3} = \frac{b S_c^2 \chi_c R_c}{b_c S^2 \chi R} \Rightarrow \frac{dy}{dS} = i \frac{1 - \frac{S_n^2 R_n}{S^2 R} \frac{C_n^2}{C^2}}{1 - \frac{b S_c^2 \chi_c R_c}{b_c S^2 \chi R}}$$

$$\begin{cases} C_n^2/C^2 \cong 1 \\ b_{\chi_c}/(b_c \chi) \cong 1 \end{cases} \Rightarrow \frac{dy}{dS} = i \frac{1 - \frac{S_n^2 R_n}{S^2 R}}{1 - \frac{S_c^2 R_c}{S^2 R}}$$

Then, $dy/ds = i = \tan \theta$.

In channels of critical slope, the backwater curves are approximately straight or horizontal.

Backwater curves in channels of strong slope, $i > i_c \wedge y_n < y_c$:

It is called channels of strong slope, when the its inclination major than the critical. At such situation is possible to have three configurations (Figure 284) for backwater curves. Its characteristics are resumed in Table 48.

Table 48 – Discretization of the backwater curves in channels of strong slope.

y	(1 – Fr) cos θ	sin θ – J	dy/dS	Backwater Curve
y > y_c	> 0	> 0	> 0	S1
y_n < y < y_c	> 0	> 0	< 0	S2
y < y_n	< 0	< 0	> 0	S3

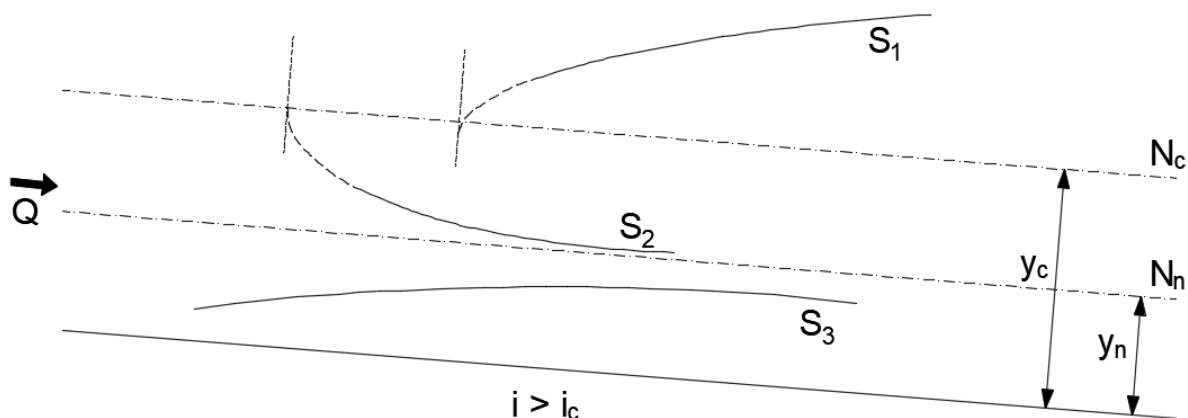


Figure 284 – Backwater curves in channels of strong slope (adapted from Barbosa, 1982).

The curve S1 assume an increase of the water height from upstream to downstream, tending to a height proximal to normal until a major deepness of water of it. At the same time, the configuration S2 presents a decrease in water deepness from the critical height until the normal height. The configuration S3 presents a water height variation for a value lower than the normal height, tending to a normal height of flow.

Backwater curves in channels of null slope (horizontal bottom), $i = 0$:

Due to non-inclination of the channel,

$$\frac{dy}{dS} = -\frac{J}{1 - Fr}$$

Analysing the last equation, by the fact that the energy losses per unit of length is always positive ($J > 0$), the quotient dy/dS is positive or negative, depending in the value of Froude, if is major or minor to a unit.

In horizontal channels is not possible to define a normal height, so will only exist two configurations of backwater curves that form when the water height of the channel is major or minor to the critical height. In Barbosa (1982), defining a H2 configuration when the water height is superior to the critical, leading to a successive decrease of the water heights until the critical height. The curve H3 happens for an increase of the water heights from lowers deepness to the critical until the critical height.

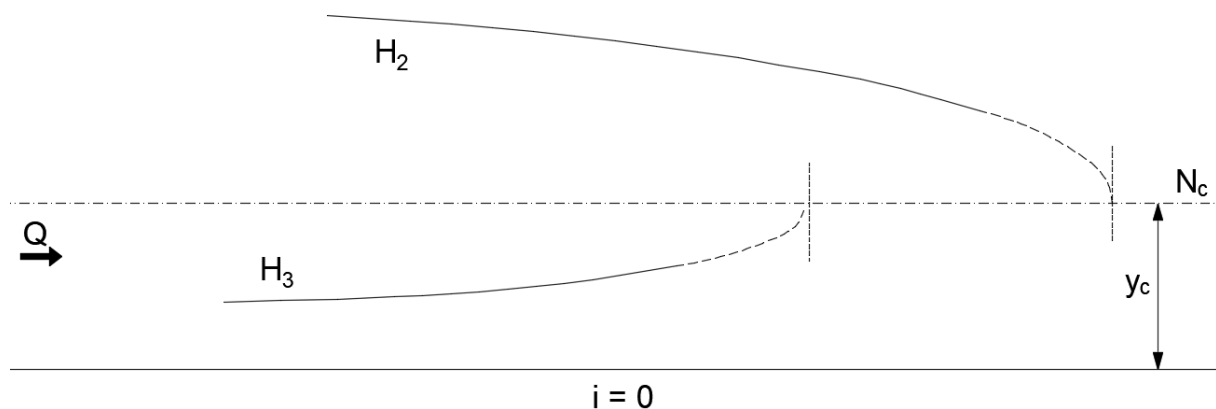


Figure 285 – Backwater curves in channels of null inclination (adapted from Barbosa, 1982).

Backwater curves in channels of negative slope, $i < 0$:

$$\frac{dy}{dS} = \frac{\sin \theta - J}{(1 - Fr) \cos \theta}; \sin \theta - J < 0$$

At this situation, the canal has an inclination opposed to the flow's direction, being impossible to determine the normal height, similar to the last situation. So, exists two configurations, N2 and N3, referred to situations where the water height is major or minor than the critical height.

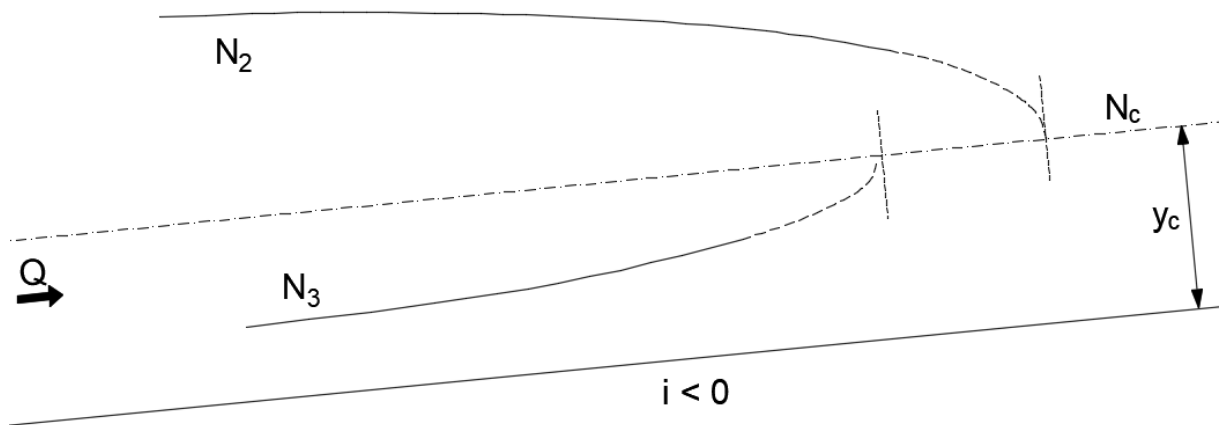


Figure 286 – Backwater curves in channels of negative slope (adapted from Barbosa, 1982).

Determination of Backwater curves:

By numerical integration:

$$\frac{dy}{dS} = \frac{\sin \theta - J}{(1 - Fr) \cos \theta} \Rightarrow dS = \frac{(1 - Fr) \cos \theta}{\sin \theta - J} dy$$

If:

$$\frac{(1 - Fr) \cos \theta}{\sin \theta - J} = \Omega y$$

Then:

$$dS = \Omega(y) dy$$

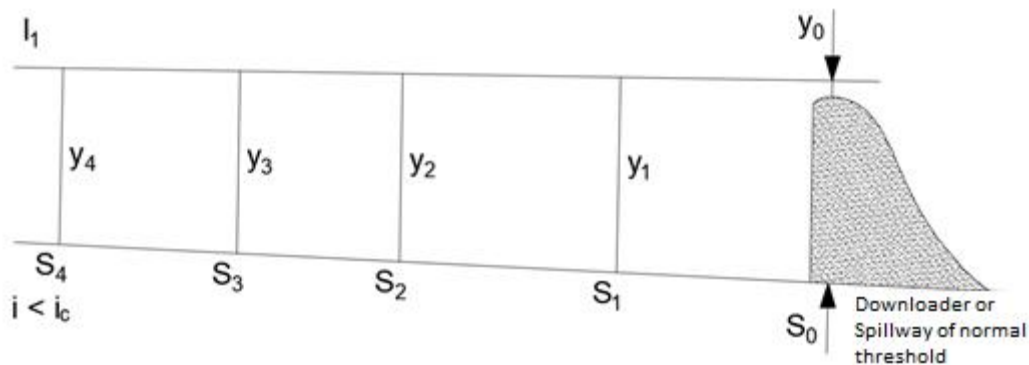


Figure 287 – Numerical integration of backwater curves.

$$S_{l+1} - S_l = \int_{y_l}^{y_{l+1}} \Omega(y) dy$$

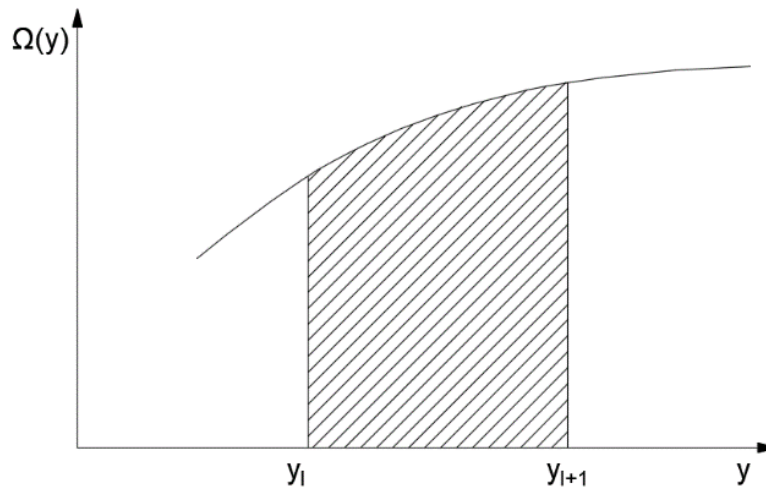


Figure 288 – Distance between S_{l+1} and S_l .

By the finite difference method with successive approximations:

To determine the length of the rebound curves by applying such method, a summation of the obtained Δs must be done, knowing the flows conditions in two successive sections, l and $l + 1$. Which means, by knowing the heights of the flow in two points of the channel is possible to determine its energy and its continuous charge losses and by the direct application of the equation is also possible to know the distance between those two sections. The summation of all Δs is the total length of the rebound curve. The precision of the result will be major as smaller are the considered intervals.

From the Bernoulli's equations:

$$\frac{d}{dS} \left(z + y \cos \theta + \frac{\alpha U^2}{2g} \right) = -J$$

Considering a part of the channel,

$$(z_{l+1} - z_l) + (y_{l+1} - y_l) \cos \theta + \left(\frac{\alpha_{l+1} U_{l+1}^2}{2g} - \frac{\alpha_l U_l^2}{2g} \right) = - \frac{J_l + J_{l+1}}{2} \Delta S$$

Where J_{l+1} and J_l represents the energy losses per unit of length in tangential uniform flows.

Procedure:

1. Fixing ΔS from the section S_l ;
2. Iterate for S_{l+1} , considering initially $J_{l+1} = J_l$;
3. Error in $y_{l+1} < \text{Tolerance}$:
 - a. Yes, progress to step 4;
 - b. No, return to step 2;
4. Proceed to next step.

11.5.3 Backwater in channels of variable flow rate

Collector channel ($\Delta M = 0 \wedge Q_1 < Q_2$)

In the case of a collector channel, it is usual to consider the total quantity of movement ($dM/ds = 0$), since the entrance or input of additional flow rate is done perpendicular to the flow (for a minimal perturbation) (Braga, 2014).

$$\begin{cases} Q = a \cdot s \\ Q_2 = a \cdot L \end{cases}$$

$$\frac{dM}{ds} = \gamma S \cdot \frac{dh}{ds} - \alpha' \frac{\gamma b}{g} \cdot \frac{Q^2}{S^2} \cdot \frac{dh}{ds} + 2\alpha' \frac{\gamma}{g} \cdot \frac{Q}{S} \cdot \frac{dQ}{ds}$$

$$\tau_0 = \gamma \cdot J \cdot R \Rightarrow \frac{dM}{ds} = \gamma S \left(\sin \theta - \frac{\tau_0}{\gamma R} \right)$$

Backwater equation for a collector channel:

$$\frac{dh}{ds} = \frac{\sin \theta - J - \frac{2Q}{gS^2} \cdot \frac{dQ}{ds}}{1 - Fr^2}$$

Spillway channel or downloader ($\Delta E = 0 \wedge Q_1 > Q_2$)

In case of a spillway channel, consider a flow with no specific energy losses ($dE/ds = 0$), since the bottom of the channel and the threshold are constant (Braga, 2014).

$$\begin{cases} Q = Q_1 - a \cdot s \\ Q_2 = Q_1 - a \cdot L \end{cases}$$

$$\frac{dE}{ds} = \cos \theta \cdot \frac{dh}{ds} - \alpha \frac{bQ^2}{gS^3} \cdot \frac{dh}{ds} + \underbrace{\alpha \cdot \frac{Q}{gS^2} \cdot \frac{dQ}{ds}}_{\text{new term}} = 0$$

Rebound equation for a lateral spillway channel:

$$\frac{dh}{ds} = - \frac{\frac{Q}{gS^2} \cdot \frac{dQ}{ds}}{1 - Fr^2}$$

Variation of flow rate along the spillway:

$$- \frac{dQ}{ds} = C \sqrt{2g(h - p^{3/2})}$$

Where, C is the discharge coefficient of the spillway or discharger.

Replacing:

$$\frac{dh}{ds} = \frac{Q}{gS^2(1 - Fr^2)} - \frac{\frac{Q}{gS^2} \cdot \frac{dQ}{ds}}{1 - Fr^2}$$

For $E = cte.$:

$$Q = S \cdot \sqrt{2g(H_0 - h)}$$

Considering a rectangular section ($S = b \cdot h$), dh/ds became:

$$\frac{dh}{ds} = \frac{2C}{b} \cdot \frac{\sqrt{(H_0 - h)(h - p^{3/2})}}{3h - 2H_0}$$

It is important to mention a case where a lateral spillway is preceded by a channel of weak slope and proceeded by a channel of strong slope. The critical regime, connecting the slow regime at upstream to the fast regime at downstream, cannot be settled after the lateral spillway (downstream section of the spillway): as an effect admitting a constant specific energy, it would have been insufficient because a necessary higher flow rate at upstream section. The critical regime at the constant specific energy hypothesis would localize at the beginning of the lateral spillway, tending to a fast regime rebound along it (Braga, 2014).

11.6 Permanent regiment rapidly varied in channels

11.6.1 General considerations

In a permanent flow rapidly varied, its characteristic varies abruptly from one section to another. Such type of flow that is highly dependent from boundaries conditions usually occurs associated to singularities and hydraulics structures. At this type of flow, the free surface line presents an accentuated curvature (Vasconcelos, 2005).

The set of peculiarities associated to this type of flow conditions the occurrence of discontinuities in the flow, resulting in the non-validity of the established equations for the study of uniform and gradually varied flows (Vasconcelos, 2005).

In a general form, such aspects of this type of flows make impossible the establishment of generic formulas that could be applied for all kind of situations. The theoretical treatment of the several cases, when it is possible, it can be done by applying the principles of Energy and Amount of Movement Conservation (Vasconcelos, 2005).

The typical cases of flow rapidly varied associated to hydraulics structures are: pourers, gates, power dissipators, obstacles, abrupt transitions, devices for flow measurements, etc (Figure 289) (Vasconcelos, 2005).

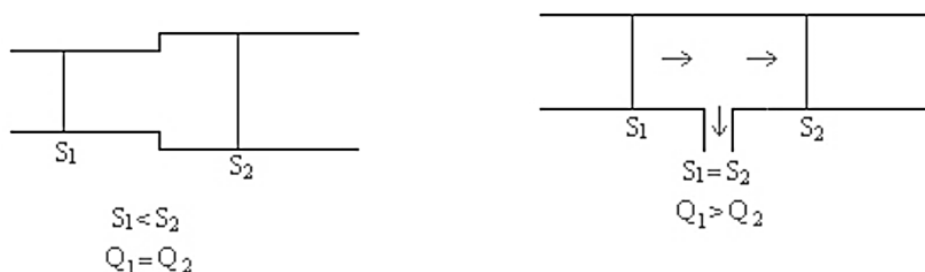


Figure 289 – Examples of permanent flows rapidly varied (Vasconcelos, 2005).

11.6.2 Hydraulic rebound

Characteristics and classifications

The hydraulics rebound is a type of flow rapidly varied. It is a flow generated by the abrupt transition from a fast flow to a lower flow, being generally a phenomenon that involves a great amount of power or energy dissipation (Nalluri & Featherstone, 2001). Such loss of energy is produced by the turbulence of the phenomenon, but also by the friction between the flow and solid boundaries (Lencastre, 1972).

The hydraulic rebound is usually used in basins of dissipation installed at downstream of spillways in hydraulic structures (Figure 290). As an effect, the flow rate downloaded by the discharge organs, flood downloaders, in fast regime, it can create downstream erosion, which is highly unsecure for such structures.

It is necessary to build a basins dissipator in order to induce an internal hydraulic rebound and the consequently change of regime, fast to slow, promoting a significant dissipation of energy or power to avoid instability problems. Then, the length of the dissipation basins will be defined based in function of the rebound length.

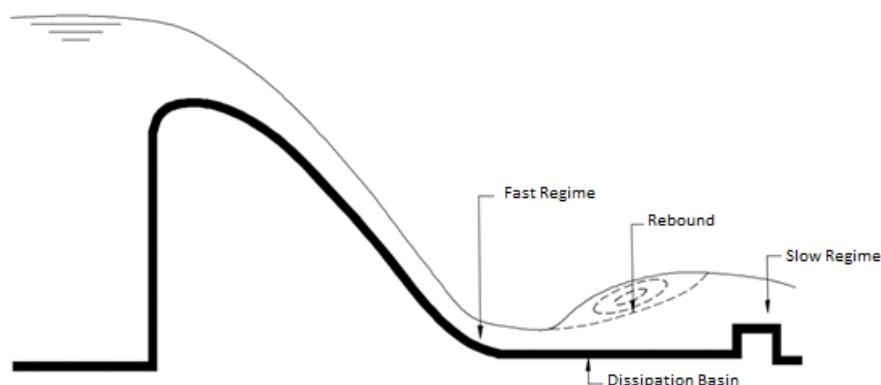


Figure 290 – Hydraulic rebound (adapted from Barbosa, 1982).

Along time, some authors have dedicated to study hydraulic rebound, in aspect such rebound length, classification, etc. by studying and analysing the aspect that influence the phenomenon, as for example, the energy dissipated during the phenomenon and the different classifications of the authors in function of the Froude parameter. By analysing different proposal from the author, it is concluded that the rebound classification depends of the Author.

Barbosa (1982), presents various types of rebounds, being its classification done in function of the number of Froude, at upstream section,

$$Fr = \frac{bQ^2}{gS_n^3 \cos \theta}$$

For number of Froude between 1 and 4, the rebound is undulated but not well defined, showing some superficial undulations as the flow follows downstream (Figure 291).

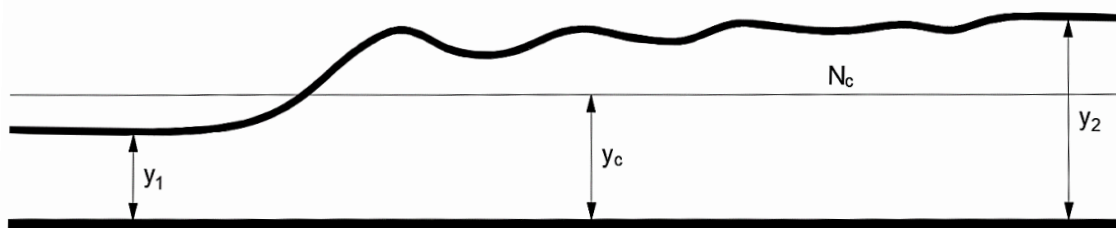


Figure 291 – Undulated hydraulic rebound (adapted from Barbosa, 1982).

For values of Froude major than 4, the rebound is called ordinary or free. Such rebound has a superpositions of vortex or swirls of horizontal axis over the expansion zone of liquid stream, and such phenomenon occurs in a small interval of time, because are abruptly dragged to a lower flow. Such phenomenon occurs massively, with great intensity and consuming a great amount of energy (Figure 292).

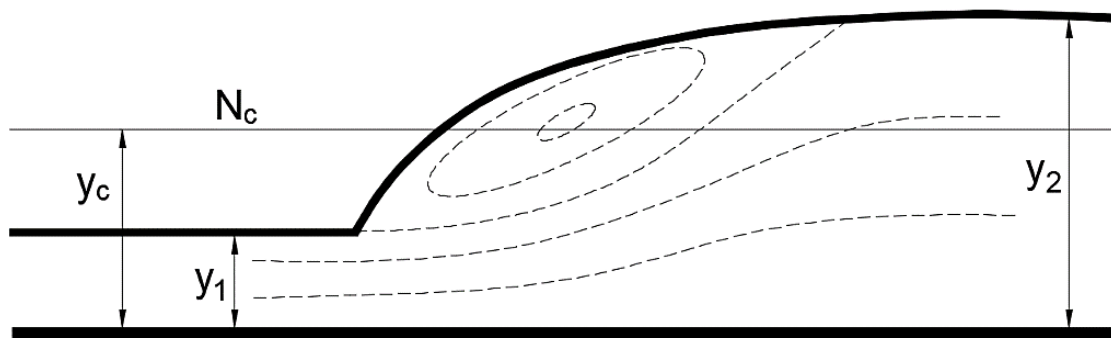


Figure 292 – Ordinary hydraulics rebound (adapted from Barbosa, 1982).

Finally, the sunken rebound (Figure 293). Such rebound could happen when an ordinary rebound suffers the effect of rising water or elevation of the level of water at downstream, which creates a backwater of elevation that push the rebound upstream until the dispositive or obstacle, that produce the fast regime (as for example, the

spillway), fixing such point. Such effect is greater as major is the difference between real water deepness and the one corresponding to a free rebound.

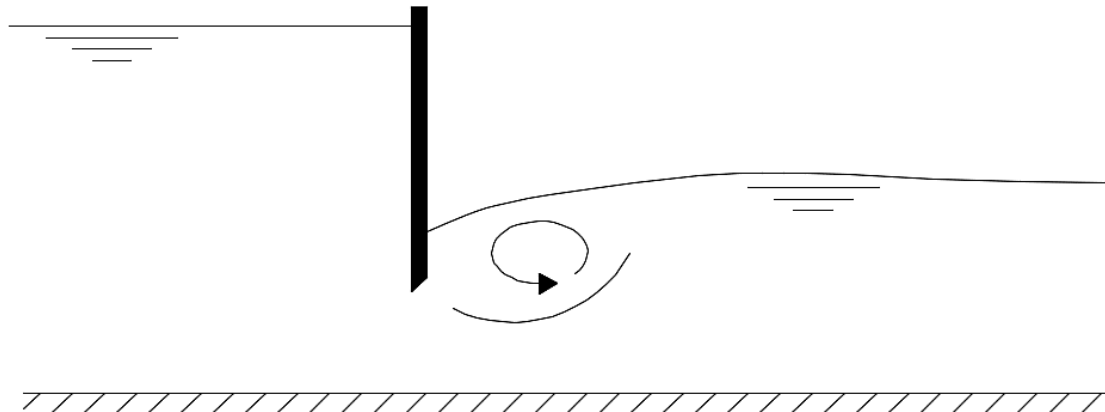


Figure 293 – Drowned rebound (adapted from Nalluri & Featherstone, 2001).

Peterka (1958) presents a different classification (Figure 294) as from Barbosa (1982); and one more time the rebound classification by the calculus of Froude's number at upstream section, being calculated by the application of the following equation:

$$Fr_1 = \frac{U_1}{\sqrt{gy_1}}$$

Where:

U_1 represent the average velocity of the flow;

y_1 is the conjugated height 1;

g is the gravitational acceleration.

For values of Froude's number lower or equal to 1, is a slow or critical regime, which have no rebounds (Lencastre A., 1983; Rijo, 2010).

For value of Froude's number between 1 and 1.7, the author classifies as undulated rebound (Figure 294b), being specially characterized by moderated undulations at surface (Peterka, 1958).

Between 1.7 e 2.5, the rebound is called weak or pre-rebound (Figure 294c), due to a roll formation (Peterka, 1958).

With the number of Froude varying from 2.5 to 4.5, the author classifies as oscillating rebound (Figure 294d) and it have strong undulations (Peterka, 1958).

For values between 4.5 and 9, the rebound is called stable (Figure 294e) and presents a well define structure, having turbulences between the rebound limits and its does not present great waving or undulations (Peterka, 1958).

In the stable rebound, the phenomenon is well characterized and localized, being favourite in design or dimensioning, principally for energy or power dissipation. At such

case the dissipation of energy or power varies between 45% and 70% of available energy at upstream.

Finally, for values superior to 9, the rebound is called as strong (Figure 294f) and it is characterized by its great turbulence (Peterka, 1958).

For a strong rebound, although of indicate a greater potential to dissipate, it is noticed mass portion rolling downstream at the beginning of the rebound, producing downstream significant waves that does not match for those dimensioning or designs. It is not used in hydraulic constructions, due to collateral effects in dissipation structures, as cavitation and abrasive processes.

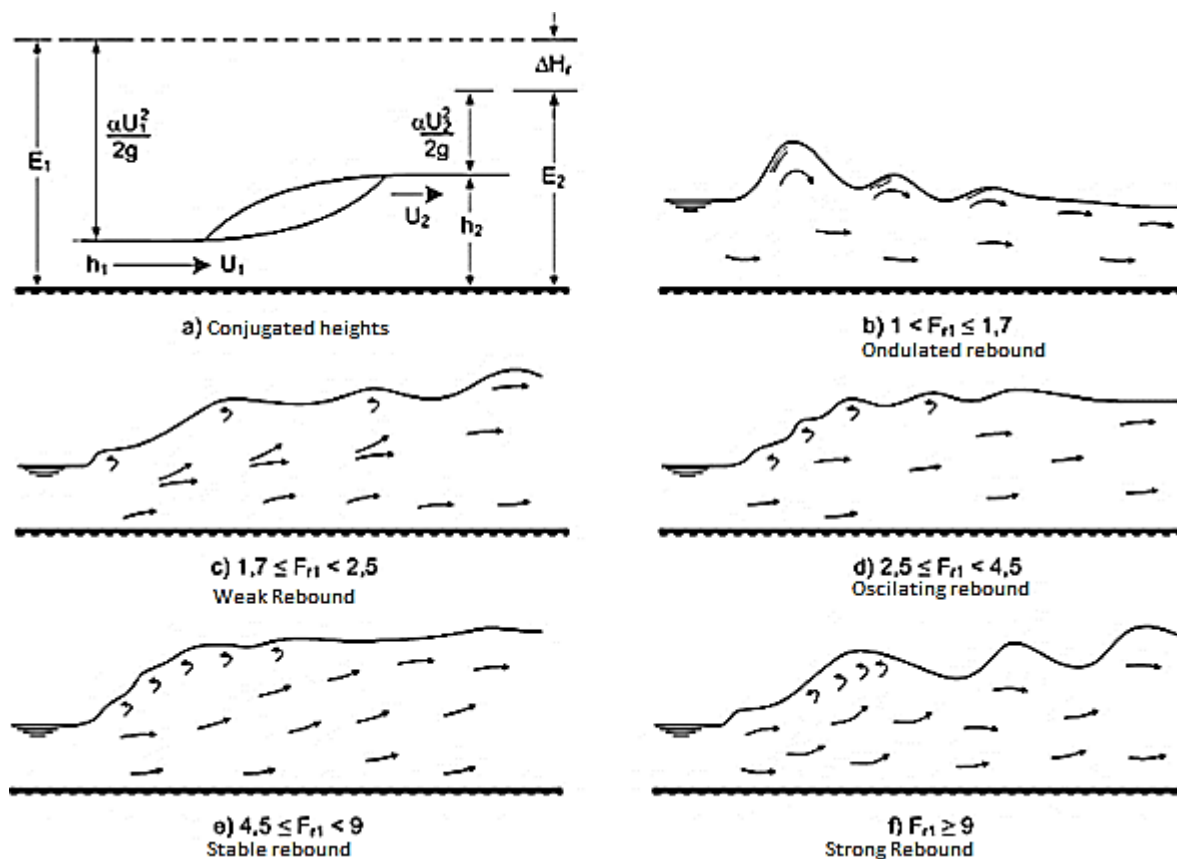


Figure 294 – Forms of hydraulic rebounds (Lencastre, 1983).

Characterization and location of hydraulic rebounds

In a study of hydraulic rebound, it is quite important to know the conjugated heights (Figure 294a). Along the years, different authors have suggested different proposals for its calculus (Lencastre A., 1972).

As for example, Barbosa (1982), apply the theorem of total amount of movement through the expression of hydrostatic distribution of pressures, at downstream and upstream sections (Lencastre A., 1972).

In this case, it is not possible to apply Bernoulli's theorem given that in the rebound there is a considerable loss of energy and this loss is not known (Lencastre A., 1972).

$$M = \gamma \left(S \eta \cos \theta + \frac{\alpha'}{g} \cdot \frac{Q^2}{S} \right)$$

In the study of such phenomenon, it is considered that during the rebound, the total amount of movement is constant. Thus:

$$M_1 = M_2$$

$$S_1 \eta_1 \cos \theta + \frac{\alpha'_1}{g} \cdot \frac{Q^2}{S_1} = S_2 \eta_2 \cos \theta + \frac{\alpha'_2}{g} \cdot \frac{Q^2}{S_2}$$

Therefore, it is possible the calculus of y_2 by applying the last equation and knowing the values of y_1 (value of the water height in the initial section), which is usually known, or vice versa.

In Quintela (2005), by using again the theorem of movement continuity the author proposed the following equations for the calculus of the conjugated heights for the study of rebounds in rectangular channels.

$$y_1^* = -\frac{y_2}{2} + \sqrt{\frac{y_2^2}{4} + \frac{2U_2^2 y_2}{g}}$$

$$y_2^* = -\frac{y_1}{2} + \sqrt{\frac{y_1^2}{4} + \frac{2U_1^2 y_1}{g}}$$

Once is presented the formulation for conjugated heights, it is possible to calculate energy losses, by Barbosa (1982).

$$\Delta E = y_1 \cos \theta + \frac{\alpha'_1}{2g} \cdot \frac{Q^2}{S_1} - \left(y_2 \cos \theta + \frac{\alpha'_2}{2g} \cdot \frac{Q^2}{S_2} \right)$$

It is even possible to graphically calculate energy losses (Figure 295), by simultaneously representing the curve of total amount of movement variation and the curve of specific energy variation (both in function of water deepness).

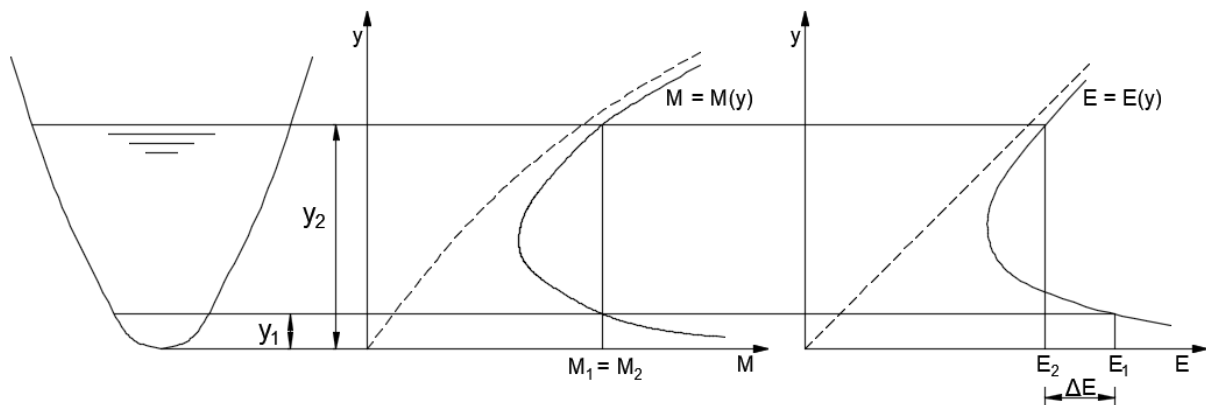


Figure 295 – Energy losses in function of the conjugated heights of the rebound (adapted from Barbosa, 1982).

Finally, in order to fully characterized the rebound, it is necessary to define its length and location.

About its length, Barbosa (1982) proposed a graphical determination for the rebound length (Figure 296) in function of the Froude number at upstream section for channels of rectangular transversal section and conjugate water height at downstream.

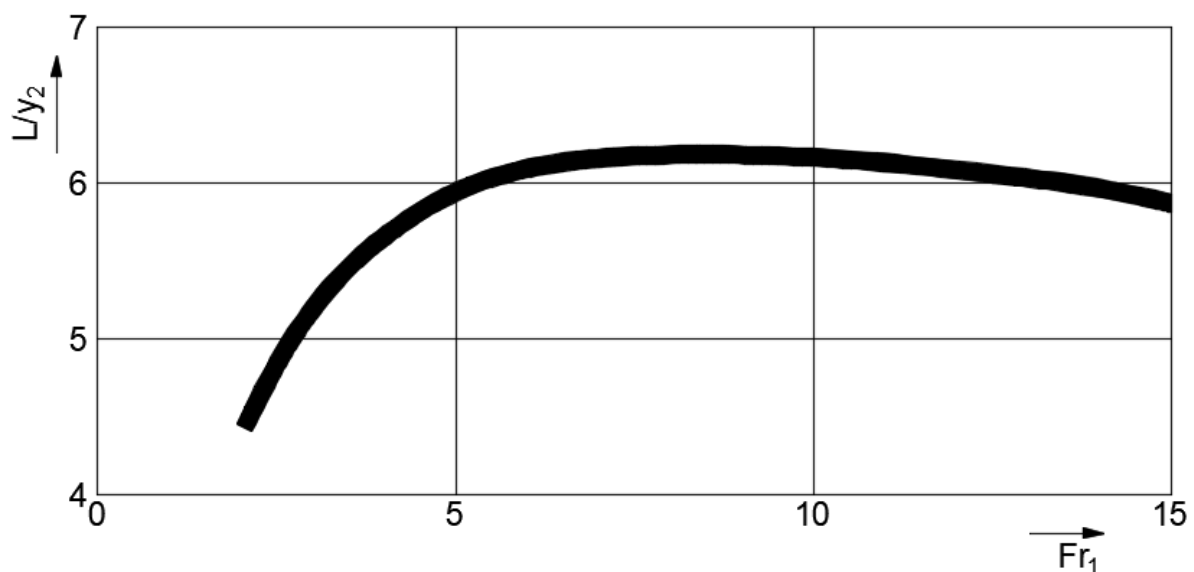


Figure 296 – Rebound length (adapted from Barbosa, 1982).

Teixeira (2003), carried out the task of collecting different mathematical proposals for the calculation of the rebound length, elaborated by different authors and different conditions and testing (Table 49).

In relation to the parameters: D_1 represents the combined height 1, D_2 the combined height 2 and Fr the Froude number at section 1.

Table 49 – Review of the proposals for the rebound length calculus.

Autor	Year	Equation
Riegel	1917	$L = 5(D_2 - D_1)$
Woycicki	1934	$L = (D_2 - D_1) \left(8 - \frac{0.05 \times D_2}{D_1} \right)$
Sanetana	1934	$L = 6(D_2 - D_1)$
Chertoussov	1935	$L = 10.3D_1(Fr - 1)^{0.81}$
Aravin	1935	$L = 5.4(D_2 - D_1)$
Bakhmeteff-Matzke	1936	$L = 5(D_2 - D_1)$
Kinney	1941	$L = 6.02(D_2 - D_1)$
Posey	1941	$L = 4.5 - 7(D_2 - D_1)$
Wu	1949	$L = 10(D_2 - D_1)Fr^{-0.16}$
Peterka	1957	$L = 6.1D_2$
Elevatorski	1959	$L = 6.9(D_2 - D_1)$
Silvester	1964	$L = 9.75D_1(Fr - 1)^{1.61}$
Marques et al.	1997	$L = 8.5(D_2 - D_1)$

To locate the rebound it is necessary to know the characteristics of the flow in two sections of control, one at upstream and one at downstream, so, being possible to be done in two forms:

- Calculating the conjugated water heights of the successive water heights determined for a backwater curve corresponding to a fast regime, obtaining then a curve of the conjugated heights when intersected with a backwater curve of a slow regime, defining the location of the rebound;
- Drawing the line of total amount of movement corresponding to the backwater curves relative to fast and slow regimes, so the intersection point corresponds to the location of the hydraulic rebound.

At the beginning of this sub-chapter, it was referred that, the rebound has its origin in the abrupt transition from fast to slow regime. Now, it is focus in the different forms to trigger such hydraulic phenomenon.

A rebound can be produced by a super-elevation, a spillway of thick edge, by the pass from a reservoir to a channel of strong slope, by the pass of a flow by a gate, or finally by the increase or decrease of the channel width.

The phenomenon of hydraulic rebound is usually applied in water supply stations or in sewers treatments plants, to promote mixture by the generated turbulence of the substances involved in the flow, which is an effective method of mixing.

The thresholds Venturi and Parshall are two more examples of hydraulic rebound application, making possible to measure flow rate or flow and the substance mixture in it by the contraction or super elevation of the transversal section of the channel but paying attention that the effect of the flow at downstream does not affect upstream flow.

The flow rate measurement through the application of threshold Venturi (Figure 297) is made by knowing the characteristics of the flow at upstream and at the section of control (contracted section). In case of a fast regime flow, the flow will tend to its normal height immediately at downstream waters. But if the regime is a slow flow, the hydraulics rebound will occur (Henriques *et al.*, 2006).

In conclusion, it can be assumed that, the Venturi's Threshold must be dimensioned in order to work in free discharge for a set of flow rate that it will work in the equipment, that is, the regime will pass through a critical regime in the narrowing section, in order to guarantee the hydraulic rebound (Henriques *et al.*, 2006).

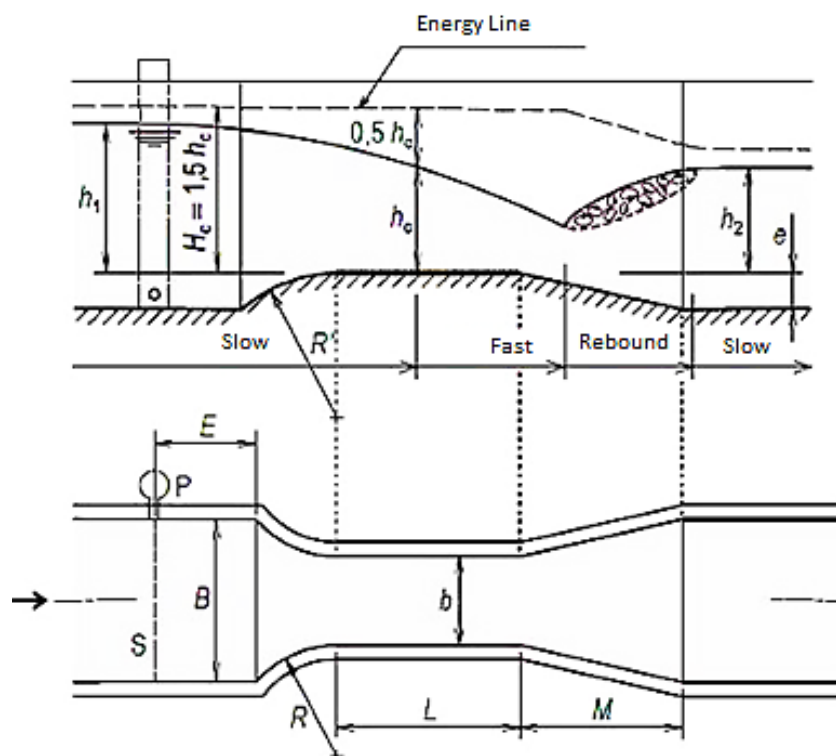


Figure 297 – Thresholds of Venturi (Henriques *et al.*, 2006).

In the thresholds of Venturi, the calculus of the flow rate is made by,

$$Q = C_d \cdot \sqrt{g} \cdot b \cdot s^{3/2} \cdot h_1^{3/2}$$

where s is given by:

$$s = \frac{1}{0.5 + \cos \left[\frac{2}{3} \cdot \sin^{-1} \left(\frac{b}{B} \right) \right]}$$

where b refers to the length of the narrowing section of the channel, s represents a constant value of the submersion relationship, h_1 is the flows height at the upstream of the contracted section, B is the total length of the channel where the Venturi's threshold is inserted, and finally C_d represents the discharge coefficient. It must be referred that, the coefficient of discharge (C_d) already includes the effect of charge losses due to friction and curvature of the current lines. Its value varies between 0.95 and 0.99.

Therefore, this equipment has some dimensional and operational conditioning (Henriques *et al.*, 2006):

- The length of the contracted zone must be major or equal to 9 cm;
- $\left(\frac{b}{B} \right) \left(\frac{h_1}{h_1 - e} \right) \leq 0.7$;
- $\frac{h_1}{b} \leq 3$;
- $0.005 \text{ m} \leq h_1 \leq 1.8 \text{ m}$.

The Parshall's threshold (Figure 298) is another example of a dispositive of flow rate measurements, being a branch of the Venturi's thresholds, but distinguished by its normalized dimensions and its angular shapes (Henriques *et al.*, 2006).

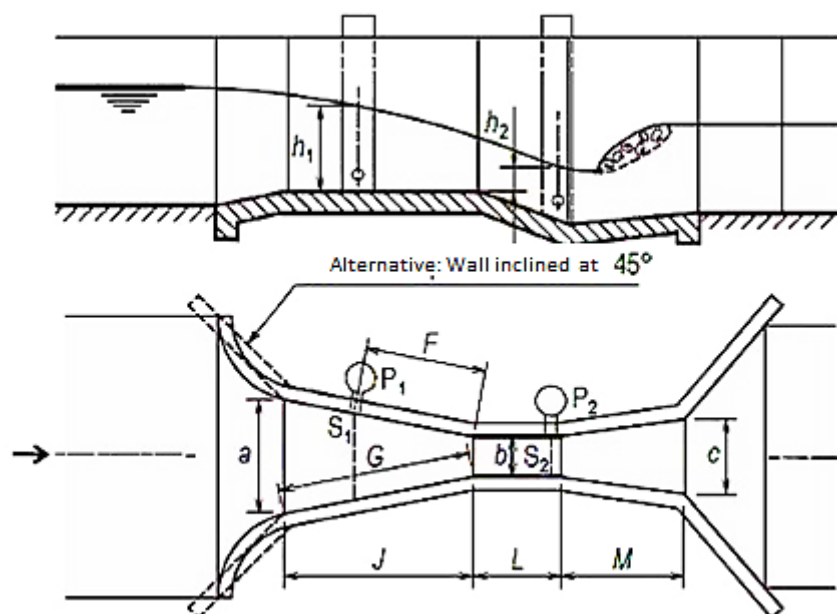


Figure 298 – Threshold of Parshall (Henriques *et al.*, 2006).

At this equipment, the water is forced to pass through a narrowing and the upstream water level is considered independently from conditions at downstream or drowning conditions (Henriques *et al.*, 2006).

The flow rate is measured through a point located at 2/3 of the channel in transition and it is generally called “point zero”. The flow rate is given by:

$$Q = K \cdot h_1^w$$

Where:

K, w are characteristic parameters of the gutter;

h_1 is the water height in section 1, located at the convergent.

Particular cases:

Rebound produced by a spillway or discharger of thick edge or super elevation

The hydraulic rebound produced by the pass of a flow by a spillway or discharger of thick wall or super elevation of the bottom of the canal (Figure 299) occurs when the flow has not enough energy to overcome the obstacle independent of the flow's regime.

In case of a slow regime has no enough energy to overcome the obstacle the flows conditions will tend to change in order to reach a minimal energy to overcome such obstacle, thus, the flow will pass through a critical regime. When the regime originally slow pass to critical, as soon as reach downstream water after super elevation, it will become a fast regime. Then, the rebound will occur in fast regime, produced by its pass over the obstacle and then becoming a slow regime at downstream waters of the obstacle (Barbosa, 1982).

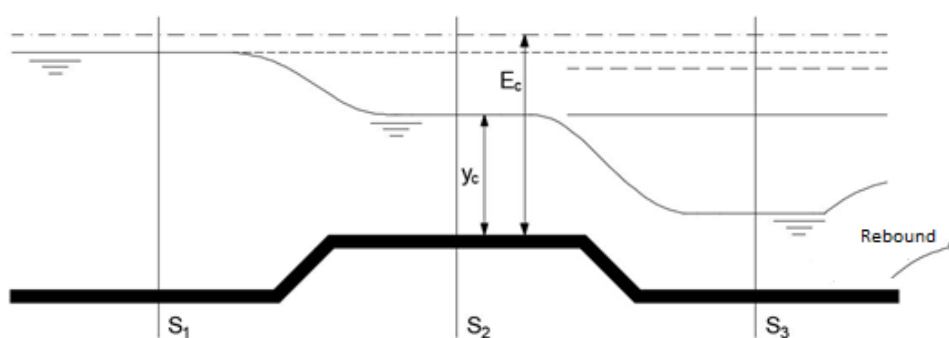


Figure 299 – Rebound at downstream waters produced by a thick threshold or super elevation (Barbosa, 1982).

In another hand, in case of a fast regime flowing without enough energy to overcome an obstacle, the rebound will occur at upstream and followed by a backwater curve of elevation (Figure 300). The level of the water will increase until the regime reaches critical conditions, and then pass to a slow regime. After becoming a slow regime and because of it is fast, it will origin a rebound at upstream waters. Finally, after the obstacle, the flow will become a fast regime again. (Barbosa, 1982).

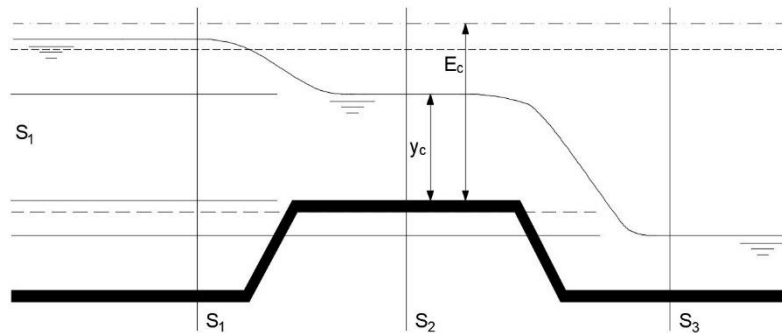


Figure 300 – Rebound at upstream waters produced by a thick threshold or super elevation (Barbosa, 1982).

Hydraulic rebound caused by a change in slopes of the channel

The hydraulic rebound caused by a change in the slope of a channel (Figure 301) occurs when the first section has a strong slope, where exists a fast regime and then come into a weak slope, finding a slow regime (Lencastre A., 1972).

The question is to know where will be located the rebound, because it can happen at any section, after or before the change of slope. When it is a fast regime, which is a flow controlled by upstream waters, it will be uniform until S_0 , where it will be followed by a backwater curve I_3 , occurring a rebound in the weak slope section (Barbosa, 1982).

If the flow is controlled by downstream waters (slow regime), the regime will stay uniform from section S_0 until section S_2 , being preceded by a backwater curve of type S_1 , occurring the rebound at the strong slope section (Barbosa, 1982).

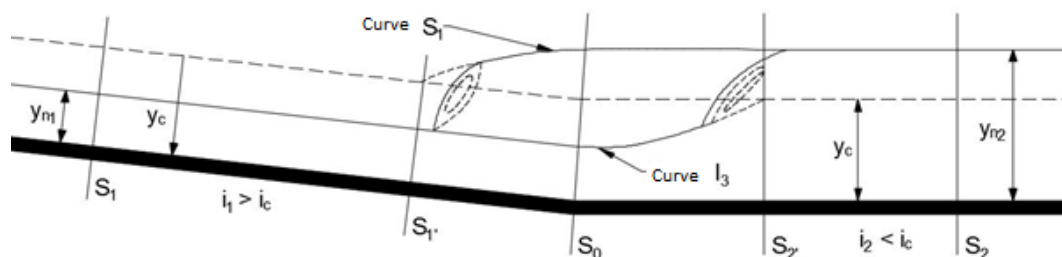


Figure 301 – Rebound produced by an abrupt change of slope (Barbosa, 1982).

Hydraulic rebound caused by the enlargement or contraction of the channel

When the flows reach a narrowing or constriction in the channel, without enough energy, its characteristics change and pass to a slow regime with an increase of water deepness. At such case, the rebound occurs at upstream waters of the narrowing of the channel. In case of a slow regime, the rebound will occur at downstream waters of the narrowing.

In the same way, by an enlargement of the channel, if exists a slow regime, it will become a fast regime in the enlargement and after it will become slow again. At that case, due to the second change, fast to slow, it will occur the rebound due to the abrupt change.

Hydraulic rebound caused by the pass of a flow through a gate

The pass of a flow through a gate (Figure 302) can originate 3 situations for hydraulic rebounds. The first case is given when the opening of the gate is inferior to the critical level of the channel of strong slope. The second case is given when the opening of the gate is lower to the critical level of the channel of weak slope, where the energy in the contracted section of the flow is the same or superior to a uniform regime. Finally, the third case refers to a drowned rebound (Barbosa, 1985).

In case of a gate opening lower than the critical level of a channel of strong slope, the rebound occurs at upstream waters of the gate, where the water rises due to the lack of energy of the flow. In this way, the rebound occurs by the abrupt pass or change from fast to slow, preceded by a backwater curve of type S_1 .

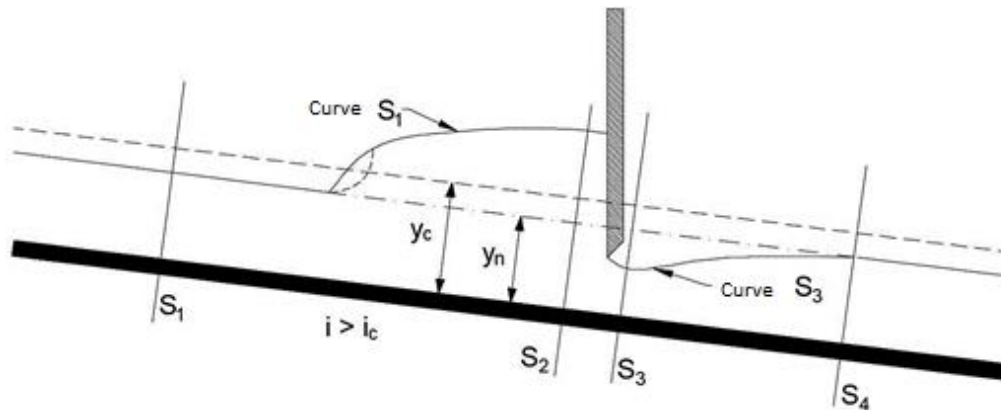


Figure 302 – Rebound caused by a gate with strong slope (Barbosa, 1982).

In case of a rebound caused with an opening lower to the critical height in a channel with weak slope (Figure 303), the flow at upstream water has a behaviour similar to the last one, because it is formed a curve of backwater type I_1 as it gets closer to the gate. at downstream, it is formed a curve of backwater type I_3 and followed by the rebound, due to the regime at downstream waters tend to be slow. Then, y_2 is equal to the normal height of flow.

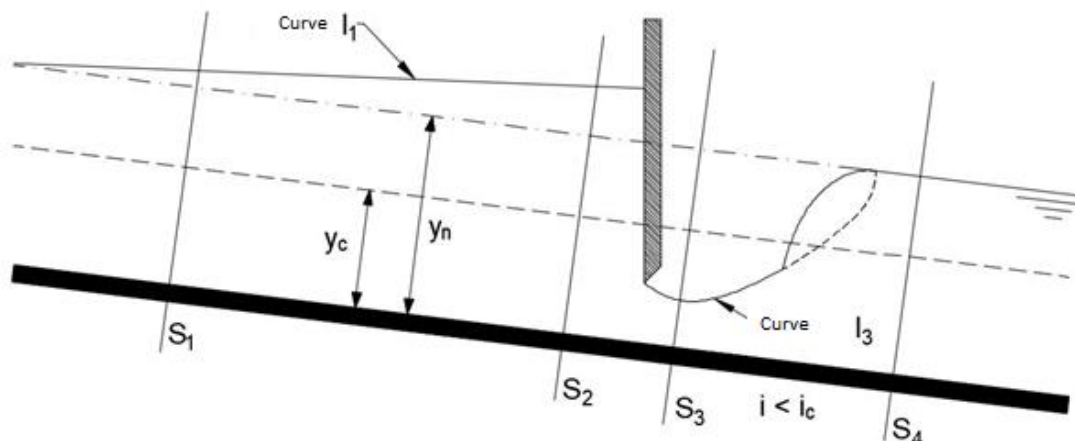


Figure 303 – Rebound caused by a gate in a channel of weak slope (Barbosa, 1982).

In case of a lack of energy at the downstream flow to re-establish the natural regime, it happens a drowned rebound (Figure 304). In such case, the water deepness rises at the contracted section in order to supply the necessary increase of energy at section S_3 , so the flow will have enough energy to return to its uniform regime.

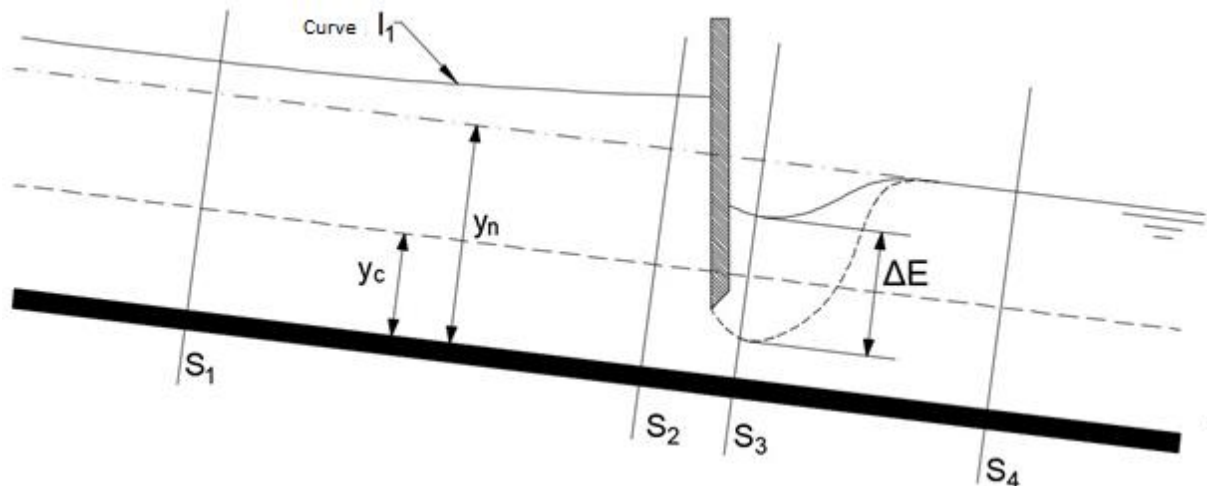


Figure 304 – Drowned rebound (Barbosa, 1982).

11.6.3 Other types of rapidly varied flows

With an exception of the rebound, the rapidly varied flows occur in the following conditions:

- Shorts sections, not associated to separation phenomenon as in the case of change of inclination and discharger or spillways;
- Shorts sections, associated to separation phenomenon as in the case of enlargements and contractions;
- Resultant steady oblique waves, as for example, change of direction.

It is important to refer that the flows rapidly varied with separation creates localized charge losses, which can lead to form stationary oblique waves turning the surface irregular, making quite difficult to define the conditions of flow (Manzanares & Quintela, 1980).

The study of rapidly varied flows is complex (theoretical) due to the mentioned conditions. Therefore, the study of such flows is made based in experimental procedures based in similarity principles and dimensional analysis (Soares A. S., 2014).

REFERENCES

- Area Mecânica. (2011). Ingeniería Mecánica: Curvas características de una bomba centrífuga (II). Obtained from Area Mecânica: <https://areamecanica.wordpress.com/2011/06/16/ingenieria-mecanica-curvas-caracteristicas-de-una-bomba-centrifuga-ii/>
- Baliño, J. L. (2017). Equações de Navier-Stokes. São Paulo, Brasil: USP.
- Barbosa, J. N. (1982). Mecânica dos fluidos e Hidráulica Geral. Porto Editora.
- Barbosa, J. N. (1985). Mecânica dos fluidos e Hidráulica Geral 2. Porto Editora.
- Braga, J. (2014). Hidráulica II. U.M.A.
- Brunetti, F. (2008). Mecânica dos Fluidos (2nd ed.). São Paulo: Pearson. Prentice Hall.
- Coelho, J. G., Brasil Junior, A. C., and Noletto, L. (2006). Escoamento Turbulento em Difusores. Rio de Janeiro: EPTT.
- Costa, A. S. (2003). Turbinas Hidráulicas e Condutos Forçados. Santa Catarina: UFSC. Obtained from <http://www.labspot.ufsc.br/~simoes/dincont/turb-hidr-2003.pdf>
- Costa, T. d., and Lança, R. (2011). Hidráulica Aplicada. Faro: Universidade do Algarve.
- Cruz, J. (2006). Aproveitamentos Hidroelétricos. Lisboa: IST.
- DRHGSA. (2007). Capítulo II. Orifícios. Piauí, Brasil: UFPI. Obtained from <http://leg.ufpi.br/subsiteFiles/ct/arquivos/files/pasta/CAP%202.pdf>
- Eisberg, R., and Resnick, R. (1979). Física Quântica - Átomos, Moléculas, Sólidos, Núcleos e Partículas (13th ed.). Editora Campus.
- Escola da Vida. (2018). Análise dimensional e leis de semelhança aplicadas as bombas hidráulicas. Obtained from Escola da Vida: http://www.escoladavida.eng.br/mecfluquimica/analise_dimensional.htm
- Filho, J. G. (2015). Turbinas Hidráulicas - Tipos e Usos. Campinas: Universidade Estadual de Campinas. Obtained from <https://docslide.com.br/documents/turbinas-hidraulicas-55ef3ff5660bb.html>
- Fletcher, B. P., and Grace, J. L. (1972). Practical guidance for estimating and controlling erosion at culvert outlets. U.S. Army Engineer Waterways Experiment Station.
- Gaspar, R. (2005). Mecânica dos Materiais. São Paulo, Brasil: Centro Universitário Nove de Julho.
- Gobbi, M., Dias, N. L., Mascarenhas, F., and Valentine, E. (2011). Introdução à Mecânica dos Fluidos e aos Fenómenos de Transporte. Paraná, Brasil: UFRP.
- Henn, É. A. (2006). Máquinas de Fluido (2nd ed.). Santa Maria: UFSM.
- Henriques, J. D., Palma, J. C., and Ribeiro, A. S. (2006). Medição de caudal em sistemas de abastecimento de água e de saneamento de águas residuais. Lisboa: LNEC.
- Ignácio, R. F., and Nóbrega, R. L. (2004). Mecânica dos Fluidos. Análise Dimensional e Semelhança Dinâmica. Paraíba, Brasil: AERH. UFCG.
- Junior, L. B. (2005). Orifícios, Bocais e Tubos curtos. Goiânia - GO, Brasil: PUC Goiás.
- Junior, N. V., and Colvara, L. D. (2010). Os modelos mentais de alunos em relação a vetores em duas e três dimensões: uma análise da dinâmica da aprendizagem e da inadequação das avaliações tradicionais. Ciências e Cognição, 55-69. Obtained from <http://pepsic.bvsalud.org/pdf/cc/v15n2/v15n2a06.pdf>

- KSB. (2003). Manual de Treinamento. Seleção e Aplicação de Bombas Centrífugas. KSB. Obtained from <https://pt.slideshare.net/EvandroTP/ksb-manual-de-selecao-e-aplicacao>
- Lencastre, A. (1972). Manual de Hidráulica Geral.
- Lencastre, A. (1983). Hidráulica Geral. Lisboa: Hidroprojeto.
- Lewis, E. V. (1988). PNA - Principles of Naval Architecture, Volume I - Stability and Strength. New Jersey, USA: SNAME.
- Manzanares, A., and Quintela, A. (1980). Hidráulica Geral II. Escoamentos Líquidos. Lisboa: AEIST.
- Martins, M. R. (2010). Hidrostática e Estabilidade. São Paulo, Brasil: USP. Obtained from http://www.ndf.poli.usp.br/~gassi/disciplinas/pnv2341/Martins_2010_Hidrost%C3%A1tica_e_Estabilidade_PNV2341.pdf
- Mata-Lima, H. (2010). Apointamentos de Hidráulica. Funchal: UMa.
- Mendonça, F. C. (2015). Hidrometria. São Paulo, Brasil: USP. Obtained from http://www.esalq.usp.br/departamentos/leb/disciplinas/Fernando/leb472/Aula_12/Aula%2012_Hidrometria.pdf
- Nalluri, C., and Featherstone, R. (2001). Civil engineering hydraulics: essential theory with worked examples. Wiley-Blackwell.
- NETeF. (2012). Análise Dimensional e Semelhança. São Paulo, Brasil: USP. Obtained from <http://www2.eesc.usp.br/netef/Oscar/Aula23>
- Netto, A. (1998). Manual de Hidraulica. Edgard Blucher Ltda.
- Oliveira, R. J. (2007). Cavitação: Como entender este fenômeno? Como identificar? Minas Gerais: MGS - Tecnologia.
- Pacífico, A. L. (2016). Introdução à Cinemática dos Flúidos. São Paulo, Brasil: USP.
- Peterka, A. J. (1958). Hydraulic design of stilling basins and energy dissipators.
- Pinho, J. L., Vieira, J. M., and Lima, M. M. (2011). Apointamentos para as Aulas de Hidráulica Geral I e II. Minho: Universidade do Minho.
- Pontes, J. d., and Mangiavacchi, N. (2013). Fenômenos de Transferência com Aplicações às Ciências Físicas e à Engenharia (Vol. I). Rio de Janeiro: UFRJ.
- Pordeus, R. V. (2015). Nota de Aula: Fenômenos de Transporte. Mecânica dos Fluidos. Tipos de Regime de Escoamento. Rio Grande do Norte, Brasil: UFRSA. Obtained from <http://www2.ufersa.edu.br/portal/view/uploads/setores/111/CAP%20V%20TIP OS%20E%20REGIME%20DE%20ESCOAMENTO.pdf>
- Queiroz, G. (2017). Vertedores. Minas Gerais, Brasil: UFOP. Obtained from <http://www.em.ufop.br/deciv/departamento/~gilbertoqueiroz/CIV225-Vertedores.pdf>
- Quintela, A. d. (2005). Hidráulica (9th ed.). Lisboa: Fundação Calouste Gulbenkian.
- Ramalho, F. J., Nicolau, G. F., and Toledo, P. A. (2015). Os Fundamentos da Física (11^a ed.). São Paulo, Brasil: Moderna.
- Rijo, M. (2010). Canais de Adução - Projecto, Operação, Controlo e Modernização (1st ed.). Lisboa: Edições Sílabo.
- Silva, G. Q. (2014). Estudo dos Orifícios e Bocais. Minas Gerais, Brasil: UFOP.
- Simões, J. G. (2011). Condutos livres. Escoamento uniforme em canais. São Paulo, Brasil: Unisanta.

- Smith, H. (1886). Hydraulics: The Flow of Water Through Orifices, Over Weirs, and Through Open Conduits and Pipes. Truebner and co.
- Soares Júnior, R. L. (2013). Projeto Conceitual de uma Turbina Hidráulica a ser utilizada na Usina Hidrelétrica Externa de Henry Borden. Rio de Janeiro: UFRJ.
- Soares, A. S. (2014). Análise Experimental das Condições de Escoamento Superficial em Zonas Urbanas na Presença de Viaturas. Lisboa: UNL.
- Soares, H. (2011). Hidráulica Geral. Minas Gerais, Brasil: UFJF. Obtained from <http://slideplayer.com.br/slide/5382800/>
- Tavares, I. T. (2014). A Influência de Difusor na Eficiência de uma Turbina Hidráulica. Brasília, DF: UnB.
- Teixeira, E. (2003). Previsão dos valores de pressão junto ao fundo em bacias de dissipação por ressalto hidráulico. Rio Grande do Sul, Brasil: UFRGS.
- UALG. (2018). Guia do princípio de Arquimedes. Obtained from UALG. Guias: <https://pt.wikipedia.org/wiki/Impuls%C3%A3o>
- UEL. (2017). Resumo de Hidráulica - Introdução. Obtained from ebah: <http://www.ebah.pt/content/ABAAAAlCKAF/resumo-hidraulica-introducao?part=3>
- Universidade Federal do ABC. (2013). Alimentação via turbo-bombas. Universidade Federal do ABC. Obtained from <https://pt.slideshare.net/edpackness/liquid-propellant-rocket-engine-motor-foguete-liquido-part11>
- Vasconcelos, M. M. (2005). Hidráulica Geral I. Évora: Universidade de Évora.
- Villa, A. A. (2011). Análise Dimensional e Semelhança. Pernambuco, Brasil: UFPEP.
- White, H. E. (1948). Modern College Physics. van Nostrand.